國立臺灣大學生物資源暨農學院生物科技研究所

博士論文

Institute of Biotechnology
College of Bioresources and Agriculture
National Taiwan University

Doctoral Dissertation

可促進植物生長之光合菌 *Rhodopseudomonas palustris* PS3 的基因體分析與培養條件優化

Genome analysis and fermentation optimization of plant growth promoting strain *Rhodopseudomonas palustris* PS3

羅凱軍

Kai-Jiun Lo

指導教授：劉啓德 博士

Advisor: Chi-Te Liu, Ph.D.

中華民國 109 年 7 月

July 2020

doi:10.6342/NTU202003422

國立臺灣大學博士學位論文
口試委員會審定書

可促進植物生長之光合菌 *Rhodopseudomonas palustris* PS3 的基因體分析與培養條件優化

Genome analysis and fermentation optimization of plant growth promoting strain *Rhodopseudomonas palustris* PS3

本論文係 羅凱軍 君（D01642012）在國立臺灣大學生物科技研究所完成之博士學位論文，於民國一零九年七月二十八日承下列考試委員審查通過及口試及格，特此證明

口試委員：劉啓德（簽名）

（指導教授）

劉啓德　　

李昆達　郭志洲

林詩舜　陳仁治

系主任、所長 劉啓德（簽名）

謝辭

當這本博士論文完成時，也代表著我的博士求學生涯告一段落了。這本論文得以完成要感謝的人實在太多了。首先，要感謝我的指導教授劉啓德博士，啓德老提供了一個很好的實驗環境讓我進行論文研究，並在我遇到困難時協助我解決難題。在學術研究外上，也給予我生活上很大的支持。時常關心我的生活狀況。從我決定攻讀博士學位到撰寫計畫書、進行實驗設計至發表研究論文的一路上，老師都是正向的鼓勵我一路往前，讓我嘗試任何想做的事情。老師給予的實驗自由度更讓我可以自由自在的進行研究，又在我迷失方向時適時拉回我。老師也提供了許多合作的機會，讓我在博士生涯裡累積了各種經驗。和老師一起經歷的事情都會是我博士班求學過程中難以忘懷並且感恩的事情。另外，也謝謝詩舜老師，雖然我們有些目標還未完成，但您是帶領我進入生物資訊領域的一個重要的人。也感謝郭志鴻老師再基因體的解序與研究上給予學生很好的指導與協助。仁治老師在分子實驗上的建議替我解決的實驗上的問題。在每週與昆達老師實驗室的會議裡，昆達老師的寶貴的建議也讓我的研究更完整。當然還要謝謝口試委員老師們仔細的閱讀我的論文、給予建議與修正，使得我的博士論文更完整。

在這段研究的路上還要感謝實驗室的成員，在實驗上提供協助、包容以及建議，也感謝這些人陪伴我渡過這些日子，這些將會是很好的經驗與回億。特別是我的戰友夥伴筱涵、郁盛、YOYO、爾傑、球球、怡儒、Aniket，雖然大家往後各奔東西，但我們的友誼將會常存。謝謝孟薇在這段時間裡，替我打理了許多事情，陪我渡過博士求學生活的日子。謝謝睦惠陪我渡過最後的衝刺階段。

最後要感謝我的弟弟凱胤，未來的日子我們一定會更好。而我最愛的母親黃瓊雀女士，是您的支持讓我得以繼續攻讀博士學位。從小到大，您一直以來都是我最大的後盾。雖然您來不及看到我穿上博士袍、無法參與我的畢業，但我完成了。這本論文也將獻給您做為禮物，您會永遠活在我的心底。

凱軍謹誌於

中華民國一百零九年七月

doi:10.6342/NTU202003422

中文摘要

沼澤紅假單胞菌 (*Rhodopseudomonas palustris*) PS3 菌株是一株由台灣水稻田土壤所篩選出的紫色非含硫光合菌。在先前研究中已證明該菌株具有促進各種作物生長的能力，並且可以提升植物氮肥使用效率。本論文的第一部份是從微生物全基因體的角度來探討光合菌與促進植物生長的關係。藉由與另一株不具促進植物生長功能之 YSC3 光合菌 (*Rhodopseudomonas palustris*)做比較分析，依基因構造、微生物生理反應以及基因表現的結果找出 PS3 菌株可能參與促進植物生長的相關基因。本研究結合了短片段與長片段定序技術，並完成序列組裝與註解後，分別得到 PS3 與 YSC3 菌株的基因體全長為 527 萬與 537 萬鹼基對，含有 4,799 以及 4,907 編碼序列。PS3 與 YSC3 菌株有極高的序列相似度（約 95.11%），而且大部分的基因群的組成與排列方式類似，都有固氮、溶磷、吲哚乙酸合成、氨基環丙烷羧酸脫胺酶等代表性的植物生長促進相關基因群。雖然 PS3 與 YSC3 菌株的生長速率沒有差異，在微生物生理試驗結果發現，添加植物的根分泌液至兩株菌的培養液中會促使 PS3 菌株的生物膜生成量以及化學趨向性的相關基因表現量都較 YSC3 菌株高。這意味著 PS3 菌株對於植物的反應可能是其促進植物生長的重要關鍵。

PS3 光合菌是具有產業化潛力的菌株，本論文的第二部分藉由數學統計模式探討最適化發酵條件，找出高產量與低成本的生產方式。在本研究中評估了各種較低成本的基質，包括了工業發酵常用的碳氮源以及農產加工副產物等作為培養基配方的可行性，並藉由回應曲面法優化培養條件。實驗結果顯示，當以 39.41 mL/L 的玉米浸漬液加上 32.35 g/L 的蔗糖糖蜜作為氮源和碳源，利用 5 公升桌上型發酵槽於 38°C，pH 7 以及溶氧濃度 30%的條件下進行 24 小時培養，得到 PS3 菌株的最大生物量約為 2.18 ± 0.01 g/L。該新配方所生產的 PS3 發酵液產量約為使用傳統光合菌培養條件的 8 倍，成本卻只需原先的 30%，而且在植物盆栽試驗上證實可以促進作物生長。

doi:10.6342/NTU202003422

在本研究中所建立的基因體資訊，可作為探討光合菌與植物間的交互作用以及促進生長機制的研究平台。此外，新開發的培養基配方是以農產加工副產物作為光合菌的主要營養基質，不僅可有效降低生產成本，也促進了農業資源的加值與循環再利用。

關鍵字：沼澤紅假單胞菌、全基因體比較分析、回應曲面法、農產加工副產物、玉米浸漬液、糖蜜、促進作物生長

doi:10.6342/NTU202003422

ABSTRACT

Rhodopseudomonas palustris PS3 is one of purple non-sulfur phototrophic bacteria that was isolated from Taiwanese paddy soils. It has been demonstrated that PS3 can promote plant growth and increase the agronomic nitrogen use efficiency of the host plant. The first part of this dissertation focuses on the elucidation of the relationship between the phototrophic bacteria and plant growth-promotion from the view of whole genomes of microorganisms. I conducted comparative analyses of genomic structures, physiological responses of microbes, and gene expression profiles with those of an ineffective *R. palustris* YSC3 strain. Based on the differential data, many putative genes that were associated with known plant growth promotional traits were identified. In this study, Illumina short-reads and PacBio long-reads technologies were integrated and assembled to obtain the whole genome sequences. PS3 and YSC3 individually contains a one circular chromosome with 5.27 and 5.37 Mb bp in size, with 4,799 and 4,907 protein-coding genes, respectively. The PS3 and YSC3 strains are closely related to each other with high identity (95.11%), and have similar genomic structures and compositions. Both strains contain the genes associated with plant growth-promotion, such as nitrogen fixation, phosphate solubilization, indole acetic acid synthesis, 1-aminocyclopropane-1-carboxylate deaminase, etc. Although there was no difference in the growth rate of PS3 and YSC3 strains, both the production of biofilm and the gene expressions of chemotaxis of PS3 were higher than those of YSC3 by the addition of root exudate in culture broth.

Since PS3 is an elite strain with commercialization potential, the second part of this dissertation focuses on the optimal fermentation conditions for PS3 through mathematical and statistical models to find out a high-yield and low-cost production strategy. In this study, I evaluated various substrates, including the carbon and nitrogen

doi:10.6342/NTU202003422

sources commonly used in industry as well as the agricultural processing by-products. The culture condition was optimized by response surface methodology. The optimum culture condition was found to be at corn steep liquor, 39.41 mL/L; molasses, 32.35 g/L; temperature, 38°C; pH, 7.0; and DO 30%. Under this condition, the maximum yield of PS3 strain was up to 2.18 ± 0.01 g/L, which was approximately 8-fold higher than that with original medium, and the medium cost was approximate 70% reduced. Moreover, the beneficial effect of the new PS3 broth on plant growth was verified by pot experiments.

The genomic information established in this study can be used as a research platform to investigate the interaction between phototrophic bacteria and plants as well as the molecular mechanisms of plant growth promotion. In addition, the newly developed medium uses agricultural processing by-products as the main nutrient substrates for phototrophic bacterium growth, which not only effectively reduces production costs, but also promotes the value-added and recycling of agricultural resources.

Keywords: *Rhodopseudomonas palustris*, whole genomic comparative analysis, response surface methodology, agricultural processing by-products, corn steep liquor, molasses, plant growth promotion

doi:10.6342/NTU202003422

CONTENTS

doi:10.6342/NTU202003422

doi:10.6342/NTU202003422

doi:10.6342/NTU202003422

doi:10.6342/NTU202003422

LIST OF FIGURES

doi:10.6342/NTU202003422

doi:10.6342/NTU202003422

LIST OF TABLE

doi:10.6342/NTU202003422

CHAPTER I

INTRODUCTION

Recently, food supply has been a major concern in the word because global warming and rise in human population greatly increase crop demand. Therefore, how to increase crop productivity is an urgent issue. Traditionally, excessive use of chemical fertilizers is a general and simple approach for farmers to increase the harvest yields of crops (Tilman, 1998). However, only a small part of the fertilizers (10% to 40%) is taken up by plants, it means more than 60% of fertilizer is lost during farming (Adesemoye and Kloepper, 2009). The excessive application of chemical fertilizers in agriculture occurs universally and results in soil acidification and reduction of arable lands (Barak *et al.*, 1997). In order to raise crop yields and reduce environmental impact, development of sustainable agriculture is required.

Plant growth promoting rhizobacteria

In 1978, Kloepper and Schroth suggested a concept of plant growth-promoting rhizobacteria, abbreviated as PGPR (Kloepper and Schroth, 1978). PGPR are diverse subgroup of rhizosphere-colonizing bacteria that exert beneficial effects on plant growth by various mechanisms (Adesemoye and Kloepper, 2009; Ahemad and Kibret, 2014; Beneduzi *et al.*, 2012; Lugtenberg and Kamilova, 2009). These bacteria are able to colonize on the roots of plants (rhizosphere), to enhance plant growth directly or indirectly. PGPR not only provides enhancement on plant growth, some PGPR can also systemically activate plant defense mechanisms (Akhtar and Siddiqui, 2011). PGPR offers an alternative way to replace chemical fertilizer, pesticide, and supplements, and can be classified as three groups: (1) biofertilizers, (2) biocontrol agents, or biocontrollers or biopesticides, (3) bioremediators (Lugtenberg and Kamilova, 2009;

doi:10.6342/NTU202003422

Vessey, 2003). The deduced modes of actions of PGPR include (1) facilitating the uptake of certain plant nutrients from soil, such as fixing nitrogen, solubilizing phosphate; (2) producing phytohormones, such as auxin and cytokinins; (3) preventing abiotic or biotic effects, by bioremediation and biocontrol traits (Goswami *et al.*, 2016). Figure 1-1 shows the general growth promoting modes of action from PGPR. To date, there are many bacterial species considered to be PGPR, such as *Azotobacter*, *Bacillus*, *Burkholderia*, *Gluconacetobacter*, *Klebsiella*, *Pseudomonas*, *Rhizobium*, etc (Kaymak, 2011). Further, several microbial species have been commercialized such as nitrogen fixation bacteria (*Azospirillum* spp., *Azotobacter* spp., *Rhizobium* spp., etc.) and phosphate solubilization bacteria (*Bacillus* spp., *Pseudomonas* spp., *Aspergillus* spp., *Penicillium* spp., etc.). The major products are based on *Bacillus* spp., including *B. thuringiensis*, *B. subtilis*, *B. amyloliquefaciens*, etc. Other species such as *Streptomyces* spp., *Pseudomonas* spp. and *Trichoderma* spp. are also used in the common products of biopesticides. Table 1-1 shows the microorganisms as potential inoculants for agricultural uses.

PGPR with nitrogen fixing ability

Biological nitrogen fixation is a process that nitrogen is converted to ammonia by nitrogenase complex of microorganisms (Kim and Rees, 1994). PGPR fix nitrogen to facilitate plant growth have been widely investigated (Garcia de Salamone *et al.*, 1996; Oberson *et al.*, 2013; Stueken *et al.*, 2015; Vessey, 2003). In general, nitrogen fixation occurs in root-nodules of leguminous plants that harbor rhizobia. It also can be carried out by the non-symbiotic bacteria, such as cyanobacteria, *Azospirillum* etc. (Kim and Rees, 1994; Oberson *et al.*, 2013). According to the metal cofactor, nitrogenase can be classified as Fe-nitrogenase, Mo-nitrogenase and V-nitrogenase (Bishop and Joerger, 1990). The gene clusters encoding nitrogenase are identified in

doi:10.6342/NTU202003422

either symbiotic or non-symbiotic bacteria (Kim and Rees, 1994). Nitrogenase complex consist of two nitrogenase, Fe nitrogenase and Mo-Fe nitrogenase (homologous to V-Fe protein). The Fe protein is encoded by *nifH* and *vnfH* (for V-nitrogenase system), respectively. While, Mo-Fe and V-Fe are encoded by *nifDK* and *vnfDK* genes, respectively. Fe-protein offers electrons with reducing power while Mo-Fe protein uses these electrons to conserve nitrogen as ammonia (Kim and Rees, 1994). For rhizobia, because these bacteria invade plant tissue to form nodule, they can directly supply the nitrogen to plants. In contrast, the free-living nitrogen fixers are able to provide nitrogen source in the rhizosphere for nourishing plants (Bhattacharyya and Jha, 2012).Nitrogen-fixation are considered an important mechanism of PGPR, and the nitrogen fixing bacteria are also used as biofertilizer in agriculture.

PGPR with phosphate solubilizing ability

Phosphorus is an important limiting nutrient for plants and abound in soil. Despite of a large quantity of phosphorus in earth's crust, low available forms can be used in soils by plants. The critical factor for this low availability is due to insoluble forms of phosphorus (Bhattacharyya and Jha, 2012). Some PGPR are reported to increase the availability of phosphorus by solubilizing phosphate from either organic or inorganic phosphates, thereby promoting plant growth (Bhattacharyya and Jha, 2012; Vassilev *et al.*, 2006). Phosphate solubiliztion is carried out by various phosphatases and organic acids which are secreted by PGPR (Rodriguez *et al.*, 2006). Comparison of both methods, bacteria secrete organic acid may be the primary mechanism, because PGPR colonize in rhizosphere can utilize sugars from root exudates to produce organic acids (Goswami *et al.*, 2014). Among the phosphate solubilizing PGPR, *Pseudomonas* and *Bacillus* have been described as effective phosphate solubilizers (Goswami *et al.*, 2015).

doi:10.6342/NTU202003422

PGPR with phytohormone producing ability

PGPR has been demonstrated that can produce phytohormones, such as auxins, cytokinins, gibberellins and ethylene, etc (Ahemad and Kibret, 2014). Particularly, auxin has been regarded as critical hormone for PGPR to promote plant growth. In plants, auxin implicates in several stages of plant growth and development, including cell elongation, cell differentiation, root development, and so on (Davies, 2010). Indole-3-acetic acid (IAA) is a most common auxin produced by PGPR. It is demonstrated that the IAA producing PGPR can increase plant growth (Ahemad and Kibret, 2014). Applying such PGPR in rhizosphere increases the endogenous IAA concentration of plants, therefore, it shows beneficial effect on plant growth (Liu *et al.*, 2016b). Bacterial IAA mainly affects the development of root system, such as increasing root size and lateral root number. All these changes result in an enhancement in its ability to uptake the nutrient from soil, therefor, improving growth capacity of plants. (Lee *et al.*, 2011; Liu *et al.*, 2016b; Ramos Solano *et al.*, 2008). IAA biosynthesis in bacteria via tryptophan dependent and independent pathways (Figure 1-2). Starting with tryptophan which is a major precursor, at least three tryptophan dependent pathways are identified (Spaepen *et al.*, 2007). First, IAA synthesized via indole-3-acetic aldehyde. The conversion of tryptophan into indole-3-acetic aldehyde via indole-3-pyruvic acid or an alternative pathway in which tryptamine, finally conversed to IAA. This pathway is found in bacteria like *Pseudomonas* (Patten and Glick, 2002). Second, IAA biosynthesis via indole-3-acetamide which are found in various bacteria such as, *Agrobacterium tumefaciens*, *Rhizobium* and *Bradyrhizobium* (Morris, 1995; Sekine *et al.*, 1989; Theunis *et al.*, 2004). Third, IAA biosynthesis via indole-3-acetonitrile is shown in *A. tumefaciens* and *Rhizobium* spp (Kobayashi *et al.*, 1995).. Although some intermediates may be different, these pathways share high similarity to those found in

doi:10.6342/NTU202003422

plants (Spaepen *et al.*, 2007). In tryptophan independent pathways, IAA is synthesized from indole-3-glycerolphosphate or indole. However, no critical enzyme related to this pathway has been identified yet. *Azospirillum brasilense* was reported to synthesize IAA through this pathway (Prinsen *et al.*, 1993).

Ethylene is another important plant hormone involved in stress response, such as salinity, drought and pathogenicity (Abeles *et al.*, 1992). It is well known that high concentration of ethylene has detrimental effect on plants, such as senescence, wilting and so on (Abeles *et al.*, 1992). PGPR have been reported that can deteriorate the biosynthesis of ethylene due to the production of 1-aminocyclopropane-1-carboxylate (ACC) deaminase (Adesemoye and Kloepper, 2009; Ahemad and Kibret, 2014). PGPR take up ACC, i.e the precursor of ethylene, and convert it into 2-oxobutanoate and NH_3 (Arshad *et al.*, 2007). Accordingly, ACC deaminase producing PGPR may protect plants from the detrimental effects of ethylene induced by various stresses (Arshad *et al.*, 2007).

Phototrophic bacteria

Phototrophic bacteria, including cyanobacteria, green bacteria and purple bacteria, convert light energy to chemical energy by photosynthesis (Pfennig, 1977). Due to the ability of photosynthesis, these bacteria have a capability to survive suing photoautotrophic and photoheterotrophic, whereas most of bacteria can only support their life by chemoheterotrophic (Van Niel, 1954). For cyanobacteria, it is similar to plants that aerobic photosynthesis is generally used. In contrast, most of phototroph bacteria such as green bacteria and purple bacteria are different from plants. They don't use water, but H_2S and H_2 as the electron donors in photosynthesis, and therefore no oxygen is produced in the reaction. Thus, this kind of photosynthesis also called as anaerobic photosynthesis and its efficiency is lower than that of aerobic photosynthesis

doi:10.6342/NTU202003422

(Allen, 2005; Van Niel, 1954).

Purple bacteria show diversity of cell colors (red, orange and yellow) due to the various photosynthetic pigment such as bacteriochlorophyll a, bacteriochlorophyll b or carotenoid and etc. The purple bacteria that use H_2S as reductant called purple sulfur bacteria, and the bacteria that perform photosynthesis without using H_2S as electron donor, that are categorized as purple non-sulfur bacteria (Madigan and Jung, 2009). In purple bacteria, the light reaction is performed by two membrane protein complex, light harvesting complex 1 and 2 (LH1 and LH2). LH2 is responsibility for collecting incoming light then the energy is transferred to LH1 where the mainly photosynthetic reaction center locates (Scheuring *et al.*, 2006).

Purple non-sulfur phototrophic bacteria

Purple non-sulfur phototrophic bacteria (PNSB) is one of the major groups of phototrophic microorganisms, which has a metabolic diversity allows them to growing in a broad range of environments (Madigan and Jung, 2009). According to their morphology, PSNB can be divided as *Rhodospirillum*, *Rhodobacter*, *Rhodopila*, *Rhodomicrobium*, *Rhodopseudomonas* and *Rhocyclus* (Madigan et al., 2006). Compare to purple sulfur phototropic bacteria, mainly PNSB can't use H_2S as electron donor but these strains still can survive under the lower concentration of H_2S. PNSB can grow under the dark by using common organic compounds or hydrogen as reductant to perform the anaerobic respiration (Brock *et al.*, 2003). Most of PNSB stains can use acetic acid as energy source, however, the metabolic pathway was quite different. The major metabolism of acetic acid was acetyl-CoA production (Laguna *et al.*, 2011). Mostly, the assimilation of acetic acid in PNSB was performed by TCA cycle and the key enzymes were isocitrate lyase and malate synthase (Albers and Gottschalk, 1976). Nevertheless, some PNSB such as *Rhodospirillumrubrum*, which lack isocitratelyase,

doi:10.6342/NTU202003422

so they conserve acetic acid as pyruvate by carboxylation, further conserved to oxaloacetate (Albers and Gottschalk, 1976). Moreover, the assimilation of acetic acid in *R. gelatinosus* is carried out via serine-hydroxypyruvate pathway (Albers and Gottschalk, 1976). It also found that PNSB can use NO^{3-}, NO^{2-} and N^2O as electron donor in electron transport chain of cellular respiration (Griffin *et al.*, 2007). All of PNSB have the ability to fix nitrogen from air. Most of PNSB can use NH_4^+, N_2 and serval organic nitrogen as nitrogen sources. In contrast, few of PNSB utilize NO_3^- as nitrogen source. However, existence of NH_4 and glutamic acid will inhibit the reaction of NO_3^- assimilation in PNSB (Imhoff and Trüper, 1992). When PNSB use N_2 and glutamic acid as nitrogen sources, the PNSB can utilize various carbon to generate CO_2 and H_2 (Imhoff and Trüper, 1992). Exactly, the hydrogen gas production of PNSB is controlled by hydrogenase and nitrogenase (Kim *et al.*, 1980). Some studies suggest that PNSB fix carbon through C4 pathway. In this pathway, CO_2 and pyruvate or phosphoenolpyruvate (PEP) will be conserved to oxaloacetate (OAA) by pyruvate, orthophosphate dikinase (PPDK), then enter to TCA cycle. Moreover, it was found that PNSB can use reduce inorganic or organic substrate, donating electron to generate NADPH by reverse electron transport (Yoch, 1978). Therefore, it was considered that electron donor is a critical factor to determine the metabolism model in PNSB (Yoch, 1978).

Application of purple non-sulfur photosynthetic bacteria

Polyhydroxybutyrate (PHB) is a polyhydroxyalkanoate (PHA) that is a form of energy storage molecule and produced via fermentation (Jendrossek and Pfeiffer, 2014). Most of PNSB have ability to produce or metabolize PHAs. On the other hand, PNSB can also accumulate PHAs and store them in intracellular (Doudoroff and Stanier, 1959; Merrick and Doudoroff, 1961). It has been reported that when *R. sphaeroides* used

doi:10.6342/NTU202003422

acetate as single carbon source or combined with malate, pyruvate, glucose or propionate in fermentation, the PHAs accumulation can approximate to 50% cell dry weight (Brandl *et al.*, 1991). Although the PHA production by PNSB is not high, using PNSB to produce PHA is still a potential strategy. Because PHA can be produced from waste materials, such as waste water of sugar refineries and palm oil waste (Ali Hassan *et al.*, 1996; Yigit *et al.*, 1999).

Many studies have shown that PNSB can be applied for waste water treatment. For example, combining the PNSB fermentation tank, aeration tank and algae culture tank in wastewater treatment program, the BOD concentration could be reduced from 1000 mg/L to 50 mg/L (Kobayash.M and Nakanish.H, 1971). In antibiotic production wastewater, lipid concentration was decreased from 1500 mg/L to 180 mg/L (about 90% removal), by *R. capsulata* and algae mixture treatment in aerobic condition (Sawada and Rogers, 1977). Harwood and Gibson found that *R. palustris* strains can metabolize diverse aromatic compounds under anaerobic and aerobic conditions (Harwood and Gibson, 1988). on the other hand, phototrophic bacterium *R. capsulate* which produces an antiviral substance that removed 97.4% of coliphage during the purification process of pigpen wastewater (Hirotani *et al.*, 1990). Recently, it was reported that PNSB can used in the application of microbial fuel cells (MFC) for electron generation (Xing *et al.*, 2008).

It has also been reported that suppling PBSB into animal feed can decrease the levels of serum cholesterol. *R. palustris* showed the potential to reduce the serum cholesterol in rats fed with high cholesterol diet (Lee *et al.*, 1990). Similar results also observed in the case that feeding diet supplemented with 2% *R. capsulatus* or 2% *R. palustris* significantly reduce the serum cholesterol levels in rats (Tsujii *et al.*, 2007). Feeding 0.04% *R. capsulatus* dramatically removed the levels of cholesterol and triglyceride from serum, liver and muscle in Broiler Meat, while the high-density

doi:10.6342/NTU202003422

Lipoprotein cholesterol cholesterol (HDL-C) in serum and unsaturated fatty acid such as oleic acid, linoeic acid, linolenic aicd in muscle were significantly increased (Salma *et al.*, 2007).

Rhodopseudomonas palustris

Rhodopseudomonas palustris, an α-poteobacteria species is one of purple nonsulfur photosynthetic bacteria, which belong to α-Proteobacteria and is widely distributed in environment (Imhoff, 2006). Because *R. palustris* has extraordinary metabolic versatility, so it can inhabit in a variety of conditions (Larimer *et al.*, 2004). These exceptional abilities of metabolism including four major modes (Figure 1-3): photoautotrophic (using light as energy sources and carbon dioxide as carbon sources), photoheterotrophic (using light as energy sources and organic compounds as carbon sources), chemoheterotrophic (using organic compounds as carbon and energy sources) and chemoautotrophic (using inorganic compounds as energy source and carbon dioxide as carbon source). Moreover, *R. palustris* is well known to inhabit in microaerobic environment with light and also grows aerobically in dark. According to these characteristics, *R. palustris* has been broadly used in industry for bioremediation, sewage treatment, and removal of phytotoxic compounds (e.g., hydrogen sulfide)(Idi *et al.*, 2015) . In addition, this bacterium can convert complex organic compounds into biomass and bioenergies, no matter the substrates are plant-derived, pollutants or aromatic compounds (Larimer *et al.*, 2004; Liu *et al.*, 2015; Oda *et al.*, 2003; Shi *et al.*, 2014; Zhang *et al.*, 2015a). On the other hand, *R. palustris* was also applied as biofertilizer to improve crop yield (Kornochalert *et al.*, 2014; Wong *et al.*, 2014).

Several studies reported that *R. palustris* can utilize citric acid, aromatic organic compounds, such benzoate, 3-hydroxybenzoate and 1,3,5-trihydozybenzene as carbon sources (Dutton and Evans, 1969). Moreover, *R. palustris* also can use acrylamide as

doi:10.6342/NTU202003422

carbon source. In contrast, it was found *Rhodospirillum rubrum* strain UR 1 and *Rhodobacter capsulatus* strain B10 can catabolize acrylamide. This result indicated that acrylamide metabolism is not a ubiquitous characteristics of PNSB (Wampler and Ensign, 2005). So far, it has suggested that *R. palustris* can catabolize various carbon sources, such as acetate, arabinose, ribose, xylose, glucose, fructose, mannose, sorbose, turanose, lyxose, arabitol, tagatose, benzoate, butyrate, caproate, caprylate, ethanol, formate, fumatate, glycerol, glycoate, lactate, malate, malonate, propionate, pyruvate, succmate, valerate, casammo acids and acrylamide, taurine, potassium 5-ketogluconate (Imhoff and Trüper, 1992; Novak *et al.*, 2004; Wampler and Ensign, 2005; Wong *et al.*, 2014).

R. palustris PS3

R. palustris PS3 was isolated from Taiwanese paddy soil (Wong *et al.*, 2014). It forms rod-shaped cells with approximately 1.0 μm in length and presents round, convex and glossy colony on the nutrient agar plate (Figure 1-4). The colonies are pearl-white under aerobic condition and turn to blood red when grow under anaerobic with illumination (Figure 1-4 b). It has been demonstrated that PS3 can utilize serval carbon sources such as glycerol, D-glucose and D-fructose, and fix atmospheric nitrogen into ammonia (Wong *et al.*, 2014). PS3 possesses the PGP traits like production of IAA and synthesis of phosphatase, etc (Wong *et al.*, 2014). PS3 not only showed beneficial effects on plant growth, but also increased the agronomic nitrogen use efficiency of plants (Wong *et al.*, 2014). Moreover, PS3 can reduce the nitrate contents of host plant, and improve both nitrogen and carbon metabolic efficiencies of plant in hydroponic system (Hsu *et al.*, 2015; Shen, 2016). It has already been proved that neither medium nor dead PS3 cells was able to promote plant growth (Wong *et al.*, 2014), and both viability (i.e., culturability) and vitality (i.e., metabolic activity) of this bacterium are

doi:10.6342/NTU202003422

crucial for the plant beneficial traits (Lee *et al.*, 2016).

Specific aims

According to the traits mentioned above suggest that PS3 can serve as a potential PGPR for agricultural applications. However, some issues remain to be elucidated: (1) the underlying mechanisms of PS3 to promote plant growth still unknown, and (2) the scale-up fermentation is required for commercialization of *R. palustris* PS3. Therefore, I would like to elucidate these two themes in this study. The outlines of the contents are as follows:

Chapter II: Whole-Genome Sequencing and Comparative Analysis of Two Plant-Associated Strains of *Rhodopseudomonas palustris* (PS3 and YSC3)

According to the 16S rDNA analysis, the phylogenetic tree indicated that PS3 has a highly close relationship with other *R. palustris* isolates. However, only PS3 showed significantly plant growth promoting effects (Wong *et al.*, 2014). To elucidate the underlying mechanisms of PS3 for promoting plant growth, I have performed the whole genome sequencing of PS3 to understand the genetic background and identify the potential genes associated with plant growth promoting by high-throughput DNA sequencing in the first part of my study. Hybrid *de novo* assembly was carried out by combination of shotgun (Illumina) and single molecule real-time (PacBio) reads. In addition, I compared the genome of PS3 with inefficient strain YSC3 strain to identify unique gene from PS3 strain involving in plant growth promoting functions. Moreover, I focused on genes involved in carbon and nitrogen metabolism as well as plant growth promoting genes. Through this study, I addressed the unique features of the PS3, which were attributed to its beneficial traits.

doi:10.6342/NTU202003422

Chapter III: Development of A Low-Cost Culture Medium For Rapid Production of Plant Growth-Promoting *Rhodopseudomonas palustris* PS3 Strain

To scale-up the fermentation of *R. palustris* PS3 for its commercialization, I optimized the culture conditions of *R. palustris* PS3 by response surface methodology. Firstly, “one-factor-at-a-time” technique was applied to screen the nitrogen and carbon source. Subsequently, the effects of selective nitrogen and carbon source as well as pH values, temperatures and dissolved oxygen were respectively evaluated for PS3 growth by fractional factorial design, and the suitable range of individual factor was estimated by steepest ascent path. Finally, according to the above data, I constructed a response surface model by central composite design. The optimization of fermentation conditions was analyzed by RSM. Besides, I also verified the effect of newly developed PS3 fermentation broth on the plat growth promotion.

doi:10.6342/NTU202003422

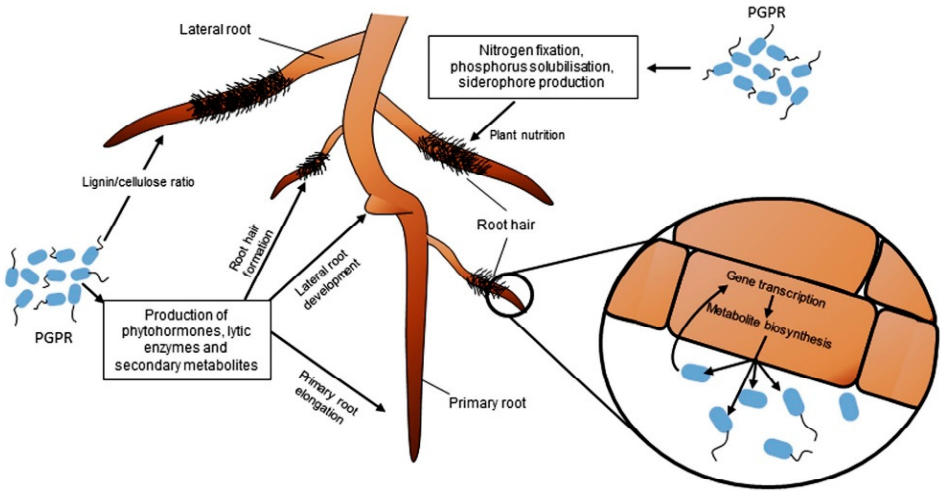

Figure 1-1. Deduced modes of action of PGPR. PGPR can promote plant growth through various mechanisms, such as production of pytohormones and secondary metabolites. These factors enhance the development of roots, especial in lateral roots and root hairs. PGPR also affect nutrition availability through nitrogen fixation or phosphorus solubilization. Besides they are also able to mediate the physiology of plants by regulating gene expression in plant cells (Adapted from (Vacheron *et al.*, 2013)).

doi:10.6342/NTU202003422

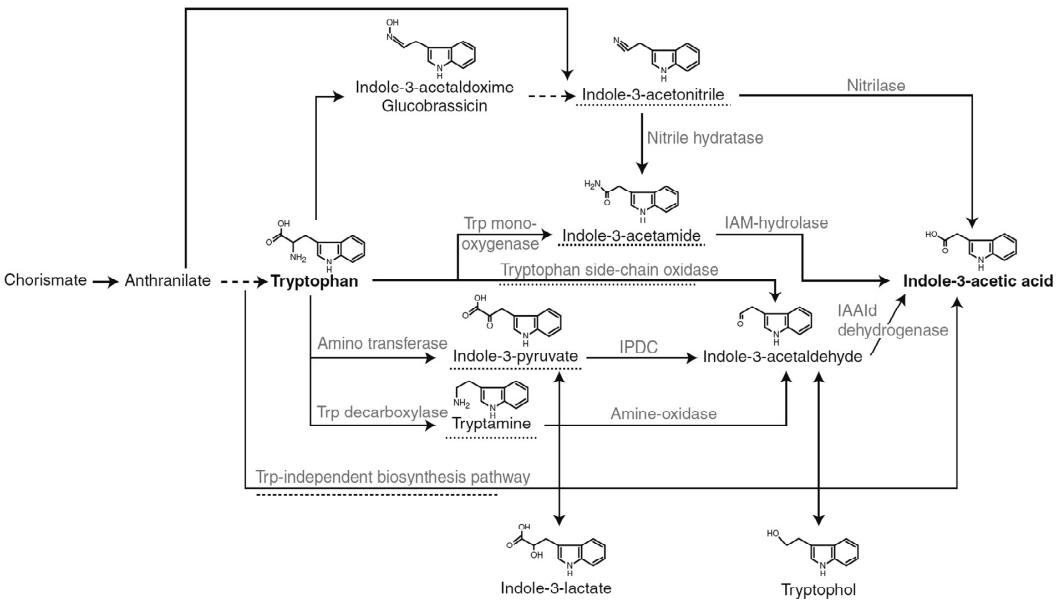

Figure 1-2. Overview of the biosynthetic pathway of IAA in bacteria. The intermediate referring to the name of the pathway or the pathway itself is underlined with a dashed line. IAAld, indole-3-acetaldehyde; IAM, indole-3-acetamide; IPDC, indole-3-pyruvate decarboxylase; Trp, tryptophan (Adapted from Spaepen *et al.* (2007)).

doi:10.6342/NTU202003422

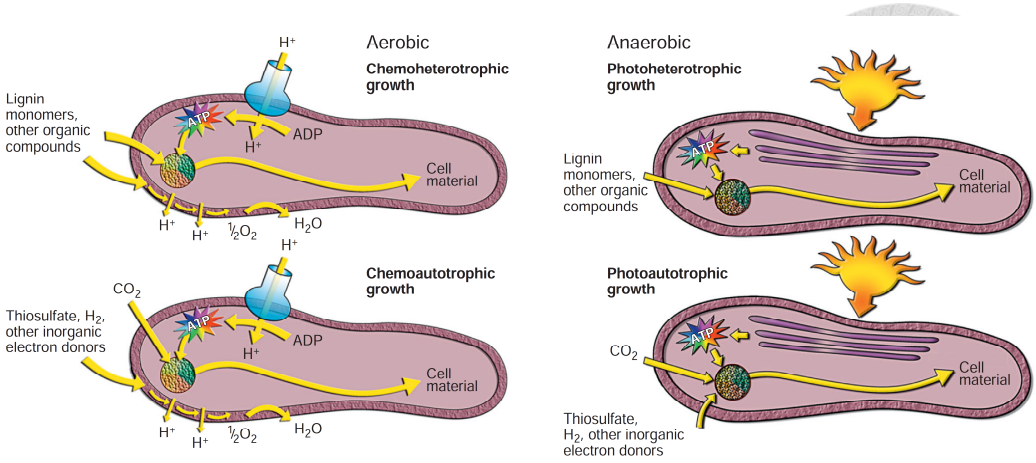

Figure 1-3. The four types of metabolism of *R. palustris* that support its growth. The multicolored circle in each cell represents the enzymatic reactions of central metabolism (Adapted from Larimer *et al.* (2004)).

doi:10.6342/NTU202003422

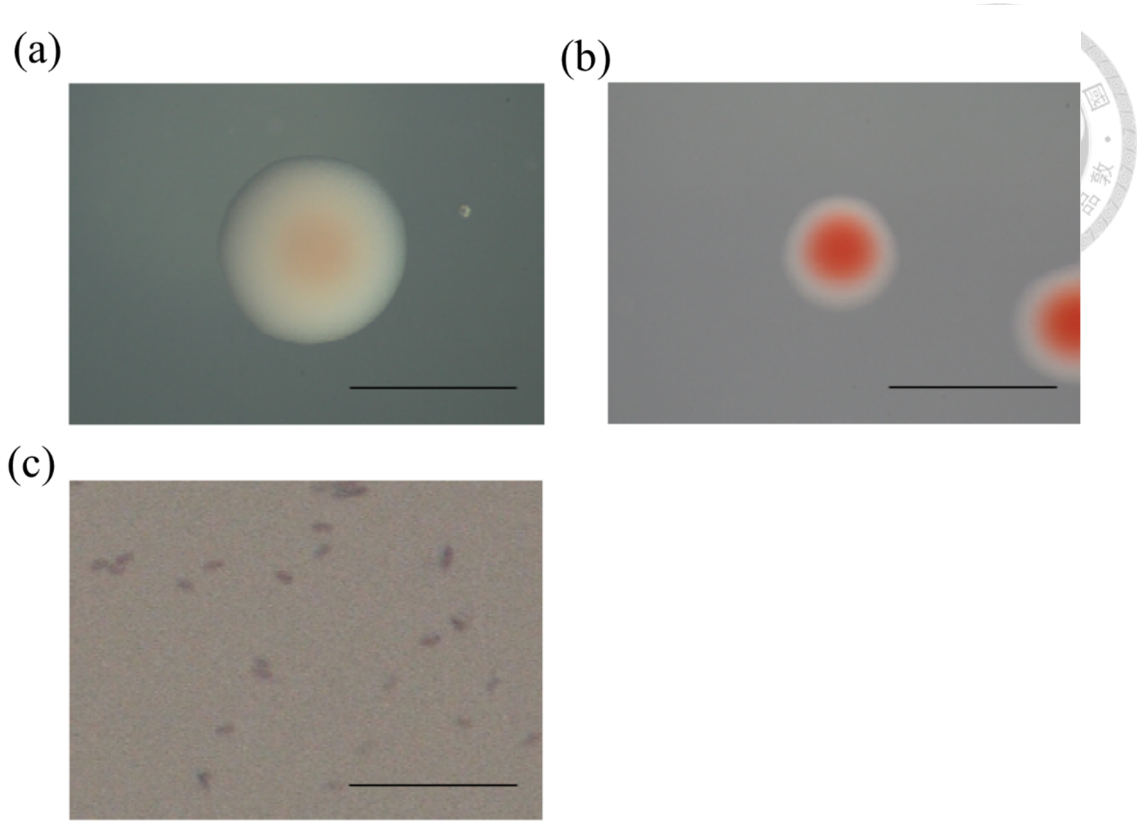

Figure 1-4. Morphology characteristics of *R. palustris* strain PS3. (a) colonies grown under aerobic condition for 4 days; (b) colonies developed under anaerobic condition for 7 days; (c) vegetative cells incubated aerobically. Scales bars equal 0.5 cm in (a) and (b), 10μm in (c). This figure was adapted from (Wong *et al.*, 2014).

doi:10.6342/NTU202003422

Table 1-1 PGPR as potential inoculants for agricultural uses. Table was made by Lo and Liu (Lo and Liu, 2020).

Strains	Crop	Mode of action	Beneficial effect	References
Achromobacter piechaudii	Tomato, Pepper	ACC deaminase	Reduced ethylene production and increased plant growth	(Mayak *et al.*, 2004)
Azospirillum brasilense	Wheat seedlings	-	Enhanced photosynthetic pigment production	(Bashan *et al.*, 2006)
Alcaligenes piechaudii	Lettuce	IAA production	Growth promotion	(Barazani and Friedman, 1999)
Azospirillum lipoferum	Maize	Gibberellins production	Increased ABA levels and alleviated drought stress	(Cohen *et al.*, 2009)
Azotobacter sp.	Maize	Nitrogen fixation	Increased nitrogen and phosphorus content of plant component	(Pandey *et al.*, 1998)
Azotobacter chroococcum	Wheat	Nitrogen fixation	Increased nitrogen nutrition in soil	(Mrkovacki and Milic, 2001)
Azospirillum sp.		IAA production, nitrogen fixation	Enhanced root growth, lateral roots formation and increasing the total N accumulation	(Arzanesh *et al.*, 2011; Boddey *et al.*, 1986)
	Maize	Nitrogen fixation	Increasing the total N accumulation	(Garcia de Salamone *et al.*, 1996)
	Rice	Nitrogen fixation	Increase in total N accumulation	(Malik *et al.*, 1997)
	Sugarcane	-	Production of IAA	(Moutia *et al.*, 2010)
Bacillus amyloliquefaciens (*velezensis*)	*Triticum aestivum*	IAA production	Increased root production	(Talboys *et al.*, 2014)

doi:10.6342/NTU202003422

	Cucumber	IAA production	Plant growth promotion	(Shao *et al.*, 2014)
	Tomato	-	Inhibited infection of *Tomato mottle virus*	(Murphy *et al.*, 2000)
	Wheat		Improvement in homeostatic mechanisms	(Kasim *et al.*, 2013)
	Canola	Production of lipopeptide antibiotics	Produced the iturin A, bacillomycin D and surfactin to suppress growth of *Leptosphaeria maculans* causing Blackleg disease	(Ramarathnam *et al.*, 2011)
	Capsicum	Bacteriocins production	Bacterial antagonism to *Ralstonia solanacearum*	(Hu *et al.*, 2010)s
Bacillus thuringiensis	Wheat	ACC deaminase	Reduced volatile emissions and increased photosynthesis	(Timmusk *et al.*, 2014)
Bacillus subtilis	*Platycladus orientalis*	Cytokinin production	Increased ABA levels in shoots and enhanced the stomatal conductance	(Liu *et al.*, 2013b)
	Soybean	IAA production	Increased production of root hairs	(Araújo *et al.*, 2005)
	Pepper	Production of antibiotics	Suppression of growth of *Myzus persicae*	(Kokalis–Burelle *et al.*, 2002)
	Tomato	Induce systemic resistance	Enhanced activities of chitinases and β-1,3-glucanase to inhibited growth of *Fusarium oxysporum* f. sp. *lycopersici* causing Tomato wilt disease	(Shanmugam and Kanoujia, 2011)
		Surfactin production	Surfactin production induced the activation of lipxygenase to against *Botrytis cinerea* growth	(Ongena *et al.*, 2007)
Bacillus pumilus	*Ocimum sanctum*	IAA production	Plant growth promotion	(Murugappan *et al.*, 2013)

doi:10.6342/NTU202003422

Bradyrhizobium sp.	Radish	IAA production	Increased the dry matter yield of radish	(Antoun *et al.*, 1998)
Burkholderia sp.	Rice	Nitrogen fixation	Increase in N content in plant	(Divan Baldani *et al.*, 2000)
Enterobacter cloacae	Rapeseed (*Brassica. napus*)	ACC deaminase	Increases in root and shoot lengths	(Saleh and Glick, 2001)
Methylobacterium fujisawaense	Canola (*Brassica campestris*)	ACC deaminase	Promoted root elongation	(Madhaiyan *et al.*, 2006)
Pseudomonas fluorescens	Pisum sativum	ACC deaminase	Induced longer roots and uptake of water	(Zahir *et al.*, 2008)
	Soybean	Cytokinin	Plant growth regulation	(García de Salamone *et al.*, 2001)
	Wheat	ACC deaminase	Increased NPK uptake and inhibited ethylene production	(Nadeem *et al.*, 2010; Shaharoona *et al.*, 2008)
	Tobacco	Induce systemic resistance	Induced salicylic acid- dependent activation of PR-1 gene against *Pseudomonas syringae* pv. *tabaci*	(Park and Kloepper, 2000)
	Green gram (*Vigna radiata*)	-	Regulated the catalase and peroxidase	(Saravanakumar *et al.*, 2011)
	Rice	Induction of systemic resistance	Against *Xanthomonas oryzae* pv.*Oryzae* in rice leaves	(Vidhyasekaran *et al.*, 2001)
Pseudomonas putida	Vigna radiata L	ACC deaminase	Inhibited ethylene production	(Mayak *et al.*, 1999)

doi:10.6342/NTU202003422

	Rice	IAA production and phosphate solubilization	Increased plant height and root length of rice	(Ashrafuzzaman *et al.*, 2009)
	Soybean	Gibberellins production	Plant growth promotion	(Kang *et al.*, 2014)
	Chickpea	Phosphate solubilization, siderophore production, and IAA production	Improved the growth and the saline tolerance of plant	(Patel *et al.*, 2012)
	Cotton	-	Regulated the ion uptake and improved production of endogenous indole acetic acid (IAA) content and reduced abscisic acid (ABA) content	(Yao *et al.*, 2010)
Rhizobium leguminosarum	Rape and lettuce	Cytokinin production	Plant growth promotion with possible involvement of the plant growth regulators indole-3-acetic acid and cytokinin	(Noel *et al.*, 1996)
Rhizobium tropici	Bean (*Phaseolus vulgaris L.*)	-	Increased nodulation as well as nitrogen fixation	(Figueiredo *et al.*, 2008)
Rhodobacter sphaeroides	Tomato	-	Enhanced quality of tomato fruit and increased ascorbic acid content	(Kondo *et al.*, 2010)
Rhodopseudomonas	Chinese	-	Plant growth promotion, increased the nitrogen use	(Hsu *et al.*, 2015;

doi:10.6342/NTU202003422

palustris	cabbage (*Brassica rapa chinensis*)		efficiency and reduced the nitrate content in plant	Wong *et al.*, 2014)
	Tobacco	Indole-3-acetic acid and 5-aminolevulinic acid production	Promote growth and germination	(Su *et al.*, 2017)
		Induces systemic resistance	Induces systemic resistance of plant to against tobacco mosaic virus	(Su *et al.*, 2017)
	Pakchoi (Brassica rapassp. Chinensis)	-	Enhanced photosynthesis and crop yield	(Xu *et al.*, 2016)

doi:10.6342/NTU202003422

CHAPTER II

Whole-Genome Sequencing and Comparative Analysis of Two Plant-Associated Strains of *Rhodopseudomonas palustris* (PS3 and YSC3)

The content in Chapter II has been published in *Scientific Reports* as shown below. This first author publication and its quality full-filled the Ph.D. thesis examination application requirements of Institution of Biotechnology, National Taiwan University. This desertion or any part of it has not been submitted for any degree, diploma, or other qualification at any other university. It is the result of my own work except where mentioned in the text.

Lo, K.J., S.S. Lin, C.W. Lu, C.H. Kuo and C.T. Liu. 2018. Whole-genome sequencing and comparative analysis of two plant-associated strains of *Rhodopseudomonas palustris* (PS3 and YSC3). Sci. Rep. 8(1): 12769. doi: 10.1038/s41598-018-31128-8

Author Contributions:

K.J. Lo carried out the experiment, experimental data analysis, bioinformatic data analysis and manuscript writing. C.W. Lu performed the bioinformatics analysis for the genome assembly. S.S. Lin provided the bioinformatic platform for data analysis. C.H. Kuo performed the bioinformatics for gene prediction and annotation as well as manuscript writing. C.T. Liu is the corresponding authors in charge of the project design and manuscript writing.

doi:10.6342/NTU202003422

Summary

Rhodopseudomonas palustris strains PS3 and YSC3 belong to purple non-sulfur phototrophic bacteria that were isolated from Taiwanese paddy soils. Strain PS3 showed beneficial effects on plant growth and enhances the agronomic nitrogen using efficiency of host plant. However, strain YSC3 has no significant effect on plant growth. According to whole genomic analyses, PS3 and YSC3 strain showed similar genomic structures, individually contains a one circular chromosome with 5,269,926 or 5,371,816 bp in size, with 4,799 or 4,907 protein-coding genes, respectively. In this study, a large class of genes associated with plant-growth promotion, such as nitrogen fixation-, IAA synthesis-, phosphate solubilization and ACC deamination-related genes, were annotated. The growth rate, biofilm formation, and the relative expression levels of several chemotaxis-associated genes were significantly higher for PS3 than for YSC3 upon treatment with root exudates. These results suggested that PS3 has a better response to the host plants, which may contribute to the successful interactions between PS3 and plant hosts. In addition, these findings indicate that the existence of gene clusters associated with plant growth promotion is required but not sufficient for bacteria to exhibit the ability of plant-growth promotion.

Introduction

In 1978, a concept of plant growth-promoting rhizobacteria (PGPR) was proposed by Kloepper and Schroth (Kloepper and Schroth, 1978). It refers as diverse soil bacteria colonize in rhizosphere, and provide beneficial effects on plant growth via various mechanisms (Kloepper and Schroth, 1978). The promotional activity of PGPRs including increasing nutrient availability (e.g., nitrogen fixation), nutrient solubilization (e.g., phosphate solubilization) as well as production of phytohormones (e.g., indole acetic acid (IAA), 2,3-butanediol, and cytokinins) (Ahemad and Kibret,

doi:10.6342/NTU202003422

2014; Goswami *et al.*, 2016; Lugtenberg and Kamilova, 2009). Moreover, PGPR can strengthen plant tolerance against environmental stress by metabolizing 1-aminocyclopropane-1-carboxylic acid (ACC), a precursor of stress hormone - ethylene (Ahemad and Kibret, 2014; Goswami *et al.*, 2016; Lugtenberg and Kamilova, 2009). In addition, PGPR can also protect plants form pathogen infection by secreting antibiotics or activating induced systemic resistances (Beneduzi *et al.*, 2012). Due to these properties of PGPR, so far, these bacteria are widely used as biofertilizers or biocontrol agents in agriculture (Lugtenberg and Kamilova, 2009). So far, several micrograms were identified as PGPR, such as *Azospirillum humicireducens* (Yu *et al.*, 2018), *Bacillus amyloliquefaciens* (Zhang *et al.*, 2015b), *Bacillus velezensis* (Chen *et al.*, 2007), *Bradyrhizobium japonicum* (Kaneko *et al.*, 2002), *Pseudomonas fluorescens* (Loper *et al.*, 2007), *Pseudomonas putida* (Ponraj *et al.*, 2012), *Rhizobium leguminosarum* (Young *et al.*, 2006), etc. These microbes were regarded as PGPR not only verified by planta experiments, but also speculated by their functional genes in genome.

Rhodopseudomonas palustris is a phototrophic purple non-sulfur bacterium (PNSB), which has the innate and extraordinary metabolic versatility. It can sustain itself by one of the four modes of metabolism, including photoautotrophic, photoheterotrophic, chemoautotrophic and chemoheterotrophic states (Larimer *et al.*, 2004). Due to this diverse metabolic property, *R. palustris* is widely distributed in nature, including river, pond water, sediments, wetlands, and paddy fields (Hiraishi and Kitamura, 1984; Oda *et al.*, 2002).

This bacterium has been widely used in industrial applications for bioremediation and sewage treatment and for the removal of phytotoxic compounds (Austin *et al.*, 2015; Idi *et al.*, 2015). In addition, this bacterium can convert complex organic compounds into biomass and bioenergy using substrates that are plant-derived

doi:10.6342/NTU202003422

compounds, pollutants, or aromatic compounds (Larimer *et al.*, 2004; Liu *et al.*, 2015; Oda *et al.*, 2003; Shi *et al.*, 2014; Zhang *et al.*, 2015a). Some studies have indicated that *R. palustris* can also be used as a biofertilizer to improve crop yields (Kornochalert *et al.*, 2014; Nunkaew *et al.*, 2014; Wong *et al.*, 2014). In our previous study, we isolated the *R. palustris* strain PS3 (abbreviated as PS3) from Taiwanese rice paddy soil (Wong *et al.*, 2014). Strain PS3 can have beneficial effects on plant growth and can enhance the utilization efficiency of fertilizers in either soil or hydroponic cultivation system (Hsu *et al.*, 2015; Wong *et al.*, 2014). Although these studies showed that strain PS3 is a promising PGPR, genomic information and the underlying molecular mechanisms for plant growth promotion (PGP) by PS3 are yet to be ascertained.

Systematic analysis of whole-genome sequences is a powerful strategy to identify either causal genes that contribute to plant growth-promoting activities or potential PGPR candidates (Gupta *et al.*, 2014; Liu *et al.*, 2016a; Magno-Perez-Bryan *et al.*, 2015; Shen *et al.*, 2013; Taghavi *et al.*, 2010). Scientists can obtain more genomic information and deduce the underlying promoting mechanisms of PGPR from whole genome sequence. As shown in Table 2-2, I listed up the whole genomic information of several PGPR strains. Furthermore, the genes associated with plant growth-promoting functions were summarized in Table 2-3.

Next-generation sequencing (NGS) technologies provide a quick and convenient approach to resolve the whole-genome sequence and investigate the transcriptomes of PGPR. The NGS technologies such as Roche/454, Illumina are widely used to study the genes of eukaryotes and prokaryotes (MacLean *et al.*, 2009). These methods used short-read (~150-300 bp) sequencing and containing some advantages, such as cost-effective, accurate, and diversity of analysis tools (Heather and Chain, 2016). However, there were some limitations of short-read sequencing, especially in highly repetitive and complex genome, including high guanine-cytosine (GC) contents, or multiple

doi:10.6342/NTU202003422

homologous elements in sequences (Nagarajan and Pop, 2013; Treangen and Salzberg, 2011). It may result in sequencing error and lose certain genomic regions (Ashley, 2016; Delaneau *et al.*, 2013; Mavromatis *et al.*, 2012). Although using the long-read sequencing technologies such as Oxford Nanopore Technologies (ONT)(Deamer *et al.*, 2016) or single-molecule sequencing technology (SMRT) Pacific Biosciences (PacBio) sequencing platforms (Levene *et al.*, 2003; Quail *et al.*, 2012) can resolve the above issues, these technologies have high relative error in sequencing with about 11-14% (Pollard *et al.*, 2018). Therefore, it is hard to assemble the complete genomic sequences with high-quality by individual sequencing technology. To address these issues, short-reads and long-reads hybrid assembly techniques were proposed to improve the genome assembly (Utturkar *et al.*, 2014). In this strategy, long reads provide the information for genomic structure and short reads improve the detailed assembly at sequencing, and can be used to correct the errors from long reads. Therefore, combination of short-read and long-read sequencing datasets appear a promising approach to completely resolve the genome assemblies with accuracy (Berbers *et al.*, 2020; De Maio *et al.*, 2019; Risse *et al.*, 2015; Sovic *et al.*, 2016; Wick *et al.*, 2017a; b).

Although few studies conducted the whole-genome sequencing of *R. palustris* strains, such as CGA009, HaA2, BisB18, and TIE (Larimer *et al.*, 2004; Oda *et al.*, 2008; Oda *et al.*, 2005), none of these strains are plant-associated. Here I focus on the elite strain *R. palustris* PS3, which was isolated from Taiwanese paddy soil and displayed plant growth-promoting (Hsu *et al.*, 2015; Wong *et al.*, 2014). In order to elucidate the potential modes of action via which *R. palustris PS3* has beneficial effects on plants, I compared the genomic characterizations of two plant-associated *R. palustris* strains- PS3 and YSC3. They are the effective PGPR strain and the ineffective strain, respectively (Wong *et al.*, 2014). For whole-genomic sequencing, I applied two NGS techniques to obtain the sequencing reads, then performed the hybrid *de novo* assembly.

doi:10.6342/NTU202003422

Identification of genes associated with plant growth-promotion and genomic comparative analyses are very important to understand the underlying mechanisms of PS3. Moreover, I also compared the genomic compositions of these two strains with the genomic representative strain for this species, *R. palustris* CGA009. Finally, I focused on genes involved in carbohydrate, nitrogen metabolism, phosphate solubilization, phytohormone production, biofilm formation, chemotaxis, and plant colonization. The flow chart of the whole genomic analysis in this chapter was described in Figure 2-1.

Materials and methods

Preparation of phototrophic bacterial inoculant

The *R. palustris* strains PS3 and YSC3 are PNSB and were both isolated from Taiwanese paddy soils (Wong *et al.*, 2014). PS3 is an effective PGPR, whereas YSC3 is not. For bacterial inoculant preparation, a single colony was picked and inoculated into 3 mL of PNSB broth as described previously (Wong *et al.*, 2014). The culture was then incubated for 24 h at 37°C (200 rpm). Subsequently, 2.5 mL of these cultures were transferred into 250-mL Erlenmeyer flasks containing 50 mL of fresh PNSB broth. The cultures were incubated under the conditions described above, and the log-phase bacterial cells were harvested for genomic DNA extraction.

Genomic DNA preparation

A 1-mL suspension of the log-phase bacterial culture was collected in a 2.0-mL Eppendorf tube and centrifuged at 3,000 × g at 4°C. Subsequently, the supernatant was removed, and the Eppendorf containing the cell pellet was snap-frozen in liquid nitrogen. The cell pellet was homogenized by adding sterile steel beads and rapidly shaking the microcentrifuge tubes back and forth at 9,000 rpm for 1 min in a SH-100 homogenizer (Kurabo, Japan). The homogenization process was repeated three times.

doi:10.6342/NTU202003422

The Gentra® Puregene® Kit (QIAGEN) was used for genomic DNA purification according to the manufacturer's protocol. The quantity and quality of the total DNA was assessed using UV spectrophotometry (Nanodrop ND-1000, J & H technology Co., Ltd.), and the OD260/280 value of the DNA was higher than 1.80. Agarose gel electrophoresis (0.75%) was used to ensure that the gDNA was intact. Samples containing greater than 25 μg of gDNA were used to perform whole-genome sequencing.

Whole-genome sequencing

We utilized the MiSeq (Illumina) and the PacBio RSII (Pacific Biosciences) platforms to perform whole-genome shotgun sequencing. The sequencing service was provided by Genomics BioSci & Tech Co., Ltd. (New Taipei City, Taiwan). For Illumina MiSeq sequencing, the DNA library was constructed using the Illumina TruSeq Nano DNA HT Sample Prep Kit according to the TruSeq DNA Sample Preparation protocol (Illumina). This library was diluted and sequenced with 600 paired-end cycles on the Illumina MiSeq instrument by following the standard protocol. For the PS3 strain, the insert size was 500 bp, and 10,471,982 read-pairs and ~3.6 Gb of raw data were obtained; and for the YSC3 strain, the insert size was 500 bp, and 11,242,474 read-pairs and ~3.8 Gb of raw data were obtained. For PacBio SMRT sequencing, the DNA library was constructed according to the PacBio SampleNet – Shared Protocol (Pacific Biosciences). After dilution, the library was loaded onto the instrument with the DNA Sequencing Kit 4.0 v2 (part number PB100-612-400) and a SMRT Cell 8 Pac for sequencing. A primary filtering analysis was performed with the RS instrument, and a secondary analysis was performed using the SMRT analysis pipeline, version 2.1.0. For the PS3 strain, the average length of the reads was 7,112 bp, and 164,831 reads and ~1.1 Gb of raw data were obtained; and for the YSC3 strain, the

doi:10.6342/NTU202003422

average length of the reads was 6,342 bp, and 192,795 reads and ~1.2 Gb of raw data were obtained.

De novo genome assembly

The *de novo* genome assembly was based on the paired-end Illumina reads and the PacBio reads. The raw Illumina reads were trimmed at the first position from both the 5'- and 3'-ends that had quality scores lower than 20. After discarding these reads, all Illumina reads were shorter than 210 bp, and high-quality sets of 10,470,949 (PS3 strain, ~2.6 Gb of raw data) and 11,241,446 paired reads (YSC3 strain, ~2.8 Gb of raw data) were obtained. These trimmed reads were individually matched with the corresponding PacBio reads and used as the input for SPAdes Genome Assembler, version 3.5(Bankevich *et al.*, 2012) with the default parameters. Finally, the whole-genome sequences were obtained, and the genomic sizes of PS3 and YSC3 were 5,269,926 bp and 5,371,816 bp, respectively.

Genome annotation

Annotations of the PS3 and YSC3 genomes were based on the procedures described by Cho *et al.* (2015). The programs RNAmmer (Lagesen *et al.*, 2007), tRNAscan-SE (Lowe and Eddy, 1997), and PRODIGAL (Hyatt *et al.*, 2010) were used for gene prediction. The genomic sequence of *R. palustris* CGA009 (Larimer *et al.*, 2004) was used as the reference, and the initial annotation of each protein-coding gene was conducted by OrthoMC (Li *et al.*, 2003) with a BLAST (Camacho *et al.*, 2009) e-value cutoff of 1e-15 and an inflation value of 1.5. Then, BLASTP(Camacho *et al.*, 2009) searches against the NCBI non-redundant (nr) protein database, BlastKOALA (Kanehisa *et al.*, 2016), and the PATRIC platform (Wattam *et al.*, 2017) were used for manual curation to improve the annotation. For functional categorization, all protein-

doi:10.6342/NTU202003422

coding genes were used to run BLASTP (Camacho *et al.*, 2009) searches against the Clusters of Orthologous Groups (COGs) functional category database as described by Galperin et al (Galperin *et al.*, 2015) with an e-value cutoff of 1e-10. The program CIRCOS (Krzywinski *et al.*, 2009) was used to plot the gene locations, GC-skew and GC content.

Phylogenetic analysis

To infer the relatedness among the *R. palustris* strains, phylogenetic trees were constructed base on multilocus sequence typing (MLST) analysis and *puf* genes. For MLST analysis, three housekeeping genes, *recA*, *rpoB* and *dnaK*, were selected. The sequences of these three genes were retrieved from GenBank. Then, individual gene sequences were validated by alignment using ClustalW multiple alignment program (Thompson *et al.*, 1994) with the default settings. Subsequently, these genes were combined to form a *recA-rpoB-dnaK* concatenated sequence by BioEdit (Hall, 1999). MEGA7.0.14 (Kumar *et al.*, 2016) was used to construct the topological tree using the maximum likelihood program (Martens *et al.*, 2008). The general time-reversible model and gamma distributed with invariant model (GTR+G+I)(Tavaré, 1986) were evaluated from the alignment in the maximum likelihood framework. To estimate the level of support for each branch, the 1,000 bootstrap (Felsenstein, 1985) samples of the alignment were generated by using the maximum likelihood program (Martens *et al.*, 2008) in MEGA7.0.14 (Kumar *et al.*, 2016). The *puf* genes consisted of *pufL* and *pufM*, which encode the core proteins of the photosynthetic reaction center. The sequences of the *puf* genes from other *R. palustris* strains were downloaded from GenBank. The individual gene sequences were aligned using BioEdit (Hall, 1999) with the ClustalW multiple alignment program (Thompson *et al.*, 1994) with the default settings. After gene concatenated, the resulting multiple sequence alignment was used to construct the

doi:10.6342/NTU202003422

phylogenetic trees by using the maximum likelihood program (Martens *et al.*, 2008) with general time-reversible model and gamma distributed with invariant model (GTR+G+I)(Tavaré, 1986). The 1,000 bootstrap (Felsenstein, 1985) replicates were used to estimate the level of support for each internal branch. For the molecular phylogeny based on all single-copy protein-coding genes conserved within the genus *Rhodopseudomonas*, the procedure was based on that described by Cho, et al (Cho *et al.*, 2015). Briefly, OrthoMCL (Li *et al.*, 2003) was used for homologous gene cluster identification; gene clusters that contained exactly one entry from each of the *Rhodopseudomonas* genomes were selected. Multiple protein sequence alignment was processed for each individual gene cluster using MUSCLE version 3.8.31 (Edgar, 2004) and then concatenated. The maximum likelihood phylogenetic inference was performed using PHYML version 20120412 (Guindon and Gascuel, 2003). The proportion of invariable sites and the gamma distribution parameter were estimated from the dataset, and the number of substitution rate categories was set to four. Bootstrap supports were estimated based on 1,000 replicates.

Biofilm formation assay

Biofilm formation assay was performed according to a protocol proposed by Tram, et al (Tram *et al.*, 2013) with some modifications. A single bacterial colony was selected, inoculated into a 10-mL sterile plastic tube containing 3 mL of PNSB broth, and then incubated at 37°C and 200 rpm for 24 h. Subsequently, 0.3 mL of the above broth was inoculated into a 10-mL sterile plastic tube containing 3 mL of fresh PNSB broth. This tube was incubated in a static state at 25°C for 5 days. After that, the broth was slowly emptied, and the residual suspension was carefully removed by pipette. The tube was rinsed with sterile distilled, deionized water (DDW) to remove the incomplete biofilm. The tube was air dried for 5 min, and then the biofilm was stained with 4 mL

doi:10.6342/NTU202003422

of 1.0% crystal violet for 15 min. The crystal violet solution was removed, and the tube was washed with DDW three times prior to observation. For biofilm quantification, 5 mL of 95% ethanol was added to the above tube and shaken vigorously by vortex. Following, the absorbance at 570 nm was determined by using a multilabel reader (VICTOR3 1420-050, PerkinElmer).

Phosphate-solubilizing activity assay

Qualitative phosphate-solubilizing activity assay was performed according to the protocol proposed by Nautiyal (Nautiyal, 1999). Bacterial strains were tested by plate assay containing dissolve phosphorus agar (DPA) medium. DPA medium was modified from National Botanical Research Institute's phosphate growth medium (NBRIP) and National Botanical Research Institute's phosphate growth medium devoid of yeast extract (NBRIY) and contained the following (L^{-1}): 10 g of glucose, 5 g of $Ca_3(PO_4)_2$, 5 g of $MgCl_2 \cdot 6H_2O$, 0.2 g of KCl, 0.1 g of $MgSO_4 \cdot 7H_2O$, 0.1 g of $(NH_4)_2SO_4$, 0.002 g of $MnSO_4$, 0.002 g of $FeSO_4 \cdot 7H_2O$ and 15 g of Bacto agar. A single bacterial colony was selected, inoculated into 3 mL of PNSB broth as described previously[7], and incubated for 24 h at 37°C under stirring (200 rpm) in darkness. Subsequently, 2.5 mL of the above broths were transferred into 250-mL Erlenmeyer flasks containing 50 mL of fresh PNSB broth. The cultures were incubated under the same conditions described above. Then, 20 μL of the bacterial cell suspensions was spotted onto DPA plates, which were then incubated at 37°C for 3 days. A *Burkholderia* sp. isolate was used as a positive strain.

Indole acetic acid production of *R. palustris*

A single bacterial colony was selected, inoculated into 3 mL of PNSB broth as described previously (Wong *et al.*, 2014), and incubated for 24 h at 37°C under stirring

doi:10.6342/NTU202003422

(200 rpm) in darkness. Following, 2.5 mL of the above broths were inoculated into 250-mL Erlenmeyer flasks containing 50 mL of fresh PNSB broth and incubated under the same conditions described above. After two days, the supernatant of the bacterial broth was filtered through a 0.22-μm filter membrane. IAA purification was performed according to a protocol proposed by Lin, et al (Lin *et al.*, 2015) with some modifications. The above filtered solution was mixed with the same volume of cold methanol. Then, the mixture was vortexed and stored at -20°C for 30 min. The supernatant was collected by centrifugation at 14,000 rpm and 4°C for 10 min and then was dried by a SpeedVac concentrator (CVE3110, EYELA) at 40°C and 1,000 rpm. Finally, the dried sample was suspended in 25% methanol with 1% acetic acid and then analyzed by high-performance liquid chromatography (HPLC). The HPLC system (600E Model, Waters-Millipore, Milford, MA, USA) equipped with a UV detector (486E, Waters-Millipore, Milford, MA, USA) was used in this study. The reversed-phase C18 column (Phenomenex Luna C18 column, 250×4.6 mm, 5 μm) with mobile phases A (0.1% acetic acid in water) and B (0.1% acetic acid in methanol) was used. Chromatographic separation was carried out by linear gradient elution with a flow rate of 1 mL/min. The gradient program was as follows: 0-30 min from 30% to 80% B and 30-40 min from 80% to 30% B. The total run time was 40 min, and an injection volume of 20 μL was used. The column temperature was set at 25°C, and the optical density was measured at a wavelength of 280 nm. Pure IAA (Sigma-Aldrich) was use as a standard.

Comparative genomic analyses

We performed comparative genomic analyses of the genomes of the PS3 and YSC3 strains and the sequenced *R. palustris* type strain CGA009(Larimer *et al.*, 2004). Pairwise alignments of all three strains were carried out by MUMmer version 3.23 (Kurtz *et al.*, 2004) with default parameters. The conserved genes and homologous gene

doi:10.6342/NTU202003422

clusters were identified using OrthoMCL (Li *et al.*, 2003) with the same settings as described above. Genes involved in metabolic pathways were analyzed by KEGG Mapper. Genome island prediction was performed by Zisland Explorer(Wei *et al.*, 2016) with default parameters.

Collection of Chinese cabbage root exudate solution

To collect the root exudates, Chinese cabbage seeds (*Brassica rapa* L. ssp. *chinesis*, "Maruba Santoh") were selected and purchased from Formosa Farming Materials Co., Ltd. (Taipei, Taiwan). The seeds were immersed in 70% alcohol for 2 min and then in 3% hydrogen peroxide solution for 7 min for surface sterilization. Then, the seeds were washed thoroughly with sterile distilled water and germinated for 1 day at 25°C in the dark. Subsequently, well-germinated seeds were transferred to soaked cotton and cultivated under continuous (24-h photoperiod) light-emitting diode lighting (~210 μmol $m^{-2}s^{-1}$). After one week, the seedlings were transferred to hydroponic tanks (35 L) in a plant factory facility (College of BioResources and Agriculture, National Taiwan University). Twenty-four seedlings were cultivated in each of the tanks, which were equipped with air pumps to homogenize the solution and maintain the dissolved oxygen. Half-strength Hoagland solution was used as a nutrient solution (NS) (0.255 g L^{-1} KNO_3, 0.245 g L^{-1} $MgSO_4•7H_2O$, 0.04 g L^{-1} NH_4NO_3, 0.034 g L^{-1} KH_2PO_4, 11.25 mg L^{-1} Fe-EDTA, 1.43 mg L^{-1} H_3BO_3, 0.0255 mg L^{-1} $CuSO_4$, 0.11 mg L^{-1} $ZnSO_4•7H_2O$, 0.95 g L^{-1} $MnCl_2•4H_2O$, 0.06 mg L^{-1} $Na_2MoO_4•2H_2O$ and 0.59 g L^{-1} $Ca(NO_3)_2•4H_2O$) (Hoagland and Arnon, 1950). The initial pH value was adjusted at 6.0 by H_3PO_4. After 7 days of cultivation, the nutrient solution containing root exudates were collected and filtered through 0.22-μm filter membranes. Sterility of these root exudate solutions was checked by plating onto nutrient agar plates.

doi:10.6342/NTU202003422

Gene expression analysis of *R. palustris* in response to root exudates

R. palustris broth was inoculated (10% (v/v)) into 200 mL of half-strength Hoagland solution and 200 mL of the abovementioned root exudate solution. The cells were then incubated at 25°C and 150 rpm in the dark. Bacterial cells were sampled at different time intervals for RNA extraction. Bacterial cell pellets were collected by centrifugation (5000 × g for 5 min at 4°C). Subsequently, the cell pellets were snap-frozen in liquid nitrogen and homogenized by adding sterile steel beads and rapidly shaking the microcentrifuge tubes back and forth at 9,000 rpm for 1 min in an SH-100 homogenizer (Kurabo, Japan). The homogenization process was repeated three times. RNA purification was performed by the Direct-zol^{TM} RNA MiniPrep Kit (Zymo Research, USA) according to the manufacturer's instructions. For reverse transcription, 2 μg of total RNA was reacted with random hexamers and the SuperScript III reagent to synthesize first-strand cDNA according to the protocol for the SuperScript® III Reverse Transcriptase (Invitrogen, USA). Quantitative PCR analysis of gene expression was performed by using the SYBR Green Real-Time PCR Master Mix Kit (Kapa Biosystems, USA), and the fluorescence intensity was measured by the LightCycler 480 system (Roche, Germany). The real-time PCR conditions were as follows: denaturation at 95°C for 3 min followed by 45 cycles of 95°C for 10 s, 60°C for 20 s and 72°C for 1 s. A program of 95°C for 5 s and 60°C for 1 min was used to obtain a melting curve. All qPCR analyses were performed in three biological replicates. The housekeeping gene *clpX* was used as the reference gene for transcript normalization. All primer pairs used for quantitative RT-PCR are listed in Table 2-1. The fold change in the expression of target genes in each treatment was calculated using the $2^{-\Delta\Delta Ct}$ method (Livak and Schmittgen, 2001).

Statistical analysis

doi:10.6342/NTU202003422

Analyses of variance were performed with *R* version 3.4.3. Fisher's least significant difference (LSD) test was used for multiple range analyses to determine significant differences between groups of data. The results were considered significant at $P < 0.05$.

Results

General characteristics of the genomes

R. palustris PS3 and YSC3 genome were sequenced and generated by *de novo* assembly from PacBio long reads and 300 bp paired-end illumina short reads. Compared with other *R. palustris* strains, PS3 has a relatively small single circular chromosome that is 5,269,926 bp in size, and encodes 4,799 protein-coding genes (Figure 2-2). The genome of YSC3 strain is composed of one circular chromosome of 5,371,816 bp and annotated to encode 4,907 proteins (Figure 2-2). The general genomic features of *R. palustris* strains are summarized in Table 2-4. Except of PS3 and YSC3 strain, other *R. palustris* have the additional tRNA gene were annotated as tRNA-OTHER, which is unknown reason. Interestingly, only CGA009 strain harbors one 8.4-kb circular plasmid (Larimer *et al.*, 2004), while other *R. palustris* strains including PS3 and YSC3 do not harbor any plasmid (Table 2-4). According to the segmental cumulative GC profile (Wei *et al.*, 2016), I deduced that no horizontally transferred genomic island exist in the PS3 genome. This result is consistent with Larimer and his colleagues' study (Larimer *et al.*, 2004), which didn't find any horizontally transferred genomic islands in the genome of *R. palustris* CGA009. In contrast, I observed that YSC3 contained one 5.6-kb genomic island, which was located at 5,229,652-5,285,897 bp, containing 60 protein-coding genes (locus tags: RPYSC3_47720-48310), and all of these genes encode hypothetical proteins (Figure 2-2 b).

Figure 2-3 shows the phylogenetic tree of the selective *R. palustris* strains, which

doi:10.6342/NTU202003422

was constructed based on multilocus sequence analysis (MLSA), functional genes and conserved amino acid sequences. The multilocus sequence analysis (MLSA) of housekeeping genes (i.e., *recA*, *rpoB*, and *dnaK*; the concatenated alignment is ~7 kb) indicated that selective strains were divided into five major groups (Figure 2-3 a). All of the *R. palustris* reference strains shared >91% nucleotide sequence identity with PS3; YSC3 is the most closely related strain, with a >99% identity, while CGA009 and TIE-1 exhibited >97% identity. On the other hand, Figure 2-3b showed the phylogenetic tree based on the *pufL* and *pufM* genes, and it presented the tree topology was identical to that of the tree generated based on the three housekeeping genes, which were consistent with PS3 and YSC3 being closely related (bootstrap support >99%). These two *puf* genes encode the two subunits of the light reaction center core protein and have been used as markers for phylogenetic analysis within the genus *Rhodopseudomonas* (Okamura *et al.*, 2009; Wong *et al.*, 2014). At the genomic level, it was identified a total of 2,515 single-copy genes that were conserved among all the *R. palustris* strains compared. Based on these genes, I calculated the average nt/aa similarity among the strains, and four main clusters were formed in the phylogenetic tree of *R. palustris* (Figure 2-3c). PS3 had a close phylogenetic relationship with YSC3, while the CGA009 and TIE strains were grouped in a nearby cluster. Moreover, according to the analysis of pairwise genome alignments, it demonstrated that PS3 shares 95.11% identity with YSC3 at the nucleotide level and exhibits a high level of synteny conservation (Figure 2-4a). In contrast, CGA009 shares 92.19% identity with PS3 (Fig. 2b). This result was consistent with the phylogenetic tree analysis (Figure 2-3 and 2-3). Although CGA009 shares 92.19% identity with PS3, it was higher than that one in other strains. Besides of YSC3, CGA009 and TIE01strain, chromosomal organization of PS3 presents the partial reverse conserved with DX-1, HaA2 as well as BisB5 strain, and lower level of synteny with BisA53 and BisB18 (Figure 2-4). It is notable that PS3 has a reversed

doi:10.6342/NTU202003422

syntenic regions with YSC3 despite there are similar to each other (Figure 2-4 a). Based on above results, I included CGA009 as a reference strain in our comparative genomic analysis. Also, CGA009 is the first sequenced *R. palustris* strain (Larimer *et al.*, 2004) and as the representative model strain of *R. palustris* in NCBI database.

The homologous gene analysis showed that the genomes of PS3, YSC3 and CGA009 were composed of 5,549 orthologous gene clusters, and 4,142 clusters were conserved among the 3 strains (Figure 2-5). On the other hand, 226 gene clusters were shared by PS3 and YSC3, while only 104 gene clusters were shared by PS3 and CGA009 (Figure 2-5). There were 260 gene clusters that were unique to the PS3 strain. Among these gene clusters, 60% encode hypothetical proteins, and of the remaining 40%, genes such as the urea ABC transporters (*UrtACD*, RPPS3_10430, RPPS3_10440 and RPA10450). COG analysis showed no significant differences in the distribution patterns of the three strains (Figure 2-6). Notably, only CGA009 has a gene belonging to the COG B group (i.e., chromatin structure and dynamics), which is associated with acetylpolyamine aminohydrolase (Larimer *et al.*, 2004). It has been suggested that acetoin can be converted to acetate by acetylpolyamine aminohydrolase upon carbon source depletion (Leipe and Landsman, 1997). With respect to the COG K group (i.e., transcription), PS3 and YSC3 exhibited a lower percentage of genes in this group than CGA009, which might indicate that CGA009 contains a larger ratio of genes encoding transcriptional factors, as described by Oda *et al.* (2008).

Carbon source utilization

R. palustris can obtain carbon from carbon dioxide and/or organic compounds (Larimer *et al.*, 2004). Core metabolic pathways, such as the Calvin-Benson-Bassham (CBB) pathway of CO_2 fixation, the complete tricarboxylic acid cycle (TCA cycle), an Embden-Meyerhof-Parnas (EMP) pathway and a pentose phosphate pathway (PPP),

doi:10.6342/NTU202003422

were found in the genomes of both PS3 and YSC3 (Figure 2-7). Larimer et al. reported that *R. palustris* CGA009 lacks genes encoding hexokinase (Larimer *et al.*, 2004), which is also the case for PS3 and YSC3. CGA009 can catabolize a variety of aromatic compounds for growth (Harwood and Gibson, 1988), and it was obtained similar results for the *R. palustris* derivatives (Oda *et al.*, 2008). Several genes in the PS3 and YSC3 strains encode dioxygenases involved in the degradation of aromatic compounds, such as 3,4-dihydroxyphenylacetate 2,3-dioxygenase (locus tags: RPPS3_16850, RPPS3_37890, RPYSC3_16530, and RPYSC3_38130), homogentisate 1,2-dioxygenase (RPPS3_46330 and RPYSC3_46820), and hydroxyquinol 1,2-dioxygenase (RPPS3_21770 and RPYSC3_21800). Genes involved in ring cleavage pathways of homogentisate and phenylacetate were also identified in PS3 and YSC3, such as the *bed* genes (RPPS3_06600 and 06630-06740; RPYSC3_06760 and 06790-06900), which are associated with anaerobic benzoate degradation (Hirakawa *et al.*, 2015). Additionally, CGA009 has been found to be able to use fatty acids and dicarboxylic acids via a conserved gene cluster associated the fatty acid beta-oxidation pathway (Harrison and Harwood, 2005; Larimer *et al.*, 2004). Similarly, it can be observed that the PS3 and YSC3 strains have a complete gene cluster for the fatty acid beta-oxidation pathway. The *R. palustris* pathways involved in degrading aromatic compounds provide not only extraordinary metabolic versatility but also high utility for bioremediation (e.g., methoxylated aromatics and aromatic amides (Austin *et al.*, 2015; Harrison and Harwood, 2005; Karpinets *et al.*, 2009) and bioenergy production (e.g., hydrogen gas (Shi *et al.*, 2014)). It was noticed that there was no monosaccharide (such as glucose, mannose, xylose, arabinose, and fructose) transporter-related gene present in any of the three *R. palustris* genomes. A previous study reported that CGA009 has limited ability to grow on sugars due to the absence of genes encoding glucose transporters, fructose *transporters* or hexokinases in its genome (Larimer *et al.*, 2004).

doi:10.6342/NTU202003422

However, some studies have reported that *R. palustris* strains could consume glucose or fructose for cell growth (Oh *et al.*, 2002; Wang *et al.*, 2010; Wong *et al.*, 2014). We also found that PS3 and YSC3 could use some monosaccharides, such as fructose and glucose in a preliminary study (Wong *et al.*, 2014). In addition, there are genes encoding TonB-dependent transporters (Schauer *et al.*, 2008) and multiple sugar ABC transport systems in the *R. palustris* genomes, which are associated with carbohydrate uptake. Therefore, this finding suggests that these *R. palustris* strains are able to transport single sugar molecules through specific outer membrane proteins. However, this hypothesis remains to be verified.

Nitrogen fixation and nitrogen utilization

Biological nitrogen fixation is the process via which nitrogen is converted to ammonia by the nitrogenase complex of microorganisms (Kim and Rees, 1994). All known diazotrophs contain at least one of the three closely related subtypes of nitrogenase related genes: *nif* (encoding molybdenum nitrogenase), *vnf* (encoding vanadium nitrogenase), and *anf* (encoding iron nitrogenase)(Bishop and Joerger, 1990). According to previous studies, CGA009 was characterized as a nitrogen-fixing bacterium and harbors the above three gene subtypes (Larimer *et al.*, 2004; Oda *et al.*, 2008). It demonstrated that both the PS3 and YSC3 strains could fix nitrogen under microaerobic conditions with light (Wong *et al.*, 2014). However, there was no *vnf*-related gene in the genomes of these strains (lower-left side in Figure 2-7 and Figure 2-8 a). According to the genomic analysis, these two strains have a gene cluster encoding the nitrate/nitrite transport pathways (RPPS3_21380-21400 and RPYSC3_21410-21430). However, no explicit nitrate reductase genes were identified in the two genomes. The PS3 and YSC3 strains have genes encoding proteins associated with denitrification (RPPS3_33410, 41010, 14290-14300 and 20700; RPYSC3_41430,

doi:10.6342/NTU202003422

1438-1439 and 20720), resembling the denitrification-associated genes in the CGA009 strain. In addition to nitrogen fixation, ferredoxin-nitrite reductase, encoded by *nirA* (RPPS3_37380 and RPYSC3_37610) can directly convert nitrite to ammonium, while the ammonium can be taken up from environment via two ammonium transporters (RPPS3_02860 and 02880; RPYSC3_02920 and 02940). As shown in Figure 2-7, ammonium can be assimilated by glutamine synthetase (RPPS3_10270, 30150 and 41690; RPYSC3_10150, 30130 and 42060) and further converted to glutamate by glutamate synthetase (RPPS3_04850 and 08970; RPYSC3_04930 and 09180) for amino acid metabolism.

Root colonization

Root colonization by bacteria is regarded as an essential step for PGPR to promote plant growth (Lugtenberg and Kamilova, 2009). I compared genes associated with root colonization, such as genes involved in chemotaxis, cell motility, and biofilm formation (Ahmad *et al.*, 2011). All three strains possess tree complete set of the *che* genes (Figure 2-9). Interestingly, both PS3 and YSC3 contain the *cheZ* gene (RPPS3_11990 and RPYSC3_11730), which is annotated as a hypothetical protein in CGA009 (Larimer *et al.*, 2004). Genes encoding methyl-accepting chemotaxis proteins (RPPS3_00100, RPPS3_04430, RPPS3_11420, RPPS3_17980, RPPS3_36270, RPPS3_42600, RPPS3_44180, RPYSC3_00110, RPYSC3_18180, RPYSC3_36490, RPYSC3_42970, RPYSC3_44590, RPA0139, RPA0431, RPA3546, RPA4302, RPA4306, RPA4307, RPA4449, RPA4638 and RPA4639) exist in all three strains. For cell motility, there were 50, 46, and 39 flagella-related genes in PS3, YSC3, and CGA009, respectively. Moreover, it was observed that the cell migration rates of the three strains varied substantially. Microscopy experiments showed that PS3 had the fastest migration speed followed by YSC3. By contrast, CGA009 was almost immobile

doi:10.6342/NTU202003422

(video data was publish on the *Scientific Reports*, (Lo *et al.*, 2018)). Several genes involved in biosynthesis or transportation of polysaccharides were identified in all three strains, for example, *exo* genes, which are responsible for exopolysaccharide (EPS) biosynthesis (Oda *et al.*, 2008). The *lptG* and *lptF* genes are responsible for lipopolysaccharide transportation (Ruiz *et al.*, 2008). Genes known to be associated with biofilm formation (as reported in the KEGG database), such as *pel*, *psl*, and *glg*, were not identified in these *R. palustris* strains. However, all three strains showed the ability to form biofilms in a crystal violet-based assay (Figure 2-10), and the CGA009 strain shown higher biofilm formation than PS3 and YSC3. In addition, biofilm formation was not significantly different between the PS3 and YSC3 strains (Figure 2-10).

Deduced plant growth promotion-related genes

The mechanisms for PGP by rhizobacteria include nitrogen fixation, improvement of nutrient availability, and phytohormone production (Lugtenberg and Kamilova, 2009; Vessey, 2003). As described above, all three strains contain the conserved gene cluster that encodes nitrogenase (Figure 2-8a), which is consistent with the positive phenotyping result obtained for nitrogen fixation. I also found that the *R. palustris* strains harbor genes encoding nitrite reductase and nitric oxide reductase, which convert nitrite to nitric oxide and nitrous oxide. These strains also contain ferredoxin-nitrite reductase (*nirA*), which can directly reduce nitrite to ammonium (Figure 2-7). These findings suggest that via enzymatic conversion processes, *R. palustris* may be able to provide plants with available sources of nitrogen.

Phosphate solubilization is also an important mode of action for plant growth (Goswami *et al.*, 2016). I identified several genes encoding phosphatases, C-P lyases, inositol-phosphate phosphatases, and organic acids in the genomes of all three strains

doi:10.6342/NTU202003422

(Figure 2-8 b). Unexpectedly, in the plate assay, these three strains did not present clear zones around the colonies, which indicates these strains are unable to solubilize phosphate (Figure 2-11). Some PGPR can produce phytohormones to stimulate plant growth (Shao *et al.*, 2014; Spaepen and Vanderleyden, 2011; Talboys *et al.*, 2014). In our previous study, it demonstrated that both PS3 and YSC3 were able to produce IAA in the presence of tryptophan (Wong *et al.*, 2014). As shown in Figure 2-8c, these two strains possess most of the genes involved in the biosynthetic pathway of IAA in bacteria (Spaepen *et al.*, 2007). However, some genes encoding essential proteins, such as tryptophan-pyruvate aminotransferase (TAA1), tryptophan aminotransferase (TAM1), aromatic amino acid decarboxylase (DDC), tryptophan 2-monooxygenase (MAO), tryptophan side chain oxidase (TSO) and tryptophan monooxygenase (IaaM), were absent in the genomes of these strains. It is unclear whether the absence of these genes is an artifact of annotation or whether these bacteria have alternative genes for these functions. I further quantified the IAA production from these three strains, and the result was consistent with our previous report (Wong *et al.*, 2014). Strains PS3, YSC3 as well as CGA009 strain showed the ability of IAA production, and IAA production was significantly increased in presence of tryptophan (Figure 2-12).

ACC deaminase genes were identified in the genomes of PS3 and YSC3 (RPPS3_24510 and RPYSC3_24830, respectively) but were absent in the genome of CGA009. *R. palustris* can produce 5-aminolevulinic acid (ALA), which is regarded as an effective compound for PGP under abiotic stress (Morales-Payan and Stall, 2005; Nishikawa and Murooka, 2001; Nunkaew *et al.*, 2014; Zhao *et al.*, 2015). The genes *hemO* and *hemA*, which are associated with the biosynthesis of ALA, were identified in all three strains (Figure 2-8 d). Detailed information about genes associated with PGP is shown in Figure 2-7.

doi:10.6342/NTU202003422

Effect of root exudates of Chinese cabbage on biofilm formation and relative gene expression levels

Root exudates and their organic acid components are considered important factors for biofilm formation and colonization by PGPR of the rhizosphere (Kloepper and Schroth, 1978). To elucidate the role of root exudates in microbial activity, I used the hydroponic solution containing root exudates for cultivation of the bacterial strains. As shown in Figure 2-13a, the growth rates of both PS3 and YSC3 increased slightly upon treatment with the root exudates (-R) in comparison with those of the control (-NS) groups. However, there was no statistically significant difference at most of the time points. As shown in Figure 2-13b, the amount of biofilm formed by PS3 was substantially enhanced in the presence of root exudates. In contrast, biofilm formation by YSC3 was not altered by the addition of root exudates.

The expression patterns of genes associated with bacterial colonization and biofilm formation in response to root exudates were analyzed in a time-course study. As shown in Figure 2-14, the relative expression levels of flagella-related genes (Figure 2-14 a and b) of YSC3 were higher than those of PS3 at most time points during growth. We found that the expression of *fliM* and *flgB* in YSC3 increased with time and that the expression of *fliE* peaked at 12 h and gradually declined. The expression of the chemotaxis-related genes *cheR*, *cheW* and *cheA* of PS3 was upregulated and peaked at 12 h, and these expression levels were significantly higher than those of YSC3 at this time point (Figure 2-14 d-f). There was no significant difference in the expression of the biofilm formation-related genes *fliE* or *exoR* or the *eps* genes between PS3 and YSC3 (Figure 2-14c, g and h).

Transcriptomic profiling of *R. palustris* PS3 response to root exudate

doi:10.6342/NTU202003422

To further understand the divergence of PS3 and YSC3 in response to host plant, I performed whole transcriptomic analyses with both PS3 and YSC3 strains. As shown in Figure 2-15, there were approximately 17-26% of PS3 and YSC3 genes significantly regulated after 24 hours by supplementation of root exudate in comparison with those of control group (p.s. at the expression fold-change was larger than 2.0). Among these different expression levels, there were about 8.4% of protein coding genes up-regulated in the genomes of PS3 strain (Figure 2-15 a). On the other hand, about 17.1% of the protein coding genes were up-regulated by root exudate in the genomes of YSC3 strain (Figure 2-15 b).

As shown in Figure 2-16, I noticed that the expression levels of the gene clusters relevant to biofilm formation, IAA biosynthesis and flagellar biosynthesis/switch were dramatically up- regulated in PS3, and higher than those in YSC3 (Figure 2-16 b). The genes involved in biofilm formation in YSC3 were down regulated while root exudate was added. These results were consistent with that of biofilm formation assay shown in Figure 2-13 b, which indicating that root exudate didn't affect the biofilm formation in YSC3 strain. Notably, most of the genes involved in chemotaxis were down-regulated at 24 hours by the addition of root exudates (Figure 2-16 b). For the genes related to carbon metabolism, most of the transcriptome in both PS3 and YSC3 were not significantly induced between different treatments (Figure 2-16 c). On the other hand, most of the genes of PS3 involved in the nitrogen metabolism, such as *glnA*, *livM*, *argC*, *his*C, and *cysD* were induced by root exudate supplementation (Figure 2-16 d). In contrast, several genes related to denitrification in YSC3 were up-regulated by root exudate supplementation (Figure 2-16 d). Furthermore, most of the carbon fixation and nitrogen fixation associated genes were down-regulated in both strains (Figure 2-16 c and d).

doi:10.6342/NTU202003422

Discussion

The *R. palustris* strains PS3 and YSC3 were isolated from paddy fields located in neighboring cities in northern Taiwan. Both strains have a closer evolutionary relationship than the other characterized *R. palustris* strains (Figure 2-3). The chromosomal organizations of these two strains were highly conserved, which shared 98.59% of the protein-coding genes (Figure 2-4). Interestingly, although these strains belong to *R. palustris*, the synteny of genomic sequence was highly different (Figure 2-4). According to the taxonomic affiliation, the 16S rRNA sequence identities of 97% or greater can be considered to be the cutoff for a species (Achtman and Wagner, 2008; Cohan and Perry, 2007). Therefore, in the previous study, PS3 and YSC3 strains were classified as *R. palustris*. However, in recent years, the whole-genome average nucleotide identity (ANI) has been considered as a sounder method for taxonomy, and the organisms belong to the same species typically showing ≥ 95% ANI (Ciufo *et al.*, 2018). If I based on the hypothesis, PS3 and the other *R. palustris* strains (except CGA009 and YSC3) could not categorize as the same species. But it was also proposed that ANI cannot strictly illustrate genome evolutionary relatedness because the orthologs also can vary broadly between pair genomes (Jain *et al.*, 2018). Despite it was confusing in the taxonomy, in consideration of the 16S rDNA (Wong *et al.*, 2014), MLSA (Figure 2-3) and ANI (Figure 2-4) analysis as well as physiological and biochemical analysis (Wong *et al.*, 2014), I classified PS3 as a *R. palutris* strain. The divergence in genomic structure may attribute to the isolation geography. PS3 and YSC3 strain were isolated from Taiwanese paddy fields, whereas the other *R. palutris* strains used for comparison in this study were isolated from Netherlands (Oda *et al.*, 2002). Although these strains were phylogenetically related with each other, only PS3 was able to promote plant growth (Hsu *et al.*, 2015; Wong *et al.*, 2014).

doi:10.6342/NTU202003422

While treating individual bacterial cultures with root exudates, substantial differences in biofilm formation and relative gene expression levels were observed between PS3 and YSC3 (Figure 2-13 and Figure 2-14). Root exudates contain various carbohydrate-derived compounds (e.g., glucose, maltose, xylose, citric acid, malic acid, and succinic acid (Ahmad *et al.*, 2011; Vacheron *et al.*, 2013), which are the most important nutrient sources for rhizospheric microorganisms. In our previous study, we proved that both PS3 and YSC3 can utilize various carbon sources, including the carbon sources mentioned above (Wong *et al.*, 2014). Furthermore, many metabolic pathways of the core carbohydrates were identified in the genomes of PS3 and YSC3 (Figure 2-7). Therefore, I inferred that these two bacteria are able to utilize carbohydrates derived from root exudates. I noticed that the bacterial growth of PS3 or YSC3 strains was not enhanced in half-strength Hoagland solution containing root exudates (Figure 2-13a). It was hypothesized that the nutrient levels in this culture medium were too low to sustain normal bacterial growth of *R. palustris*. Especially, carbon source was lack in this Hoagland solution.

In addition to carbohydrates, aromatic hydrocarbons are another type of abundant plant-derived compounds in the rhizosphere. Aromatic hydrocarbons are mainly derived from secondary *metabolites* (such as flavonoids and phenols) and lignin structures (Adler, 1977). *R. palustris* can degrade a variety of aromatic compounds (Austin *et al.*, 2015; Harwood *et al.*, 1998; Larimer *et al.*, 2004). In the present study, several genes associated with degradation of aromatic compounds were identified in the PS3 and YSC3 genomes. These putative enzymes are involved in either oxygenase-dependent ring cleavage pathways or the anaerobic benzoate degradation pathway. Accordingly, this finding suggests that the *R. palustris* strains can utilize a variety of carbon sources at different levels of oxygen, even under low-oxygen conditions (hypoxia). This result may explain why PS3 can have beneficial effects on plant growth

doi:10.6342/NTU202003422

in either soil (aerobic) or hydroponic solution (aerobic-anaerobic interfaces)(Hsu *et al.*, 2015; Wong *et al.*, 2014). It would be advantageous for *R. palustris* to act as a PGPR to utilize additional nutrients in agricultural systems in conditions where oxygen demand exceeds supply, such as during flooding of the rice rhizosphere.

Efficient colonization by PGPR of roots has been considered a key trait to confer beneficial effects to plants, and this ability is closely associated with chemotaxis and biofilm formation (Ramey *et al.*, 2004). I found that the genetic arrangement of the chemotaxis-related gene cluster (*cheA*, *cheB*, *cheW*, *cheR* and *cheY*) and the flagellar biosynthesis-related gene cluster (*flhA*, *flhB*, *fliP*, *fliQ*, and *fliR*) are very similar among the genomes of PS3, YSC3 and CGA009 (Figure 2-7). Moreover, genes associated with biosynthesis of exopolysaccharides were identified in the three strains, such as the *exo*, *kps*, and *upp* genes. The *upp* gene has already been elucidated as an important gene in the mediation of biofilm formation by *R. palustris* under photoheterotrophic growth conditions (Fritts *et al.*, 2017). Although these gene clusters showed very similar genetic arrangements in the three bacteria, the abilities of these strains to form biofilms differed. As shown in Figure 2-10, CGA009 produced more biofilm than the other two strains did.

Rhizobia are able to supply nitrogen sources to host plants via symbiotic nitrogen fixation in root nodules. In contrast, free-living nitrogen-fixing bacteria release the ammonia synthesized by cells into the environment, and some of this ammonia is converted to nitrite/nitrate (Bhattacharyya and Jha, 2012). In a preliminary study, we found that upon inoculating PS3 into a hydroponic nutrient solution, the concentration of ammonia or nitrate in the nutrient solution did not change substantially (unpublished data). This finding suggests that neither N_2-fixation by free-living bacteria nor nitrification occurred under aerobic conditions that were suitable for plant growth. Accordingly, we deduced that biological nitrogen fixation is not the main mode of

doi:10.6342/NTU202003422

action by which PS3 promotes plant growth.

Phosphorus is one of the most important macronutrients, but the availability of phosphorus in soil is limited. Phosphate solubilizing bacteria can convert insoluble phosphorus (both organic and inorganic) to available forms for plant utilization, and this property is regarded as an essential mode of action for PGP (Goswami *et al.*, 2016; Lugtenberg and Kamilova, 2009). PS3 and YSC3 as well as CGA009 contained many genes involved in phosphate solubilization, such as *phn*, *gcd* and *pqq* (Figure 2-8 b). The *phn* gene family encodes phosphonatases and C-P lyases, which are the enzymes that perform C-P cleavage in organophosphonates (Rodriguez *et al.*, 2006). Furthermore, this gene family is also associated with the release of phosphate ions from organic matter, such as fertilizers. On the other hand, genes involved in phosphate solubilization via the production of organic acids were also identified in these *R. palustris* strains. For example, the *gcd* gene, encoding glucose dehydrogenase, and the *pqq* gene, encoding pyrroloquinoline quinone (PQQ), are associated with the production of gluconic acid (GA), which is a well-known organic acid-based mechanism of inorganic phosphate solubilization (Rodriguez *et al.*, 2006). However, we noted that all three strains lacked orthologs of the *pqqA* gene in the PQQ synthetic pathway (Figure 2-8 b). This finding suggests that these three strains may be unable to synthesize GA. In addition, these bacteria did not harbor related genes encoding phosphatases or phytases, which are the most relevant proteins associated with phosphate solubilization in the environment (Rodriguez *et al.*, 2006). Moreover, our data showed that these three strains were not capable of solubilizing inorganic phosphorus from insoluble compounds (Figure 2-11) even though these strains possess most of the phosphate solubilization-related genes. This result is also consistent with previous reports that *R. palustris* lacks the ability to solubilize phosphate (Batool *et al.*, 2017; Koh and Song, 2007). The commonly observed absence of phosphate-

doi:10.6342/NTU202003422

solubilization activity among *R. palustris* strains indicates that this function is probably no longer required for sustaining the growth of these bacteria in the environment. Bacteria generally lose some essential biosynthetic functions when the corresponding metabolite is present in sufficient amounts in the bacterial growth environment or is provided by a consortium of organisms (D'Souza and Kost, 2016). Whether the reduction of metabolic burden for basic cellular processes in *R. palustris* results in adaptive benefits over other genotypes (D'Souza *et al.*, 2014) as well as the causal mechanisms that explain this observation remain unclear.

In previously, we observed that PS3 could modulate root system architectures and promote plant growth (Hsu *et al.*, 2015; Wong *et al.*, 2014), indicating the production of phytohormones and other signals during the interactions between *R. palustris* and host plants. It has been demonstrated that enhanced root proliferation, such as increasing root size and lateral root number, is closely associated with bacterial IAA levels (Shao *et al.*, 2014). IAA biosynthesis in bacteria can be divided into tryptophan-dependent and tryptophan-independent pathways (Spaepen *et al.*, 2007). However, we noted that genes involved in the conversion of tryptophan to other intermediates were absent in the annotation (Figure 2-7 and Figure 2-8 c). I identified some genes involved in the synthesis of indole-3-glycerolphosphate and indole in PS3 and YSC3 as well as in CGA009; these genes included *trpBA* (RPPS3_00730, RPPS3_00740, RPYSC3_00730, RPYSC3_00740, RPA0069 and RPA0070) and *tnaA* (RPPS3_35930, RPYSC3_36170 and RPA3564). These intermediates are predictive precursors of IAA synthesis in tryptophan-independent pathways (Prinsen *et al.*, 1993), suggesting that these *R. palustris* strains are able to synthesize IAA via an as yet unidentified pathway(s).

Some genes associated with environmental stress tolerance were identified in the genomes of the *R. palustris* strains. Examples of these genes include *acdS* (ACC

doi:10.6342/NTU202003422

deaminase; locus tags: RPPS3_24510 and RPYSC3_24830) and *hemO*/*hemA* (RPPS3_08610, RPYSC3_08830 and RPA0854 for PS3, YSC3 and CGA009, respectively) and the *hemA* genes (RPPS3_15310, RPYSC3_15390 and RPA1554 for PS3, YSC3 and CGA009, respectively), which encode 5-aminolevulinic acid (ALA) synthase (Figure 2-8 d). In many PGPR, such as *Pseudomonas fluorescens*, *Achromobacter piechaudii* and *P. putida*, ACC deaminase can alleviate the detrimental effects of environmental stress and can enhance the stress tolerance of plants by degrading the ethylene precursor ACC (Mayak *et al.*, 2004; Saravanakumar and Samiyappan, 2007). ALA is a precursor of porphyrin-containing compounds, such as vitamin B12, chlorophyll, heme and phytochrome(Bykhovsky *et al.*, 2008; Sasaki *et al.*, 2002; Tabuchi *et al.*, 2009; Wang *et al.*, 2005). Several studies have indicated that the exogenous application of ALA can effectively promote plant growth and aid the stress tolerance of plants (Korkmaz *et al.*, 2010; Liu *et al.*, 2013a; Naeem *et al.*, 2012; Youssef and Awad, 2008). For example, Nunkaew et al. found that applying the broths of *R. palustris* TK103 and PP803 could promote the growth of rice under high-salt conditions due to the high ALA content (Nunkaew *et al.*, 2014).

As described above, PS3 and YSC3 exhibited a very close phylogenetic relationship and shared several conserved regions and genetic arrangements in their chromosomes. The conservation of genetic arrangement is usually used to predict functions of protein-coding genes (Tamames, 2001). Although we identified many putative genes that were associated with known PGP traits in both *R. palustris* strains, only PS3 can successfully promote the growth of plants (Wong *et al.*, 2014). Previous studies have indicated that root exudates can regulate transcription in PGPR (Wu *et al.*, 2015; Yuan *et al.*, 2015; Zhang *et al.*, 2015b). As shown in Figure 2-13 and Figure 2-14, root exudates of Chinese cabbage had an effect on microbial activities such as biofilm formation as well as on gene expression patterns specific to flagella-related

doi:10.6342/NTU202003422

genes (*fliM, fliB, fliE*) and chemotaxis-related genes (*cheR, cheW,* and *cheA*) of PS3 and YSC3. Flagella of bacteria are primarily involved in cellular motility but also have sensory functions to sense changes in the environment (Chilcott and Hughes, 2000). *C*hemotaxis is the movement of bacteria in response to stimuli; the bacteria move toward favorable chemicals or away from unfavorable chemicals (Wadhams and Armitage, 2004). Furthermore, as the transcriptomic data shown in Figure 2-16, the genes related to biofilm formation, flagellar biosynthesis or switch were significantly induced in PS3 strain in the presence of root exudate. It could be speculated that PS3 strain could sense the root exudate components secreted from plants and activated its cell motility related genes via methyl-accepting proteins, then swum to the root surface for attachment. Thereafter, the genes involved in metabolism of various substrates were induced, and the genes related to biofilm formation in PS3 were up-regulated and stimulated its cell aggregation, thus allowing the colonization of PS3. Finally, the genes associated to PGP functions were stimulated and contributed to plant growth promoting traits. Therefore, I deduced that the differences in the effectiveness of PGP by the two bacterial strains was due to the different physiological responses of these strains to specific compounds in the root exudates that act as signal molecules.

Recent studies have indicated that quorum sensing (QS) by PGPR is involved in biofilm formation, plant colonization and PGP and in triggering induced systemic resistance (Jung *et al.*, 2017; Zuniga *et al.*, 2017; Zuniga *et al.*, 2013). These beneficial effects are mediated via QS signaling molecules, such as N-acylhomoserine lactone (*AHL*), which regulate gene expression in response to bacterial population density and interactions with the plants(Degrassi *et al.*, 2002; Imran *et al.*, 2014). Surprisingly, *R. palustris* uses *p*-coumaroyl-HSL (pC-HSL), an aryl-HSL, as a signaling molecule (Schaefer *et al.*, 2008). The pC-HSL synthase was also identified in the genomes of the PS3 and YSC3 strains (RPPS3_03320 and RPYSC3_03390). The

doi:10.6342/NTU202003422

synthesis of pC-HSL requires an exogenous source of *p*-coumarate, which is usually present in root exudates (Badri and Vivanco, 2009; Eisenhauer *et al.*, 2017). Accordingly, we inferred that this aromatic compound triggers the synthesis of the QS molecule of *R. palustris* and mediates interactions with the plant host. pC-HSL is conserved in PGPR strains other than *R. palustris*, such as *Bradyrhizobium* BTAi1 (Schaefer *et al.*, 2008). Therefore, it is possible that *R. palustris* can use pC-HSL to have beneficial effects on plant growth.

This is the first study to carry out a comparative analysis of *R. palustris* strains that are effective and ineffective in PGP. The PS3 and YSC3 strains are closely related to each other and have similar genomic structures and compositions. Although these strains have many plant growth promoting genes in common, only the former exhibited PGP. This result suggests that the presence of PGP-associated genes in a bacterium is not sufficient for the bacterium to have beneficial effects on plant growth. Rather, physiological responses to the presence of plant hosts and successful establishment of interactions with the host appear to be a critical step. To elucidate the underlying molecular *mechanisms* associated with PGP by *R. palustris* PS3, further experiments are needed. For example, gene deletion and parallel analyses can be used to determine the phenotypic and functional properties associated with plant-bacteria interactions.

doi:10.6342/NTU202003422

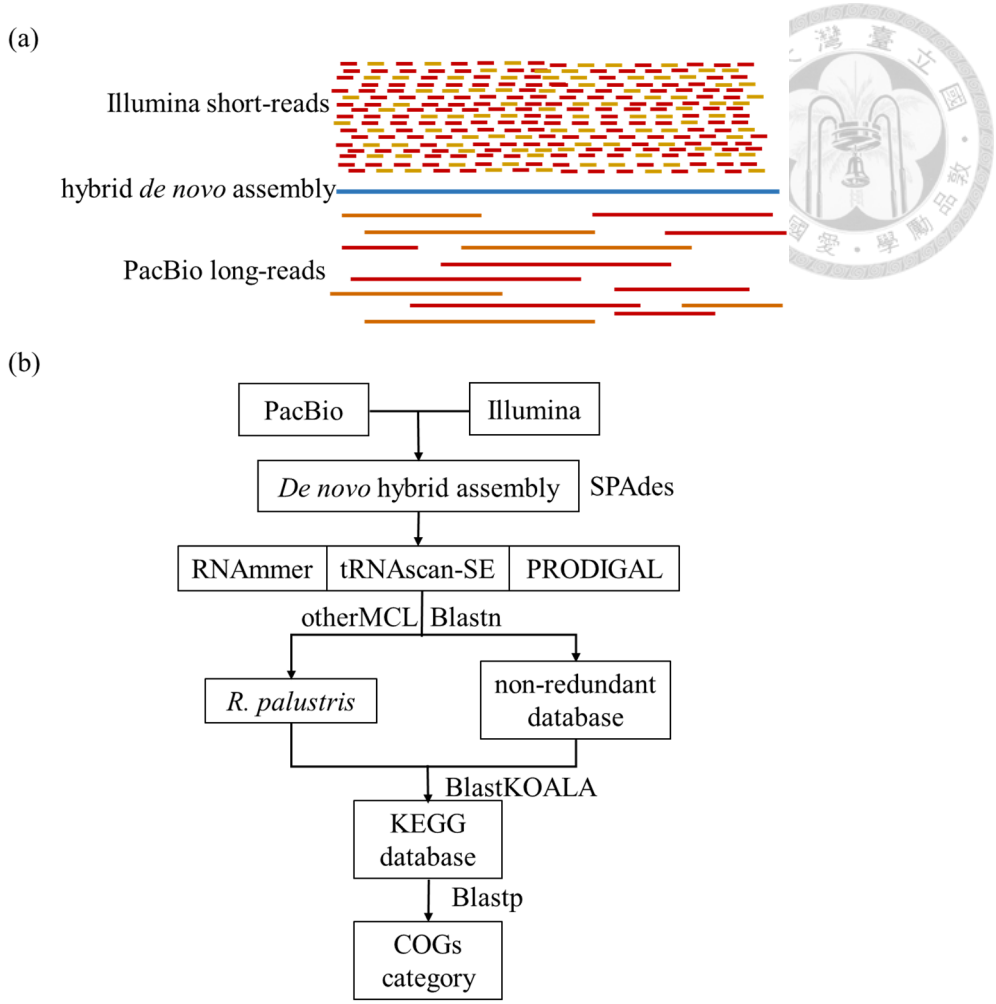

Figure 2-1. Assembly scheme and annotation pipeline in this study (modified from (Lo and Liu, 2020). (a) Scheme of hybrid *de novo* assembly of *R. palutris* genome with Illumin short-reads and PacBio long-reads. (b) flowchart for whole genomic sequencing and protein-coding genes prediction: 1. raw reads of genomic sequences were obtained from shotgun (MiSeq platform, Illumina) and single molecule real-time (SMRT) (PacBio RSII platform, Pacific Biosciences) sequencing. Hybrid *de novo* assembly was performed by SPAdes Genome Assembler version 3.5 (Bankevich *et al.*, 2012). rRNA, tRNA and protein coding genes were predicted by RNAmmer (Lagesen *et al.*, 2007), tRNAscan-SE (Lowe and Eddy, 1997), and PRODIGAL (Hyatt *et al.*, 2010). Initially functional genes annotation was performed by OrthoMCL (Li *et al.*, 2003) with BLASTP (Camacho *et al.*, 2009) against homologous genes database. Then, BLASP (Camacho *et al.*, 2009) searches against the NCBI non-redundant (nr) protein database. Finally, putative genes were against the KEGG database to correct the annotation by BlastKOALA (Kanehisa *et al.*, 2016). Finally, functional categorization were performed by BLASTP (Camacho *et al.*, 2009) searches against the Clusters of Orthologous Groups (COGs) functional category database as described by Galperin et al (Galperin *et al.*, 2015).

doi:10.6342/NTU202003422

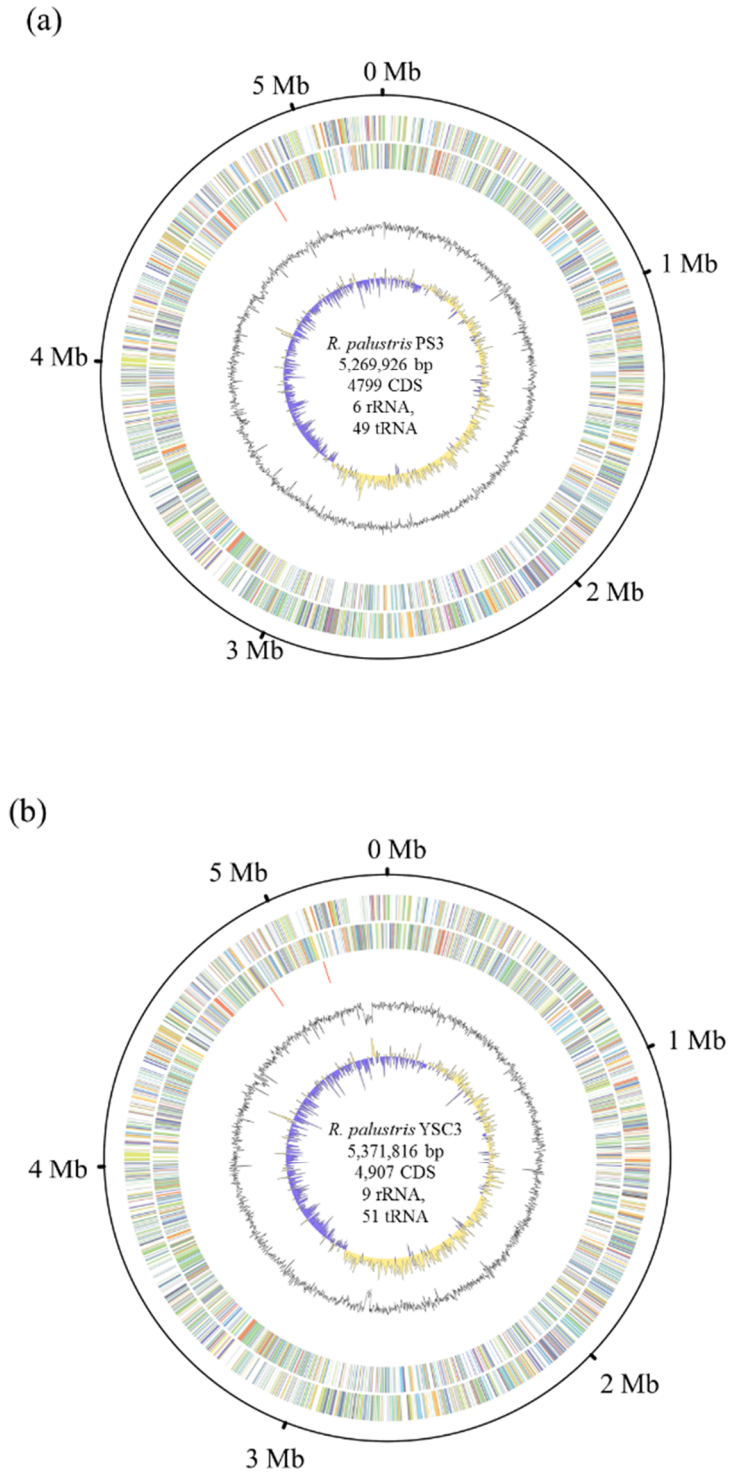

Figure 2-2. Genome map of *R. palustris* PS3 (a) and YSC3 (b). Rings from the outside are scale marks (unit, Mb), genomic island, protein-coding genes on the forward strand colored by COG category, protein-coding genes on the reverse strand (same color scheme as the second circle), rRNA genes, GC content (deviation from average), and GC skew in blue (below average) and yellow (above average)

doi:10.6342/NTU202003422

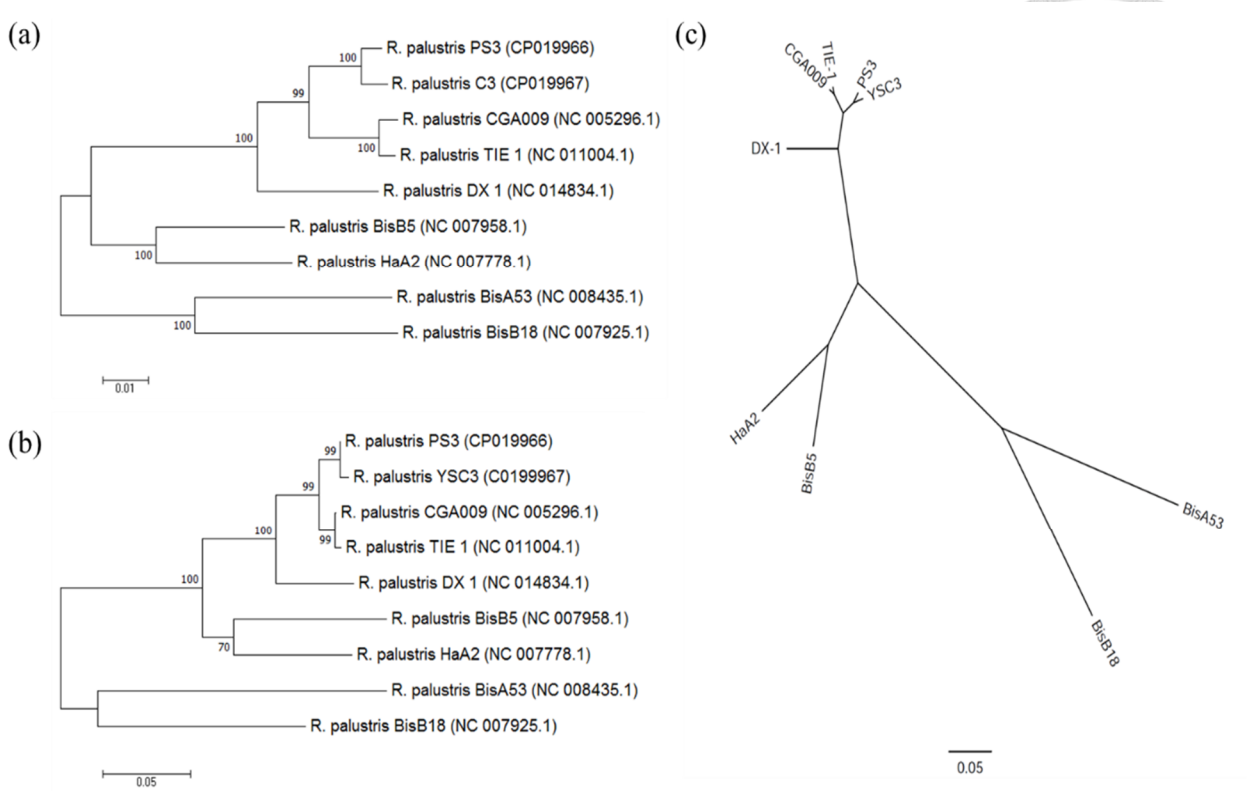

Figure 2-3. Phylogenetic tree of *R. palustris* strains based on housekeeping, functional genes and conserved amino acid sequences. Maximum-likelihood tree based on concatenated *recA-rpoB-dnaK* gene sequences (a), *puf* gene sequences (b) and concatenated amino acid sequences of 2,515 single-copy conserved genes shared in *R. palustris* strains (c), which show the relationships among the genus *Rhodopseudomonas*. All of the bootstrap values (1000 replicates) are given at branch points and generated in MEGA7.

doi:10.6342/NTU202003422

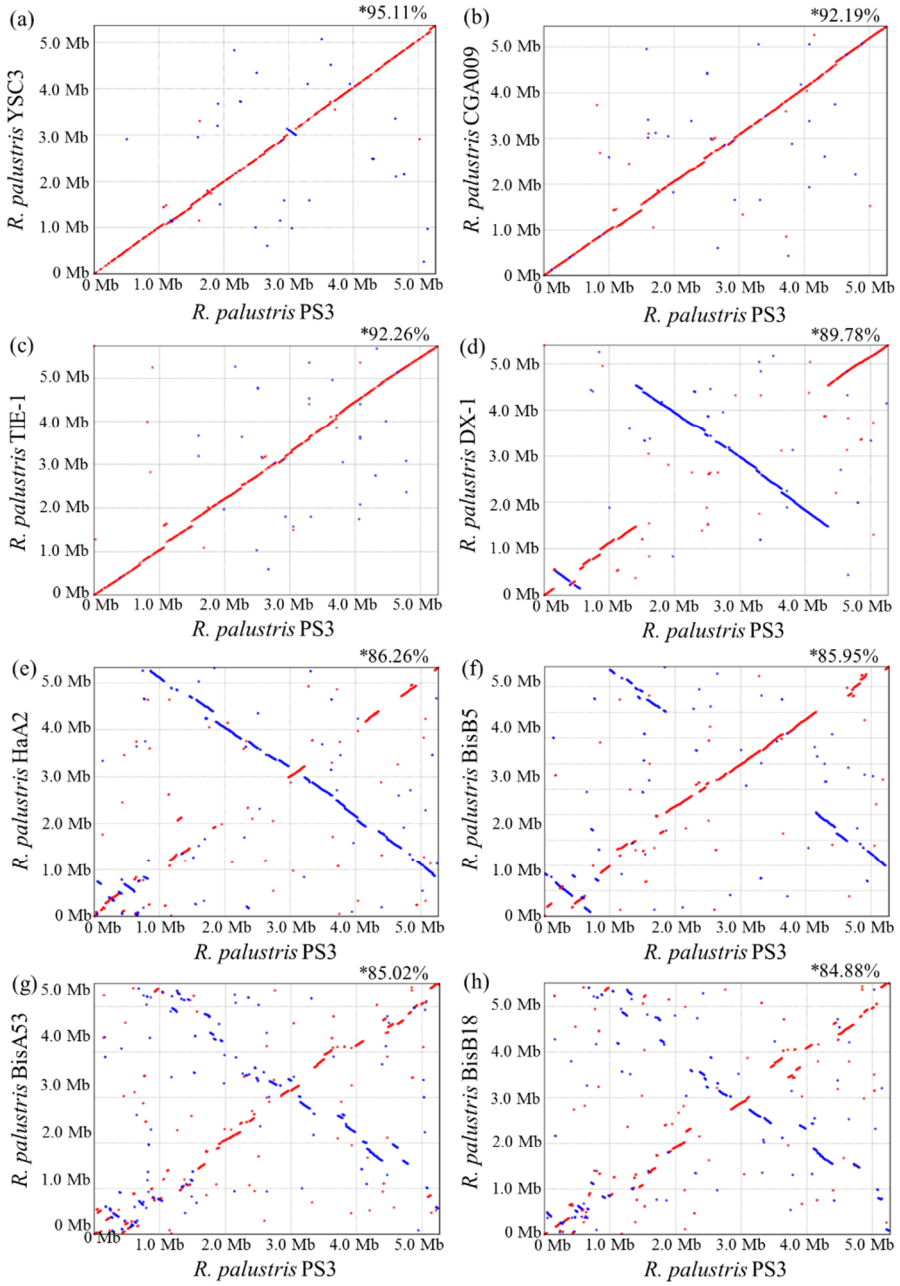

Figure 2-4 Pairwise genome alignments between *R. palustris* PS3 and other related strains. Synteny plots show the comparison of the PS3 genome (each vertical axis) with the genomes of *R. palustris* (each horizontal axis). Forward matches are plotted in red, and reverse matches are plotted in blue. "*" indicates the sequence similarities that were calculated based on nucleotides.

doi:10.6342/NTU202003422

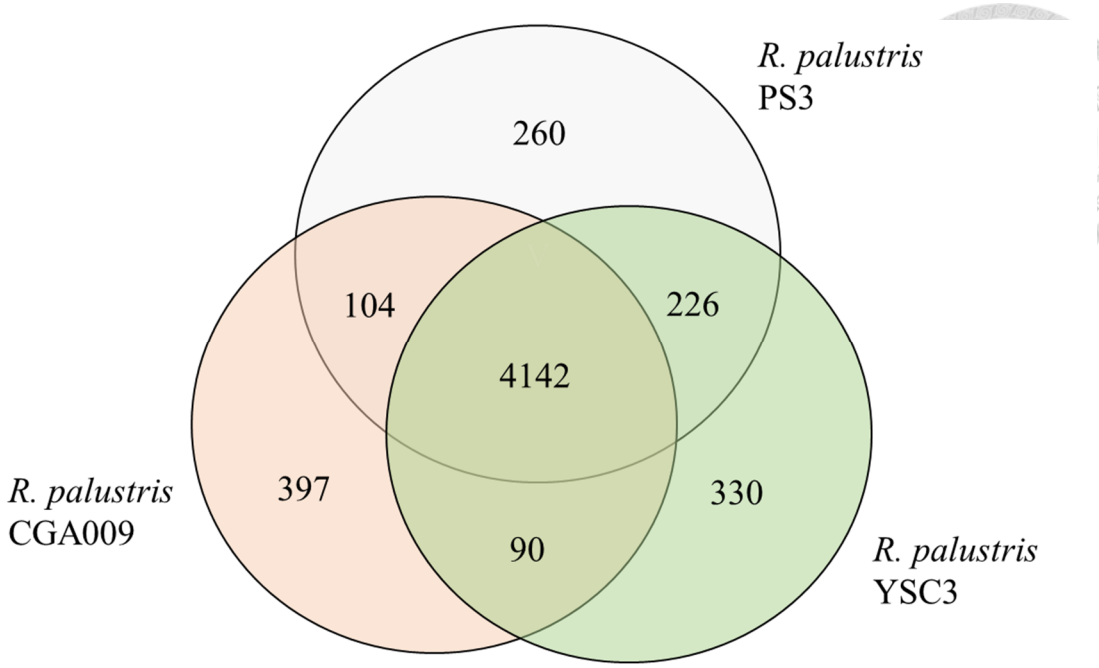

Figure 2-5. Distribution patterns of homologous gene clusters. The homologous gene clusters are those located at the intersection of *R. palustris* PS3, YSC3 and CGA009.

doi:10.6342/NTU202003422

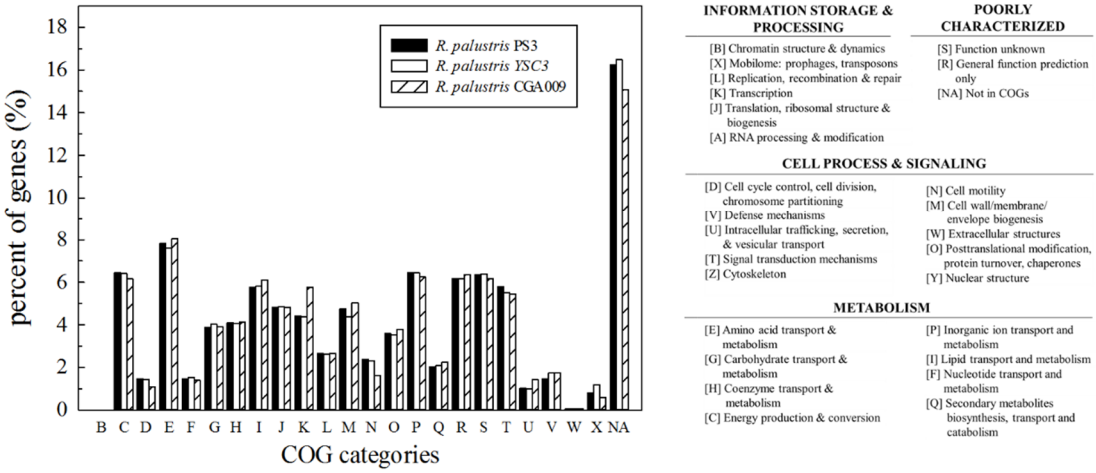

Figure 2-6. COG categories in the three *R. palustris* strains. Functional categorization of genes was performed by the COG database (Galperin *et al.*, 2015).

doi:10.6342/NTU202003422

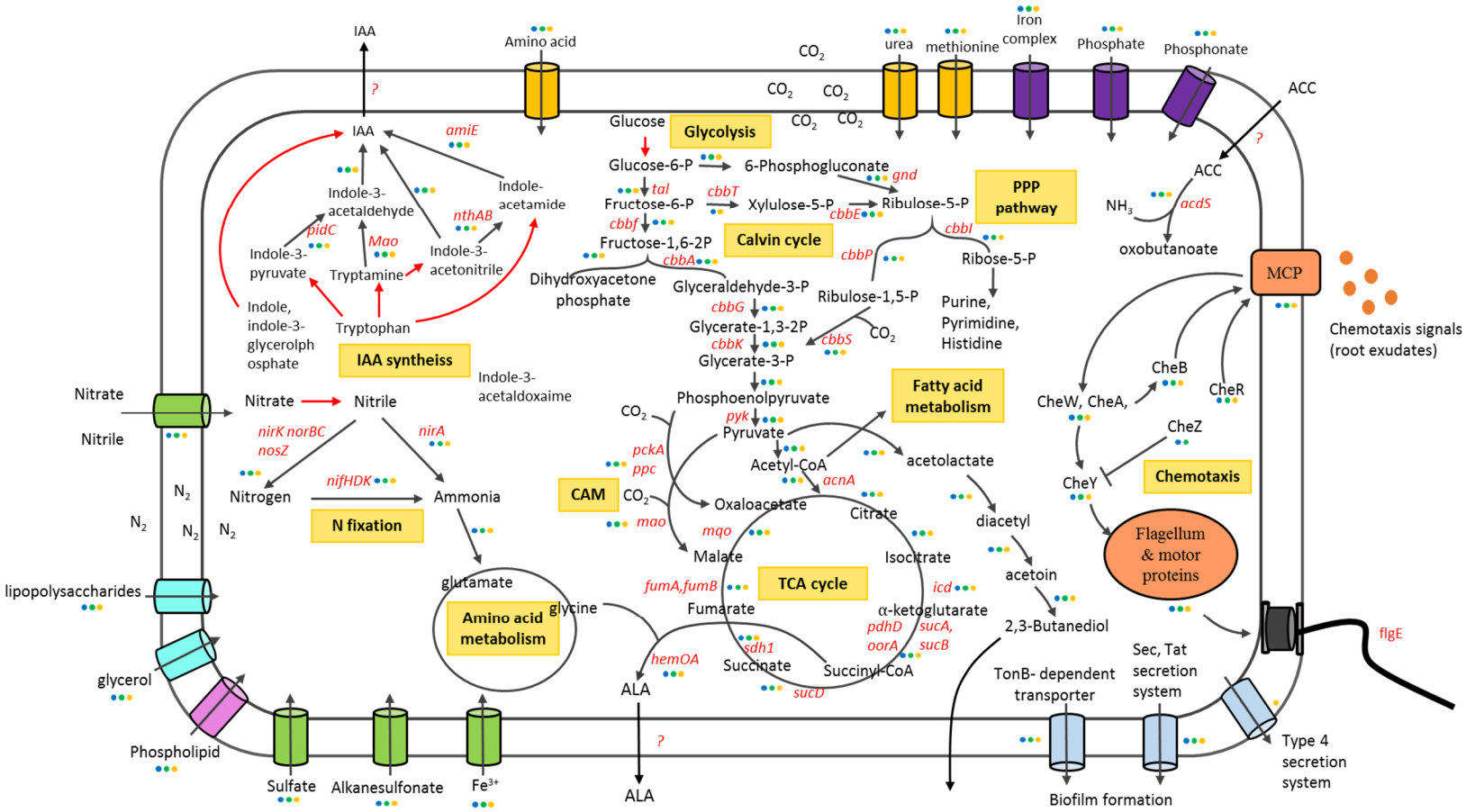

Figure 2-7. Schematic depiction of genes involved in metabolism (PPP pathway, TCA cycle, glycolysis, nitrogen assimilation), rhizosphere adaptation and plant growth promotion in *R. palustris*. Genes annotated in each strain are marked with colored circles representing PS3 (blue), YSC3 (green), and CGA009 (orange), respectively. Red arrows represent non-specific genes that were annotated among the three strains. "?" represents unknown function.

doi:10.6342/NTU202003422

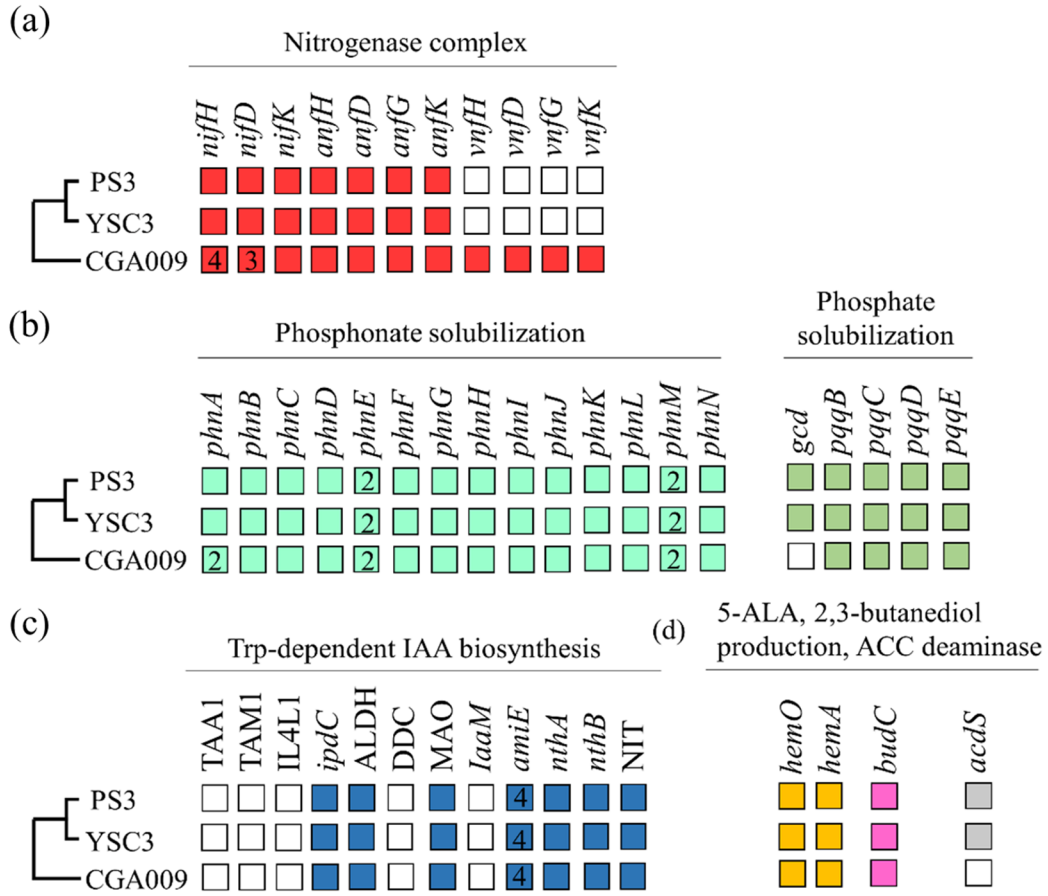

Figure 2-8. Putative genes related to plant growth-promotion in the genomes and biofilm production of PS3, YSC3 and CGA009 strains. The comparative summary of the presence (colored) and absence (empty) of genes for (a) nitrogenases, (b) phosphate solubilization, 5-ALA, 2,3-butanediol production, ACC deaminase and Trp-dependent IAA biosynthesis. The multi-copy genes are labeled by their copy number inside the filled square. (c) The biofilm production of *R. palustris* strains in tubes under static condition for 5 days. TAA1, tryptophan-pyruvate aminotransferase; TAM1, tryptophan aminotransferase; IL4L1, amino-acid oxidase; ALDH, aldehyde dehydrogenase; DDC, aromatic amino acid decarboxylase; TSO, tryptophan side-chain oxidase; MAO, monoamine oxidase; NIT, nitrilase.

doi:10.6342/NTU202003422

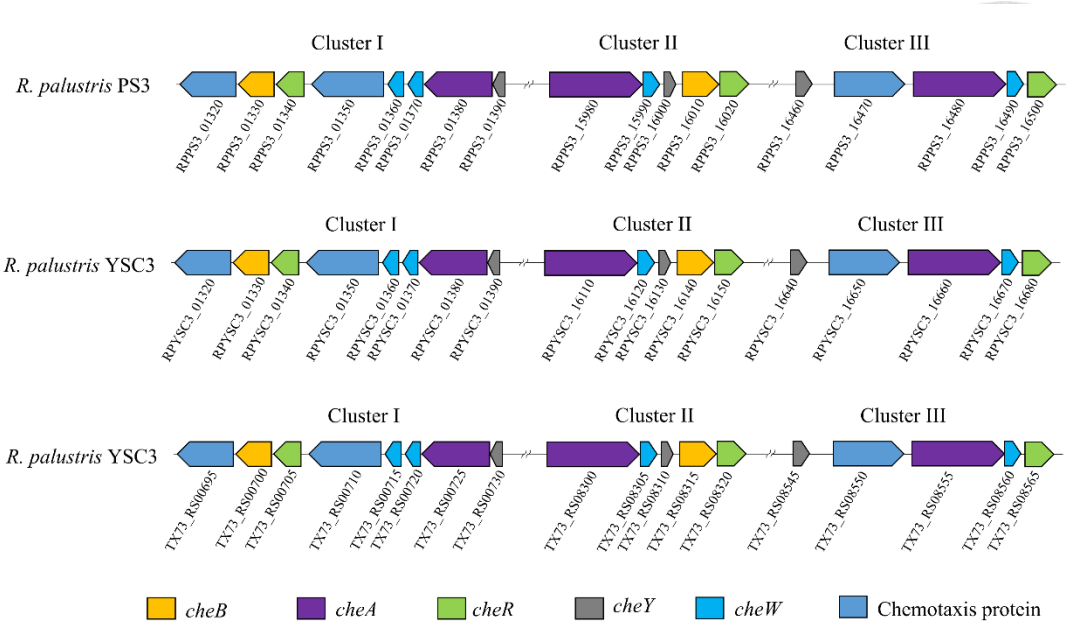

Figure 2-9. Comparison of the chemotaxis (*che*) gene clusters in *R. palustris* PS3, YSC3 and CGA009 strains. The chemotaxis genes were predicted in this study by BLASTP searches against the NCBI non-redundant (nr) protein database and KEGG database

doi:10.6342/NTU202003422

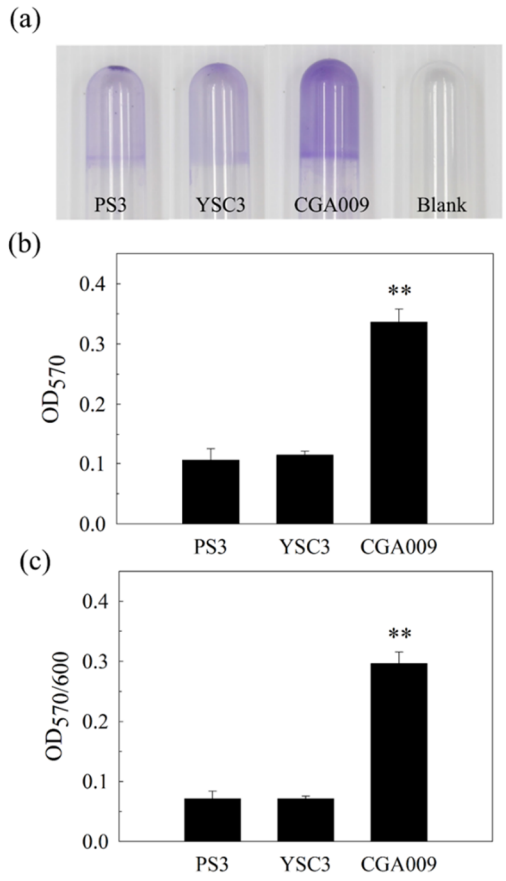

Figure 2-10. Qualification and quantification of biofilm formation assay in *R. palustris* PS3, YSC3 and CGA009. (a) The photograph of biofilm staining by 1% crystal violet. (b) Biofilm production and (c) biofilm productivity of *R. palustris strains*.

doi:10.6342/NTU202003422

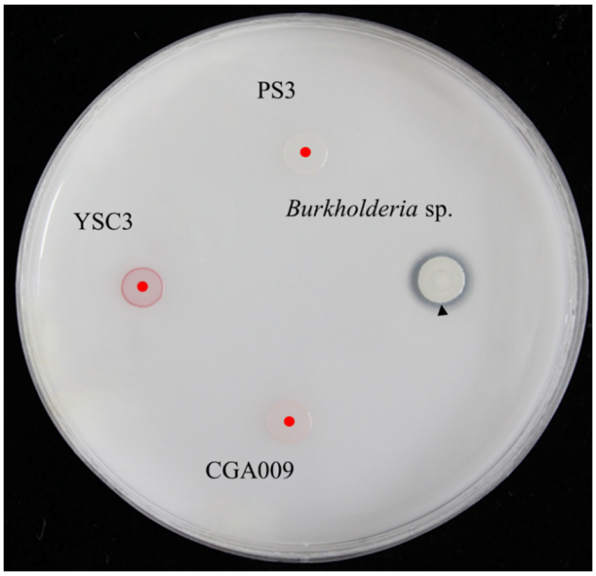

Figure 2-11. The phosphate solubilizing activity assay of *R. palustris* strains on the dissolve phosphorus agar (DPA) medium. The bacterial broths were dropped on the agar surface then incubated at 28°C for 3 days. *Burkholderia* sp. was used as positive strains and presence a clear zone around colony. The red points represent the location of *R. palustris* strains.

doi:10.6342/NTU202003422

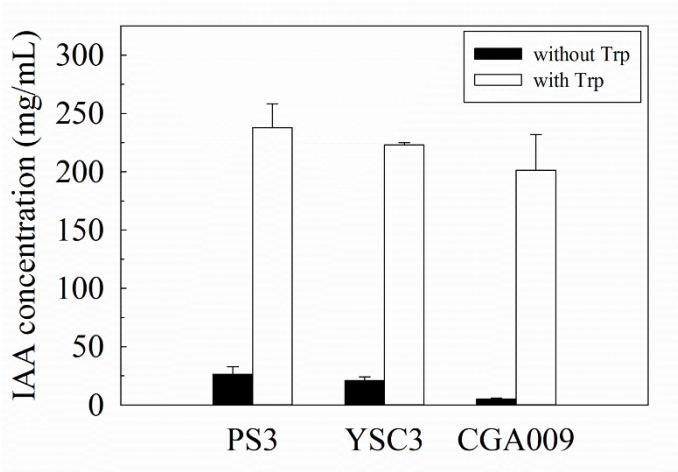

Figure 2-12 Indole-3-acetic acid production of *R. palustris* PS3, YSC3 and CGA009 strains. Indole-3-acetic acid was measured by high-performance 167 liquid chromatography with a C18 reverse column. Bar charts colored in gray and black 168 represent bacteria cultured in PNSB medium with/without tryptophan.

doi:10.6342/NTU202003422

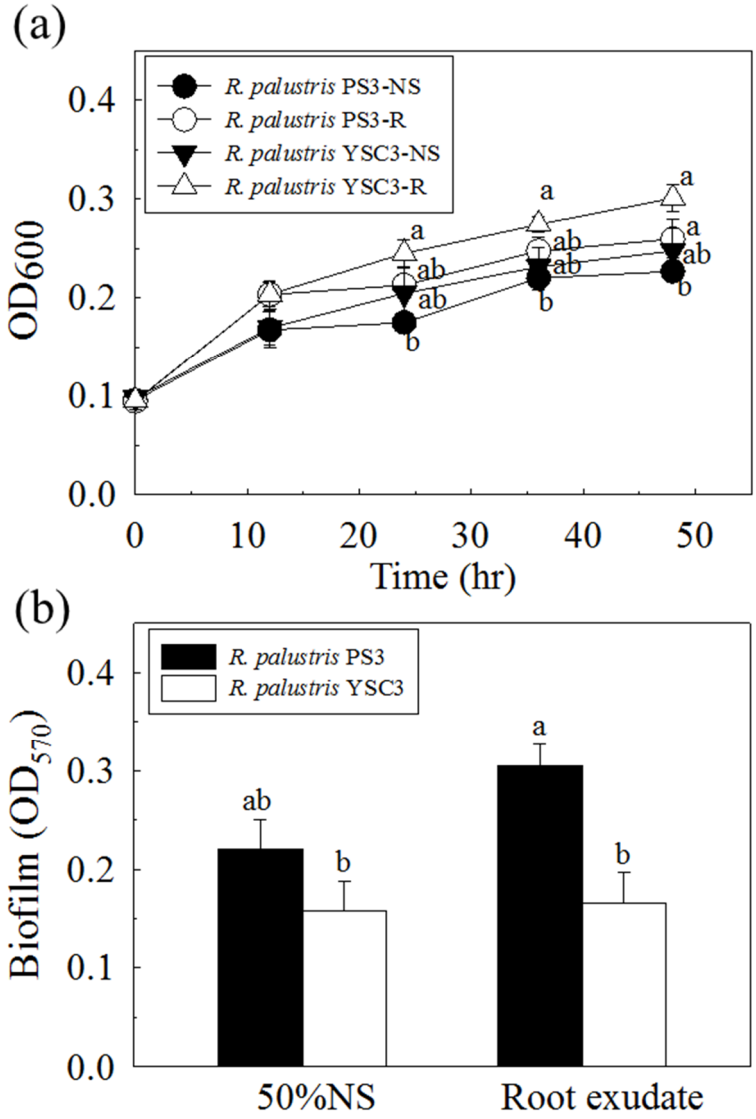

Figure 2-13. Effects of Chinese cabbage root exudates on growth and biofilm formation of the *R. palustris* PS3 and YSC3 strains. (a) Growth curve of *R. palustris* strains in half-strength Hoagland solution (NS) and root exudate solution. (b) Biofilm formation was evaluated by 0.1% crystal violet staining for 15 min at 24 h postincubation. Both *R. palustris* strains were incubated in either half-strength Hoagland NS or root exudate solution (10% (v/v)). The letters indicate statistically significant differences based on Student's t-test ($P < 0.05$).

doi:10.6342/NTU202003422

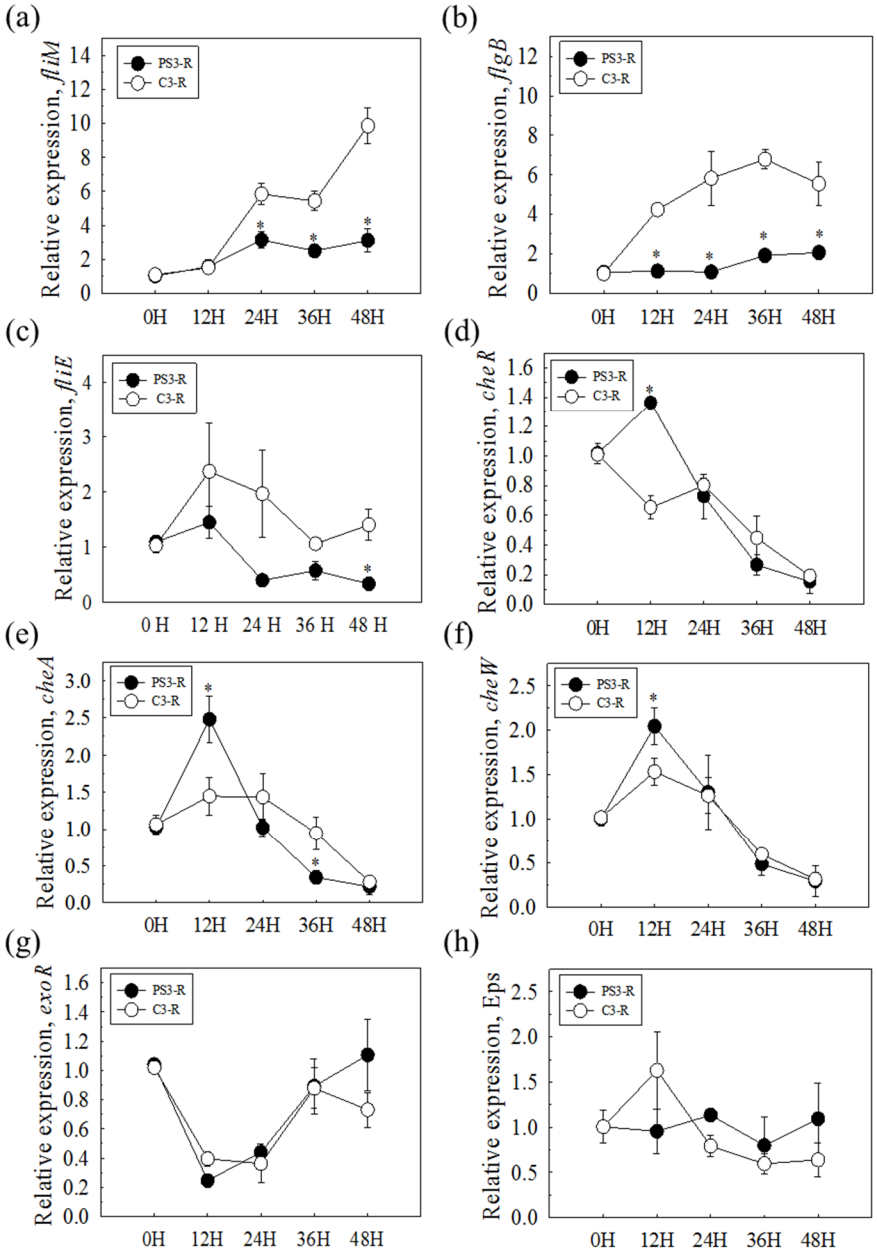

Figure 2-14. Genes expression patterns of *R. palustris* strains in response to Chinese cabbage root exudate solution. *R. palustris* strains were incubated with Chinese cabbage root exudates, and then, the expression of flagella (*fliM*, *flgB*, *fliE*), chemotaxis (*cheR*, *cheW*, *cheA*) and biofilm formation genes (Eps and *exo*) were determined by qPCR relative to an internal control gene, *clpX*. Relative expression values (SE) were obtained from three biological repeats and measured for three technical repeats. Asterisks indicate significant differences based on Student's t-test ($P < 0.05$).

doi:10.6342/NTU202003422

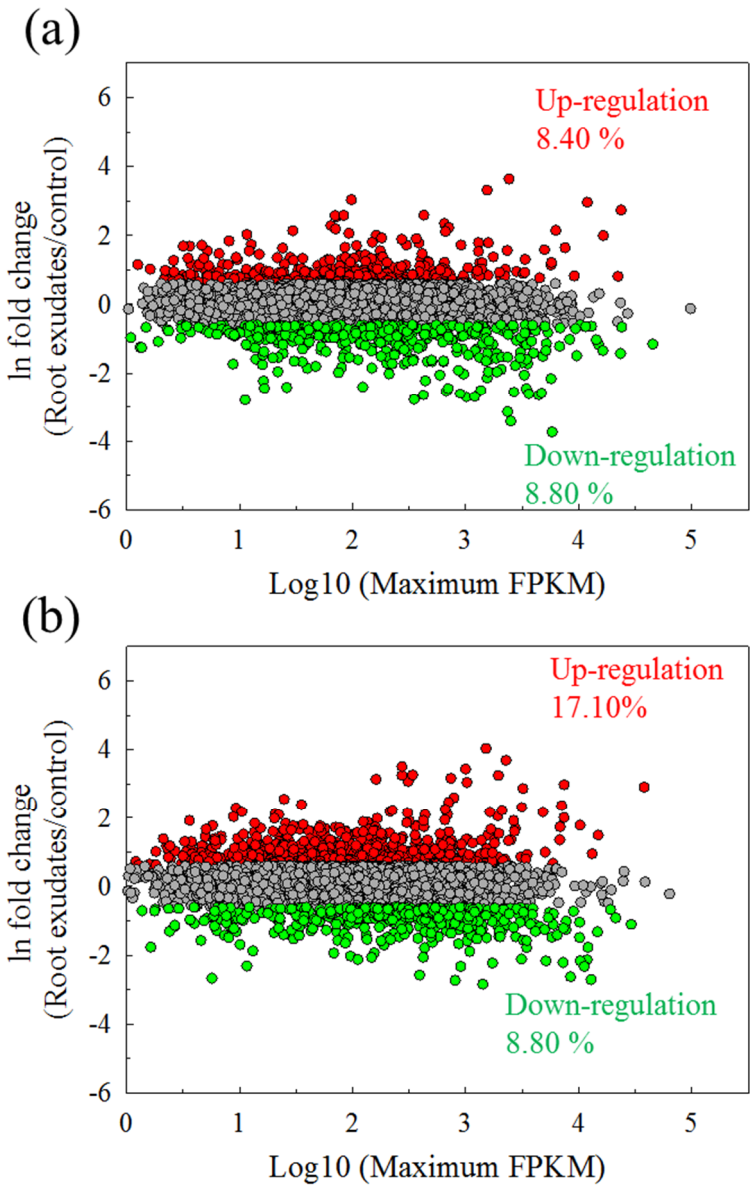

Figure 2-15. Genome-wide analysis of gene expression patterns in *R. palustris* PS3 (a) and YSC3 (b) strains in the presence of root exudates at 24 h. Every point represents the fold change for individual gene expression levels derived from those in the presence versus those in the absence of root exudate. FPKM represents the fragments per kilobase unique exon sequence per megabase of library mapped. Gray color denotes genes with no significant differences between the two transcriptomes, red color shows the up-regulation and green color means down-regulation.

doi:10.6342/NTU202003422

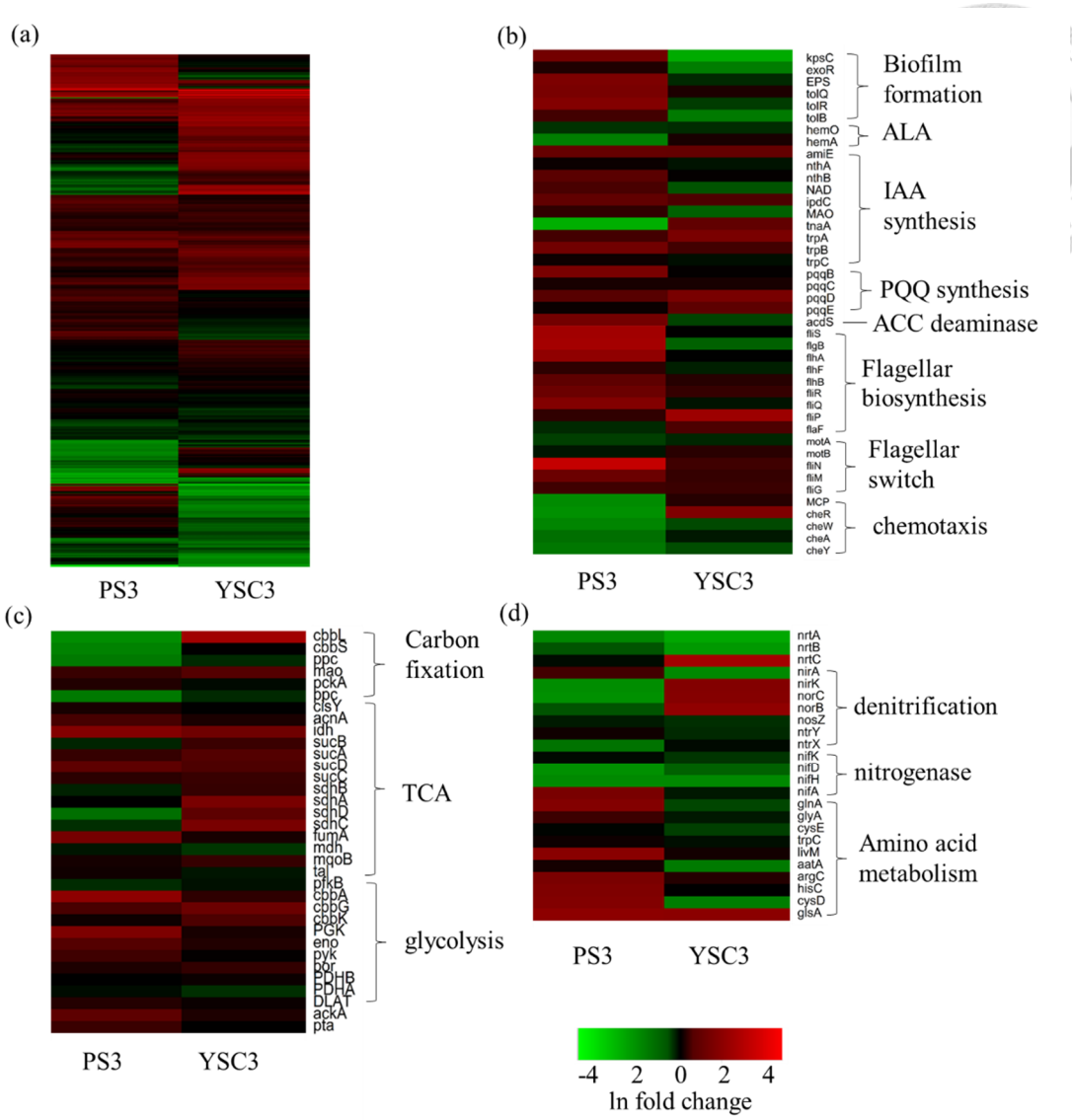

Figure 2-16. Gene expression profiles of *R. palustris* PS3 and YSC3 strains in response to root exudate for overall view and several representative categories. (a) Overall view, (b) PGP related genes, (c) carbon metabolism and (d) nitrogen assimilation.

doi:10.6342/NTU202003422

Table 2-1 Primer sequences used and product sizes in this study.

Genes	Forward primer (5'→3') Reverse primer (5'→3')	Amplicon size (bp)	References
clpX	GCGGTCCACAATCACTACAA TGTTCGACTTCGCCAGTTC	73	(Bose and Newman, 2011)
flgB	ATAACAAGGGCGGCTTCC GGCGTAGTCCATCTGGTTG	95	This study
fliM	TGCACATCGACATGGAAGA GGTTCGATCGTGGCGTAT	67	This study
fliE	TTCGGCAACCTGGTCAAG TCACCACATCCATCACGTT	111	This study
cheR	TTGCCGAACTGATCGAAGA AGCATCAGACGTTTGGCATT	61	This study
cheW	GTAACGATCGGGTTCAAAGC GAGTCCGATCATCACCACCT	68	This study
cheA	TCTCGTGACCGTGAAGGAC GGAACTGATGGATTTCCTGGT	122	This study
exoR	GCTGTTCAACGGCGAGAAG AAGGCCTTGTTGTAGCTGTC	120	This study
eps	CGGTCGAAGTGGAATCGTAT GCGCTCTCGACGCTCATA	97	This study

doi:10.6342/NTU202003422

Table 2-2 Whole genome information of PGPR strains. Table was made by Lo and Liu (Lo and Liu, 2020).

Species	Strain	Genome size (bp)	GC content (%)	Number of CDSs	Reference
Azospirillum humicireducens	SgZ-5T	6,834,379	67.55	5,969	(Yu et al., 2018)
Bacillus atrophaeus	GQJK17	4,325,818	43.30	4,181	(Ma et al., 2018)
Bacillus amyloliquefaciens	Co1-6	3,922,431	46.85	3,913	(Koberl et al., 2015)
Bacillus velezensis	FZB42	3,918,589	46.40	3,693	(Chen et al., 2007)
	SQR9	4,117,023	46.10	4,078	(Zhang et al., 2015b)
Bacillus pumilus	TUAT1	3,723,433	41.40	3,778	(Okazaki et al., 2019)
Bradyrhizobium japonicum	USDA110	9,105,828	64.10	8,317	(Kaneko et al., 2002)
Burkholderia sp.	B-AU4i	9,267,974	66.00	8,649	(Martina et al., 2018)
Enterobacteriaceae spp.	CPCRI-1	4,475,442	56.00	4,056	(Gupta *et al.*, 2014)
	CPCRI-3	4,669,355	54.80	4,286	(Gupta *et al.*, 2014)
Klebsiella sp.	D5A	5,540,009	57.15	4,999	(Liu *et al.*, 2016a)
Leifsonia xyli	SE134	3,596,761	70.02	3,466	(Kang et al., 2016)
Paenibacillus riograndensis	SBR5T	7,893,056	50.97	6,705	(Brito et al., 2015)
Pantoea agglomerans	P5	5,082,485	55.40	4,674	(Shariati et al., 2017)
Pseudomonas aeruginosa	M18	6,327,754	66.50	5,690	(Wu et al., 2011)
Pseudomonas chlororaphis	HT66	7,298,823	62.60	6,455	(Chen et al., 2015)
	GP-72	6,663,241	62.89	6,091	(Shen et al., 2012)
	30-84	6,665,021	62.90	5,869	(Chen et al., 2015)
	O6	6,977,251	62.80	6,236	(Chen et al., 2015)
Pseudomonas fluorescens	F113	6,845,832	60.80	5,862	(Redondo-Nieto et al., 2012)

doi:10.6342/NTU202003422

	PICF7	6,136,735	60.40	5,567	(Martinez-Garcia et al., 2015)
	Pf-5	7,074,893	63.30	6,142	(Paulsen et al., 2005)
	PCL1751	6,143,950	60.40	5,534	(Cho et al., 2015)
	SBW25	6,722,539	60.50	5.921	(Silby et al., 2009)
Pseudomonas protegens	CHA0	6,867,980	63.40	6,115	(Jousset et al., 2014)
Pseudomonas putida	S11	5,970,799	62.40	6,076	(Ponraj et al., 2012)
Pseudomonas sp.	UW4	6,183,388	60.10	5,423	(Duan et al., 2013)
Pseudomonas spp.	CPCRI-2	5,285,206	63.60	4,596	(Gupta *et al.*, 2014)
Pseudomonas stutzeri	A1501	4,567,418	63.88	4,135	(Li et al., 2010)
Rhizobium leguminosarum	Rlv3841	5,057,142	61.10	4,736	(Young et al., 2006)
Serratia marcescens	UENF-22GI,	5,001,184	59.70	4,528	(Matteoli et al., 2018)
Streptomyces albireticuli	MDJK11	8,144,417	72.80	6,550	(Wang et al., 2018)
Streptomyces alboflavus	MDJK44	9,622,415	72.10	7,285	(Wang et al., 2018)

doi:10.6342/NTU202003422

Table 2-3 Functional genes encoding PGPR traits. Table was made by Lo and Liu (Lo and Liu, 2020).

Function	Gene
Phosphate solubilization	*pqqB*, *pqqC*, *pqqD*, *pqqE*, *pqqF*, *pqqG*, *gcd*, *phnH*, *phnN*, *phnI*, *phnK*, *phnJ*, *phnG*, *phnA*, *phnP*, *phnB*, *phnL*, *phnO*, *phnE*, *phnF*
2,4-Diacetylphloroglucinol synthesis	*phlA*, *phlB*, *phlC*, *phlD*
Hydrogen cyanide synthesis	*hcnA, hcnB, hcnC*
Acetoine/2,3-butanediol synthesis	*budA, budB, budC*
Nitric oxide synthesis	*nirK*
Auxin synthesis	*ipdC, ppdC*
Cytokinin	*miaA*
Gibberellin	*cyp112*, *cyp114*, *cyp117*
ACC deamination	*acdS*
Nitrogen fixation	*nifD*, *nifH*, *nifK*
5-aminolevulinic acid synthesis	*hemA*, *hemL*
Enterobactin siderophore	*EntD*, *EntF*, *EntC*, *EntE*, *EntB*, *EntA*
Pyoverdines biosynthesis	*pvdA*, *pvdE*, *pvdF*, *pvdG*, *pvdH*, *pvdI*, *pvdJ*, *pvdM*, *pvdN*, *pvdO*, *pvdP*, *pvdQ*, *pvdS*
Pyochelin	*pchA*, *pchC*, *pchD*, *pchH*, *pchI*, *pchK*, *pchP*, *pchR*
Surfactin biosynthesis	*srfA*, *srfB*, *srfC*, *srfD*
BacillomycinD biosynthesis	*bmyC*, *bmyB*, *bmyA*, *bmyD*
Fengycin biosynthesis	*fenA*, *fenB*, *fenC*, *fenD*, *fenE*
Bacillibactin biosynthesis	*dhbA*, *dhbB*, *dhbC*, *dhbD*, *dhbE*, *dhbF*
Bacilysin/anticapsin biosynthesis	*bacA*, *bacB*, *bacC*, *bacD*, *bacE, ywfG*
Macrolactin biosynthesis	*mlnA*, *mlnB*, *mlnC*, *mlnD*, *mlnE*, *mlnF*, *mlnG*, *mlnH*, *mlnI*

doi:10.6342/NTU202003422

Bacillaene biosynthesis	*baeB*, *baeC*, *baeD*, *baeE, acpK, baeG*, *baeH*, *baeI*, *baeJ*, *baeL*, *baeM*, *baeN*, *baeR*, *baeS*
Difficidin biosynthesis	*dfnA*, *dfnY*, *dfnX*, *dfnB*, *dfnC*, *dfnD*, *dfnE*, *dfnF*, *dfnG*, *dfnH*, *dfnI*, *dfnJ*, *dfnK*, *dfnL*, *dfnM*
Gamma-aminobutyric acid biosynthesis	*gabD*, *gabT*
N-acyl homoserine lactone synthesis	*traI*, *raiI*, *cinI*, *sinI*, *melI*

doi:10.6342/NTU202003422

Table 2-4 General features of sequenced strains of *R. palustris*.

Feature	Accession	Size (bp)	G+C content	rRNA	tRNA	CDS	Plasmid
PS3	CP019966	5,269,926	65.30%	6	48	4,799	none
YSC3	CP019967	5,371,816	65.20%	6	48	4,907	none
CGA009	NC_005296.1	5,459,213	65.00%	6	49	4,841	1 (8,427 bp)
TIE-1	NC_011004.1	5,744,041	64.90%	6	51	5,355	none
DX-1	NC_014834.1	5,404,117	65.40%	6	49	5,019	none
HaA2	NC_007778.1	5,331,656	66%	3	49	4,792	none
BisB5	NC_007958.1	4,892,717	64.80%	6	49	4,397	none
BisA53	NC_008435.1	5,505,494	64.40%	6	49	4,993	none
BisB18	NC_007925.1	5,513,844	64.9	6	52	5,050	none

The characteristic analyses of genomes of *R. palustris* PS3 and YSC3 were performed in this study and other genomic data of *R. palustris* strains were download from NCBI database. CDS: Coding DNA Sequence. Data were collected on 06/28/2020.

doi:10.6342/NTU202003422

CHAPTER III

Development of A Low-Cost Culture Medium For Rapid Production of Plant Growth-Promoting *Rhodopseudomonas palustris* PS3 Strain

The content in Chapter III has been published in PLoS ONE as shown below. This first author publication and its quality full-filled the Ph.D. thesis examination application requirements of Institution of Biotechnology, National Taiwan University. This desertion or any part of it has not been submitted for any degree, diploma, or other qualification at any other university. It is the result of my own work except where mentioned in the text.

Lo, K.J., S.S. Lee, C.T. Liu. 2020. Development of a low-cost culture medium for the rapid production of plant growthpromoting *Rhodopseudomonas palustris* strain PS3. PLoS ONE 15(7): e0236739. doi: 10.1371/journal.pone.0236739

Authors Contribution

K.J. Lo, S.K. Lee and C.T. Liu conceived and designed research. K.J. Lo conducted experiments and contributed data analysis. K.J. Lo, S.K. Lee and C.T. Liu wrote the manuscript. All authors read and approved the manuscript.

doi:10.6342/NTU202003422

Summary

Rhodopseudomonas palustris PS3 is one of the purple phototrophic non-sulfur bacteria (PNSB), which have plant growth-promoting effects on various plants. To expand the scale of PS3 fermentation in a time- and cost-effective fashion, the purpose of this work was to evaluate the use of low-cost materials as culture media and to optimize the culture conditions via response surface methodology. Corn steep liquor (CSL) and molasses were identified as potential materials to replace the nitrogen and carbon sources, respectively, in the conventional growth medium. The optimum culture conditions identified through central composite design were CSL, 39.41 mL/L; molasses, 32.35 g/L; temperature, 38°C; pH, 7.0; and DO 30%. Under the optimized conditions, the biomass yield reached 2.18 ± 0.01 g/L at 24 hours, which was 7.8-fold higher than that under the original medium (0.28 ± 0.01 g/L). The correlation between the predicted and experimental values of the model was over 98%, which verified the validity of the response models. Furthermore, we verified the effectiveness of the *R. palustris* PS3 inoculant grown under the newly developed culture conditions for plant growth promotion. This study provides a potential strategy for improving the fermentation of *R. palustris* PS3 in low-cost media for large-scale industrial production.

Introduction

Rhodopseudomonas palustris is one of the purple phototrophic non-sulfur bacteria (PSNB). Since it can process nutrients through various metabolic pathways, such as photosynthetic, photoheterotrophic, chemoheterotrophic and chemoautotrophic pathways, *R. palustris* can inhabit a variety of environments (Larimer *et al.*, 2004). It is already known that *R. palustris* contains many useful characteristics and is broadly used in industry for bioremediation, sewage treatment, removal of phytotoxic compounds, etc. (Austin *et al.*, 2015; Idi *et al.*, 2015). This strain is able to convert

doi:10.6342/NTU202003422

complex organic compounds into biomass and bioenergy, regardless of whether the substrates are plant-derived, pollutant or aromatic compounds (Larimer *et al.*, 2004; Liu *et al.*, 2015; Oda *et al.*, 2003; Shi *et al.*, 2014; Zhang *et al.*, 2015a). *R. palustris* has also been reported to act as a promising biofertilizer for promoting crop yield and improving soil fertility (Kornochalert *et al.*, 2014; Nunkaew *et al.*, 2014; Wong *et al.*, 2014). Previously, we isolated an *R. palustris* strain, called as the PS3, from Taiwanese paddy soil that not only had beneficial effects on plant growth but also enhanced the efficiency of the uptake of the applied fertilizer nutrients (Hsu *et al.*, 2015; Wong *et al.*, 2014). Accordingly, this strain has been considered an elite microbial inoculant for agricultural applications.

For the purpose of the commercialization or the large-scale field application of the selected microbes, fermentation production is an essential prerequisite. The yield per unit biomass of the mass production is influenced by several factors, such as the medium composition (carbohydrate and nitrogen sources, minerals, etc.), the culture conditions (pH, temperature, agitation and aeration, etc.) and the mode of fermentation (batch, fed-batch and continuous fermentations) (Yang, 2010). The scaling-up of microbial processes is commonly undertaken in lab-scale process development with expensive medium components such as yeast extract, beef extract, and peptone (Crater and Lievense, 2018). These high-cost media result in a limitation on commercialization. To reduce the cost of fermentation, complex raw materials derived from plant and animal residues, as well as from agricultural and food industrial wastes, are mainly used (Thomsen, 2005). For example, cheese whey, corn steep liquor (CSL), corn syrup, distillery yeast, molasses, soybean and starch are widely applied (Cha *et al.*, 2007; Moraes *et al.*, 1991; Shamala *et al.*, 2012; Xiao *et al.*, 2007; Yang *et al.*, 2013). These relatively inexpensive raw materials have already been used as suitable nutrients for ensuring the growth of bacteria and for the production of different primary and secondary metabolites

doi:10.6342/NTU202003422

(Dhaliwal *et al.*, 2011; Liu *et al.*, 2010; Shen *et al.*, 2016; Yang *et al.*, 2013).

In order to optimize the growth and/or products formed by cells, the qualification and quantification of nutrimental and physical variables is required. In traditional, the optimization of fermentation processes is conducted using "one-factor-at-a-time" technique (Czitrom, 1999). Unfortunately, because the interaction effects of factors on the response are not considered in the procedure, it may fail to find out the region of optimum response (Bezerra *et al.*, 2008). Response surface methodology (RSM), also called the Box–Wilson methodology, is a useful tool to optimize the factors of fermentation processes by applying mathematics and statistics (Bezerra *et al.*, 2008). This technique is an experimental design based on the fit of a polynomial regression model for testing the multiple factors that influence the responses by varying the factors simultaneously, and fewer experiments are needed to study the effects of all factors (Yolmeh and Jafari, 2017; Zhang *et al.*, 2017). Through RSM, the interaction effects of individual factors can also be determined. The common experimental designs for RSM are central composite design (CCD) and Box-Behnken design (BBD). Although BBD has been suggested to reduce the number of trials required for a large number of variables, this advantage will disappear when in four or more factors (Bezerra *et al.*, 2008). Moreover, because CCD consists of a factorial or fractional factorial design with center points augmented with a group of axial points, it is often applied in sequential experiments and can be used in the estimation of model curvature (Bezerra *et al.*, 2008). Overall, the RSM procedure includes the selection of independent variables, the delimitation of the experimental factor region, the evaluation of the model's fitness, and finally, the attainment of optimum values and verification (Bezerra *et al.*, 2008; Yolmeh and Jafari, 2017).

The van Niel medium and modified van Niel medium have been designed for *R. palustris* fermentation (Dönmez *et al.*, 1999; van Niel, 1944). Du et al (Du *et al.*, 2003)

doi:10.6342/NTU202003422

cultivated *R. palustris* strain DH with the original van Niel medium for 7 days, and the derived biomass was ~0.3 g/L. Carlozzi and Sacchi (Carlozzi and Sacchi, 2001) incubated *R. palustris* strain 42OL in a modified van Niel medium to which sodium acetate was added, and the derived biomass was 1.42 g/L/d. Chang et al (Chang *et al.*, 2020) modified the original medium with sodium acetate and peptone, and the derived biomass of *R. palustris* strain YSC3 was 0.36 g/L after 2 days of incubation. However, the use of these media may be uneconomical for industrial application due to their high cost and long incubation time. The cost is primarily due to expensive nitrogen sources, such as yeast extract and peptone. On the other hand, some media have low-cost sources; for example, Xu et al (Xu *et al.*, 2013) used *Stevia* residue extractions supplied with NH_4Cl as a medium to culture *R. palustris*, and the highest obtained biomass was 1.5 (OD_{660}) (approximately equivalent to 0.77 g/L) after 96 hours of cultivation. Kornochalert et al (Kornochalert *et al.*, 2014) obtained the 0.9 g/L *R. palustris* in latex rubber sheet wastewater supplied with pineapple extract after 96 hours of fermentation. In our previous study, we used a modified van Niel medium with malate and yeast extract as the carbon and nitrogen sources for the fermentation of *R. palustris* PS3, and the biomass was 0.07 g/L after 24 hours of cultivation. Although this broth showed promising plant growth-promoting effects on several crops (Hsu *et al.*, 2015; Lee *et al.*, 2016; Wong *et al.*, 2014), the cost was too high for industrial application. Therefore, the purpose of this study was to develop an optimal fermentation protocol for *R. palustris* PS3 that is cost-effective, results in high biomass yield, and has a short fermentation time. We evaluated some agro-industrial by-products, including corn steep liquor (CSL), beetroot extract (BRE), soybean flour (SF), soybean protein isolate (SPI), molasses and corn starch, for use as substrates for *R. palustris* PS3 cultivation in terms of cost reduction and tested them with RSM to obtain the optimal fermentation conditions. Furthermore, we inoculated the newly developed fermentation broth into

doi:10.6342/NTU202003422

plants to verify its plant growth-promoting effect. The process of RSM is shown as Figure 3-1.

Materials and Methods

Microorganism and bacterial preparation

R. palustris PS3 was isolated from Taiwanese paddy soil and showed promising beneficial effects on plant growth in our previous studies (Hsu *et al.*, 2015; Wong *et al.*, 2014). This bacterium was grown in 3 mL of modified van Niel medium (Wong *et al.*, 2014) (designated PNSB medium hereafter) at 37°C and 200 rpm. The PNSB medium consisted of KH_2PO_4 1.0 g/L, NH_4Cl 1.0 g/L, $MgSO_4 \cdot 7H_2O$ 0.2 g/L, $FeSO_4 \cdot 7H_2O$ 0.01 g/L, $CaCl_2$ 0.02 g/L, $MnCl_2 \cdot 4H_2O$ 0.002 g/L, $Na_2MoO_4 \cdot 2H_2O$ 0.001 g/L, yeast extract 0.5 g/L, and malate 5.0 g/L, pH=7.0. After 24 hours incubation, 2 mL of the above bacterial broth was incubated in a 250 mL Erlenmeyer flask containing 50 mL PNSB medium and then cultured at 37°C with shaking at 200 rpm. After 24 hours incubation, the bacterial broth was diluted with fresh PNSB medium and adjusted to an optical density approximately equal to OD_{600} = 1.0. This diluted bacterial broth was used as a seed culture for further experiments.

Measurement of cell growth

The population of PS3 cells was estimated by a standard plate count method. Enrichment culture broth was serially diluted by fresh PNSB medium, and spread onto PNSB agar plate. Incubated the plate at 37°C in the dark and then calculated the number of colony forming unit (CFU) per milliliter. On the other hand, the cell concentration was also measured by optical density with a spectrophotometer at 600 nm. The bacterial culture broth was diluted in distilled water to obtain an optical density less than 0.6, and the OD_{600} was multiplied by the dilution times. Biomass (grams per liter) was

doi:10.6342/NTU202003422

assayed from the OD_{600} value by using a calibration standard curve. Viable counts were determined by the plate counting method.

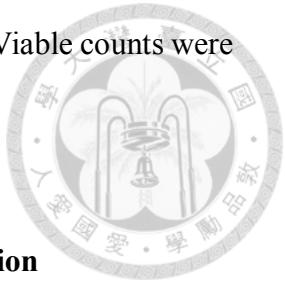

Screening of nitrogen and carbon sources for medium optimization

Different nitrogen (yeast extract, NH_4Cl, corn steep liquor (CSL) (TAIROUN PRODUCTS Co., Ltd., Taiwan), beetroot extract (BRE) (Hauert HBG Dünger AG, Switzerland), soybean flour (SF), soybean protein isolate (SPI) and NH_4NO_3) and carbon (malate, sodium acetate, glucose, fructose, molasses (TAIWAN SUGAR Co. Ltd., Taiwan) and corn starch (TAIROUN PRODUCTS Co., Ltd., Taiwan)) sources were used to optimize the composition of the PNSB medium. The initial concentrations of the individual carbon and nitrogen sources followed those in the PNSB medium described above and were sterilized separately by autoclave. For preliminary screening of alternative nitrogen sources, a final concentration of 1.5 g/L of each nitrogen-containing candidate material was introduced to substitute NH_4Cl (1.0 g/L) as well as yeast extract (0.5 g/L) in the presence of 5.0 g/L malate (carbon source). For preliminary screening of alternative carbon sources, a final concentration of 5.0 g/L of each carbon-containing candidate material was introduced to substitute malate (5.0 g/L) in the presence of CSL (1.5 g/L) as the selected nitrogen source.

For the experiments, the seed culture mentioned above was centrifuged at 3,000 rpm for 5 min at 4°C and then suspended in phosphate buffer solution (PBS). The final OD_{600} was adjusted to 1.0, inoculated (10% v/v) into 50 mL of the respective modified media in a 250 mL Erlenmeyer flask, and then cultured at 37°C with shaking at 200 rpm.

Evaluate the effects of fermentation factors on the growth of *R. palustris* by fractional factorial design (FFD)

doi:10.6342/NTU202003422

The effects of two medium components (carbon and nitrogen) and three fermentation conditions (dissolved oxygen (DO), temperature and pH) on *R. palustris* PS3 biomass production were investigated with a two-level fractional factorial design (FFD). The 2^{5-2} FFD was performed in R software with the package "rsm" and resulted in a total of 8 experiments (Lenth, 2009). Before performing a regression analysis, the factors will be normalized. Codification of the levels of variables needs transforming the real studied value to the range without dimension (-1 to +1). The various factors were coded according to the following equation, Eq. (3-1):

$x_i = \frac{E_i - E_0}{\Delta E_i}$ Eq. (3-1)

where X_i is the coded variable of the factor, E_i is study value of variable, E_0 is the real value of the variable at the center point, and ΔE_i is the step-altered value, which represents the difference from the real value in the higher or lower value from the real value at the central point. The various factors and levels for the FFD are shown in Table 3- 1.

For FFD, the variable levels, coded variables and experimental design and results are shown in Table 3-2. Here, X_1, X_2, X_3, X_4 and X_5 represent CSL, molasses, DO, temperature and pH, respectively. All of the experimental data for the FFD were fitted with a standard first-order equation by a multiple regression technique. The standard first-order regression equation is shown as follows, Eq. (3-2):

$Y = \beta_0 + \sum_{i=1}^{k} \beta_i X_i$ Eq. (3-2)

where Y is the predicted response of the biomass (g/L) of *R. palustris*, β_0 is the intercept, and β_i and X_i are the linear constant coefficients and coded independent variables for factors, respectively. The quality of fit of the first-order equation model to the data was analyzed by the coefficient of determination, R-squared, and ANOVA. The statistical software used was R, version 3.6.2 (R Core Team, 2019). All experiments

doi:10.6342/NTU202003422

were performed in a bioreactor.

Maximum region improvement of factors by steepest ascent method

To maximize the region of each factor and achieve a maximum for the response of interest, the path of steepest ascent method was applied in this study. The search direction and length of the step were estimated according to the ratio of coefficients in Eq. (3-3), and adjusted from the central operating conditions in FFD. Eq. (3-3) (shown in result section) was generated by data collected from FFD and fitted with first-order regression equation Eq. (3-2). The search direction and length of each factor were CSL 5 mL/L, molasses 3.82 g/L, temperature 0.7°C and pH -0.3, respectively. The experimental design and result are shown in Table 3-3. All experiments were performed in a bioreactor and fermentation was performed in 24 hours.

Construction of the response surface model by central composite design (CCD)

Based on the results of factor screening, the following independent variables, including the medium components (molasses and CSL) as well as the fermentation conditions (temperature and pH), were selected for optimization by central composite design (CCD). The CCD consists of three parts: a factorial design, a central points, and axial points (Bezerra *et al.*, 2008). In order to reduce the experimental trials, fractional factorial design was substituted for factorial design. For CCD construction, we performed a 2^{4-1} (four factors) fractional factorial design (FFD) using R software with the package “rsm”. Then, the design was augmented by eight axial points and four replications of the center points. This design resulted in a total of 20 experiments (Lenth, 2009). The distance of the axial points from the central point was developed by the software with the default settings (rotatable if possible)(Lenth, 2009). Before performing a regression analysis, the factors will be normalized. Codification of the

doi:10.6342/NTU202003422

levels of variables needs transforming the real studied value to the range without dimension (-1 to +1). The various factors were coded according to Eq. (1). The various factors and levels for the CCD are shown in Table 3-4. The matrix corresponding to the CCD and the total experimental data from 20 runs are shown in Table 3-5. The trail no. 1 to 8 represented fractional factorial design (FFD); trail no. 9 to 12 were attributed to center point; and trail no. 13 to 20 were referred as axial points. The experimental data of the CCD were fitted with a quadratic second-order polynomial equation by a multiple regression technique. The regression equation is shown as Eq. (3-4):

$$Y = \beta_0 + \sum_{i=1}^{k} \beta_i x_i + \sum_{i=1}^{k} \beta_{ii} x_i^2 + \sum_{i=1}^{k-1} \sum_{j=1+i}^{k} \beta_{ij} x_i x_j \quad \text{Eq. (3-4)}$$

where Y is the predicted response, β_0 is the intercept, and β_i, β_{ii}, and β_{ij} are the linear, quadratic and cross-interaction regression constant coefficients, respectively. x_i and x_j are the coded independent variables for factors. The quality of the fitting of the second-order equation model to the data was described by the coefficient of determination R-squared, and the statistical significance was evaluated by the F-test. The significance of the regression coefficients was analyzed by a t-test. The computer software used was R, version 3.6.2 (R Core Team, 2019).

Batch-culture experiments in a benchtop bioreactor

To perform the response surface methodology assay, a 5-L stirred tank bioreactor (BTF-A5L, BIOTOP Inc, Taiwan) was used to carry out all of the batch-culture experimental trials. We inoculated 300 mL of bacterial culture into 3 L of fresh medium. The conditions for molasses, CSL, temperature and pH value were set according to the experimental design matrix corresponding to the CCD described. The pH value of the cultures was controlled by pH-stat and automatically adjusted with 2 N NaOH and 2 N HCl.

doi:10.6342/NTU202003422

Quantification of total organic carbon

The total organic carbon in fermentation broth was quantified by Walkley-Black chromic acid wet oxidation method (Nelson and Sommers, 1982) with some modification. Weighed 5.0 g of fermentation broth into a 500 mL erlenmeyer flask. Add 10 mL of 0.1N $K_2Cr_2O_7$ and swirl the flask gently to disperse the sample in the solution. Rapidly, 20 mL of concentrated H_2SO_4 was added into above mix solution. Subsequently, the flask was stood on an insulated sheet for 30 min in a fume hood. After that, 200 mL of D.D. water was added into the flask and mix with 10 mL of 85% H_3PO_4. Finally, 30 drops of barium diphenylamine sulfonate indicator were added into above mix solution and titrated the solution with 0.5 M $(NH_4)_2$ $Fe(SO_4)_2$•$6H_2O$. At the end-point of titration, the color changes sharply to brilliant green. The total organic carbon (g/Kg) was calculated by equation as below Eq. (3-5):

$$Total\ organic\ carbon\ (g/Kg) = V \times \left(1 - \frac{V_s}{V_b}\right) \times \frac{12}{4 \times 1000} \times 1.3 \times \frac{1000}{sample\ (g)} \quad \text{Eq. (3-5)}$$

Where, the V is the volume of 0.1N $K_2Cr_2O_7$ (mL), V_s is the volume of titrant in 0.5 M $(NH_4)_2$ $Fe(SO_4)_2$•$6H_2O$ (mL) and V_s is the volume of titrant in blank, D.D. water (mL).

Quantification of total nitrogen

Quantification of total nitrogen was carried out by Kjeldahl method (Bremner and Mulvaney, 1982) with some modification. Weighted 1.0 g fermentation broth and mix with 1.g catalyst, which is consists of K_2SO_4, $CuSO_4$•$5H_2O$ and Selenium (100:10:1 in weight). After that, 10 mL concentrated sulfuric acid was added. The above mixture was heated for 2 hours. After cooling, the mixture was filtered to obtain the clear supernatant. The above 10 mL solution was mixed with 5 mL 10N NaOH and 0.2 g Devarda's Alloy, then this mixture was heated to liberate ammonia which is distilled

doi:10.6342/NTU202003422

by steam through a condenser, the tip of which is submerged in a flask containing 10 mL 2% boric acid containing Tashiro indicator (2 volume of 0.2% methyl red in 90% ethanol + 1 volume of 0.2% methylene blue in 90% ethanol). After the distillation was finished, titrate the ammonia with 0.1 N HCl. The total nitrogen was calculated according to Eq. (3-6) as shown below:

$$Total\ \ nitrogen\ (g/Kg) = \frac{(V_s - V_b) \times 0.09780 \times 14 \times V_{tse}}{W_S \times V_{se} \times recorver\ rate} \quad \text{Eq. (3-6)}$$

Where, V_s is the volume of titrant in 0.01N HCl, V_b is the volume of titrant in blank (D.D. water), V_{tse} is the volume of total sample extraction solution (one mL in this study), W_s is the weight of sample and V_{se} is the volume of reaction sample extraction (one mL in this study). Recover rate was calculated according Eq. (3-7) as shown in below, and 10 N NH_4Cl was used as standard reagent.

$$Recovery\ \ rate\ (\%) = \frac{(V_{std} - V_b) \times 0.09780 \times 14 \times 100\%}{C_{std} \times \frac{V_{STD}}{1000}} \quad \text{Eq. (3-7)}$$

Where, V_{std} is the volume of titrant in 10 N NH_4Cl, V_b is the volume of titrant in blank (D.D. water), 0.09789 is the standard equivalent concentration of 0.1 N HCl which was calibrated by titration with 0.1 N NaOH. C_{std} is the equivalent concentration of NH_4Cl (10 N) and V_{STD} is the volume (10 mL).

In planta experiments to verify the plant-growth promotion effect of the newly developed fermentation broth

Chinese cabbage seeds (*Brassica rapa* L. spp. *pekinensis* cv. "Michelle") were purchased from Formosa Farming Materials Co., Ltd. (Taipei, Taiwan). The seeds were immersed in 70% alcohol for 3 min and then in 3% hydrogen peroxide solution for 7 min for surface sterilization, followed by a thorough washing with sterile distilled water. These seeds were germinated for 1 day at 25°C in the dark. For hydroponic cultivation, well-germinated seeds were transferred to completely wet cotton and cultivated under

doi:10.6342/NTU202003422

continuous (24-h photoperiod) light-emitting diode (LED) light (~210 μmol $m^{-2}s^{-1}$). After one week, the seedlings were transferred to hydroponic tanks (35 L) in a plant factory facility (College of BioResources and Agriculture, National Taiwan University). Twenty-four seedlings were cultivated in each tank, and each tank was equipped with an air pump to homogenize the solution and maintain the dissolved oxygen. Hoagland's solution (0.51 g L^{-1} KNO_3, 0.49 g L^{-1} $MgSO_4$•$7H_2O$, 0.08 g L^{-1} NH_4NO_3, 0.068 g L^{-1} KH_2PO_4, 22.5 mg L^{-1} Fe-EDTA, 2.86 mg $L^{-1}H_3BO$, 0.051 mg L^{-1} $CuSO_4$, 0.22 mg L^{-1} $ZnSO_4$•$7H_2O$, 1.81 g L^{-1} $MnCl_2$•$4H_2O$, 0.12 mg L^{-1} Na_2MoO_4•$2H_2O$ and 1.18 g L^{-1} $Ca(NO_3)_2$•$4H_2O$) was used as a nutrient sources (Hoagland and Arnon, 1950). The concentrations of the hydroponic nutrient solution were measured by an electrical conductivity meter (EC meter) (Spectrum® Technologies, Inc.) and adjusted with concentrated hydroponic nutrient solution to maintain an EC value of 1.2-1.3 dS m^{-1}. The initial pH value of the hydroponic nutrient solution was adjusted by H_3PO_4 and 2N KOH to 7.0. The cultivation environment was set at 25°C, 70% humidity, and 210 μmol m^{-2} s^{-1} light intensity for 16 hours. We poured 250 mL of the liquid culture (OD_{600}= 0.1, equivalent to ~ 10^8 colony-forming units [CFU]/mL) into the tank, resulting in a final bacterial concentration of 10^6 CFU/mL. After seven days post inoculation (7 dpi), another 250 mL of the liquid culture was applied to each tank. Seventeen days after planting (DAP), the Chinese cabbages were harvested, and the fresh and dry weights were measured. For soil cultivation, well-germinated seeds were transferred to cultivatable soil under controlled illumination with a 16-hour photoperiod (~210 μmol $m^{-2}s^{-1}$). After one week, the seedlings were transferred to pots containing approximately 300 g cultivatable soil. The cultivation environment was set to be consistent with that under hydroponic cultivation. Two milliliters of the respective culture broth (OD_{600}= 0.1, equivalent to ~ 10^8 colony-forming units [CFU]/mL) and 0.05g chemical fertilizer were added into each pot once a week as described previously (Wong *et al.*, 2014). The

doi:10.6342/NTU202003422

chemical fertilizer was purchased from SINON Co., Ltd. (New Taipei City, Taiwan) which consists of 14% ammonium nitrogen, 15% citric acid-soluble Phosphorus (13.5% water-soluble phosphorus), and 10% water- soluble potassium. At 28 DAP, the Chinese cabbages were harvested, and their fresh and dry weights were measured.

Statistical analysis

Analyses of variance (ANOVA) were performed with R version 3.6.2 (R Core Team, 2019). Fisher's least significant difference (LSD) test was used for multiple range analyses to determine the significant differences between the groups of data. The results were considered significant at P = 0.05.

Results

Selection of appropriate components for optimization of *R. palustris* strain PS3 medium

Carbon and nitrogen sources provide important nutrients for bacterial growth. To screen suitable carbon and nitrogen sources for viable PS3 cell production, a "one-factor-at-a-time" method (OFAT, or single-variable *optimization* strategy) was used. I selected corn steep liquor (CSL), beetroot extract, soybean flour (SF), soybean protein isolate (SPI), and NH_4NO_3 as the individual nitrogen sources and malate, sodium acetate, glucose, fructose, molasses, and corn starch as the individual carbon sources. These materials are common, low-cost agro-industrial byproducts and are the most common nutrient sources in industrial fermentations (Liu, 2017; Thomsen, 2005). Figure 3-2 shows the effect of the different selected nitrogen and carbon sources on the growth of the *R. palustris* PS3 strain. In the presence of 5 g/L malate as single carbon source, the highest turbidity (OD_{600}) was observed when using SF or SPI as the sole nitrogen source, followed by that of the strain incubated with CSL, BRE and PNSB and

doi:10.6342/NTU202003422

that from fermentation in NH_4NO_3 (Figure 3-2a). As shown in Figure 3-2b, when using CSL as the sole nitrogen source, the cell viability of *R. palustris* PS3 was $1.14 \pm 0.72 \times 10^9$ CFU/mL, which was comparable to that with the original nitrogen source (NH_4Cl and yeast extract in PNSB medium) and higher than with the other nitrogen sources. Although the soybean flour (SF) and soybean protein isolate (SPI) also showed high OD_{600} values, their CFUs were dramatically lower than the others. This implied that the turbidities (OD_{600}) of these two microbial samples did not reflect the number of viable cells produced (CFU). This inconsistency may be attributed to their poor solubility in the individual media, which interfered with the turbidity readout. Accordingly, CSL is considered a potential nitrogen source for the production of *R. palustris* PS3. After 1.5 mL/L CSL was determined as the nitrogen source for the modified medium, we further screened appropriate carbon sources. It was found that molasses and sodium acetate significantly increased the biomass of *R. palustris* PS3 compared with those under the other carbon sources (Figure 3-2c), with OD_{600} values of 0.641 ± 0.033 and 0.628 ± 0.032, respectively. On the other hand, higher viable cell counts were present in the molasses and malate treatments than in the other treatments, and the biomass was approximately 10^9 CFU/mL (Figure 3-2d). I noticed that when sugars were used as carbons (i.e., glucose and fructose), the corresponding cell viability (CFU/mL) was significantly lower than that resulting from the use of organic acid (i.e., malate and sodium acetate) or molasses. Accordingly, molasses could be a suitable substrate to replace malate as a carbon source for *R. palustris* PS3 cultivation. Taken together, I selected CLS and molasses as nitrogen and carbon sources for future experiments.

Screening suitable fermentation conditions by FFD

I further evaluated the effect of some operating variables of fermentation (dissolved oxygen, pH value and temperature) on the growth of *R. palustris* PS3 via a

doi:10.6342/NTU202003422

two-level fraction factorial design (FFD) experiment. All of the experiments were performed in the 5 L desktop bioreactor as described above. The factor screening process and the experimental design for the range and levels of test variables, as well as results for the FFD are shown in Table 3-2. The experimental data were analyzed by ANOVA with a first-order regression model, Eq. (3-2). The results of the regression analyses are shown in Table 3-6 and were analyzed by Fisher's F-test and Student's t-test. Student's t-test was used to evaluate the significance of the factor regression coefficients. The proposed linear model for the biomass (g/L) of *R. palustris* PS3 is shown in Eq. (3-8).

$$Biomass\ (g/L) = 1.36149 + 0.393X_1 + 0.29241X_4 + 0.00226X_3 + 0.17893X_4 - 0.04288X_5 \quad \text{Eq. (3-8)}$$

The variables X_1, X_2, X_3, $X_4$and X_5 represent the CSL, molasses, dissolved oxygen, temperature and pH value, respectively. As shown in Table 3-6, the model *p* value is significantly lower than 0.05, and the coefficient and adjusted coefficient of determination R^2 were calculated to be 0.9999 and 0.9996, respectively. The coefficients of the factors are 0.76188 (CSL), 0.58188 (molasses), 0.00438 (dissolved oxygen), 0.34688 (temperature) and -0.08312 (pH), respectively (Table 3-6). In addition, for the regression *p* value, all of the target factors showed a significant effect except that of dissolved oxygen (DO). Therefore, I set the dissolved oxygen as constant at 30% for the subsequent experiments. To further identify the appropriate range of variables for RSM, I conducted the steepest ascent path method to clarify the levels of factors. The steepest ascent path was designed according to Eq. (3-8), and the results are shown in Table 3-3. The search direction and length of each factor were CSL 5 mL/L, molasses 3.82 g/L, temperature 0.7°C and pH -0.3, respectively. Based on the data, I found that the biomass significantly increased with each step, reaching 2.44 g/L in step 4. After step 5, the biomass of *R. palustris* PS3 dramatically decreased and was

doi:10.6342/NTU202003422

even lower than the original biomass.

Optimization of culture conditions by RSM

According to the results of the FFD, I took CSL, molasses, temperature and pH as the major variables affecting the performance of *R. palustris* PS3 growth. I conducted a four-coded-level central composite design (CCD) to optimize the levels of these variables. The corresponding experimental results of the CCD design are shown in Table 3-5 and were fitted with a second–order polynomial equation, Eq. (3-4). The proposed polynomial model for biomass production in *R. palustris* PS3 is shown in Eq. (3-9):

$$\text{Biomass (g/L)} = 4.2267 - 0.1918x_1 - 0.0562x_2 - 0.6582x_3 + 0.4321x_4 - 0.3882x_1^2 - 0.0442x_2^2 - 0.7315x_3^2 - 1.0302x_4^2 + 0.0165x_1x_2 - 0.1448x_1x_3 + 0.2340x_1x_4 \quad \text{Eq. (3-9)}$$

The variables x_1, x_2, x_3 and x_4 represent the CSL, molasses, temperature and pH value, respectively. The results of the regression analyses were evaluated by Fisher's *F*-test and Student's *t*-test. As shown in Table 3-7, the regression coefficients and corresponding *p* values of the linear terms of CSL, temperature, pH value and interaction terms between CSL and temperature or pH value had a significant effect on *R. palustris* PS3 biomass production (*p* value < 0.05). However, the molasses term and other interaction terms were not significant at the 5% level. Moreover, other interaction terms between molasses, temperature and pH value were omitted from the predicted model. The coefficient and adjusted coefficient of determination, R^2, for the regression model fit were calculated to be 0.9962 and 0.9896, respectively. This means that more than 98% of the variability of the regression model could be explained by the regression equation. The response-surface full quadratic model of biomass for *R. palustris* PS3 was also tested by ANOVA. The *F* value of the model was 151.99, and the *p* value was

doi:10.6342/NTU202003422

less than 0.0001 (2.84×10^{-7}), indicating that the model was highly significant (Table 3-7). The lack-of-fit *F* value and *p* value were 3.16 and 0.186, respectively, which implied that the lack of fit was insignificant. These results supported that the second-order model adequately approximated the response surface of *R. palustris* PS3 biomass production. After canonical transformation of Eq. (3-9), the optimum fermentation combination was obtained as follows: CSL, 39.41 mL/L; molasses, 32.35 g/L, temperature, 38°C, pH 7.0 and the DO was constant at 30%. The model predicted that the maximum response of *R. palustris* PS3 biomass production would be 2.31 g/L.

Effects of various factors on *R. palustris* PS3 biomass production

The 3D response surface contour plots were constructed in R software to analyze the interaction effects of four variables (CSL, molasses, temperature and pH value). The plots showed the effect of two variables on the response while the other factors were set at the "zero" level; the levels tested were 40 mL/L CSL, 35 g/L molasses, 38.5°C temperature and 6.9 pH (Figure 3-3). These contour plots represent the projection maps the 3D response surfaces onto two-dimensions planes with contours delineating changes in 3D space, which provide relative clear pictures of the responses derived from each factor. As shown in Figure 3-3 a b and e, the elliptical and inclined form of contour plots inferred that the interactions between CSL and molasses, CSL and temperature, CSL and pH value are evident. These results can also be confirmed by the variance analysis of regression model for biomass production (Table 3-6). On the other hand, the biomass production of *R. palustris* PS3 significantly increased with increasing CSL, temperature and pH. However, too high a concentration or condition level of these factors resulted in the opposite effect. On the other hand, it was noted that molasses did not acutely affect the biomass production of *R. palustris* PS3 under our experimental design, although increasing the concentration resulted in a slight increase-

doi:10.6342/NTU202003422

then-decrease pattern. These results were consistent with the polynomial regression analyses (Table 3-6), i.e., biomass production was significantly influenced by CSL, temperature and pH value. On the other hand, the 3D surface projection was confined to the smallest curve of the contour diagram suggesting that it contained an optimum condition in the levels of variables. Moreover, the 3D response surface presented a "roof form". Taken together, these data suggest that the model has a maximum stationary point, which contains the maximum biomass production of *R. palustris* PS3 strain.

Verification of optimization

To verify the predicted biomass production of *R. palustris* PS3, confirmation fermentation with the predicted optimal culture conditions (CSL, 39.41 mL/L; molasses, 32.35 g/L, temperature, 38°C, pH 7.0 and DO 30%) was performed. As shown in Table 3-8, after 24 hours of fermentation, the biomass production of *R. palustris* PS3 was 2.18 ± 0.01 g/L, which was approximately 7.8 times higher than that obtained in the original PNSB medium (0.28 ± 0.01g/L). The validated biomass production showed a high correlation (95%) with the predicted biomass from the response model. This result suggests that the proposed model Eq. (3-9) is effective for *R. palustris* PS3 biomass production. The estimated cost of this newly developed medium was about 0.16 US$/L, which was approximately 30% of the original PNSB medium (0.53 US$/L). The detailed material cost of each component in respective medium was shown in Table 3-9.

Validation of the plant growth-promoting effect of the newly developed fermentation broth

To confirm the plant growth-promoting effect of PS3 with the newly developed

doi:10.6342/NTU202003422

fermentation broth, we cultivated Chinese cabbage in either hydroponic or soil system with different treatments. As shown in Table 3-10, the fermented culture broth of PS3 contained 0.05±0.17 g/Kg of total organic carbon and 16.98 ±0.17 g/Kg of total nitrogen (Table 3-10), indicating the C/N ratio of this broth was approximated 1.77. The morphologies of 17 DAP and 28 DAP Chinese cabbage cultivated under different treatments are shown in Figure 3-4 (a-c) and Figure 3-5 (a-c), respectively. In the hydroponic system, the Chinese cabbage treated with the PS3 inoculant was obviously larger than that treated with CF or conventional growth medium. There was no significant difference in the size of Chinese cabbage treated with the medium and with CF. The fresh and dry shoot weights of Chinese cabbage cultivated in the hydroponic system with different treatments are shown in Figure 3-4 d and e (fresh/dry weight of CF: 45.87 ± 1.39 g/2.51 ± 0.076 g, PS3: 57.20 ± 1.54 g/2.81 ± 0.078 g, medium: 48.86 ± 1.14 g/2.35 ± 0.067 g). Compared to those of the CF group, the fresh and dry shoot weights of the PS3 treatment increased by 25% and 12%, respectively. Likewise, the fresh and dry shoot weights of PS3 Chinese cabbage cultivated in the soil system were also superior to those of the other treatments (fresh/dry weight of CF: 11.11 ± 0.84 g/1.75 ± 0.36 g, PS3: 14.27 ± 0.71 g/2.50 ± 0.23 g, medium: 13.31 ± 0.71 g/2.12 ± 0.24 g, respectively) (Figure 3-5 d and e). Compared to those of the CF group, the fresh and dry shoot weights were 28% and 48% increased, respectively, with the PS3 treatment. We confirmed that the fermentation broth of *R. palustris* PS3 produced under the newly developed culture conditions had beneficial effects on plant growth.

Discussion

R. palustris PS3 has been shown to have beneficial effects on several crops (Hsu *et al.*, 2015; Lee *et al.*, 2016; Wong *et al.*, 2014). To scale up the biomass production of PS3 for commercial purposes, we developed optimal fermentation conditions that

doi:10.6342/NTU202003422

are cost-effective and have a high product yield and a short fermentation time. Based on the derived RSM model (Eq. (3-9)), the predicted optimal culture conditions were 39.41 mL/L CSL, 32.35 g/L molasses, 38°C and 7.0 pH. As shown in Table 3-8, the optimized medium resulted in *R. palustris* PS3 biomass production (2.18 ± 0.01 g/L at 24 hours fermentation) that was 7.8-fold higher than that with the original PNSB medium (0.28 ± 0.01g/L at 24 hours fermentation). Accordingly, this optimal fermentation condition for *R. palustris* PS3 is not only highly productive but also cost- and time-effective. It has been indicated that the sources of nitrogen and carbon play a critical role in the production of microbial secondary metabolites (Singh *et al.*, 2016). Variation in fermentation condition results in changes in the yields and compositions of these secondary metabolites, which potentially affect activity, biomass and original effectiveness of microorganisms (Comelli *et al.*, 2016; Navarrete-Bolaños, 2012; Waites *et al.*, 2001). Therefore, I deduced that the secondary metabolites of PS3 using CLS and molasses as nitrogen and carbon sources can effectively stimulate the growth of this bacterium, although the profiles of the substances remains to be elucidated.

For industrial fermentation, the composition of the medium is critical, since it significantly affects the product concentration, yield and volumetric productivity. Furthermore, the cost of raw materials can range from 40% to 80% of the total costs of fermentation and affect the ease and cost of downstream product separation (Li *et al.*, 2014). *R. palustris* is already known as the most metabolically versatile bacteria , which was able to catabolize various carbon and nitrogen sources, such as glucose, fructose, malic acid, acetic acid, ammonium nitrate, glutamine, yeast extract and so on (Dönmez *et al.*, 1999; Imhoff and Trüper, 1992; Wong *et al.*, 2014). In this study, we evaluated several low-cost materials derived from common nutrients or agro-industrial byproducts for the fermentation of *R. palustris* PS3 and found that a variety of nitrogen and carbon sources could be utilized (Figure 3-2). These results may be attributed to

doi:10.6342/NTU202003422

the extraordinary metabolic versatility of *R. palustris* PS3 (Lo *et al.*, 2018). Noteworthily, the growth rates of *R. palustris* PS3 varied in response to different carbon or nitrogen sources (Figure 3-2). For nitrogen sources, the viable count of PS3 cultured with complex substrates, such as CSL, BRE or yeast extract supplied with NH_4Cl (i.e., the PNSB treatment), was significantly higher than that of PS3 cultured with a sole nitrogen source (i.e., NH_4NO_3) (Figure 3-2 b). These complex substrates all contain nitrogen-rich substances (Hull *et al.*, 1996; Mirmiran *et al.*, 2020; Silveira *et al.*, 2001; Xiao *et al.*, 2012), and were well solubilized in our cultivation medium. On the other hand, although SF and SPI are also complex nitrogen sources, the cell counts of these two treatments were relatively low (Figure 3-2b). I deduced that it was due to their low solubility in the medium as described above or because their primary components (β-conglycinin, glycinin, and lipophilic proteins) are not easily metabolized by *R. palustris* PS3. However, further experimentation is still needed.

For carbon sources, as shown in Figure 3-2 d, the viable count of PS3 cultured with molasses was higher than those of PS3 cultured with sugars (i.e., glucose or fructose). Molasses is a by-product of the sugar manufacturing process and may be obtained from beet or sugarcane; it contains abundant saccharides (such as sucrose, glucose, and fructose) and small amounts of organic acids (such as acetic acid and lactic acid) (Najafpour and Shan, 2003; Nelson, 1929). It has been reported that *R. palustris* biomass production is stimulated by the co-utilization of multiple carbon sources (Govindaraju *et al.*, 2019). Similar phenomenon was also observed in other microorganisms. For example, the growth rate of cultivated *E. coli* was higher with a combination of two substrates (i.e., mannose, xylose, glycerol, maltose or glucose supplemented with succinate, pyruvate, oxaloacetate, glycerol or glucose, respectively) than with a single substrate (mannose, xylose, glycerol, maltose or glucose, respectively) (Hermsen *et al.*, 2015). *Lactobacillus brevis* subsp. *lindneri* CB1 cultivated with

doi:10.6342/NTU202003422

maltose and citrate mixtures resulted in a faster cell growth rate than that of the strain cultivated with maltose alone, and the growth rate and viable counts (OD_{620}) derived from the former media were 1.8-fold and 1.2-fold higher, respectively (Gobbetti and Corsetti, 1996). Comparison with either glucose alone or malate alone as a carbon source, the growth rate of *B. subtilis* 168 increased 1.25-fold when cultured in medium containing glucose and malate mixtures (Kleijn *et al.*, 2010). It is already known that *R. palustris* can readily utilize organic acids as carbon sources (McKinlay and Harwood, 2011). Since organic acids such as acetic acid and lactic acid are contained in molasses (Nelson, 1929), it is possible that *R. palustris* co-metabolized several of the carbon sources in molasses, although further experimentation is needed.

The relationship between the target factors and *R. palustris* PS3 biomass production was explained by mathematical models and ANOVA. The linear regression model and ANOVA in FFD suggested that increasing the concentration of molasses could increase biomass production (Table 3-2 and Table 3-6). This result is quite reasonable because bacterial cells require carbon sources to survive. However, the results of the second-order regression model and ANOVA (Table 3-7) indicated that molasses did not significantly influence the growth of *R. palustris* PS3 (Eq. (3-9) and Table 3-7). I inferred that this discrepancy between the first- and second-order regression models might be attributed to CSL, which contains organic acids (Xiao *et al.*, 2012). Increasing the concentration of CSL might supply a carbon source to partially substitute for molasses. In a previous study, it was mentioned that CSL could serve as a supplement to replace carbon sources for some microorganisms (Liggett and Koffler, 1948). It also indicated that the carbon source was already sufficient in our CCD experiments. The effects of molasses concentration can also be observed in Figure 2 a, c and d. Increasing or reducing the concentration of molasses did not significantly alter the biomass of *R. palustris* PS3.

doi:10.6342/NTU202003422

In contrast, the factors CSL, temperature and pH value significantly influenced the growth of *R. palustris* PS3 (Table 3-7). It was observed that for greater and lower levels of CSL, temperature and pH value, there was a reduction in the response (Figture 3-2). Not surprisingly, a higher or lower pH value reduced the growth of *R. palustris* PS3, while the optimal pH value proposed by the RSM model for the fermentation of *R. palustris* was 7.0 (Table 3-8). This result was consistent with our previous study, which found that the pH range for *R. palustris* PS3 growth was 5.0 to 9.0, and the optimum pH was 7.0 (Wong *et al.*, 2014). Interestingly, the mathematical model suggested that the optimal temperature for *R. palustris* PS3 fermentation was 38°C, which was different from our previous finding (30ºC)(Wong *et al.*, 2014). I inferred that this dissimilarity could be attributed to the culture medium composition. Our proposed model showed that the interaction between CSL and temperature dramatically influenced *R. palustris* PS3 biomass production (Table 3-7). However, no study has indicated the effects of temperature and nutrients on *R. palustris* metabolism. Likewise, a higher temperature suppressed the growth of *R. palustris* PS3, though Eq. (3-8) indicated that increasing the temperature could increase *R. palustris* PS3 biomass production (Figure 2b, c and f). In the CCD experiments, the biomass production in trials No. 1, 3, 4, 5 and 17 was significantly lower than that in the other trials (Table 3-5). Regarding the effect of CSL on the growth of *R. palustris* PS3, I considered that an extra nitrogen source was absolutely important to *R. palustris* growth. It is known that *R. palustris* can obtain nitrogen from air by biological nitrogen fixation (BNF) (Larimer *et al.*, 2004). However, BNF is very sensitive to the O_2 concentration and is only carried out under microaerobic conditions. Thus, under the aerobic culture conditions of this study, BNF did not occur. Accordingly, supplementation with exogenous nitrogen in the culture medium was necessary.

Molasses and CSL can be applied individually as fertilizers in agriculture. For

doi:10.6342/NTU202003422

example, it has been found that the soil quality was remarkably improved by the application of molasses (Bagheri *et al.*, 2019; Pyakurel *et al.*, 2019). There were also reports showing that molasses could increase the yield and quality of crops (Samavat and Samavat, 2014; Şanlı *et al.*, 2015). CSL was shown to have beneficial effects on plants (Chinta *et al.*, 2014; Zhu *et al.*, 2019), and supplementation of with exogenous CSL in soil promoted the growth of the root system of soybean (Zhu *et al.*, 2019). It has been suggested that the organic nitrogen in CSL is converted to nitrate via microbial ammonification and nitrification and directly utilized by plants (Shinohara *et al.*, 2011). However, it has also been reported that CSL and molasses might have negative effects on plant growth. Zhu et al (Zhu *et al.*, 2019) reported that high concentration of CSL (more than 2%) will inhibit plant growth. In addition, fertilization of molasses singly or in combination with some PGPRs (*Bacillus* spp. *Azospirillum* spp. or *Azotobacter* spp.) showed a negative influence on seed germination *in vitro* (Suliasih and Widawati, 2017). In this study, the newly developed medium containing molasses (32.35 g/L) and CSL (39.41 mL/L) was verified for its effect on plant growth. Since the PS3 fermentation broth showed positive effects on plant growth in both soil and hydroponic systems (Figure 3-4 and Figure 3-5). It suggests that this medium is suitable not only for phototrophic bacteria production but for application in agricultural production. Such an approach to farming is regarded as environmentally friendly and can be used to reduce excessive chemical fertilizer application and ensure sustainable crop production.

Furthermore, it is notable that PS3 fermentation broth obtained from newly developed medium that is consistent with PS3 cultured in modified PNSB, it shown the plant growth promotion effect (Figure 3). In our previous work (Wong *et al.*, 2014), to examine whether the plant beneficial effects of *R. palustris* PS3 were elicited by viable cells or conferred by organic compounds from the PNSB medium or dead/ decaying cells, the 65°C heat-killed bacterial suspension was applied to replace the vegetative *R.*

doi:10.6342/NTU202003422

palustris cells. The results showed that neither medium nor dead *R. palustris* cells was able to promote plant growth (Wong *et al.*, 2014). These results indicated that the effectiveness observed were mainly exerted by the viable cells of *R. palustris* PS3. Notably, it was also demonstrated that not only the population (i.e viability) but also the metabolic activity (i.e vitality) of PS3 cells is crucial for the plant beneficial traits (Lee *et al.*, 2016). On the other hand, in our another study (Lo *et al.*, 2018), we carried out a comparative analysis of effective (strain PS3) as well as ineffective (strain YSC3) *R. palustris* strains in plant-growth promotion. PS3 and YSC3 exhibited a very close phylogenetic relationship and shared several conserved regions and genetic arrangements in their chromosomes. Although these strains have many plant growth-promoting (PGP) genes in common, only PS3 exhibited beneficial traits. It noticed that the transcripts of genes associated with bacterial colonization and biofilm formation in response to root exudates were higher in PS3 than those in YSC3 strain (Lo *et al.*, 2018). These data suggested that PS3 responds better to the presence of plant hosts. These results indicate that the physiological responses of this bacterium to its plant hosts as well as successful establishment of interactions with plant hosts appear to be critical factors for PS3 to promote plant growth. Taken together, I deduced that the beneficial effects of PS3 were mainly offered by the viable cells of this bacterium through interactions with the host.

This study presented an experimental design for the optimization of *R. palustris* PS3 biomass production with an alternative, low-cost medium containing agricultural byproducts. CSL and molasses were identified as potential nitrogen and carbon sources for *R. palustris* fermentation. The utilization of CSL and molasses as raw materials for *R. palustris* fermentation can aid in reducing agro-industrial waste. The response surface methodology revealed the factors that greatly influence *R. palustris* PS3 growth, namely, CLS, temperature and pH value. *R. palustris* PS3 biomass production increased

doi:10.6342/NTU202003422

significantly, by 7.8-fold, from 0.28 ± 0.01 g/L to 2.18 ± 0.01 g/L, compared to that under the basal medium/conditions when the strain was cultivated in the optimal culture conditions (CSL, 39.41 mL/L; molasses, 32.35 g/L; temperature, 38°C; pH, 7.0 and DO 30%) developed by statistical experimental methods. The in planta experiments verified that the newly developed fermentation broth retained the plant growth-promoting functions of *R. palustris* PS3. Compared with those in previous studies, our newly developed fermentation process could successfully produce high levels of *R. palustris* in a shorter time. This study described the prospective uses of agro-industrial techniques for *R. palustris* biofertilizer production.

doi:10.6342/NTU202003422

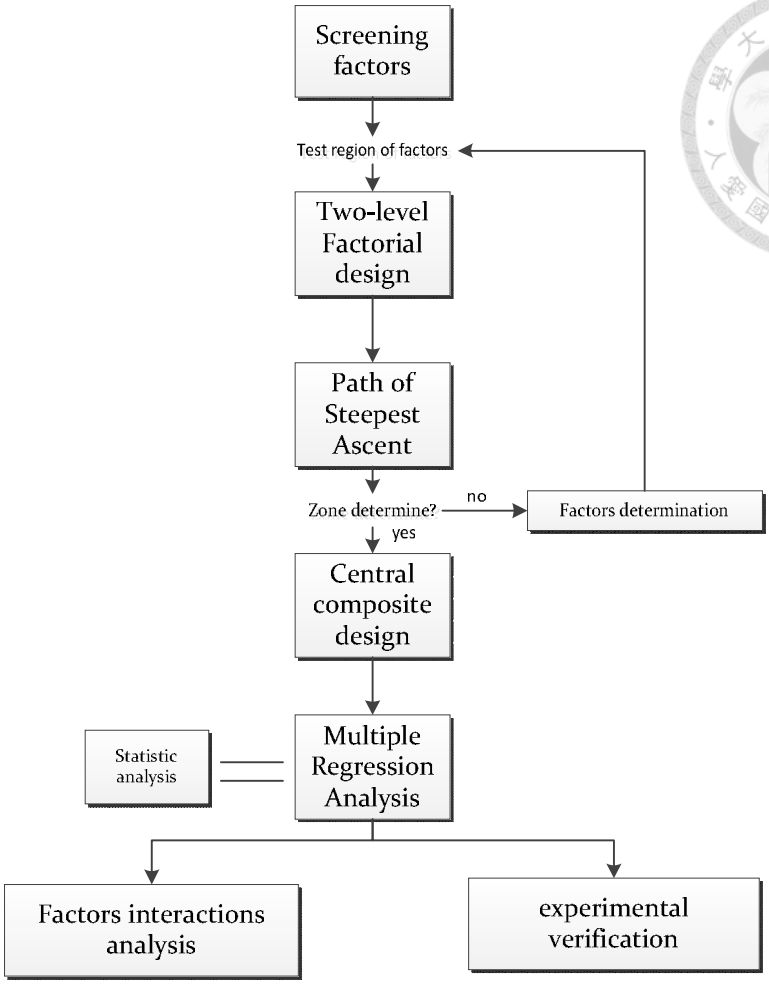

Figure 3-1. Scheme of RSM process. For construction of RSM model contains several steps. Firstly, Determine the variables and operating range of experiments by two-level factorial design. Then, evaluate whether the factor range include polar points. If the operating range contains polar points, constructing central composite design. Subsequently, building a mathematical model of response surface by regression analysis. Then, examine adaptability of model. Finally, determine the polar points and verify the model.

doi:10.6342/NTU202003422

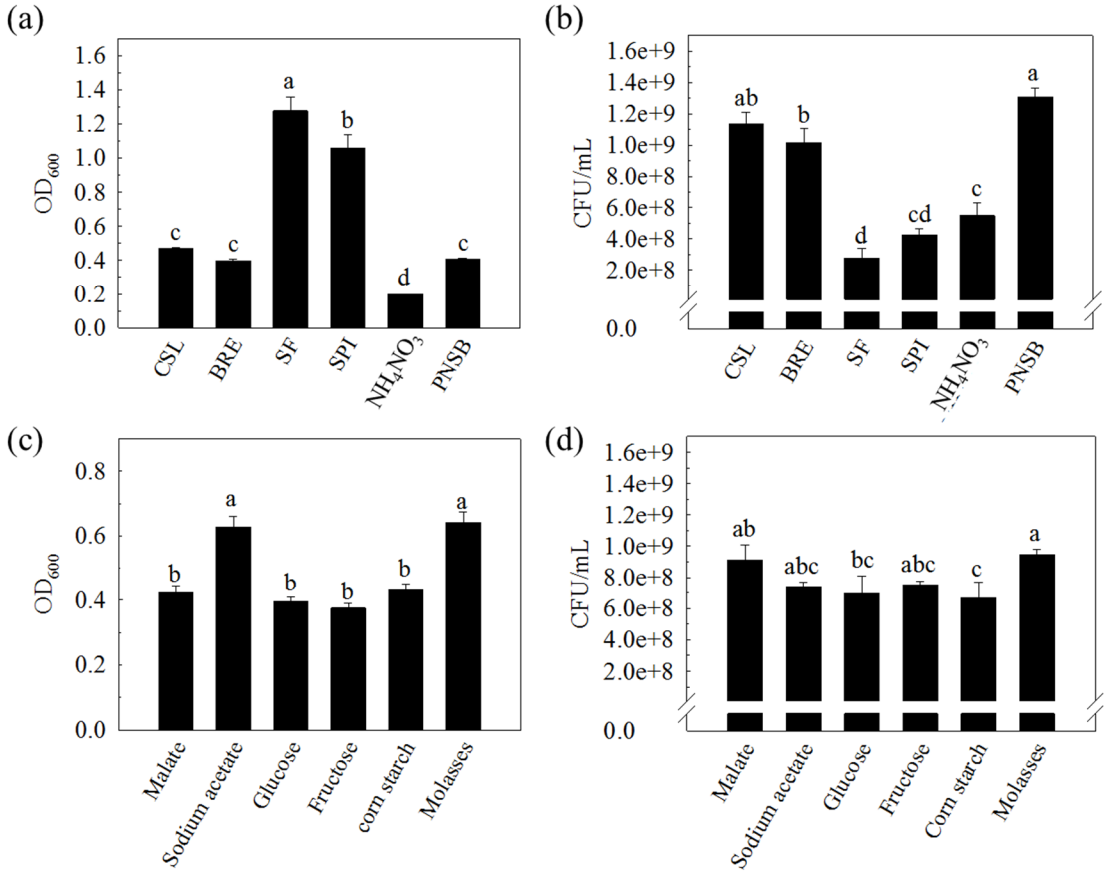

Figure 3-2. Selection of appropriate components for an optimized *R. palustris* medium. The effect of different nitrogen (A, B) and carbon sources (C, D) on the growth of *R. palustris* PS3 culture under 200 rpm and 37°C for 24 hours. In the nitrogen source screening experiments (A and B), each nitrogen source (1.5 g/L) was used to replace 1.0 g/L NH_4Cl and 0.5 g/L yeast extract in the PNSB treatment. In the carbon source screening experiments (C and D), 1.5 g/L CSL was used as the nitrogen source in the medium, and the concentration of each carbon source was set at 5 g/L. CSL: corn steep liquor; BRE: beetroot extract; SF: soybean flour; SPI: soybean protein isolate; PNSB: modified van Niel medium (8). Vertical bars represent the standard error of each mean, and bars with different letters indicate statistically significant differences at P = 0.05 according to LSD test.

doi:10.6342/NTU202003422

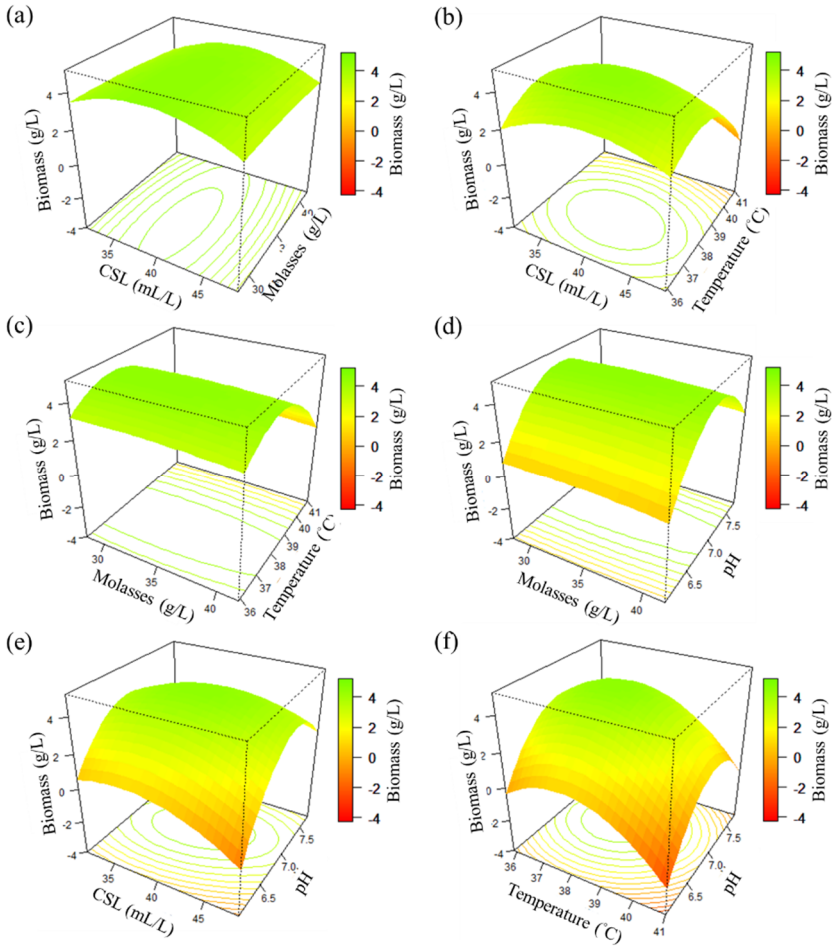

Figure 3-3. Three-dimensional response surfaces and contour plots of the effects of three factors on *R. palustris* PS3 biomass production. When two factors were plotted, the other two factors were set at the coded level, zero. Each condition was as follows: CSL, 40 mL/L; molasses, 35 g/L; temperature, 38.5°C and pH value, 6.9. (a): CSL and molasses were plotted at 38.5°C and pH 6.9; (b) CSL and temperature were plotted at 35 g/L molasses and pH 6.9; (c) molasses and temperature were plotted at 40 mL/L CSL and pH 6.9; (d) molasses and pH were plotted at 40 mL/L CSL and 38.5°C; (e): CSL and pH were plotted at 35 g/L molasses and 38.5°C; (f): temperature and pH were plotted at 40 mL/L and 35 g/L molasses. CSL: corn steep liquor.

doi:10.6342/NTU202003422

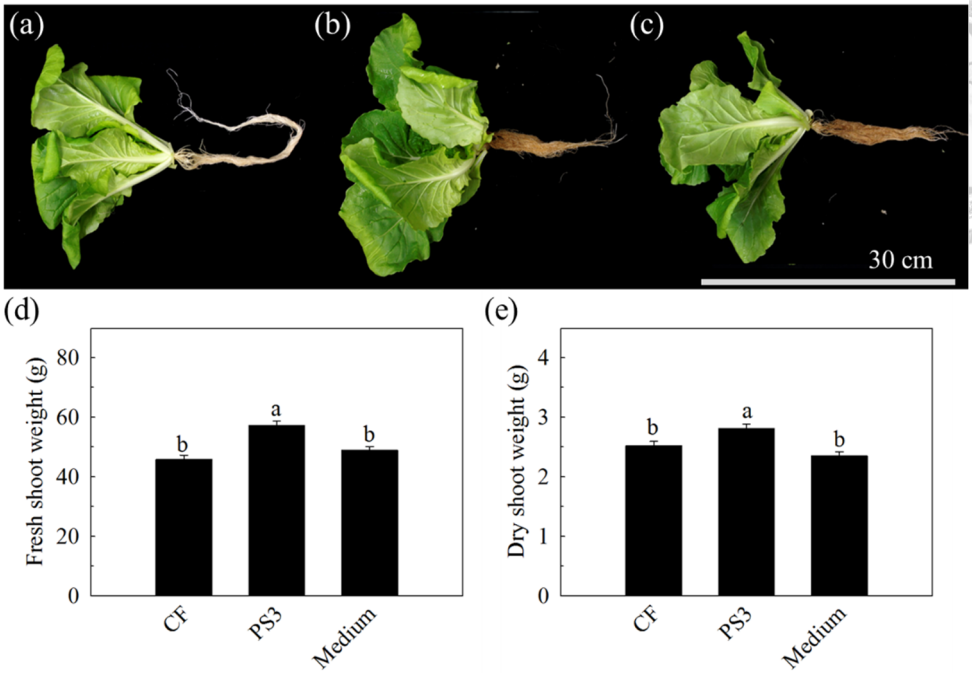

Figure 3-4. Plant growth-promoting effects of *R. palustris* PS3 incubated with the newly developed culture conditions on leafy vegetable in hydroponic system. *Brassica rapa chinensis* (Chinese cabbage) was cultivated with/without PS3 inoculum. The "CF" indicates the control group (Hoagland's solution). The "PS3" indicates the treatment (CF) supplemented with the fermentation broth of *R. palustris* PS3, "medium" indicates the treatment (CF) supplemented with fresh medium, respectively. (a)-(c) show the morphology of Chinese cabbage (a: CF, b: PS3 and c: medium) with the different treatments at 17 DAP. (d) and (e) are the fresh and dry shoot weights of Chinese cabbage. Vertical bars represent the standard error and bars with different letters indicate statistically significant differences at P = 0.05 according LSD test.

doi:10.6342/NTU202003422

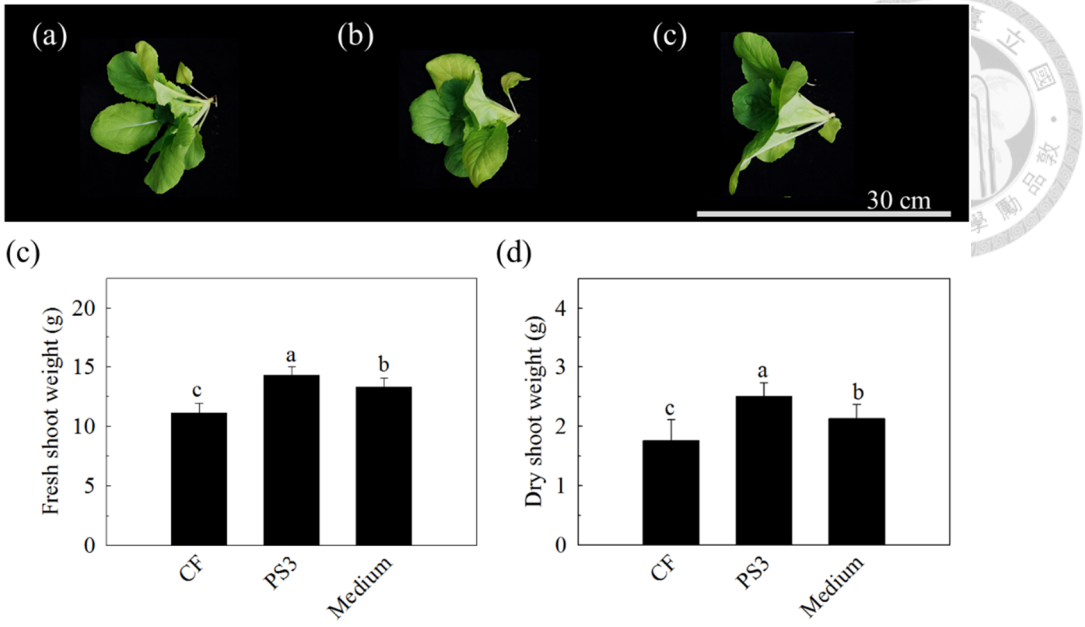

Figure 3-5. Plant growth-promoting effects of *R. palustris* PS3 incubated with the newly developed culture conditions on leafy vegetable in soil system. *Brassica rapa chinensis* (Chinese cabbage) was cultivated with pure chemical fertilizer under soil system. "CF" indicates the control group (chemical fertilizer treatment), "PS3" indicates the treatment (CF) supplemented with the fermentation broth of *R. palustris* PS3, "medium" indicates the treatment (CF) supplemented with fresh medium, respectively. (a)-(c) show the morphology of Chinese cabbage (a: CF, b: PS3 and c: medium) with the different treatments at 28 DAP. (d) and (e) are the fresh and dry shoot weights of Chinese cabbage. Vertical bars represent the standard error and bars with different letters indicate statistically significant differences at P = 0.05 according LSD test.

doi:10.6342/NTU202003422

Table 3-1. Level and code of variables in the FFD experiments.

Independent variable	Coded levels		
	-1	0	1
Corn steep liquor (mL/L)	35	40	45
Molasses (g/L)	31	35	39
Temperature (°C)	37	38.5	40
pH	6.4	6.9	7.4

The various factors were coded according to Eq. (3-1).

doi:10.6342/NTU202003422

Table 3-2. Level codes of the variables, experimental design and results from the FFD.

Trial No.	Coded levels of factors					Biomass
	X_1	X_2	X_3	X_4	X_5	(g/L)
1	-1(10)	+1(30)	-1(10)	-1(34)	+1(7.5)	1.03
2	+1(30)	+1(30)	-1(10)	+1(40)	-1(6.5)	2.3
3	-1(10)	+1(30)	+1(50)	-1(34)	-1(6.5)	1.13
4	-1(10)	-1(10)	+1(50)	+1(40)	-1(6.5)	0.89
5	+1(30)	-1(10)	-1(10)	-1(34)	-1(6.5)	1.32
6	-1(10)	-1(10)	-1(10)	+1(40)	+1(7.5)	0.82
7	+1(30)	-1(10)	+1(50)	-1(34)	+1(7.5)	1.25
8	+1(30)	+1(30)	+1(50)	+1(40)	+1(7.5)	2.18

The various factors were coded according to Eq. (3-1).

Letters: X_1 = CSL (mL/L), X_2 = molasses (g/L), X_3 = dissolved oxygen, X_4 = temperature (°C) and X_5= pH value.

doi:10.6342/NTU202003422

Table 3-3. The experimental design and results from the path of steepest ascent method.

Step	Variance of Factors				Response
	Corn steep liquor (ml/L)	Molasses (g/L)	Temperature (°C)	pH	Biomass (g/L)
Original point	20	20	37	7	1.48
Step 1	25	23.82	37.7	6.97	1.8
Step 2	30	27.64	38.4	6.95	2.27
Step 3	35	31.46	39.1	6.92	2.36
Step 4	40	35.27	39.7	6.89	2.44
Step 5	45	39.09	40.4	6.86	0.8

The interval between each step was determined according to the ratio of coefficients in Eq. (3-3). The fermentation was performed in 24 hours.

doi:10.6342/NTU202003422

Table 3-4. Level and code of variables in the CCD experiments.

Independent variable	Coded levels				
	-1.682	-1	0	1	1.682
Corn steep liquor (mL/L)	31.59	35	40	45	48.41
Molasses (g/L)	28.27	31	35	39	41.73
Temperature (°C)	35.9	37	38.5	40	41
pH	6.06	6.4	6.9	7.4	7.74

The various factors were coded according to Eq. (3-1).

doi:10.6342/NTU202003422

Table 3-5. The coded levels and real values for the experimental design and results of CCD.

Trial no.	Coded levels of factors				Biomass (g/L)	
	x_1	x_2	x_3	x_4	Experimental	Predicted
1	-1	+1	+1	-1	0.88	0.74
2	-1	-1	-1	-1	1.45	1.34
3	+1	+1	+1	+1	0.91	0.86
4	+1	-1	+1	-1	0.25	0.21
5	-1	-1	+1	+1	1.09	1.02
6	-1	+1	-1	+1	1.59	1.47
7	+1	+1	-1	-1	1.09	1.00
8	+1	-1	-1	+1	1.75	1.72
9	0	0	0	0	2.29	2.18
10	0	0	0	0	2.21	2.18
11	0	0	0	0	2.31	2.18
12	0	0	0	0	2.23	2.18
13	+1.682	0	0	0	1.43	1.44
14	-1.682	0	0	0	1.63	1.78
15	0	+1.682	0	0	1.94	2.06
16	0	-1.682	0	0	2.13	2.16
17	0	0	+1.682	0	0.47	0.54
18	0	0	-1.682	0	1.59	1.68
19	0	0	0	+1.682	1.01	1.05
20	0	0	0	-1.682	0.18	0.30

Letters: x_1= CSL (mL/L), x_2= molasses (g/L), x_3= temperature (°C) and x_4=pH value. Trial no. 1 to 8 represented fractional factorial design (FFD), trial no. 9 to 12 were referred as central point, and trial no. 13 to 20 were represented as axial points. The coefficient of determination, R^2, between the predicted and experimental values was calculated to be 0.98.

doi:10.6342/NTU202003422

Table 3-6. The variance analysis of the first-order model regression to biomass production.

Source	DF	Adj SS	Adj MS	F-Value	Effect	Coef	P-Value
Model	5	8.37027	1.67405	3169.8			0.00032
Linear	5	8.37027	1.67405	3169.8			0.00032
X_1	1	4.64363	4.64363	8792.67	1.52375	0.76188	0.00011
X_2	1	2.70863	2.70863	5128.76	1.16375	0.58188	0.00021
X_3	1	0.00015	0.00015	0.29	0.00875	0.00438	0.644
X_4	1	0.96258	0.96258	1822.63	0.69375	0.34688	0.00055
X_5	1	0.05528	0.05528	104.67	-0.16625	-0.08312	0.00942
Error	2	0.00106	0.00053				
Total	7	8.37132					

Letters: X_1 = CSL (mL/L), X_2 = molasses (g/L), X_3 = Dissolved oxygen, X_4 = temperature (°C) and X_5= pH value.

doi:10.6342/NTU202003422

Table 3-7. The variance analysis of the second-order regression model for biomass production.

Source	DF	SS	MS	*F*-value	Coef.	*p*-value
Model	12	31.9509	2.6626	151.99		2.84E-07
Blocks	1	0.4613	0.4613	26.33		0.0003
Linear	4	9.0117	2.2529	128.6		1.2E-06
x_1	1	0.5024	0.5024	28.68	-0.1918	0.00104
x_2	1	0.0432	0.0432	2.46	-0.0562	0.15911
x_3	1	5.9164	5.9164	337.72	-0.6582	2.8E-07
x_4	1	2.5498	2.5498	145.55	0.4321	6E-06
Square	4	21.5663	5.3916	307.76		5.9E-08
x_1^2	1	2.143	2.143	122.33	-0.3882	1E-05
x_2^2	1	0.0278	0.0278	1.59	-0.0442	0.23298
x_3^2	1	7.6097	7.6097	434.38	-0.7315	1.4E-07
x_4^2	1	15.0951	15.0951	861.66	-1.0302	1.3E-08
2-Way Interaction	3	0.608	0.2027	11.57		0.00412
x_1x_2	1	0.0022	0.0022	0.12	0.0165	0.73435
x_1x_3	1	0.1677	0.1677	9.57	-0.1448	0.0172
x_1x_4	1	0.4382	0.4382	25.01	0.234	0.00153
Error	7	0.1226	0.0175			
Lack-of-Fit	4	0.0991	0.0248	3.16		0.186
Pure Error	3	0.0235	0.0078			
Total	19	32.0735				

Letters: x_1= CSL (mL/L), x_2= molasses (g/L), x_3= temperature (°C) and x_4=pH value.

doi:10.6342/NTU202003422

Table 3-8. Comparison of PNSB medium and optimal medium parameters for *R. palustris* PS3 biomass production for 24 hours.

Factor	PNSB medium	Optimal medium
Molasses (g/L)	-	32.35
Malate (g/L)	5	-
CSL (mL/L)	-	39.41
Yeast extract (g/L)	1	-
NH_4Cl (g/L)	0.5	-
Agitation (rpm)	200	-
Aeration (vvm)	1.22	-
pH	7	7
Temperature (°C)	37	38
Biomass (g/L)	0.28 ± 0.01	2.18 ± 0.01
Material cost (US$/L)	0.53	0.16

The fermentation experiments were carried out in a 5-L bioreactor. Material cost was calculated in Jun. 2020.

doi:10.6342/NTU202003422

Table 3-9. The cost of different medium component for *R. palustris* PS3 fermentation.

Composed	Purchased source/brand	Package size (g)	Cost (US$/Kg)	Concentration in medium (g/L)	Cost for medium of per liter (US$)	
					PNSB medium	Newly developed medium
Ammonium chloride (NH_4Cl)	J.T. Baker	1000	66.72	1	0.06672	0.06672
Dipotassium phosphate (K_2HPO_4)	J.T. Baker	500	60.66	1	0.0606564	0.0606564
Sodium chloride (NaCl)	Bio BASIC INC.	1000	35.38	0.5	0.01769145	0.01769145
Magnesium sulfate ($MgSO_4•7H_20$)	Bio BASIC INC.	1000	30.33	0.2	0.00606564	0.00606564
Ferrous sulfate ($FeSO_4$)	J.T. Baker	500	51.56	0.01	0.000515579	0.000515579
Calcium chloride ($CaCl_2$)	Bio BASIC INC.	500	153.80	0.02	0.003075953	0.003075953
Manganese chloride ($MnCl_2$)	Sigma	100	454.92	0.002	0.000909846	0.000909846
Sodium molybdate (Na_2MoO_4)	Sigma	100	585.33	0.001	0.000585334	0.000585334
Yeast extract	Bio BASIC INC.	500	70.77	0.5	0.0353829	-
Malate	Alfa Aesar	500	67.40	5	0.33698	-
Sodium acetate	KATAYAMA	500	22.24	2	-	-
Molasses	TAIWAN SUGAR Co. Ltd.	25000	0.67	32.35	-	0.021802606
Corn steep liquor	TAIROUN PRODUCTS Co., Ltd.	25000	0.61	39.41	-	0.023904687

Material cost was calculated in Jun. 2020.

doi:10.6342/NTU202003422

Table 3-10. Quantification of total organic carbon and total nitrogen.

	Newly developed *R palustis* PS3 fermentation broth
Total organic carbon (g/Kg)	30.05±0.17
Total nitrogen (g/Kg)	16.98 ±0.17
C/N	1.77

Bacterial fermentation was performed according the optimal culture conditions in this study.

doi:10.6342/NTU202003422

Chapter IV

Concluding remarks and discussion

R. palustris exhibits distinctive metabolic pathways, which is a suitable model microorganism for researching bacterial metabolic mechanisms (Larimer *et al.*, 2004). It has been demonstrated that this bacterium can be employed in bioremediation of environmental pollutants, biological hydrogen production, or animal feed probiotics, etc. However, only few studies were related to the applications in agriculture (Batool *et al.*, 2017; Hsu *et al.*, 2015; Nunkaew *et al.*, 2014; Shen, 2016; Su *et al.*, 2019; Wong *et al.*, 2014; Xu *et al.*, 2016). *R. palustris* PS3 is an elite strain for developing biofertilizer, which remarkably promotes plant growth and increases the agronomic nitrogen use efficiency of plant hosts (Wong *et al.*, 2014). On the other hand, there was another *R. palustris* YSC3, which has no significant effect on plant growth. I employed whole genome sequencing and genomic comparative analysis to educate the mechanisms of plant growth-promoting effects derived from the effective strain of *R. palustris*. To develop an optimal fermentation protocol for producing *R. palustris* PS3 broth, high cost-effectiveness, high biomass yield, and short fermentation time were considered as the essential criteria. I evaluated some agro-industrial by-products, including corn steep liquor (CSL), beetroot extract (BRE), soybean flour (SF), soybean protein isolate (SPI), molasses and corn starch, for use as substrates for *R. palustris* PS3 cultivation.

In **Chapter II**, I combined the short-read illumina and long-read PacBio techniques to conduct whole-genome sequencing for the effective *R. palustris* PS3 as well as the ineffective YSC3. I successfully obtained two circular contigs via *de novo* assembly. So far, there were nine complete genomes of *R. palustris* strains available in GenBank, including those of PS3 and YSC3 strains (Table 2-4). I found that the genomic sizes of PS3 and YSC3 are similar to the other *R. palustris*, about 5.3 Mb

doi:10.6342/NTU202003422

(Table 2-4). I also observed that they shared the conserved genes with each other (Figure 2-5, Figure 2-6 and Figure 2-7). In the PS3 genome, several plant growth-promotion associated genes were identified (Figure 2-8). However, these genes were also annotated in the YSC3 genome. In general, the genetic background can assist us to more understand the detailed characteristics of microorganisms and help us to develop more potential applications. It tends to be considered that the microorganisms with the plant growth-promoting genes are potential PGPR. However, in this study, I found that even the bacteria contained the plant growth-promoting genes are insufficient to claim their beneficial effects on plant growth. For example, the nitrogen fixation-, IAA synthesis-, phosphate solubilization and ACC deamination-associated genes, were also annotated in the ineffective YSC3 strain (Figure 2-8). Notably, I observed that the growth rate, biofilm formation, and gene expression pattern of PS3 responded to root exudate of host plants were significantly higher than those in the YSC3 strain (Figure 2-13 and Figure 2-14). It indicated that the regulation of these genes of respective strain in response to the host plant were diverged. Our data proposed that the physiological responses to the plant hosts as well as the interactions between bacteria and host plant may be the critical steps for the effective strain to promote plant growth. These results also explained that not all of the *R. palustris* are PGPR.

Comparative genomic analyses of PGPR can provide insight into genomic features to identify the conserved "core genome" (i.e the genes present in all strains) involved in plant growth promoting (PGP) functions (Belbahri *et al.*, 2017). For example, a genomic analysis for multiple PGPR strains of *B. velezensis* showed that all of the strains containing IAA synthesis genes (Chen, 2020; Chen *et al.*, 2007; Liu, 2018; Zhang *et al.*, 2015b). In this study, a comparative analysis of *R. palustris* strains that are effective and ineffective in PGP. The PS3 and YSC3 strains are closely related to each other and have similar genomic structures and compositions. Although these

doi:10.6342/NTU202003422

strains have many plant growth-promoting genes in common, only the former exhibited PGP. This result suggests that the presence of PGP-associated genes in a bacterium is not sufficient for the bacterium to have beneficial effects on plant growth. Rather, physiological responses to the presence of plant hosts and successful establishment of interactions with the host appear to be critical. Similar phenomenon in our other study was also found. We sequenced two *B. velezensis* strains (WF02 and EN01) by NGS and found that they have similar genomic structures and compositions (unpublished data). However, their biocontrol spectrum and efficacy were varied (Chen, 2020). Another evidence was in the case of phosphate solubilization in this study. I identified a serious of genes related to microbial phosphate-solubilization in the genome of PS3 (Figure 2-8 b). However, this bacterium showed no phosphate solubilizing activity in the plate assay (Figure 2-11). Taken together, these findings indicate that the existence of gene clusters associated with PGP is required but not sufficient for a bacterium to exhibit phenotypes associated with these functions.

Another noteworthy issue is related to genome annotation for protein-coding genes. In general, the functional annotation of predicted genes dependents on the database. I predicted the protein-coding genes of PS3 based on BLASTP search against several databases, however, the current genomic information of PS3 is still incompleted. For instance, I demonstrated that PS3 could synthesize IAA, and IAA production was increased with adding tryptophan (Figure 2-12). However, the genomic data presents that PS3 lacks some genes encoding essential proteins (Figure 2-8 c). Similarly, PS3 stain could grow in the medium containing glucose as single carbon source (Figure 3-2), but there was no hexokinase-coding gene found in PS3 genome. Due to the current limitations in functional annotation by BLASTP against database (Altenhoff and Dessimoz, 2009; Araujo *et al.*, 2018; Tekaia, 2016), we can't exclude the possibility that there are ortholog gene(s) in PS3. On the other hand, even though several PGP

doi:10.6342/NTU202003422

genes were identified in the PS3 genome, it still not enough to elucidate the mechanics of PGP exerted by this bacterium. Although I found several gene transcriptions of PS3 related to PGP function were up-regulated by root exudate (Figure 2-16), whether these induction of transcriptome contributes to the traits of plant growth promotion is still unclear. To elucidate the underlying molecular mechanisms associated with PGP, further experiments, such as gene muatagenesis and genome-wide transcriptome profiling analyses, are needed to determine the phenotypic and functional properties. So far, the technique barrier for analyzing the transcriptome of PGPR is hard to efficiently collected the mRNAs of the bacterial cells from root surface. It is partially due to the attaching cells on the root surface are too few to isolate enough their mRNA, and this issue may be resolved by a single-cell sequencing technique as described by (Tang *et al.*, 2019). This technique can achieve sequencing and derive sequence information from individual cells, also provide reveal cell-to-cell variability in altering environments (Saliba *et al.*, 2014).

A promising direction of further research is to identify the key-molecules that are involved in the signal transduction between PGPR and their host plants. This study could be done by investigating the secretome of PS3 before and post- plant-microbe interactions as those described by Adeniji et al (Adeniji *et al.*, 2020). On the other hand, the investigation derived from planta side would also assist us to verify the interactions. In a yet published study conducted in our lab, we evaluated various plant physiological responses to inoculation with different bacterial inoculants (Hsu et al., submitted in 2020). We found that the nitrate uptake efficiency was dramatically increased in the PS3 inoculated plants; however, nitrate was not accumulated in the leaves. We also noticed that the endogenous IAA levels as well as cell division rate in the leaves of PS3-inoculated plants were significantly higher than those of YSC3-inoculated plants. We deduced that PS3 inoculation could promote plant growth via enhancing nitrogen

doi:10.6342/NTU202003422

uptake efficiency and stimulating the accumulation of endogenous auxin in young expanding leaves to increase the proliferation of leaf cells during leaf development.

In **Chapter III**, optimization of culture conditions was performed by response surface methodology (RSM). When I started this research, there were only few studies related to the biomass production of *R. palustris* (Choorit *et al.*, 2011; Saikeur *et al.*, 2009). Since phototrophic bacteria are regarded as efficient producers for 5-aminolevulinic acid (5-ALA) and hydrogen (Bolatkhan *et al.*, 2019; Liu *et al.*, 2005), most studies focus on the production of these products (Choorit *et al.*, 2011; Merugu *et al.*, 2011; Nunkaew *et al.*, 2018; Saikeur *et al.*, 2009; Shi *et al.*, 2014; Zhang *et al.*, 2015a). In our previous studies, we proved that the beneficial effects of PS3 were mainly exerted by the viable cells through interactions with the host plants (Lee *et al.*, 2016; Lo *et al.*, 2018). To maximize the cell viability of PS3, I optimized the culture conditions for large scale fermentation, and remarkably reduced time and cost (70%) compared with former condition (Table 3-8).

Based on my current results, I propose that CSL and molasses are promising substrates for *R. palustris* fermentation. This suggestion is convincing due to (1) The biomass of PS3 is significantly increased using the modified medium (Figure 3-2). (2) CSL and molasses are agro-industrial byproducts which are available with a relative lower cost (Thomsen, 2005). (3) CSL and molasses can be used directly as organic fertilizers in agriculture (Bagheri *et al.*, 2019; Chinta *et al.*, 2014; Pyakurel *et al.*, 2019; Samavat and Samavat, 2014; Şanlı *et al.*, 2015; Shinohara *et al.*, 2011; Zhu *et al.*, 2019). Notably, I confirmed that under the optimized conditions, the biomass of PS3 was raised 7.8-fold (from 0.28 ± 0.01 g/L to 2.18 ± 0.01 g/L), and medium cost was reduced approximately 30% compared with that of the original PNSB medium (i.e from 0.53 US$/L to 0.16 US$/L) (Table 3-8). The fermentation broth of *R. palustris* PS3 produced under the newly developed culture conditions has been proved to exert beneficial

doi:10.6342/NTU202003422

effects on plant growth (Figure 3-4 and Figure 3-5).

In general, microbes favor t certain nutrients to sustain their growth, whereas utilization of the other substrate is restricted until the favored one is not available (Harder and Dijkhuizen, 1982). CSL and molasses are both complex substrates, which are used as nutrient sources in the newly developed medium (Nelson, 1929; Xiao *et al.*, 2012). However, PS3 didn't present a "diauxic growth or tow phase growth" pattern (Harder and Dijkhuizen, 1982) while grows under the newly developed medium. It remains to be elucidate that whether PS3 strain can simultaneously utilize multiple carbon and nitrogen sources, and how to coordinate the complex metabolism networks would be interesting. In a recent study indicate that *R. palustris* is able to co-utilize acetate and lactate (Govindaraju *et al.*, 2019). Govindaraju et al quantified the residual organic acids in the post-fermentation broth by Shimadzu high-performance liquid chromatograph (Govindaraju *et al.*, 2019).

With respect to CSL and molasses, since these two products are derived from agriculture processing, their compositions highly depend on the material sources and the extracting procedures (Clarke, 2003; Loy and Lundy, 2019). It has been known that either the biomass yields or the secondary metabolites of microbes are affected by the compositions of nutrient substrates (Choorit *et al.*, 2011; Merugu *et al.*, 2011; Ruiz *et al.*, 2010). In consideration of commercialization, quality control of the main nutrient substrates, i.e CSL and molasses, is indispensable for PS3 fermentation. This issue could be addressed by construction of chromatographic fingerprints as described by Xai et al (Xiao *et al.*, 2013). Such studies on the analysis of chromatographic fingerprints of medium as well as identification of the main substrates for PS3 utilization, could assist us to control the quality and yield of large scale fermentation.

Overall, my studies expand the insights on *R. palustris* PS3 in plant growth promoting and fermentation. Firstly, I identified several PGP-associated genes in the

doi:10.6342/NTU202003422

PS3 genome. Secondary, I proposed that the presence of PGP-associated genes in a bacterium is not sufficient for the bacterium to have beneficial effects on plant growth. Rather, physiological responses to the presence of plant hosts and successful establishment of interactions with the host appear to be a critical step. Thirdly, CSL and molasses could be used as low-cost substrates for PS3 fermentation.

doi:10.6342/NTU202003422

References

Abeles, F.B., P.W. Morgan and M.E. Saltveit Jr. 1992. CHAPTER 4 - Regulation of Ethylene Production by Internal, Environmental, and Stress Factors. In "Ethylene in Plant Biology (Second Edition)", pp. 56-119. New York: Academic Press.

Achtman, M. and M. Wagner. 2008. Microbial diversity and the genetic nature of microbial species. Nat. Rev. Microbiol. 6(6):431-440. doi: 10.1038/nrmicro1872

Adeniji, A.A., O.O. Babalola and D.T. Loots. 2020. Metabolomic applications for understanding complex tripartite plant-microbes interactions: Strategies and perspectives. Biotechnology Reports 25:e00425. doi: 10.1016/j.btre.2020.e00425

Adesemoye, A.O. and J.W. Kloepper. 2009. Plant-microbes interactions in enhanced fertilizer-use efficiency. Appl. Microbiol. Biotechnol. 85(1):1-12. doi: 10.1007/s00253-009-2196-0

Adler, E. 1977. Lignin chemistry - past, present and future. Wood Sci. Technol. 11(3):169-218.

Ahemad, M. and M. Kibret. 2014. Mechanisms and applications of plant growth promoting rhizobacteria: Current perspective. J. King. Saud. Univ. Sci. 26(1):1-20. doi: 10.1016/j.jksus.2013.05.001

Ahmad, F., F.M. Husain and I. Ahmad. 2011. Rhizosphere and root colonization by bacterial inoculants and their monitoring methods: A critical area in PGPR research. In "Microbes and microbial technology: Agricultural and environmental applications", ed. I. Ahmad, F. Ahmad and J. Pichtel, pp. 363-391. New York: Springer New York.

Akhtar, M.S. and Z.A. Siddiqui. 2011. Role of plant growth promoting rhizobacteria in biocontrol of plant diseases and sustainable agriculture. In "Plant growth and health promoting bacteria", ed. D. K. Maheshwari, pp. 157-195. Berlin, Heidelberg: Springer Berlin Heidelberg.

Albers, H. and G. Gottschalk. 1976. Acetate metabolism in *Rhodopseudomonas gelatinosa* and several other *Rhodospirillaceae*. Arch. Microbiol. 111(1-2):45-49. doi: 10.1007/bf00446548

Ali Hassan, M., Y. Shirai, N. Kusubayashi, M. Ismail Abdul Karim, K. Nakanishi and K. Hashimoto. 1996. Effect of organic acid profiles during anaerobic treatment of palm oil mill effluent on the production of polyhydroxyalkanoates by *Rhodobacter sphaeroides*. J. Ferment. Bioeng. 82(2):151-156. doi: 10.1016/0922-338X(96)85038-0

doi:10.6342/NTU202003422

Allen, J.F. 2005. A redox switch hypothesis for the origin of two light reactions in photosynthesis. FEBS Lett. 579(5):963-968. doi: 10.1016/j.febslet.2005.01.015

Altenhoff, A.M. and C. Dessimoz. 2009. Phylogenetic and functional assessment of orthologs inference projects and methods. PLoS Comput. Biol. 5(1). doi: 10.1371/journal.pcbi.1000262

Antoun, H., C.J. Beauchamp, N. Goussard, R. Chabot and R. Lalande. 1998. Potential of *Rhizobium* and *Bradyrhizobium* species as plant growth promoting rhizobacteria on non-legumes: Effect on radishes (*Raphanus sativus* L.). Plant Soil 204(1):57-67. doi: 10.1023/A:1004326910584

Araújo, F.F., A.A. Henning and M. Hungria. 2005. Phytohormones and antibiotics produced by *Bacillus subtilis* and their effects on seed pathogenic fungi and on soybean root development. World J. Microbiol. Biotechnol. 21(8):1639-1645. doi: 10.1007/s11274-005-3621-x

Araujo, F.A., D. Barh, A. Silva, L. Guimaraes and R.T.J. Ramos. 2018. GO FEAT: a rapid web-based functional annotation tool for genomic and transcriptomic data. Sci. Rep. 8. doi: 10.1038/s41598-018-20211-9

Arshad, M., M. Saleem and S. Hussain. 2007. Perspectives of bacterial ACC deaminase in phytoremediation. Trends Biotechnol. 25(8):356-362. doi: 10.1016/j.tibtech.2007.05.005

Arzanesh, M.H., H.A. Alikhani, K. Khavazi, H.A. Rahimian and M. Miransari. 2011. Wheat (*Triticum aestivum* L.) growth enhancement by *Azospirillum* sp. under drought stress. World J. Microbiol. Biotechnol. 27(2):197-205. doi: 10.1007/s11274-010-0444-1

Ashley, E.A. 2016. Towards precision medicine. Nat. Rev. Genet. 17(9):507-522. doi: 10.1038/nrg.2016.86

Ashrafuzzaman, M., F.A. Hossen, M. Ismail, M. Hoque, M.Z. Islam, s. Shahidullah and all. 2009. Efficiency of plant growth-promoting rhizobacteria (PGPR) for the enhancement of rice growth. Afr. J. Biotechnol. 8(7):1247-1252.

Austin, S., W.S. Kontur, A. Ulbrich, J.Z. Oshlag, W. Zhang, A. Higbee and all. 2015. Metabolism of multiple aromatic compounds in corn stover hydrolysate by *Rhodopseudomonas palustris*. Environ. Sci. Technol. 49(14):8914-8922. doi: 10.1021/acs.est.5b02062

Badri, D.V. and J.M. Vivanco. 2009. Regulation and function of root exudates. Plant. Cell. Environ. 32(6):666-681. doi: 10.1111/j.1365-3040.2009.01926.x

Bagheri, B., A. Karimi-Jashni and M.M. Zerafat. 2019. Application of molasses as draw solution in forward osmosis desalination for fertigation purposes. Environ. Technol.:1-11. doi: 10.1080/09593330.2019.1645215

doi:10.6342/NTU202003422

Bankevich, A., S. Nurk, D. Antipov, A.A. Gurevich, M. Dvorkin, A.S. Kulikov and all. 2012. SPAdes: a new genome assembly algorithm and its applications to single-cell sequencing. J. Comput. Biol. 19(5):455-477. doi: 10.1089/cmb.2012.0021

Barak, P., B.O. Jobe, A.R. Krueger, L.A. Peterson and D.A. Laird. 1997. Effects of long-term soil acidification due to nitrogen fertilizer inputs in Wisconsin. Plant Soil 197(1):61-69. doi: 10.1023/A:1004297607070

Barazani, O. and J. Friedman. 1999. Is IAA the major root growth factor secreted from plant-growth-mediating bacteria? J. Chem. Ecol. 25(10):2397-2406. doi: 10.1023/A:1020890311499

Bashan, Y., J.J. Bustillos, L.A. Leyva, J.P. Hernandez and M. Bacilio. 2006. Increase in auxiliary photoprotective photosynthetic pigments in wheat seedlings induced by *Azospirillum brasilense*. Biol. Fertil. Soils 42(4):279-285. doi: 10.1007/s00374-005-0025-x

Batool, K., F. Tuz Zahra and Y. Rehman. 2017. Arsenic-redox transformation and plant growth promotion by purple nonsulfur bacteria *Rhodopseudomonas palustris* CS2 and *Rhodopseudomonas faecalis* SS5. BioMed Res. Int. 2017:6250327. doi: 10.1155/2017/6250327

Belbahri, L., A. Chenari Bouket, I. Rekik, F.N. Alenezi, A. Vallat, L. Luptakova and all. 2017. Comparative genomics of *Bacillus amyloliquefaciens* strains reveals a core genome with traits for habitat adaptation and a secondary metabolites rich accessory genome. Front. Microbiol. 8:1438. doi: 10.3389/fmicb.2017.01438

Beneduzi, A., A. Ambrosini and L.M.P. Passaglia. 2012. Plant growth-promoting rhizobacteria (PGPR): Their potential as antagonists and biocontrol agents. Genet. Mol. Biol. 35(4):1044-1051.

Berbers, B., A. Saltykova, C. Garcia-Graells, P. Philipp, F. Arella, K. Marchal and all. 2020. Combining short and long read sequencing to characterize antimicrobial resistance genes on plasmids applied to an unauthorized genetically modified *Bacillus*. Sci. Rep. 10(1):4310. doi: 10.1038/s41598-020-61158-0

Bezerra, M.A., R.E. Santelli, E.P. Oliveira, L.S. Villar and L.A. Escaleira. 2008. Response surface methodology (RSM) as a tool for optimization in analytical chemistry. Talanta 76(5):965-977. doi: 10.1016/j.talanta.2008.05.019

Bhattacharyya, P.N. and D.K. Jha. 2012. Plant growth-promoting rhizobacteria (PGPR): Emergence in agriculture. World J. Microbiol. Biotechnol. 28(4):1327-1350. doi: 10.1007/s11274-011-0979-9

Bishop, P.E. and R.D. Joerger. 1990. Genetics and molecular biology of alternative nitrogen fixation systems. Annu. Rev. Plant Phys. Plant Mol. Biol. 41(1):109-

doi:10.6342/NTU202003422

125. doi: 10.1146/annurev.pp.41.060190.000545

Boddey, R.M., V.L.D. Baldani, J.I. Baldani and J. Döbereiner. 1986. Effect of inoculation of *Azospirillum* spp. on nitrogen accumulation by field-grown wheat. Plant Soil 95(1):109-121. doi: 10.1007/BF02378857

Bolatkhan, K., B.D. Kossalbayev, B.K. Zayadan, T. Tomo, T.N. Veziroglu and S.I. Allakhuerdiev. 2019. Hydrogen production from phototrophic microorganisms: Reality and perspectives. Int. J. Hydrogen. Energ. 44(12):5799-5811. doi: 10.1016/j.ijhydene.2019.01.092

Bose, A. and D.K. Newman. 2011. Regulation of the phototrophic iron oxidation (pio) genes in *Rhodopseudomonas palustris* TIE-1 is mediated by the global regulator, FixK. Mol. Microbiol. 79(1):63-75. doi: 10.1111/j.1365-2958.2010.07430.x

Brandl, H., R.A. Gross, R.W. Lenz, R. Lloyd and R.C. Fuller. 1991. The accumulation of poly(3-Hydroxyalkanoates) in *Rhodobacter sphaeroides*. Arch. Microbiol. 155(4):337-340.

Bremner, J.M. and C.S. Mulvaney. 1982. Salicylic acid-thiosulfate modification on Kjeldahl method to include nitrate and nitrite. In "Methods of Soil Analysis Part 2 Chemical and Microbiological Properties", ed. A. L. Page, pp. 621-622. New York, USA.: Academic Press.

Brito, L., E. Bach, J. Kalinowski, C. Rückert, D. Wibberg, L. Passaglia and all. 2015. Complete genome sequence of *Paenibacillus riograndensis* SBR5T, a gram-positive diazotrophic rhizobacterium. J. Biotechnol. 207:30-31. doi: 10.1016/j.jbiotec.2015.04.025

Brock, T.D., M.T. Madigan, J.M. Martinko and J. Parker. 2003. Brock biology of microorganisms. 10th ed. ed Upper Saddle River (N.J.) : Prentice-Hall

Bykhovsky, V.Y., A.L. Demain and N.I. Zaitseva. 2008. The crucial contribution of starved resting cells to the elucidation of the pathway of vitamin B12 biosynthesis. Crit. Rev. Biotechnol. 17(1):21-37. doi: 10.3109/07388559709146605

Camacho, C., G. Coulouris, V. Avagyan, N. Ma, J. Papadopoulos, K. Bealer and all. 2009. BLAST+: Architecture and applications. BMC Bioinf. 10:421-429. doi: 10.1186/1471-2105-10-421

Carlozzi, P. and A. Sacchi. 2001. Biomass production and studies on *Rhodopseudomonas palustris* grown in an outdoor, temperature controlled, underwater tubular photobioreactor. J. Biotechnol. 88(3):239-249. doi: 10.1016/S0168-1656(01)00280-2

Cha, S.H., J.S. Lim, C.S. Yoon, J.H. Koh, H.I. Chang and S.W. Kim. 2007. Production of mycelia and exo-biopolymer from molasses by *Cordyceps sinensis* 16 in

doi:10.6342/NTU202003422

submerged culture. Bioresour. Technol. 98(1):165-168. doi: 10.1016/j.biortech.2005.11.007

Chang, T.H., R. Wang, Y.H. Peng, T.H. Chou, Y.J. Li and Y.H. Shih. 2020. Biodegradation of hexabromocyclododecane by *Rhodopseudomonas palustris* YSC3 strain: A free-living nitrogen-fixing bacterium isolated in Taiwan. Chemosphere 246:125621. doi: 10.1016/j.chemosphere.2019.125621

Chen, E.N. (2020) Comparative analyses of two *Bacillus* sp. isolates (*B. velezensis* EN01 and *B. amyloliquefaciens* WF02) and evaluation of thir biocontrol effets in the presence of Edible *Asteraceae* plant. Taipei, Taiwan: National Taiwan University. Institute of Biotechnology.

Chen, X.H., A. Koumoutsi, R. Scholz, A. Eisenreich, K. Schneider, I. Heinemeyer and all. 2007. Comparative analysis of the complete genome sequence of the plant growth-promoting bacterium *Bacillus amyloliquefaciens* FZB42. Nat. Biotechnol. 25(9):1007-1014. doi: 10.1038/nbt1325

Chen, Y., X. Shen, H. Peng, H. Hu, W. Wang and X. Zhang. 2015. Comparative genomic analysis and phenazine production of *Pseudomonas chlororaphis*, a plant growth-promoting rhizobacterium. Genom. Data 4:33-42. doi: 10.1016/j.gdata.2015.01.006

Chilcott, G.S. and K.T. Hughes. 2000. Coupling of flagellar gene expression to flagellar assembly in *salmonella enterica* serovar typhimurium and *Escherichia coli*. Microbiol. Mol. Biol. R. 64(4):694-708. doi: 10.1128/Mmbr.64.4.694-708.2000

Chinta, Y.D., K. Kano, A. Widiastuti, M. Fukahori, S. Kawasaki, Y. Eguchi and all. 2014. Effect of corn steep liquor on lettuce root rot (*Fusarium oxysporum* f.sp. *lactucae*) in hydroponic cultures. J. Sci. Food Agr. 94(11):2317-2323. doi: 10.1002/jsfa.6561

Cho, S.T., H.H. Chang, D. Egamberdieva, F. Kamilova, B. Lugtenberg and C.H. Kuo. 2015. Genome analysis of *Pseudomonas fluorescens* PCL1751: A rhizobacterium that controls root diseases and alleviates salt stress for its plant host. PLoS One 10(10):e0140231. doi: 10.1371/journal.pone.0140231

Choorit, W., A. Saikeur, P. Chodok, P. Prasertsan and D. Kantachote. 2011. Production of biomass and extracellular 5-aminolevulinic acid by *Rhodopseudomonas palustris* KG31 under light and dark conditions using volatile fatty acid. J. Biosci. Bioeng. 111(6):658-664. doi: 10.1016/j.jbiosc.2011.01.014

Ciufo, S., S. Kannan, S. Sharma, A. Badretdin, K. Clark, S. Turner and all. 2018. Using average nucleotide identity to improve taxonomic assignments in prokaryotic genomes at the NCBI. Int. J. Syst. Evol. Microbiol. 68(7):2386-2392. doi: 10.1099/ijsem.0.002809

doi:10.6342/NTU202003422

Clarke, M.A. 2003. Syrups. In "Encyclopedia of food sciences and nutrition", ed. B. Caballero, pp. 5711-5717. Oxford: Academic Press.

Cohan, F.M. and E.B. Perry. 2007. A systematics for discovering the fundamental units of bacterial diversity. Curr. Biol. 17(10):R373-386. doi: 10.1016/j.cub.2007.03.032

Cohen, A.C., C.N. Travaglia, R. Bottini and P.N. Piccoli. 2009. Participation of abscisic acid and gibberellins produced by endophytic *Azospirillum* in the alleviation of drought effects in maize. Botany 87(5):455-462. doi: 10.1139/B09-023

Comelli, R.N., L.G. Seluy and M.A. Isla. 2016. Optimization of a low-cost defined medium for alcoholic fermentation - a case study for potential application in bioethanol production from industrial wastewaters. New Biotechnol. 33(1):107-115. doi: 10.1016/j.nbt.2015.09.001

Crater, J.S. and J.C. Lievense. 2018. Scale-up of industrial microbial processes. FEMS Microbiol. Lett. 365(13). doi: 10.1093/femsle/fny138

Czitrom, V. 1999. One-factor-at-a-time versus designed experiments. Am. Stat. 53(2):126-131. doi: 10.2307/2685731

Dönmez, G.Ç., A. Öztürk and L. çakmakçı. 1999. Properties of the *Rhodopseudomonas palustris* strains isolated from an alkaline lake in turkey. Turk. J. Biol. 23(4):457–463.

D'Souza, G. and C. Kost. 2016. Experimental evolution of metabolic dependency in bacteria. PLoS Genet. 12(11):e1006364. doi: 10.1371/journal.pgen.1006364

D'Souza, G., S. Waschina, S. Pande, K. Bohl, C. Kaleta and C. Kost. 2014. Less is more: Selective advantages can explain the prevalent loss of biosynthetic genes in bacteria. Evolution 68(9):2559-2570. doi: 10.1111/evo.12468

Davies, P.J. 2010. The plant hormones: Their nature, occurrence, and functions. In "Plant hormones: Biosynthesis, signal transduction, action!", ed. P. J. Davies, pp. 1-15. Dordrecht: Springer Netherlands.

De Maio, N., L.P. Shaw, A. Hubbard, S. George, N.D. Sanderson, J. Swann and all. 2019. Comparison of long-read sequencing technologies in the hybrid assembly of complex bacterial genomes. Microb. Genom. 5(9). doi: 10.1099/mgen.0.000294

Deamer, D., M. Akeson and D. Branton. 2016. On 'three decades of nanopore sequencing' reply. Nat. Biotechnol. 34(5):482-482.

Degrassi, G., C. Aguilar, M. Bosco, S. Zahariev, S. Pongor and V. Venturi. 2002. Plant growth-promoting *Pseudomonas putida* WCS358 produces and secretes four cyclic dipeptides: Cross-talk with quorum sensing bacterial sensors. Curr. Microbiol. 45(4):250-254. doi: 10.1007/s00284-002-3704-y

doi:10.6342/NTU202003422

Delaneau, O., B. Howie, A.J. Cox, J.F. Zagury and J. Marchini. 2013. Haplotype estimation using sequencing reads. Am. J. Hum. Genet. 93(4):687-696. doi: 10.1016/j.ajhg.2013.09.002

Dhaliwal, S.S., H.S. Oberoi, S.K. Sandhu, D. Nanda, D. Kumar and S.K. Uppal. 2011. Enhanced ethanol production from sugarcane juice by galactose adaptation of a newly isolated thermotolerant strain of *Pichia kudriavzevii*. Bioresour. Technol. 102(10):5968-5975. doi: 10.1016/j.biortech.2011.02.015

Divan Baldani, V.L., J.I. Baldani and J. Döbereiner. 2000. Inoculation of rice plants with the endophytic diazotrophs *Herbaspirillum seropedicae* and *Burkholderia* spp. Biol. Fertil. Soils 30(5):485-491. doi: 10.1007/s003740050027

Doudoroff, M. and R.Y. Stanier. 1959. Role of poly-beta-hydroxybutyric acid in the assimilation of organic carbon by bacteria. Nature 183(4673):1440-1442. doi: 10.1038/1831440a0

Du, C., J. Zhou, J. Wang, B. Yan, H. Lu and H. Hou. 2003. Construction of a genetically engineered microorganism for CO_2 fixation using a *Rhodopseudomonas*/*Escherichia coli* shuttle vector. FEMS Microbiol. Lett. 225(1):69-73. doi: 10.1016/S0378-1097(03)00482-8

Duan, J., W. Jiang, Z.Y. Cheng, J.J. Heikkila and B.R. Glick. 2013. The complete genome sequence of the plant growth-promoting bacterium *Pseudomonas* sp. UW4. PLoS One 8(3):e58640. doi: 10.1371/journal.pone.0058640

Dutton, P.L. and W.C. Evans. 1969. The metabolism of aromatic compounds by *Rhodopseudomonas palustris*. A new, reductive, method of aromatic ring metabolism. Biochem. J. 113(3):525-536. doi: 10.1042/bj1130525

Edgar, R.C. 2004. MUSCLE: multiple sequence alignment with high accuracy and high throughput. Nucleic Acids Res. 32(5):1792-1797. doi: 10.1093/nar/gkh340

Eisenhauer, N., A. Lanoue, T. Strecker, S. Scheu, K. Steinauer, M.P. Thakur and all. 2017. Root biomass and exudates link plant diversity with soil bacterial and fungal biomass. Sci. Rep. 7. doi: 10.1038/srep44641

Felsenstein, J. 1985. Confidence limits on phylogenies - an approach using the bootstrap. Evolution 39(4):783-791. doi: 10.2307/2408678

Figueiredo, M.V.B., C.R. Martinez, H.A. Burity and C.P. Chanway. 2008. Plant growth-promoting rhizobacteria for improving nodulation and nitrogen fixation in the common bean (*Phaseolus vulgaris* L.). World J. Microbiol. Biotechnol. 24(7):1187-1193. doi: 10.1007/s11274-007-9591-4

Fritts, R.K., B. LaSarre, A.M. Stoner, A.L. Posto and J.B. McKinlay. 2017. A Rhizobiales-specific unipolar polysaccharide adhesin contributes to

doi:10.6342/NTU202003422

Rhodopseudomonas palustris biofilm formation across diverse photoheterotrophic conditions. Appl. Environ. Microbiol. 83(4):e03035-03016. doi: 10.1128/AEM.03035-16

Galperin, M.Y., K.S. Makarova, Y.I. Wolf and E.V. Koonin. 2015. Expanded microbial genome coverage and improved protein family annotation in the COG database. Nucleic Acids Res. 43(Database issue):D261-269. doi: 10.1093/nar/gku1223

Garcia de Salamone, I.E., J. Döbereiner, S. Urquiaga and R.M. Boddey. 1996. Biological nitrogen fixation in *Azospirillum* strain-maize genotype associations as evaluated by the 15N isotope dilution technique. Biol. Fertil. Soils 23(3):249-256. doi: 10.1007/BF00335952

García de Salamone, I.E., R.K. Hynes and L.M. Nelson. 2001. Cytokinin production by plant growth promoting rhizobacteria and selected mutants. Can. J. Microbiol. 47(5):404-411. doi: 10.1139/w01-029

Gobbetti, M. and A. Corsetti. 1996. Co-metabolism of citrate and maltose by *Lactobacillus brevis* subsp. *lindneri* CB1 citrate-negative strain: Effect on growth, end-products and sourdough fermentation. Eur. Food Res. Technol. 203(1):82-87. doi: 10.1007/BF01267775

Goswami, D., K. Patel, S. Parmar, H. Vaghela, N. Muley, P. Dhandhukia and all. 2015. Elucidating multifaceted urease producing marine *Pseudomonas aeruginosa* BG as a cogent PGPR and bio-control agent. Plant Growth Regul. 75(1):253-263. doi: 10.1007/s10725-014-9949-1

Goswami, D., S. Pithwa, P. Dhandhukia and J.N. Thakker. 2014. Delineating Kocuria turfanensis 2M4 as a credible PGPR: a novel IAA-producing bacteria isolated from saline desert. J. Plant Interact. 9(1):566-576. doi: 10.1080/17429145.2013.871650

Goswami, D., J.N. Thakker and P.C. Dhandhukia. 2016. Portraying mechanics of plant growth promoting rhizobacteria (PGPR): a review. Cogent Food Agric. 2(1):1127500-1127518. doi: 10.1080/23311932.2015.1127500

Govindaraju, A., J.B. McKinlay and B. LaSarre. 2019. Phototrophic lactate utilization by *Rhodopseudomonas palustris* is stimulated by coutilization with additional substrates. Appl. Environ. Microbiol. 85(11). doi: 10.1128/AEM.00048-19

Griffin, B.M., J. Schott and B. Schink. 2007. Nitrite, an electron donor for anoxygenic photosynthesis. Science 316:1870.

Guindon, S. and O. Gascuel. 2003. A simple, fast, and accurate algorithm to estimate large phylogenies by maximum likelihood. Syst. Biol. 52(5):696-704. doi: 10.1080/10635150390235520

Gupta, A., M. Gopal, G.V. Thomas, V. Manikandan, J. Gajewski, G. Thomas and all.

doi:10.6342/NTU202003422

2014. Whole genome sequencing and analysis of plant growth promoting bacteria isolated from the rhizosphere of plantation crops coconut, cocoa and arecanut. PLoS One 9(8):e104259. doi: 10.1371/journal.pone.0104259

Hall, T.A. 1999. BioEdit: a user-friendly biological sequence alignment editor and analysis program for Windows 95/98/NT. Nucleic Acids Symp. Ser. 41:95-98. doi: citeulike-article-id:691774

Harder, W. and L. Dijkhuizen. 1982. Strategies of mixed substrate utilization in microorganisms. Philos. Trans. R. Soc. Lond. B. Biol. Sci. 297(1088):459-480. doi: 10.1098/rstb.1982.0055

Harrison, F.H. and C.S. Harwood. 2005. The *pimFABCDE* operon from *Rhodopseudomonas palustris* mediates dicarboxylic acid degradation and participates in anaerobic benzoate degradation. Microbiology 151(Pt 3):727-736. doi: 10.1099/mic.0.27731-0

Harwood, C.S., G. Burchhardt, H. Herrmann and G. Fuchs. 1998. Anaerobic metabolism of aromatic compounds via the benzoyl-CoA pathway. FEMS Microbiol. Rev. 22(5):439-458. doi: 10.1111/j.1574-6976.1998.tb00380.x

Harwood, C.S. and J. Gibson. 1988. Anaerobic and aerobic metabolism of diverse aromatic compounds by the photosynthetic bacterium *Rhodopseudomonas palustris*. Appl. Environ. Microbiol. 54(3):712-717.

Heather, J.M. and B. Chain. 2016. The sequence of sequencers: The history of sequencing DNA. Genomics 107(1):1-8. doi: 10.1016/j.ygeno.2015.11.003

Hermsen, R., H. Okano, C. You, N. Werner and T. Hwa. 2015. A growth-rate composition formula for the growth of *E.coli* on co-utilized carbon substrates. Mol. Syst. Biol. 11(4):801. doi: 10.15252/msb.20145537

Hiraishi, A. and H. Kitamura. 1984. Distribution of phototrophic purple nonsulfur bacteria in activated-sludge systems and other aquatic environments. B. Jpn. Soc. Sci. Fish. 50(11):1929-1937.

Hirakawa, H., Y. Hirakawa, E.P. Greenberg and C.S. Harwood. 2015. BadR and BadM proteins transcriptionally regulate two operons needed for anaerobic benzoate degradation by *Rhodopseudomonas palustris*. Appl. Environ. Microbiol. 81(13):4253-4262. doi: 10.1128/AEM.00377-15

Hirotani, H., Y. Agui, M. Kobayashi and E. Takahashi. 1990. Removal of coliphages from wastewater effluent by phototrophic bacteria. Water Sci. Technol. 22(9):59-63. doi: 10.2166/wst.1990.0067

Hoagland, D.R. and D.I. Arnon. 1950. The Water-culture method for growing plants without soil University of California, College of Agriculture, Agricultural Experiment Station

Hsu, S.H., K.J. Lo, W. Fang, H.S. Lur and C.T. Liu. 2015. Application of phototrophic

doi:10.6342/NTU202003422

bacterial inoculant to reduce nitrate content in hydroponic leafy vegetables. Crop Environ. Bioinf. 12:30-41.

Hu, H.Q., X.S. Li and H. He. 2010. Characterization of an antimicrobial material from a newly isolated *Bacillus amyloliquefaciens* from mangrove for biocontrol of capsicum bacterial wilt. Biol. Control 54(3):359-365. doi: 10.1016/j.biocontrol.2010.06.015

Hull, S.R., B.Y. Yang, D. Venzke, K. Kulhavy and R. Montgomery. 1996. Composition of corn steep water during steeping. J. Agr. Food Chem. 44(7):1857-1863. doi: 10.1021/jf950353v

Hyatt, D., G.L. Chen, P.F. Locascio, M.L. Land, F.W. Larimer and L.J. Hauser. 2010. Prodigal: Prokaryotic gene recognition and translation initiation site identification. BMC Bioinf. 11:119-129. doi: 10.1186/1471-2105-11-119

Idi, A., M.H.M. Nor, M.F.A. Wahab and Z. Ibrahim. 2015. Photosynthetic bacteria: an eco-friendly and cheap tool for bioremediation. Rev. Environ. Sci. Bio. 14(2):271-285. doi: 10.1007/s11157-014-9355-1

Imhoff, J.F. 2006. The Phototrophic alpha-proteobacteria. In "The Prokaryotes: Volume 5: Proteobacteria: Alpha and beta subclasses", ed. M. Dworkin, S. Falkow, E. Rosenberg, K.-H. Schleifer and E. Stackebrandt, pp. 41-64. New York: Springer New York.

Imhoff, J.F. and H.G. Trüper. 1992. The genus *Rhodospirillum* and related genera. In "The prokaryotes", ed. A. Balows, H. G. Trüper, M. Dworkin, W. Harder and K.-H. Schleifer, pp. 2141-2155. New York: Springer-Verlag.

Imran, A., M.J.A. Saadalla, S.U. Khan, M.S. Mirza, K.A. Malik and F.Y. Hafeez. 2014. *Ochrobactrum* sp Pv2Z2 exhibits multiple traits of plant growth promotion, biodegradation and N-acyl-homoserine-lactone quorum sensing. Ann. Microbiol. 64(4):1797-1806. doi: 10.1007/s13213-014-0824-0

Jain, C., L.M. Rodriguez-R, A.M. Phillippy, K.T. Konstantinidis and S. Aluru. 2018. High throughput ANI analysis of 90K prokaryotic genomes reveals clear species boundaries. Nature Communications 9(1):5114. doi: 10.1038/s41467-018-07641-9

Jendrossek, D. and D. Pfeiffer. 2014. New insights in the formation of polyhydroxyalkanoate granules (carbonosomes) and novel functions of poly(3-hydroxybutyrate). Environ. Microbiol. 16(8):2357-2373. doi: 10.1111/1462-2920.12356

Jousset, A., J. Schuldes, C. Keel, M. Maurhofer, R. Daniel, S. Scheu and all. 2014. Full-genome sequence of the plant growth-promoting bacterium *Pseudomonas protegens* CHA0. Genome Announc. 2(2). doi: 10.1128/genomeA.00322-14

Jung, B.K., A.R. Khan, S.J. Hong, G.S. Park, Y.J. Park, H.J. Kim and all. 2017.

doi:10.6342/NTU202003422

Quorum sensing activity of the plant growth-promoting rhizobacterium *Serratia glossinae* GS2 isolated from the sesame (*Sesamum indicum* L.) rhizosphere. Ann. Microbiol. 67(9):623-632. doi: 10.1007/s13213-017-1291-1

Kanehisa, M., Y. Sato and K. Morishima. 2016. BlastKOALA and GhostKOALA: KEGG tools for functional characterization of genome and metagenome sequences. J. Mol. Biol. 428(4):726-731. doi: 10.1016/j.jmb.2015.11.006

Kaneko, T., Y. Nakamura, S. Sato, K. Minamisawa, T. Uchiumi, S. Sasamoto and all. 2002. Complete genomic sequence of nitrogen-fixing symbiotic bacterium *Bradyrhizobium japonicum* USDA110. DNA Res. 9(6):189-197. doi: 10.1093/dnares/9.6.189

Kang, S.-M., R. Radhakrishnan, A.L. Khan, M.-J. Kim, J.-M. Park, B.-R. Kim and all. 2014. Gibberellin secreting rhizobacterium, *Pseudomonas putida* H-2-3 modulates the hormonal and stress physiology of soybean to improve the plant growth under saline and drought conditions. Plant Physiol. Biochem. 84:115-124. doi: 10.1016/j.plaphy.2014.09.001

Kang, S.M., S. Asaf, S.J. Kim, B.W. Yun and I.J. Lee. 2016. Complete genome sequence of plant growth-promoting bacterium *Leifsonia xyli* SE134, a possible gibberellin and auxin producer. J. Biotechnol. 239:34-38. doi: 10.1016/j.jbiotec.2016.10.004

Karpinets, T.V., D.A. Pelletier, C. Pan, E.C. Uberbacher, G.V. Melnichenko, R.L. Hettich and all. 2009. Phenotype fingerprinting suggests the involvement of single-genotype consortia in degradation of aromatic compounds by *Rhodopseudomonas palustris*. PLoS One 4(2):e4615. doi: 10.1371/journal.pone.0004615

Kasim, W.A., M.E. Osman, M.N. Omar, I.A. Abd El-Daim, S. Bejai and J. Meijer. 2013. Control of drought stress in wheat using plant-growth-promoting bacteria. J. Plant Growth Regul. 32(1):122-130. doi: 10.1007/s00344-012-9283-7

Kaymak, H.C. 2011. Potential of PGPR in agricultural innovations. In "Plant growth and health promoting bacteria", ed. D. K. Maheshwari, pp. 45-79. Berlin, Heidelberg: Springer Berlin Heidelberg.

Kim, J., K. Ito and H. Takahashi. 1980. The relationship between nitrogenase activity and hydrogen evolution in *Rhodopseudomonas palustris*. Agric. Biol. Chem. 44(4):827-833.

Kim, J. and D.C. Rees. 1994. Nitrogenase and biological nitrogen fixation. Biochemistry 33(2):389-397. doi: 10.1021/bi00168a001

Kleijn, R.J., J.M. Buescher, L. Le Chat, M. Jules, S. Aymerich and U. Sauer. 2010. Metabolic fluxes during strong carbon catabolite repression by malate in

doi:10.6342/NTU202003422

Bacillus subtilis. J. Biol. Chem. 285(3):1587-1596. doi: 10.1074/jbc.M109.061747

Kloepper, J.W. and M.N. Schroth. (1978) In S. d. P. V. e. Phyto-Bactériologie (ed.), *Proceedings of the 4th international conference on plant pathogenic bacteria*, Gilbert-Clarey, Tours, France, Vol. 2, pp. 879-882.

Kobayash.M and Nakanish.H. 1971. Studies on photosynthetic bacteria .28. construction of a purification plant for polluted water using photosynthetic bacteria. J Ferment. Technol. 49(9):817.

Kobayashi, M., T. Suzuki, T. Fujita, M. Masuda and S. Shimizu. 1995. Occurrence of enzymes involved in biosynthesis of indole-3-acetic-acid from indole-3-acetonitrile in plant-associated bacteria, *Agrobacterium* and *Rhizobium*. Proc. Natl. Acad. Sci. U. S. A. 92(3):714-718. doi: 10.1073/pnas.92.3.714

Koberl, M., R.A. White, S. Erschen, N. Spanberger, T.F. El-Arabi, J.K. Jansson and all. 2015. Complete genome sequence of *Bacillus amyloliquefaciens* strain Co1-6, a plant growth-promoting rhizobacterium of *Calendula officinalis*. Microbiol. Resour. Announc. 3(4). doi: 10.1128/genomeA.00862-15

Koh, R.H. and H.G. Song. 2007. Effects of application of *Rhodopseudomonas* sp. on seed germination and growth of tomato under axenic conditions. J. Microbiol. Biotechnol. 17(11):1805-1810.

Kokalis–Burelle, N., C.S. Vavrina, E.N. Rosskopf and R.A. Shelby. 2002. Field evaluation of plant growth-promoting *Rhizobacteria amended* transplant mixes and soil solarization for tomato and pepper production in Florida. Plant Soil 238(2):257-266. doi: 10.1023/A:1014464716261

Kondo, K., N. Nakata and E. Nishihara. 2010. Effect of the purple non-sulfur bacterium (*Rhodobacter sphaeroides*) on the Brix, titratable acidity, ascorbic acid, organic acid, lycopene and beta-carotene in tomato fruit. J. Food Agric. Environ. 8:743-746.

Korkmaz, A., Y. Korkmaz and A.R. Demirkiran. 2010. Enhancing chilling stress tolerance of pepper seedlings by exogenous application of 5-aminolevulinic acid. Environ. Exp. Bot. 67(3):495-501. doi: 10.1016/j.envexpbot.2009.07.009

Kornochalert, N., D. Kantachote, S. Chaiprapat and S. Techkarnjanaruk. 2014. Use of *Rhodopseudomonas palustris* P1 stimulated growth by fermented pineapple extract to treat latex rubber sheet wastewater to obtain single cell protein. Ann. Microbiol. 64(3):1021-1032. doi: 10.1007/s13213-013-0739-1

Krzywinski, M., J. Schein, I. Birol, J. Connors, R. Gascoyne, D. Horsman and all. 2009. Circos: An information aesthetic for comparative genomics. Genome Res. 19(9):1639-1645. doi: 10.1101/gr.092759.109

Kumar, S., G. Stecher and K. Tamura. 2016. MEGA7: Molecular evolutionary

doi:10.6342/NTU202003422

genetics analysis version 7.0 for bigger datasets. Mol. Biol. Evol. 33(7):1870-1874. doi: 10.1093/molbev/msw054

Kurtz, S., A. Phillippy, A.L. Delcher, M. Smoot, M. Shumway, C. Antonescu and all. 2004. Versatile and open software for comparing large genomes. Genome Biol. 5(2):R12. doi: 10.1186/gb-2004-5-2-r12

Lagesen, K., P. Hallin, E.A. Rodland, H.H. Staerfeldt, T. Rognes and D.W. Ussery. 2007. RNAmmer: Consistent and rapid annotation of ribosomal RNA genes. Nucleic Acids Res. 35(9):3100-3108. doi: 10.1093/nar/gkm160

Laguna, R., F.R. Tabita and B.E. Alber. 2011. Acetate-dependent photoheterotrophic growth and the differential requirement for the Calvin-Benson-Bassham reductive pentose phosphate cycle in *Rhodobacter sphaeroides* and *Rhodopseudomonas palustris*. Arch. Microbiol. 193(2):151-154. doi: 10.1007/s00203-010-0652-y

Larimer, F.W., P. Chain, L. Hauser, J. Lamerdin, S. Malfatti, L. Do and all. 2004. Complete genome sequence of the metabolically versatile photosynthetic bacterium *Rhodopseudomonas palustris*. Nat. Biotechnol. 22(1):55-61. doi: 10.1038/nbt923

Lee, M.G., M. Kobayashi and K. Yasumoto. 1990. Hypocholesterolemic effect of phototrophic bacterial cells in rats. J. Nutr. Sci. Vitaminol. 36(5):475-483. doi: 10.3177/jnsv.36.475

Lee, S.K., H.S. Lur, K.J. Lo, K.C. Cheng, C.C. Chuang, S.J. Tang and all. 2016. Evaluation of the effects of different liquid inoculant formulations on the survival and plant-growth-promoting efficiency of *Rhodopseudomonas palustris* strain PS3. Appl. Microbiol. Biotechnol. 100(18):7977-7987. doi: 10.1007/s00253-016-7582-9

Lee, Y.C., J.M. Johnson, C.T. Chien, C. Sun, D.G. Cai, B.G. Lou and all. 2011. Growth promotion of Chinese cabbage and *Arabidopsis* by *Piriformospora indica* is not stimulated by mycelium-synthesized auxin. Mol. Plant Microbe. Interact. 24(4):421-431. doi: 10.1094/Mpmi-05-10-0110

Leipe, D.D. and D. Landsman. 1997. Histone deacetylases, acetoin utilization proteins and acetylpolyamine amidohydrolases are members of an ancient protein superfamily. Nucleic Acids Res. 25(18):3693-3697. doi: 10.1093/nar/25.18.3693

Lenth, R.V. 2009. Response-surface methods in R, using rsm. J. Stat. Softw. 32(7):1-17. doi: 10.18637/jss.v032.i07

Levene, M.J., J. Korlach, S.W. Turner, M. Foquet, H.G. Craighead and W.W. Webb. 2003. Zero-mode waveguides for single-molecule analysis at high concentrations. Science 299(5607):682-686. doi: 10.1126/science.1079700

doi:10.6342/NTU202003422

Li, D., Y. Yan, S. Ping, M. Chen, W. Zhang, L. Li and all. 2010. Genome-wide investigation and functional characterization of the beta-ketoadipate pathway in the nitrogen-fixing and root-associated bacterium *Pseudomonas stutzeri* A1501. BMC Microbiol. 10:36. doi: 10.1186/1471-2180-10-36

Li, K.X., S. Liu and X.H. Liu. 2014. An overview of algae bioethanol production. Int. J. Energ. Res. 38(8):965-977. doi: 10.1002/er.3164

Li, L., C.J. Stoeckert, Jr and D.S. Roos. 2003. OrthoMCL: Identification of ortholog groups for eukaryotic genomes. Genome Res. 13(9):2178-2189. doi: 10.1101/gr.1224503

Liggett, R.W. and H. Koffler. 1948. Corn steep liquor in microbiology. Bacteriol. Rev. 12(4):297-311. doi: 10.1128/Mmbr.12.4.297-311.1948

Lin, G.-H., C.Y. Chang and H.-R. Lin. 2015. Systematic profiling of indole-3-acetic acid biosynthesis in bacteria using LC–MS/MS. J. Chromatogr. B. 988:53-58. doi: doi.org/10.1016/j.jchromb.2015.02.025

Liu, B.B., M.H. Yang, B.K. Qi, X.R. Chen, Z.G. Su and Y.H. Wan. 2010. Optimizing L-(+)-lactic acid production by thermophile *Lactobacillus plantarum* As 1 3 using alternative nitrogen sources with response surface method. Biochem. Eng. J. 52(2-3):212-219. doi: 10.1016/j.bej.2010.08.013

Liu, D., L.T. Wu, M.S. Naeem, H.B. Liu, X.Q. Deng, L. Xu and all. 2013a. 5-Aminolevulinic acid enhances photosynthetic gas exchange, chlorophyll fluorescence and antioxidant system in oilseed rape under drought stress. Acta Physiol. Plant. 35(9):2747-2759. doi: 10.1007/s11738-013-1307-9

Liu, F., S. Xing, H. Ma, Z. Du and B. Ma. 2013b. Cytokinin-producing, plant growth-promoting rhizobacteria that confer resistance to drought stress in *Platycladus orientalis* container seedlings. Appl. Microbiol. Biotechnol. 97(20):9155-9164. doi: 10.1007/s00253-013-5193-2

Liu, S. 2017. Chapter 2 - An overview of biological basics. In "Bioprocess Engineering", ed. S. Liu, pp. 21-80 Elsevier.

Liu, W.X., Q.L. Wang, J.Y. Hou, C. Tu, Y.M. Luo and P. Christie. 2016a. Whole genome analysis of halotolerant and alkalotolerant plant growth-promoting rhizobacterium *Klebsiella* sp. D5A. Sci. Rep. 6:26710-26719. doi: 10.1038/srep26710

Liu, X.Y., X.Y. Xu, Q.I. Ma and W.H. Wu. 2005. Biological formation of 5-aminolevulinic acid by photosynthetic bacteria. J. Environ. Sci. 17(1):152-155.

Liu, Y., L. Chen, N. Zhang, Z. Li, G. Zhang, Y. Xu and all. 2016b. Plant-microbe communication enhances auxin biosynthesis by a root-associated bacterium, *Bacillus amyloliquefaciens SQR9*. Mol. Plant Microbe. Interact. 29(4):324-

doi:10.6342/NTU202003422

330. doi: 10.1094/mpmi-10-15-0239-r

Liu, Y., D. Ghosh and P.C. Hallenbeck. 2015. Biological reformation of ethanol to hydrogen by *Rhodopseudomonas palustris* CGA009. Bioresour. Technol. 176:189-195. doi: 10.1016/j.biortech.2014.11.047

Liu, Y.Y. (2018) Evaluation of the multifunctional effects of *Bacillus amyloliquefaciens* strain WF02 formulated with a phytogenic additive *Bidens pilosa* against bacterial fruit lotch of melon. Taipei, Taiwan: National Taiwan University. Institute of Biotechnology.

Livak, K.J. and T.D. Schmittgen. 2001. Analysis of relative gene expression data using real-time quantitative PCR and the 2(T)(-delta delta C) method. Methods 25(4):402-408. doi: 10.1006/meth.2001.1262

Lo, K.J., S.S. Lin, C.W. Lu, C.H. Kuo and C.T. Liu. 2018. Whole-genome sequencing and comparative analysis of two plant-associated strains of *Rhodopseudomonas palustris* (PS3 and YSC3). Sci. Rep. 8(1):12769. doi: 10.1038/s41598-018-31128-8

Lo, K.J. and C.T. Liu. 2020. Application of genomics technology in gariculture bactera. In "Application and prospect of genomics technology in the research of agriculture", ed. J. R. Liu and M. C. Shih, pp. 126-156. Taiwan: National Taiwan University Education Center for Agriculture Innovation and Industrialization.

Loper, J.E., D.Y. Kobayashi and I.T. Paulsen. 2007. The Genomic sequence of *Pseudomonas fluorescens* Pf-5: Insights into biological control. Phytopathology 97(2):233-238. doi: 10.1094/phyto-97-2-0233

Lowe, T.M. and S.R. Eddy. 1997. tRNAscan-SE: A program for improved detection of transfer RNA genes in genomic sequence. Nucleic Acids Res. 25(5):955-964.

Loy, D.D. and E.L. Lundy. 2019. Nutritional poperties and feeding value of corn and its coproducts. In "Corn ", ed. S. O. Serna-Saldivar, pp. 633-659. Oxford: AACC International Press.

Lugtenberg, B. and F. Kamilova. 2009. Plant-growth-promoting rhizobacteria. Annu. Rev. Microbiol. 63:541-556. doi: 10.1146/annurev.micro.62.081307.162918

Ma, J., C. Wang, H. Wang, K. Liu, T. Zhang, L. Yao and all. 2018. Analysis of the complete genome sequence of *Bacillus atrophaeus* GQJK17 reveals its biocontrol characteristics as a plant growth-promoting rhizobacterium. BioMed Res. Int. 2018:9473542. doi: 10.1155/2018/9473542

MacLean, D., J.D. Jones and D.J. Studholme. 2009. Application of 'next-generation' sequencing technologies to microbial genetics. Nat. Rev. Microbiol. 7(4):287-296. doi: 10.1038/nrmicro2122

doi:10.6342/NTU202003422

Madhaiyan, M., S. Poonguzhali, J. Ryu and T. Sa. 2006. Regulation of ethylene levels in canola (*Brassica campestris*) by 1-aminocyclopropane-1-carboxylate deaminase-containing *Methylobacterium fujisawaense*. Planta 224(2):268-278. doi: 10.1007/s00425-005-0211-y

Madigan, M.T. and D.O. Jung. 2009. An overview of purple bacteria: Systematics, physiology, and habitats. In "The purple phototrophic bacteria", ed. C. N. Hunter, F. Daldal, M. C. Thurnauer and J. T. Beatty, pp. 1-15. Dordrecht: Springer Netherlands.

Madigan, M.T., J.M. Martinko and T.D. Brock. 2006. Brock biology of microorganisms. Upper Saddle River, NJ: Pearson Prentice Hall

Magno-Perez-Bryan, M.C., P.M. Martinez-Garcia, J. Hierrezuelo, P. Rodriguez-Palenzuela, E. Arrebola, C. Ramos and all. 2015. Comparative genomics within the *Bacillus genus* reveal the singularities of two robust *Bacillus amyloliquefaciens* biocontrol strains. Mol. Plant Microbe. Interact. 28(10):1102-1116. doi: 10.1094/Mpm1-02-15-0023-R

Malik, K.A., R. Bilal, S. Mehnaz, G. Rasul, M.S. Mirza and S. Ali. 1997. Association of nitrogen-fixing, plant-growth-promoting rhizobacteria (PGPR) with kallar grass and rice. Plant Soil 194(1):37-44. doi: 10.1023/A:1004295714181

Martens, M., P. Dawyndt, R. Coopman, M. Gillis, P. De Vos and A. Willems. 2008. Advantages of multilocus sequence analysis for taxonomic studies: a case study using 10 housekeeping genes in the genus Ensifer (including former *Sinorhizobium*). Int. J. Syst. Evol. Microbiol. 58(Pt 1):200-214. doi: 10.1099/ijs.0.65392-0

Martina, P., M. Leguizamon, C.I. Prieto, S.A. Sousa, P. Montanaro, W.O. Draghi and all. 2018. *Burkholderia puraquae* sp. nov., a novel species of the *Burkholderia cepacia* complex isolated from hospital settings and agricultural soils. Int. J. Syst. Evol. Microbiol. 68(1):14-20. doi: 10.1099/ijsem.0.002293

Martinez-Garcia, P.M., D. Ruano-Rosa, E. Schiliro, P. Prieto, C. Ramos, P. Rodriguez-Palenzuela and all. 2015. Complete genome sequence of *Pseudomonas fluorescens* strain PICF7, an indigenous root endophyte from olive (*Olea europaea* L.) and effective biocontrol agent against *Verticillium dahliae*. Stand. Genomic Sci. 10:10. doi: 10.1186/1944-3277-10-10

Matteoli, F.P., H. Passarelli-Araujo, R.J.A. Reis, L.O. da Rocha, E.M. de Souza, L. Aravind and all. 2018. Genome sequencing and assessment of plant growth-promoting properties of a *Serratia marcescens* strain isolated from vermicompost. BMC Genomics 19(1):750. doi: 10.1186/s12864-018-5130-y

Mavromatis, K., M.L. Land, T.S. Brettin, D.J. Quest, A. Copeland, A. Clum and all. 2012. The fast changing landscape of sequencing technologies and their

doi:10.6342/NTU202003422

impact on microbial genome assemblies and annotation. PLoS One 7(12). doi: 10.1371/journal.pone.0048837

Mayak, S., T. Tirosh and B.R. Glick. 1999. Effect of wild-type and mutant plant growth-promoting rhizobacteria on the rooting of mung bean cuttings. J. Plant Growth Regul. 18(2):49-53. doi: 10.1007/PL00007047

Mayak, S., T. Tirosh and B.R. Glick. 2004. Plant growth-promoting bacteria that confer resistance to water stress in tomatoes and peppers. Plant Sci. 166(2):525-530. doi: 10.1016/j.plantsci.2003.10.025

McKinlay, J.B. and C.S. Harwood. 2011. Calvin cycle flux, pathway constraints, and substrate oxidation state together determine the H-2 biofuel yield in photoheterotrophic bacteria. mbio 2(2). doi: 10.1128/mBio.00323-10

Merrick, J.M. and M. Doudoroff. 1961. Enzymatic synthesis of poly-beta-hydroxybutyric acid in bacteria. Nature 189:890-892. doi: 10.1038/189890a0

Merugu, R., M.P.P. Rudra, A.S. Rao, D. Ramesh, B. Nageshwari, K. Rajyalaxmi and all. 2011. Influence of different cultural conditions on photoproduction of hydrogen by *Rhodopseudomonas palustris* KU003. ISRN Renew. Energy 2011:6. doi: 10.5402/2011/328984

Mirmiran, P., Z. Houshialsadat, Z. Gaeini, Z. Bahadoran and F. Azizi. 2020. Functional properties of beetroot (*Beta vulgaris*) in management of cardio-metabolic diseases. Nutr. Metab. 17(1). doi: 10.1186/s12986-019-0421-0

Moraes, I.O., D.M.F. Capalbo and R.O. Moraes. 1991. Multiplicação de agentes de controle biológico. In "Controle biológico de doenças de plantas", pp. 253-272. Brasília: EMBRAPA.

Morales-Payan, J.P. and W.M. Stall. 2005. Papaya transplant growth as affected by 5-aminolevulinic acid and nitrogen fertilization. Flori. Stat. Hortic. Soc. 118:263-265.

Morris, R.O. 1995. Genes specifying auxin and cytokinin biosynthesis in prokaryotes. In "Plant hormones: Physiology, biochemistry and molecular biology", ed. P. J. Davies, pp. 318-339. Dordrecht: Springer Netherlands.

Moutia, J.-F.Y., S. Saumtally, S. Spaepen and J. Vanderleyden. 2010. Plant growth promotion by *Azospirillum* sp. in sugarcane is influenced by genotype and drought stress. Plant Soil 337(1):233-242. doi: 10.1007/s11104-010-0519-7

Mrkovacki, N. and V. Milic. 2001. Use of *Azotobacter chroococcum* as potentially useful in agricultural application. Ann. Microbiol. 51:145-158.

Murphy, J.F., G.W. Zehnder, D.J. Schuster, E.J. Sikora, J.E. Polston and J.W. Kloepper. 2000. Plant growth-promoting rhizobacterial mediated protection in tomato against tomato mottle virus. Plant Dis. 84(7):779-784. doi: 10.1094/pdis.2000.84.7.779

doi:10.6342/NTU202003422

Murugappan, R.M., S. Begum and R. Roobia. 2013. Symbiotic influence of endophytic *Bacillus pumilus* on growth promotion and probiotic potential of the medicinal plant *Ocimum sanctum*. Symbiosis 60(2):91-99. doi: 10.1007/s13199-013-0244-0

Nadeem, S., Z. Zahir, M. Naveed, H. Asghar and M. Arshad. 2010. Rhizobacteria capable of producing ACC-deaminase may mitigate salt stress in wheat. Soil Sci. Soc. Am. J. 74(2):533–542. doi: 10.2136/sssaj2008.0240

Naeem, M.S., H. Warusawitharana, H.B. Liu, D. Liu, R. Ahmad, E.A. Waraich and all. 2012. 5-Aminolevulinic acid alleviates the salinity-induced changes in *Brassica napus* as revealed by the ultrastructural study of chloroplast. Plant Physiol. Biochem. 57:84-92. doi: 10.1016/j.plaphy.2012.05.018

Nagarajan, N. and M. Pop. 2013. Sequence assembly demystified. Nat. Rev. Genet. 14(3):157-167. doi: 10.1038/nrg3367

Najafpour, G.D. and C.P. Shan. 2003. Enzymatic hydrolysis of molasses. Bioresour. Technol. 86(1):91-94. doi: 10.1016/s0960-8524(02)00103-7

Nautiyal, C.S. 1999. An efficient microbiological growth medium for screening phosphate solubilizing microorganisms. FEMS Microbiol. Lett. 170(1):265-270. doi: 10.1111/j.1574-6968.1999.tb13383.x

Navarrete-Bolaños, J.L. 2012. Improving traditional fermented beverages: How to evolve from spontaneous to directed fermentation. Eng. Life Sci. 12(4):410-418. doi: 10.1002/elsc.201100128

Nelson, D.W. and L.E. Sommers. 1982. Total carbon, organic carbon, and organic matter. In "Methods of soil analysis", ed. A. L. Page, pp. 539-579

Nelson, E.K. 1929. Some organic acids of sugar cane molasses. J. Am. Chem. Soc. 51(9):2808-2810. doi: 10.1021/ja01384a030

Nishikawa, S. and Y. Murooka. 2001. 5-Aminolevulinic acid: Production by fermentation, and agricultural and biomedical applications. Biotechnol. Genet. Eng. Rev. 18:149-170.

Noel, T.C., C. Sheng, C.K. Yost, R.P. Pharis and M.F. Hynes. 1996. *Rhizobium leguminosarum* as a plant growth-promoting rhizobacterium: direct growth promotion of canola and lettuce. Can. J. Microbiol. 42(3):279-283. doi: 10.1139/m96-040

Novak, R.T., R.F. Gritzer, E.R. Leadbetter and W. Godchaux. 2004. Phototrophic utilization of taurine by the purple nonsulfur bacteria *Rhodopseudomonas palustris* and *Rhodobacter sphaeroides*. Microbiology 150(Pt 6):1881-1891. doi: 10.1099/mic.0.27023-0

Nunkaew, T., D. Kantachote, S. Chaiprapat, T. Nitoda and H. Kanzaki. 2018. Use of wood vinegar to enhance 5-aminolevulinic acid production by selected

doi:10.6342/NTU202003422

Rhodopseudomonas palustris in rubber sheet wastewater for agricultural use. Saudi J. Biol. Sci. 25(4):642-650. doi: 10.1016/j.sjbs.2016.01.028

Nunkaew, T., D. Kantachote, H. Kanzaki, T. Nitoda and R.J. Ritchie. 2014. Effects of 5-aminolevulinic acid (ALA)-containing supernatants from selected *Rhodopseudomonas palustris* strains on rice growth under NaCl stress, with mediating effects on chlorophyll, photosynthetic electron transport and antioxidative enzymes. Electron. J. Biotechn. 17(1):19-26. doi: 10.1016/j.ejbt.2013.12.004

Oberson, A., E. Frossard, C. Bühlmann, J. Mayer, P. Mäder and A. Lüscher. 2013. Nitrogen fixation and transfer in grass-clover leys under organic and conventional cropping systems. Plant Soil 371(1):237-255. doi: 10.1007/s11104-013-1666-4

Oda, Y., F.W. Larimer, P.S.G. Chain, S. Malfatti, M.V. Shin, L.M. Vergez and all. 2008. Multiple genome sequences reveal adaptations of a phototrophic bacterium to sediment microenvironments. Proc. Natl. Acad. Sci. U. S. A. 105(47):18543-18548. doi: 10.1073/pnas.0809160105

Oda, Y., S.K. Samanta, F.E. Rey, L. Wu, X. Liu, T. Yan and all. 2005. Functional genomic analysis of three nitrogenase isozymes in the photosynthetic bacterium *Rhodopseudomonas palustris*. J. Bacteriol. 187(22):7784-7794. doi: 10.1128/Jb.187.22.7784-7794.2005

Oda, Y., B. Star, L.A. Huisman, J.C. Gottschal and L.J. Forney. 2003. Biogeography of the purple nonsulfur bacterium *Rhodopseudomonas palustris*. Appl. Environ. Microbiol. 69(9):5186-5191. doi: 10.1128/Aem.69.9.5186-5191.2003

Oda, Y., W. Wanders, L.A. Huisman, W.G. Meijer, J.C. Gottschal and L.J. Forney. 2002. Genotypic and phenotypic diversity within species of purple nonsulfur bacteria isolated from aquatic sediments. Appl. Environ. Microbiol. 68(7):3467-3477. doi: 10.1128/Aem.68.7.3467-3477.2002

Oh, Y.K., E.H. Seol, E.Y. Lee and S. Park. 2002. Fermentative hydrogen production by a new chemoheterotrophic bacterium *Rhodopseudomonas palustris* P4. Int. J. Hydrogen. Energ. 27(11-12):1373-1379. doi: 10.1016/S0360-3199(02)00100-3

Okamura, K., K. Takata and A. Hiraishi. 2009. Intrageneric relationships of members of the genus *Rhodopseudomonas*. J. Gen. Appl. Microbiol. 55(6):469-478.

Okazaki, S., N. Sano, T. Yamada, K. Ishii, K. Kojima, S. Djedidi and all. 2019. Complete genome sequence of plant growth-promoting *Bacillus pumilus* TUAT1. Microbiol. Resour. Announc. 8(21):e00076-00019. doi: 10.1128/MRA.00076-19

Ongena, M., E. Jourdan, A. Adam, M. Paquot, A. Brans, B. Joris and all. 2007.

doi:10.6342/NTU202003422

Surfactin and fengycin lipopeptides of *Bacillus subtilis* as elicitors of induced systemic resistance in plants. Environ. Microbiol. 9(4):1084-1090. doi: 10.1111/j.1462-2920.2006.01202.x

Pandey, A., E. Sharma and L.M.S. Palni. 1998. Influence of bacterial inoculation on maize in upland farming systems of the *Sikkim Himalaya*. Soil Biol. Biochem. 30(3):379-384. doi: 10.1016/S0038-0717(97)00121-1

Park, K.S. and J.W. Kloepper. 2000. Activation of PR-1a promoter by rhizobacteria that induce systemic resistance in tobacco against *Pseudomonas syringae* pv. *tabaci*. Biol. Control 18(1):2-9. doi: 10.1006/bcon.2000.0815

Patel, D., D.C. Jha, N. Tank and M. Saraf. 2012. Growth enhancement of chickpea in saline soils using plant growth-promoting rhizobacteria. J. Plant Growth Regul. 31(1):53-62. doi: 10.1007/s00344-011-9219-7

Patten, C.L. and B.R. Glick. 2002. Role of *Pseudomonas putida* indoleacetic acid in development of the host plant root system. Appl. Environ. Microbiol. 68(8):3795-3801. doi: 10.1128/aem.68.8.3795-3801.2002

Paulsen, I.T., C.M. Press, J. Ravel, D.Y. Kobayashi, G.S. Myers, D.V. Mavrodi and all. 2005. Complete genome sequence of the plant commensal *Pseudomonas fluorescens* Pf-5. Nat. Biotechnol. 23(7):873-878. doi: 10.1038/nbt1110

Pfennig, N. 1977. Phototrophic green and purple bacteria: a comparative, systematic survey. Annu. Rev. Microbiol. 31:275-290. doi: 10.1146/annurev.mi.31.100177.001423

Pollard, M.O., D. Gurdasani, A.J. Mentzer, T. Porter and M.S. Sandhu. 2018. Long reads: Their purpose and place. Hum. Mol. Genet. 27(R2):R234-R241. doi: 10.1093/hmg/ddy177

Ponraj, P., M. Shankar, D. Ilakkiam, J. Rajendhran and P. Gunasekaran. 2012. Genome sequence of the plant growth-promoting rhizobacterium *Pseudomonas putida* S11. J. Bacteriol. 194(21):6015-6015. doi: 10.1128/jb.01509-12

Prinsen, E., A. Costacurta, K. Michiels, J. Vanderleyden and H. Vanonckelen. 1993. *Azospirillum brasilense* indole-3-acetic acid biosynthesis: evidence for a non-tryptophan dependent pathway. Mol. Plant Microbe. Interact. 6(5):609-615. doi: 10.1094/mpmi-6-609

Pyakurel, A., B. Dahal and S. Rijal. 2019. Effect of molasses and organic fertilizer in soil fertility and yield of spinach in Khotang, Nepal. Int. J. Appl. Sci. Biotechnol. 7:49-53. doi: 10.3126/ijasbt.v7i1.23301

Quail, M.A., M. Smith, P. Coupland, T.D. Otto, S.R. Harris, T.R. Connor and all. 2012. A tale of three next generation sequencing platforms: comparison of ion torrent, pacific biosciences and Illumina MiSeq sequencers. BMC Genomics

doi:10.6342/NTU202003422

13:341. doi: 10.1186/1471-2164-13-341

R Core Team. (2019). R Foundation for Statistical Computing, Vienna, Austria.

Ramarathnam, R., W.G.D. Fernando and T. de Kievit. 2011. The role of antibiosis and induced systemic resistance, mediated by strains of *Pseudomonas chlororaphis*, *Bacillus cereus* and *B. amyloliquefaciens*, in controlling blackleg disease of canola. Biocontrol 56(2):225-235. doi: 10.1007/s10526-010-9324-8

Ramey, B.E., M. Koutsoudis, S.B. von Bodman and C. Fuqua. 2004. Biofilm formation in plant-microbe associations. Curr. Opin. Microbiol. 7(6):602-609. doi: 10.1016/j.mib.2004.10.014

Ramos Solano, B., J. Barriuso and F.J. Gutiérrez Mañero. 2008. Physiological and Molecular Mechanisms of Plant Growth Promoting Rhizobacteria (PGPR). In "Plant-Bacteria Interactions", pp. 41-54 Wiley-VCH Verlag GmbH & Co. KGaA.

Redondo-Nieto, M., M. Barret, J.P. Morrisey, K. Germaine, F. Martinez-Granero, E. Barahona and all. 2012. Genome sequence of the biocontrol strain *Pseudomonas fluorescens* F113. J. Bacteriol. 194(5):1273-1274. doi: 10.1128/Jb.06601-11

Risse, J., M. Thomson, S. Patrick, G. Blakely, G. Koutsovoulos, M. Blaxter and all. 2015. A single chromosome assembly of *Bacteroides fragilis* strain BE1 from Illumina and MinION nanopore sequencing data. Gigascience 4:60. doi: 10.1186/s13742-015-0101-6

Rodriguez, H., R. Fraga, T. Gonzalez and Y. Bashan. 2006. Genetics of phosphate solubilization and its potential applications for improving plant growth-promoting bacteria. Plant Soil 287(1-2):15-21. doi: 10.1007/s11104-006-9056-9

Ruiz, B., A. Chavez, A. Forero, Y. Garcia-Huante, A. Romero, M. Sanchez and all. 2010. Production of microbial secondary metabolites: Regulation by the carbon source. Crit. Rev. Microbiol. 36(2):146-167. doi: 10.3109/10408410903489576

Ruiz, N., L.S. Gronenberg, D. Kahne and T.J. Silhavy. 2008. Identification of two inner-membrane proteins required for the transport of lipopolysaccharide to the outer membrane of *Escherichia coli*. Proc. Natl. Acad. Sci. U. S. A. 105(14):5537-5542. doi: 10.1073/pnas.0801196105

Saikeur, A., W. Choorit, P. Prasertsan, D. Kantachote and K. Sasaki. 2009. Influence of precursors and inhibitor on the production of extracellular 5-aminolevulinic acid and biomass by *Rhodopseudomonas palustris* KG31. Biosci. Biotech. Bioch. 73(5):987-992. doi: 10.1271/bbb.80682

doi:10.6342/NTU202003422

Saleh, S.S. and B.R. Glick. 2001. Involvement of *gacS* and *rpoS* in enhancement of the plant growth-promoting capabilities of *Enterobacter cloacae* CAL2 and UW4. Can. J. Microbiol. 47(8):698-705. doi: 10.1139/w01-072

Saliba, A.-E., A.J. Westermann, S.A. Gorski and J. Vogel. 2014. Single-cell RNA-seq: Advances and future challenges. Nucleic Acids Res. 42(14):8845-8860. doi: 10.1093/nar/gku555

Salma, U., A.G. Miah, T. Maki, M. Nishimura and H. Tsujii. 2007. Effect of dietary *Rhodobacter capsulatus* on cholesterol concentration and fatty acid composition in broiler meat. Poultry Sci. 86(9):1920-1926. doi: 10.1093/ps/86.9.1920

Samavat, S. and S. Samavat. 2014. The effects of fulvic acid and sugar cane molasses on yield and qualities of tomato. Int. Res. J. Appl. Basic. Sci. 8(3):266-268.

Şanlı, A., T. Karadoğan and B. Tosun. 2015. The effects of sugar beet molasses applications on root yield and sugar content of sugar beet (*Beta vulgaris* L.). Tarla Bitkileri Merkez Araştırma Enstitüsü Dergisi 24(2):103-108.

Saravanakumar, D., M. Kavino, T. Raguchander, P. Subbian and R. Samiyappan. 2011. Plant growth promoting bacteria enhance water stress resistance in green gram plants. Acta Physiol. Plant. 33(1):203-209. doi: 10.1007/s11738-010-0539-1

Saravanakumar, D. and R. Samiyappan. 2007. ACC deaminase from *Pseudomonas fluorescens* mediated saline resistance in groundnut (*Arachis hypogea*) plants. J. Appl. Microbiol. 102(5):1283-1292. doi: 10.1111/j.1365-2672.2006.03179.x

Sasaki, K., M. Watanabe, T. Tanaka and T. Tanaka. 2002. Biosynthesis, biotechnological production and applications of 5-aminolevulinic acid. Appl. Microbiol. Biotechnol. 58(1):23-29.

Sawada, H. and P. Rogers. 1977. Photosynthetic bacteria in waste treatment. J Ferment. Technol. 55:297-310.

Schaefer, A.L., E.P. Greenberg, C.M. Oliver, Y. Oda, J.J. Huang, G. Bittan-Banin and all. 2008. A new class of homoserine lactone quorum-sensing signals. Nature 454(7204):595-599. doi: 10.1038/nature07088

Schauer, K., D.A. Rodionov and H. de Reuse. 2008. New substrates for TonB-dependent transport: do we only see the 'tip of the iceberg'? Trends Biochem. Sci. 33(7):330-338. doi: 10.1016/j.tibs.2008.04.012

Scheuring, S., R.P. Goncalves, V. Prima and J.N. Sturgis. 2006. The photosynthetic apparatus of *Rhodopseudomonas palustris*: Structures and organization. J. Mol. Biol. 358(1):83-96. doi: 10.1016/j.jmb.2006.01.085

Sekine, M., K. Watanabe and K. Syono. 1989. Molecular cloning of a gene for indole-3-acetamide hydrolase from *Bradyrhizobium japonicum*. J. Bacteriol.

doi:10.6342/NTU202003422

171(3):1718. doi: 10.1128/jb.171.3.1718-1724.1989

Shaharoona, B., M. Naveed, M. Arshad and Z.A. Zahir. 2008. Fertilizer-dependent efficiency of *Pseudomonads* for improving growth, yield, and nutrient use efficiency of wheat (*Triticum aestivum* L.). Appl. Microbiol. Biotechnol. 79(1):147-155. doi: 10.1007/s00253-008-1419-0

Shamala, T.R., S.V. Vijayendra and G.J. Joshi. 2012. Agro-industrial residues and starch for growth and co-production of polyhydroxyalkanoate copolymer and alpha-amylase by *Bacillus* sp. CFR-67. Braz. J. Microbiol. 43(3):1094-1102. doi: 10.1590/S1517-838220120003000036

Shanmugam, V. and N. Kanoujia. 2011. Biological management of vascular wilt of tomato caused by *Fusarium oxysporum* f.sp *lycospersici* by plant growth-promoting rhizobacterial mixture. Biol. Control 57(2):85-93. doi: 10.1016/j.biocontrol.2011.02.001

Shao, J., Z. Xu, N. Zhang, Q. Shen and R. Zhang. 2014. Contribution of indole-3-acetic acid in the plant growth promotion by the rhizospheric strain *Bacillus amyloliquefaciens* SQR9. Biol. Fertil. Soils 51(3):321-330. doi: 10.1007/s00374-014-0978-8

Shariati, J.V., M.A. Malboobi, Z. Tabrizi, E. Tavakol, P. Owilia and M. Safari. 2017. Comprehensive genomic analysis of a plant growth-promoting rhizobacterium *Pantoea agglomerans* strain P5. Sci. Rep. 7(1):15610. doi: 10.1038/s41598-017-15820-9

Shen, M.W. (2016) Effect of *Rhodopseudomonas palustris* PS3 on nitrogen and carbon metabolism in the *Brassica rapa* L. ssp. *chinesis*. Taipei, Taiwan: National Taiwan University. Department of Biochemical Science and Technology.

Shen, N.K., S.M. Liao, Q.Y. Wang, Y. Qin, Q.X. Zhu, J. Zhu and all. 2016. Economical succinic acid production from sugarcane juice by *Actinobacillus succinogenes* supplemented with corn steep liquor and peanut meal as nitrogen sources. Sugar. Tech. 18(3):292-298. doi: 10.1007/s12355-015-0401-2

Shen, X., M. Chen, H. Hu, W. Wang, H. Peng, P. Xu and all. 2012. Genome sequence of *Pseudomonas chlororaphis* GP72, a root-colonizing biocontrol strain. J. Bacteriol. 194(5):1269-1270. doi: 10.1128/JB.06713-11

Shen, X., H. Hu, H. Peng, W. Wang and X. Zhang. 2013. Comparative genomic analysis of four representative plant growth-promoting rhizobacteria in *Pseudomonas*. BMC Genomics 14:271-290. doi: 10.1186/1471-2164-14-271

Shi, X.Y., W.W. Li and H.Q. Yu. 2014. Optimization of H-2 photo-fermentation from benzoate by *Rhodopseudomonas palustris* using a desirability function

doi:10.6342/NTU202003422

approach. Int. J. Hydrogen. Energ. 39(9):4244-4251. doi: 10.1016/j.ijhydene.2014.01.016

Shinohara, M., C. Aoyama, K. Fujiwara, A. Watanabe, H. Ohmori, Y. Uehara and all. 2011. Microbial mineralization of organic nitrogen into nitrate to allow the use of organic fertilizer in hydroponics. Soil. Sci. Plant. Nutr. 57(2):190-203. doi: 10.1080/00380768.2011.554223

Silby, M.W., A.M. Cerdeno-Tarraga, G.S. Vernikos, S.R. Giddens, R.W. Jackson, G.M. Preston and all. 2009. Genomic and genetic analyses of diversity and plant interactions of *Pseudomonas fluorescens*. Genome Biol. 10(5):R51. doi: 10.1186/gb-2009-10-5-r51

Silveira, M.M., E. Wisbeck, I. Hoch and R. Jonas. 2001. Production of glucose-fructose oxidoreductase and ethanol by *Zymomonas mobilis* ATCC 29191 in medium containing corn steep liquor as a source of vitamins. Appl. Microbiol. Biotechnol. 55(4):442-445. doi: 10.1007/s002530000569

Singh, V., S. Haque, R. Niwas, A. Srivastava, M. Pasupuleti and C.K. Tripathi. 2016. Strategies for fermentation medium optimization: An in-depth review. Front. Microbiol. 7:2087. doi: 10.3389/fmicb.2016.02087

Sovic, I., K. Krizanovic, K. Skala and M. Sikic. 2016. Evaluation of hybrid and non-hybrid methods for de novo assembly of nanopore reads. Bioinformatics 32(17):2582-2589. doi: 10.1093/bioinformatics/btw237

Spaepen, S. and J. Vanderleyden. 2011. Auxin and plant-microbe interactions. Cold Spring Harb. Perspect. Biol. 3(4):a001438. doi: 10.1101/cshperspect.a001438

Spaepen, S., J. Vanderleyden and R. Remans. 2007. Indole-3-acetic acid in microbial and microorganism-plant signaling. FEMS Microbiol. Rev. 31(4):425-448. doi: 10.1111/j.1574-6976.2007.00072.x

Stueken, E.E., R. Buick, B.M. Guy and M.C. Koehler. 2015. Isotopic evidence for biological nitrogen fixation by molybdenum-nitrogenase from 3.2 Gyr. Nature 520(7549):666-669. doi: 10.1038/nature14180

Su, P., X.Q. Tan, C.G. Li, D.Y. Zhang, J.E. Cheng, S.B. Zhang and all. 2017. Photosynthetic bacterium *Rhodopseudomonas palustris* GJ-22 induces systemic resistance against viruses. Microb. Biotechnol. 10(3):612-624. doi: 10.1111/1751-7915.12704

Su, P., D.Y. Zhang, Z. Zhang, A. Chen, M.R. Hamid, C.G. Li and all. 2019. Characterization of *Rhodopseudomonas palustris* population dynamics on tobacco phyllosphere and induction of plant resistance to Tobacco mosaic virus. Microb. Biotechnol.:1453-1463. doi: 10.1111/1751-7915.13486

Suliasih, A. and S. Widawati. (2017), *The 1st Science and Technology Research Partnership for Sustainable Development Program (SATREPS)*, Bogor,

doi:10.6342/NTU202003422

Indonesia, pp. 94-99.
Tabuchi, K., H. Mizuta and H. Yasui. 2009. Promotion of callus propagation by 5-aminolevulinic acid in a *Laminaria japonica* sporophyte. Aquac. Res. 41(1):1-10. doi: 10.1111/j.1365-2109.2009.02294.x
Taghavi, S., D. van der Lelie, A. Hoffman, Y.B. Zhang, M.D. Walla, J. Vangronsveld and all. 2010. Genome sequence of the plant growth promoting endophytic *bacterium Enterobacter* sp. 638. PLoS Genet. 6(5):e1000943. doi: 10.1371/journal.pgen.1000943
Talboys, P.J., D.W. Owen, J.R. Healey, P.J.A. Withers and D.L. Jones. 2014. Auxin secretion by *Bacillus amyloliquefaciens* FZB42 both stimulates root exudation and limits phosphorus uptake in *Triticum aestivum*. BMC Plant Biol. 14(1):51. doi: 10.1186/1471-2229-14-51
Tamames, J. 2001. Evolution of gene order conservation in prokaryotes. Genome Biol. 2(6):research0020.0021–research0020.0011.
Tang, X., Y. Huang, J. Lei, H. Luo and X. Zhu. 2019. The single-cell sequencing: new developments and medical applications. Cell Biosci. 9:53. doi: 10.1186/s13578-019-0314-y
Tavaré, S. 1986. Some probabilistic and statistical problems in the analysis of DNA sequences. In "American mathematical society: Lectures on mathematics in the life sciences", pp. 57-86 Amer Mathematical Society.
Tekaia, F. 2016. Inferring orthologs: open questions and perspectives. Genom Insights:17-28. doi: 10.4137/Geiei.S37925
Theunis, M., H. Kobayashi, W.J. Broughton and E. Prinsen. 2004. Flavonoids, NodD1, NodD2, and nod-box NB15 modulate expression of the y4wEFG locus that is required for indole-3-acetic acid synthesis in *Rhizobium* sp strain NGR234. Mol. Plant Microbe. Interact. 17(10):1153-1161. doi: 10.1094/Mpmi.2004.17.10.1153
Thompson, J.D., D.G. Higgins and T.J. Gibson. 1994. CLUSTAL W: improving the sensitivity of progressive multiple sequence alignment through sequence weighting, position-specific gap penalties and weight matrix choice. Nucleic Acids Res. 22(22):4673-4680.
Thomsen, M.H. 2005. Complex media from processing of agricultural crops for microbial fermentation. Appl. Microbiol. Biotechnol. 68(5):598-606. doi: 10.1007/s00253-005-0056-0
Tilman, D. 1998. The greening of the green revolution. Nature 396(6708):211-212. doi: 10.1038/24254
Timmusk, S., A.A. Islam, D. El, C. Lucian, T. Tanilas and A. Kannaste. 2014. Drought-tolerance of wheat improved by rhizosphere bacteria from

doi:10.6342/NTU202003422

harshenvironments: Enhanced biomass production and reduced emissions of stressvolatiles. PLoS One 9:1-13. doi: 10.1371/journal.pone.0096086

Tram, G., V. Korolik and C.J. Day. 2013. MBDS solvent: An improved method for assessment of biofilms. Adv. Microbiol. 3(2):200-204. doi: 10.4236/aim.2013.32030

Treangen, T.J. and S.L. Salzberg. 2011. Repetitive DNA and next-generation sequencing: Computational challenges and solutions. Nat. Rev. Genet. 13(1):36-46. doi: 10.1038/nrg3117

Tsujii, H., M. Nishioka, U. Salma, A.G. Miah, T. Maki and M.G. Lee. 2007. Comparative study on hypocholesterolemic effect of *Rhodopseudomonas palustris* and *Rhodobacter capsulatus* on rats fed a high cholesterol diet. Anim. Sci. J. 78(5):535-540. doi: 10.1111/j.1740-0929.2007.00473.x

Utturkar, S.M., D.M. Klingeman, M.L. Land, C.W. Schadt, M.J. Doktycz, D.A. Pelletier and all. 2014. Evaluation and validation of de novo and hybrid assembly techniques to derive high-quality genome sequences. Bioinformatics. doi: 10.1093/bioinformatics/btu391

Vacheron, J., G. Desbrosses, M.-L. Bouffaud, B. Touraine, Y. Moënne-Loccoz, D. Muller and all. 2013. Plant growth-promoting rhizobacteria and root system functioning. Front. Plant. Sci. 4:356. doi: 10.3389/fpls.2013.00356

van Niel, C.B. 1944. The culture, general physiology, morphology, and classification of the non-sulfur purple and brown bacteria. Bacteriol. Rev. 8(1):1-118.

Van Niel, C.B. 1954. The chemoautotrophic and photosynthetic bacteria. Annu Rev Microbiol 8:105-132. doi: 10.1146/annurev.mi.08.100154.000541

Vassilev, N., M. Vassileva and I. Nikolaeva. 2006. Simultaneous P-solubilizing and biocontrol activity of microorganisms: potentials and future trends. Appl. Microbiol. Biotechnol. 71(2):137-144. doi: 10.1007/s00253-006-0380-z

Vessey, J.K. 2003. Plant growth promoting rhizobacteria as biofertilizers. Plant Soil 255(2):571-586. doi: 10.1023/A:1026037216893

Vidhyasekaran, P., N. Kamala, A. Ramanathan, K. Rajappan, V. Paranidharan and R. Velazhahan. 2001. Induction of systemic resistance by *Pseudomonas fluorescens* Pf1 against *Xanthomonas oryzae* pv. *Oryzae* in rice leaves. Phytoparasitica 29(2):155. doi: 10.1007/BF02983959

Wadhams, G.H. and J.P. Armitage. 2004. Making sense of it all: Bacterial chemotaxis. Nat. Rev. Mol. Cell. Bio. 5(12):1024-1037. doi: 10.1038/nrm1524

Waites, M.J., N.L. Morgan, J.S. Rockey and G. Higton. 2001. Industrial microbiology: An introduction Wiley

Wampler, D.A. and S.A. Ensign. 2005. Photoheterotrophic metabolism of acrylamide by a newly isolated strain of *Rhodopseudomonas palustris*. Appl. Environ.

doi:10.6342/NTU202003422

Microbiol. 71(10):5850-5857. doi: 10.1128/aem.71.10.5850-5857.2005
Wang, C., Y. Wang, J. Ma, Q. Hou, K. Liu, Y. Ding and all. 2018. Screening and whole-genome sequencing of two streptomyces species from the rhizosphere Soil of Peony reveal their characteristics as plant growth-promoting rhizobacteria. BioMed Res. Int. 2018:2419686. doi: 10.1155/2018/2419686
Wang, L.J., W.B. Jiang, H. Liu, W.Q. Liu, L. Kang and X.L. Hou. 2005. Promotion by 5-aminolevulinic acid of germination of pakchoi (*Brassica campestris* ssp *chinensis* var. *communis* Tsen et Lee) seeds under salt stress. J. Integr. Plant. Biol. 47(9):1084-1091. doi: 10.1111/j.1744-7909.2005.00150.x
Wang, Y.Z., Q. Liao, X. Zhu, X. Tian and C. Zhang. 2010. Characteristics of hydrogen production and substrate consumption of *Rhodopseudomonas palustris* CQK 01 in an immobilized-cell photobioreactor. Bioresour. Technol. 101(11):4034-4041. doi: 10.1016/j.biortech.2010.01.045
Wattam, A.R., J.J. Davis, R. Assaf, S. Boisvert, T. Brettin, C. Bun and all. 2017. Improvements to PATRIC, the all-bacterial bioinformatics database and analysis resource center. Nucleic Acids Res. 45(D1):D535-D542. doi: 10.1093/nar/gkw1017
Wei, W., F. Gao, M.Z. Du, H.L. Hua, J. Wang and F.B. Guo. 2016. Zisland explorer: Detect genomic islands by combining homogeneity and heterogeneity properties. Brief. Bioinform. 18(3):357-366. doi: 10.1093/bib/bbw019
Wick, R.R., L.M. Judd, C.L. Gorrie and K.E. Holt. 2017a. Completing bacterial genome assemblies with multiplex MinION sequencing. Microb. Genom. 3(10):e000132. doi: 10.1099/mgen.0.000132
Wick, R.R., L.M. Judd, C.L. Gorrie and K.E. Holt. 2017b. Unicycler: Resolving bacterial genome assemblies from short and long sequencing reads. PLoS Comput. Biol. 13(6):e1005595. doi: 10.1371/journal.pcbi.1005595
Wong, W.T., C.H. Tseng, S.H. Hsu, H.S. Lur, C.W. Mo, C.N. Huang and all. 2014. Promoting effects of a single *Rhodopseudomonas palustris* inoculant on plant growth by *Brassica rapa chinensis* under low fertilizer input. Microbes Environ. 29(3):303-313. doi: 10.1264/jsme2.ME14056
Wu, D.Q., J. Ye, H.Y. Ou, X. Wei, X. Huang, Y.W. He and all. 2011. Genomic analysis and temperature-dependent transcriptome profiles of the rhizosphere originating strain *Pseudomonas aeruginosa* M18. BMC Genomics 12:438. doi: 10.1186/1471-2164-12-438
Wu, L., J. Wang, W. Huang, H. Wu, J. Chen, Y. Yang and all. 2015. Plant-microbe rhizosphere interactions mediated by *Rehmannia glutinosa* root exudates under consecutive monoculture. Sci. Rep. 5:15871. doi: 10.1038/srep15871
Xiao, X., Y. Hou, J. Du, Y. Liu, Y. Liu, L. Dong and all. 2012. Determination of main

doi:10.6342/NTU202003422

categories of components in corn steep liquor by near-infrared spectroscopy and partial least-squares regression. J. Agr. Food Chem. 60(32):7830-7835. doi: 10.1021/jf3012823

Xiao, X., Y. Hou, Y. Liu, Y. Liu, H. Zhao, L. Dong and all. 2013. Classification and analysis of corn steep liquor by UPLC/Q-TOF MS and HPLC. Talanta 107:344-348. doi: 10.1016/j.talanta.2013.01.044

Xiao, Z.J., P.H. Liu, J.Y. Qin and P. Xu. 2007. Statistical optimization of medium components for enhanced acetoin production from molasses and soybean meal hydrolysate. Appl. Microbiol. Biotechnol. 74(1):61-68. doi: 10.1007/s00253-006-0646-5

Xing, D., Y. Zuo, S. Cheng, J.M. Regan and B.E. Logan. 2008. Electricity generation by *Rhodopseudomonas palustris* DX-1. Environ. Sci. Technol. 42(11):4146-4151. doi: 10.1021/es800312v

Xu, J., Y. Feng, Y. Wang and X. Lin. 2013. Characteristics of purple nonsulfur bacteria grown under stevia residue extractions. Lett. Appl. Microbiol. 57(5):420-426. doi: 10.1111/lam.12129

Xu, J., Y. Feng, Y. Wang, X. Luo, J. Tang and X. Lin. 2016. The foliar spray of *Rhodopseudomonas palustris* grown under Stevia residue extract promotes plant growth via changing soil microbial community. J. Soils Sediments 16(3):916-923. doi: 10.1007/s11368-015-1269-1

Yang, T.W., Z.M. Rao, X. Zhang, M.J. Xu, Z.H. Xu and S.T. Yang. 2013. Effects of corn steep liquor on production of 2,3-butanediol and acetoin by *Bacillus subtilis*. Process. Biochem. 48(11):1610-1617. doi: 10.1016/j.procbio.2013.07.027

Yang, X. 2010. Scale-up of microbial fermentation process. In "Manual of industrial microbiology and biotechnology", ed. D. A. Baltz R, Davies J, Bull A, Junker B, Katz L, Lynd L, Masurekar P, Reeves C, Zhao H, pp. 669-675. Washington, DC: American Society of Microbiology.

Yao, L., Z. Wu, Y. Zheng, I. Kaleem and C. Li. 2010. Growth promotion and protection against salt stress by *Pseudomonas putida* Rs-198 on cotton. Eur. J. Soil Biol. 46(1):49-54. doi: 10.1016/j.ejsobi.2009.11.002

Yigit, D.O., U. Gunduz, L. Turker, M. Yucel and I. Eroglu. 1999. Identification of by-products in hydrogen producing bacteria; *Rhodobacter sphaeroides* OU 001 grown in the waste water of a sugar refinery. J. Biotechnol. 70(1-3):125-131. doi: 10.1016/S0168-1656(99)00066-8

Yoch, D.C. 1978. In "The photosynthetic bacteria", ed. R. K. Clayton and W. R. Sistrom, pp. 657-672. New York: Plenum Press.

Yolmeh, M. and S.M. Jafari. 2017. Applications of response surface methodology in

doi:10.6342/NTU202003422

the food industry processes. Food Bioprocess Tech. 10(3):413-433. doi: 10.1007/s11947-016-1855-2

Young, J.P.W., L.C. Crossman, A.W.B. Johnston, N.R. Thomson, Z.F. Ghazoui, K.H. Hull and all. 2006. The genome of *Rhizobium leguminosarum* has recognizable core and accessory components. Genome Biol. 7(4):R34-R34. doi: 10.1186/gb-2006-7-4-r34

Youssef, T. and M.A. Awad. 2008. Mechanisms of enhancing photosynthetic gas exchange in date palm seedlings *(Phoenix dactylifera* L.) under salinity stress by a 5-aminolevulinic acid-based fertilizer. J. Plant Growth Regul. 27(1):1-9. doi: 10.1007/s00344-007-9025-4

Yu, Z., G. Yang, X. Liu, Y. Wang, L. Zhuang and S. Zhou. 2018. Complete genome sequence of the nitrogen-fixing bacterium Azospirillum humicireducens type strain SgZ-5T. Stand. Genomic Sci. 13(1):28. doi: 10.1186/s40793-018-0322-2

Yuan, J., N. Zhang, Q. Huang, W. Raza, R. Li, J.M. Vivanco and all. 2015. Organic acids from root exudates of banana help root colonization of PGPR strain *Bacillus amyloliquefaciens* NJN-6. Sci. Rep. 5:13438. doi: 10.1038/srep13438

Zahir, Z.A., A. Munir, H.N. Asghar, B. Shaharoona and M. Arshad. 2008. Effectiveness of rhizobacteria containing ACC deaminase for growth promotion of peas (*Pisum sativum*) under drought conditions. J. Microbiol. Biotechnol. 18(5):958-963.

Zhang, B., S. Guowei, C. Bao, J. Cao and Y. Tan. 2017. Optimization of culture medium for *Lactobacillus bulgaricus* using box-behnken design. Acta Univ. Cibiniensis, Ser. E: Food Technol. 21. doi: 10.1515/aucft-2017-0001

Zhang, D., N. Xiao, K.T. Mahbubani, E.A. del Rio-Chanona, N.K.H. Slater and V.S. Vassiliadis. 2015a. Bioprocess modelling of biohydrogen production by *Rhodopseudomonas palustris*: Model development and effects of operating conditions on hydrogen yield and glycerol conversion efficiency. Chem. Eng. Sci. 130:68-78. doi: 10.1016/j.ces.2015.02.045

Zhang, N., D. Yang, D. Wang, Y. Miao, J. Shao, X. Zhou and all. 2015b. Whole transcriptomic analysis of the plant-beneficial rhizobacterium *Bacillus amyloliquefaciens* SQR9 during enhanced biofilm formation regulated by maize root exudates. BMC Genomics 16:685. doi: 10.1186/s12864-015-1825-5

Zhao, Y.Y., F. Yan, L.P. Hu, X.T. Zhou, Z.R. Zou and L.R. Cui. 2015. Effects of exogenous 5-aminolevulinic acid on photosynthesis, stomatal conductance, transpiration rate, and PIP gene expression of tomato seedlings subject to salinity stress. Genet. Mol. Res. 14(2):6401-6412. doi:

doi:10.6342/NTU202003422

10.4238/2015.June.11.16

Zhu, M.M., E.Q. Liu, Y. Bao, S.L. Duan, J. She, H. Liu and all. 2019. Low concentration of corn steep liquor promotes seed germination, plant growth, biomass production and flowering in soybean. Plant Growth Regul. 87(1):29-37. doi: 10.1007/s10725-018-0449-6

Zuniga, A., R.A. Donoso, D. Ruiz, G.A. Ruz and B. Gonzalez. 2017. Quorum-sensing systems in the plant growth-promoting bacterium *Paraburkholderia phytofirmans* PsJN exhibit cross-regulation and are involved in biofilm formation. Mol. Plant Microbe. Interact. 30(7):557-565. doi: 10.1094/Mpmi-01-17-0008-R

Zuniga, A., M.J. Poupin, R. Donoso, T. Ledger, N. Guiliani, R.A. Gutierrez and all. 2013. Quorum sensing and indole-3-acetic acid degradation play a role in colonization and plant growth promotion of *Arabidopsis thaliana* by *Burkholderia phytofirmans* PsJN. Mol. Plant Microbe. Interact. 26(5):546-553. doi: 10.1094/Mpmi-10-12-0241-R

doi:10.6342/NTU202003422

APPENDIX

Lo, K.J., S.S. Lin, C.W. Lu, C.H. Kuo and C.T. Liu. 2018. Whole-genome sequencing and comparative analysis of two plant-associated strains of *Rhodopseudomonas palustris* (PS3 and YSC3). Sci. Rep. 8(1):12769. doi: 10.1038/s41598-018-31128-8.

Lo, K.J., S.S. Lee, C.T. Liu. 2020. Development of a low-cost culture medium for the rapid production of plant growthpromoting *Rhodopseudomonas palustris* strain PS3. PLoS ONE 15(7): e0236739. doi: 10.1371/journal.pone.0236739

doi:10.6342/NTU202003422

SCIENTIFIC REPORTS

OPEN

Whole-genome sequencing and comparative analysis of two plant-associated strains of *Rhodopseudomonas palustris* (PS3 and YSC3)

Received: 12 March 2018
Accepted: 13 August 2018
Published online: 24 August 2018

Kai-Jiun Lo[1], Shih-Shun Lin[1,2,6,7], Chia-Wei Lu[8], Chih-Horng Kuo[3,4,5] & Chi-Te Liu[1,2]

Rhodopseudomonas palustris **strains PS3 and YSC3 are purple non-sulfur phototrophic bacteria isolated from Taiwanese paddy soils. PS3 has beneficial effects on plant growth and enhances the uptake efficiency of applied fertilizer nutrients. In contrast, YSC3 has no significant effect on plant growth. The genomic structures of PS3 and YSC3 are similar; each contains one circular chromosome that is 5,269,926 or 5,371,816 bp in size, with 4,799 or 4,907 protein-coding genes, respectively. In this study, a large class of genes involved in chemotaxis and motility was identified in both strains, and genes associated with plant growth promotion, such as nitrogen fixation-, IAA synthesis- and ACC deamination-associated genes, were also identified. We noticed that the growth rate, the amount of biofilm formation, and the relative expression levels of several chemotaxis-associated genes were significantly higher for PS3 than for YSC3 upon treatment with root exudates. These results indicate that PS3 responds better to the presence of plant hosts, which may contribute to the successful interactions of PS3 with plant hosts. Moreover, these findings indicate that the existence of gene clusters associated with plant growth promotion is required but not sufficient for a bacterium to exhibit phenotypes associated with plant growth promotion.**

In 1978, Kloepper and Schroth proposed the concept of plant growth-promoting rhizobacteria (PGPRs)[1]. PGPRs are a diverse subgroup of rhizosphere-colonizing bacteria that can have beneficial effects on soil quality and crop growth and can sustain soil health via various mechanisms[1]. PGPRs can facilitate plant growth by increasing nutrient availability (e.g., nitrogen fixation) and nutrient solubilization (e.g., phosphate solubilization) and by producing phytohormones such as indole acetic acid (IAA), 2,3-butanediol, and cytokinins[2–4]. In addition, PGPRs can improve plant tolerance to environmental stress by metabolizing 1-aminocyclopropane-1-carboxylic acid (ACC), a precursor of ethylene, as a stress hormone[2–4]. Moreover, PGPR can also protect plants from pathogen infection by producing antibiotics or activating induced systemic resistance[5]. Due to these properties of PGPRs, these bacteria are widely used as biofertilizers and biocontrol agents[3].

Rhodopseudomonas palustris is a phototrophic purple non-sulfur bacterium (PNSB) that can sustain itself in different metabolic states, including photoautotrophic, photoheterotrophic, chemoautotrophic and chemoheterotrophic states[6]. This bacterium has been widely used in industrial applications for bioremediation and sewage treatment and for the removal of phytotoxic compounds[7,8]. In addition, this bacterium can convert complex

[1]Institute of Biotechnology, National Taiwan University, Taipei, 106, Taiwan. [2]Agricultural Biotechnology Research Center, Academia Sinica, Taipei, 115, Taiwan. [3]Institute of Plant and Microbial Biology, Academia Sinica, Taipei, 115, Taiwan. [4]Molecular and Biological Agricultural Sciences Program, Taiwan International Graduate Program, National Chung Hsing University and Academia Sinica, Taipei, 115, Taiwan. [5]Graduate Institute of Biotechnology, National Chung Hsing University, Taichung City, 402, Taiwan. [6]Center of Biotechnology, National Taiwan University, Taipei, 106, Taiwan. [7]National Center for High-Performance Computing, National Applied Research Laboratories, Hsinchu, 300, Taiwan. [8]Center for Shrimp Disease Control and Genetic Improvement, National Cheng Kung University, Tainan, 701, Taiwan. Correspondence and requests for materials should be addressed to C.-H.K. (email: chk@gate.sinica.edu.tw) or C.-T.L. (email: chiteliu@ntu.edu.tw)

Feature	PS3	YSC3	CGA009
Accession	CP019966	CP019967	NC_005296.1
Size (bp)	5,269,926	5,371,816	5,459,213
G + C content	65.3%	65.2%	65.0%
rRNA	6	6	6
tRNA	48	48	49
Protein-coding genes	4,799	4,907	4,841
Hypothetical genes	942	1,331	1,379
Plasmid	none	none	1
Reference	This study	This study	[6]

Table 1. General features of sequenced strains of *Rhodopseudomonas palustris*. The characteristics of the genomes of *R. palustris* PS3 and YSC3 were analyzed in this study, and genomic data pertaining to *R. palustris* CGA009 (GenBank accession no. NC_005296) were downloaded from the NCBI database.

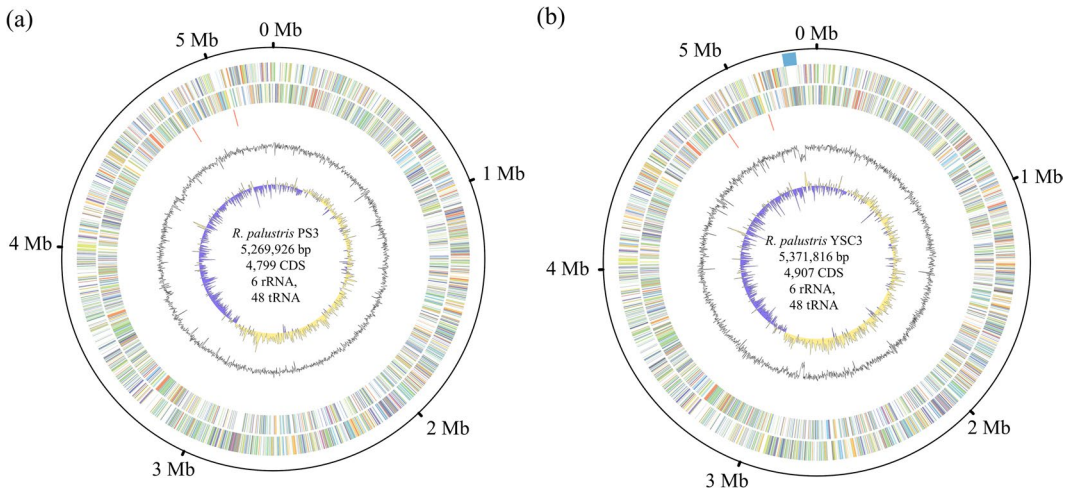

Figure 1. Genome map of *Rhodopseudomonas palustris* PS3 (**a**) and YSC3 (**b**). Rings from the outside as follows: (1) scale marks (unit, Mb), (2) genomic island, (3) protein-coding genes on the forward strand colored by COG category, (4) protein-coding genes on the reverse strand (same color scheme as the second circle), (5) rRNA genes, (6) GC content (deviation from average), and (7) GC skew in blue (below average) and yellow (above average).

organic compounds into biomass and bioenergy using substrates that are plant-derived compounds, pollutants, or aromatic compounds[6,9–12]. Some studies have indicated that *R. palustris* can also be used as a biofertilizer to improve crop yield[13–15]. *R. palustris* strain PS3 can have beneficial effects on plant growth and can enhance the efficiency of fertilizers used in either soil or hydroponic cultivation systems[13,16]. Although PS3 is a promising PGPR, genomic information and the underlying molecular mechanisms for plant growth promotion (PGP) by PS3 have yet to be ascertained.

Systematic analysis of whole-genome sequences is a powerful approach to identify either causal genes that contribute to plant growth-promoting activities or potential PGPR candidates[17–21]. Some studies have conducted genomic analyses of *R. palustris* strains such as CGA009, HaA2, BisB18, and TIE[6,22,23]. However, none of these strains are plant-associated strains. In this study, we performed a genomic characterization of two plant-associated *R. palustris* strains. One strain is the effective PGPR strain PS3, and the other is YSC3, which has been shown to be ineffective in PGP[13]. To elucidate the potential modes of action via which *R. palustris* PS3 has beneficial effects on plants, we compared the genomic compositions of these two strains as well as that of *R. palustris* CGA009, which is the genomic representative of this species, and the sequence derived from the NCBI database. We focused on genes involved in carbohydrate and nitrogen metabolism, phosphate solubilization, phytohormone production, biofilm formation, chemotaxis, and plant colonization.

Results

General characteristics of the genomes. The general genomic features of the *R. palustris* strains are summarized in Table 1 and Fig. 1. All three strains have a single circular chromosome that is ~5.3 Mb and encodes 6 rRNAs and ~4,800–4,900 protein-coding genes. CGA009 has an additional tRNA gene annotated as tRNA-OTHER, which may be an artifact. CGA009 harbors one 8.4-kb circular plasmid[6], while PS3 and YSC3 do not harbor any plasmid. Based on the anomalous G + C contents determined by an online tool, Zisland Explorer[24], we found that no horizontally transferred genomic island of DNA is present in the PS3 and CGA009 genomes.

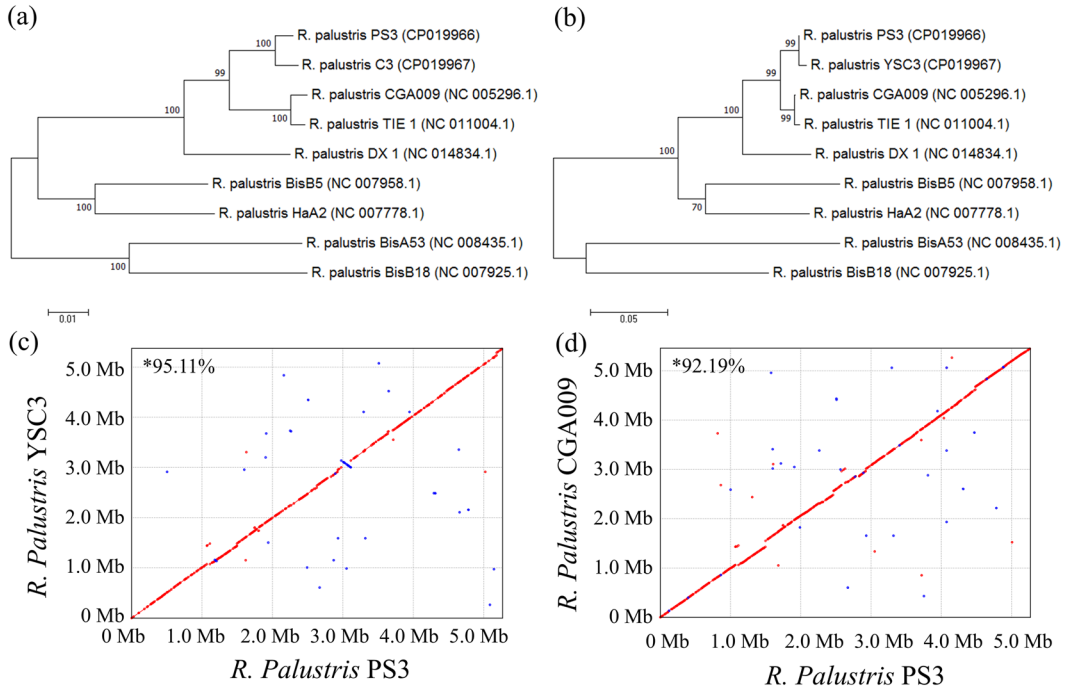

Figure 2. Phylogenetic tree and genome alignments of *R. palustris* based on housekeeping and functional genes and nucleotide levels. Maximum-likelihood tree based on concatenated *recA-rpoB-dnaK* gene sequences (**a**) and *puf* gene sequences (**b**) showing the relationships among the *R. palustris* strains. Both bootstrap values (1000 replicates) are given at branch points and generated in MEGA7. (**c**,**d**) Pairwise genome alignments among *R. palustris* PS3, YSC3 and CGA009. Synteny plots show the comparison of the PS3 genome (c and d, vertical axis) with the genomes of YSC3 (c, horizontal axis) and CGA009 (d, horizontal axis). Forward matches are plotted in red, and reverse matches are plotted in blue. The nucleotide sequence similarities were calculated by software MUMmer[100] with the nucmer function and represented as "*".

Furthermore, Larimer *et al*. also indicated that there were no horizontally transferred genomic islands in the genome of *R. palustris* CGA009[6]. In contrast, YSC3 contained one 56-kb genomic island located at 5,229,652–5,285,897 bp (Fig. 1). This genomic island contains 60 protein-coding genes (locus tags: RPYSC3_47720-48310), and all of these genes encode hypothetical proteins.

The phylogenetic tree of the nine *R. palustris* strains was constructed based on concatenated multilocus sequence analysis (MLSA) of three housekeeping genes (i.e., *recA*, *rpoB*, and *dnaK*; the concatenated alignment is ~7 kb) and is shown in Fig. 2a. The strains were divided into five major groups. All of the *R. palustris* reference strains shared >91% nucleotide sequence identity with PS3; YSC3 was the most closely related strain, with a >99% identity, while CGA009 and TIE-1 exhibited >97% identity. We also constructed a phylogenetic tree based on the *pufL* and *pufM* genes (Fig. 2b). These two genes encode the two subunits of the light reaction center core protein and have been used as markers for phylogenetic analysis within the genus *Rhodopseudomonas*[13,25]. As shown in Fig. 2b, the tree topology is identical to that of the tree generated based on the three housekeeping genes, which is consistent with PS3 and YSC3 being closely related (bootstrap support >99%). At the genomic level, we identified a total of 2,515 single-copy genes that were conserved among all the *R. palustris* strains compared. Based on these genes, we calculated the average nt/aa similarity among the strains, and four main clusters were formed in the phylogenetic tree of *R. palustris* (Supplementary Fig. S1). PS3 had a close phylogenetic relationship with YSC3, while the CGA009 and TIE strains were grouped in a nearby cluster. Based on these results, we included CGA009 as a reference strain in our comparative genomic analysis. CGA009, the first sequenced *R. palustris* strain, is a representative model strain, and the sequence of this strain is available in the NCBI database.

Pairwise genome alignments demonstrated that PS3 shares 95.11% identity with YSC3 at the nucleotide level and exhibits a high level of synteny conservation (Fig. 2c). In contrast, CGA009 shares 92.19% identity with PS3 (Fig. 2d). This result is consistent with the phylogenetic tree analysis (Fig. 2a,b and Supporting Information Fig. S1). Gene homology analysis showed that the genomes of PS3, YSC3 and CGA009 were composed of 5,549 orthologous gene clusters, and 4,142 clusters were conserved among the 3 strains (Fig. 3 and Supplementary Table S1). On the other hand, 226 gene clusters were shared by PS3 and YSC3, while only 104 gene clusters were shared by PS3 and CGA009 (Fig. 3). There were 260 gene clusters that were unique to the PS3 strain (Supplementary Table S2). Sixty percent of these genes encode hypothetical proteins, and the remaining 40% include genes such as those encoding the urea ABC transporters (*UrtACD*, RPPS3_10430, RPPS3_10440 and RPPS3_10450). The list of unique gene clusters in strains YSC3 and CGA009 are shown in Supplementary Tables S3 and S4, respectively. As shown in Fig. 4, the distribution patterns of the Clusters of Orthologous Groups (COG)-assigned proteins for these three strains highly resemble each other. Detailed analyses for the annotation of protein-coding genes in PS3 and YSC3 are shown in Supplementary Tables S5 and S6, respectively. Notably,

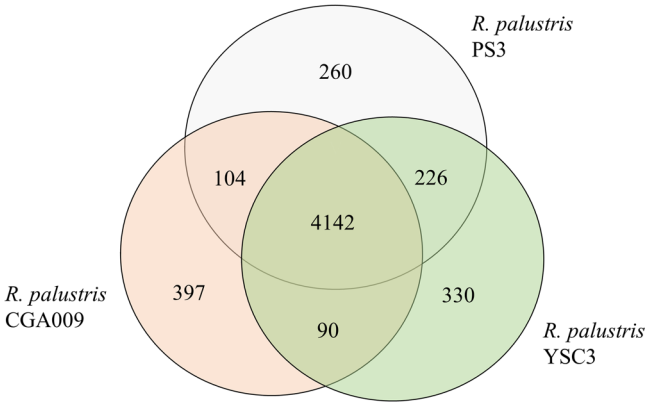

Figure 3. Distribution patterns of homologous gene clusters. The homologous gene clusters are those located at the intersection of *R. palustris* PS3, YSC3 and CGA009.

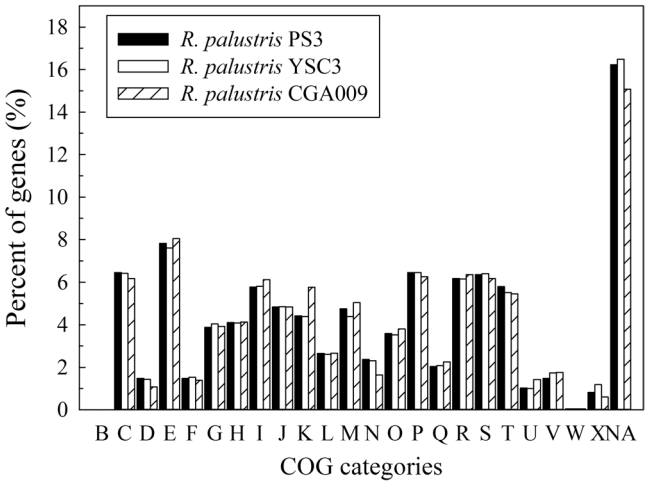

Figure 4. COG categories in the three *R. palustris* strains. Functional categorization of genes was performed by the COG database[92]. The y-axis indicates the percentage of genes assigned with the COG category relative to all genes. The x-axis represents the COG functional category. The groups in each COG category are as follows: (B) chromatin structure and dynamics; (C) energy production and conversion; (D) cell cycle control, cell division and chromosome partitioning; (E) amino acid transport and metabolism; (F) nucleotide transport and metabolism; (G) carbohydrate transport and metabolism; (H) coenzyme transport and metabolism; (I) lipid transport and metabolism; (J) translation, ribosomal structure and biogenesis; (K) transcription; (L) replication, recombination and repair; (M) cell wall/membrane/envelope biogenesis; (N) cell motility; (O) posttranslational modification, protein turnover and chaperones; (P) inorganic ion transport and metabolism; (Q) secondary metabolite biosynthesis, transport and catabolism; (R) general function prediction only; (S) function unknown; (T) signal transduction mechanisms; (U) intracellular trafficking, secretion and vesicular transport; (V) defense mechanisms; (W) extracellular structures; (X) mobilome: prophages and transposons; and (NA) no COG assignment.

only CGA009 has a gene belonging to the COG B group (i.e., chromatin structure and dynamics), which is associated with acetylpolyamine aminohydrolase[6]. It has been suggested that acetoin can be converted to acetate by acetylpolyamine aminohydrolase upon carbon source depletion[26]. We noticed that CGA009 exhibited a higher percentage of genes in the COG K group (i.e., transcription) than did PS3 or YSC3. We further analyzed the gene contents in the K group and found that CGA009 contains a larger ratio of genes encoding transcriptional regulators (Supplementary Table S7).

Carbon source utilization. *R. palustris* can obtain carbon from carbon dioxide and/or organic compounds[6]. Core metabolic pathways, such as the Calvin-Benson-Bassham (CBB) pathway of CO_2 fixation, the complete tricarboxylic acid (TCA) cycle, an Embden-Meyerhof-Parnas (EMP) pathway and a pentose phosphate pathway (PPP), were found in the genomes of both PS3 and YSC3 (Fig. 5). Larimer *et al.* reported that *R. palustris* CGA009 lacks genes encoding hexokinase[6], which is also the case for PS3 and YSC3. CGA009 can catabolize a variety of aromatic compounds for growth[27], and we obtained similar results for the *R. palustris* derivatives[22]. Several

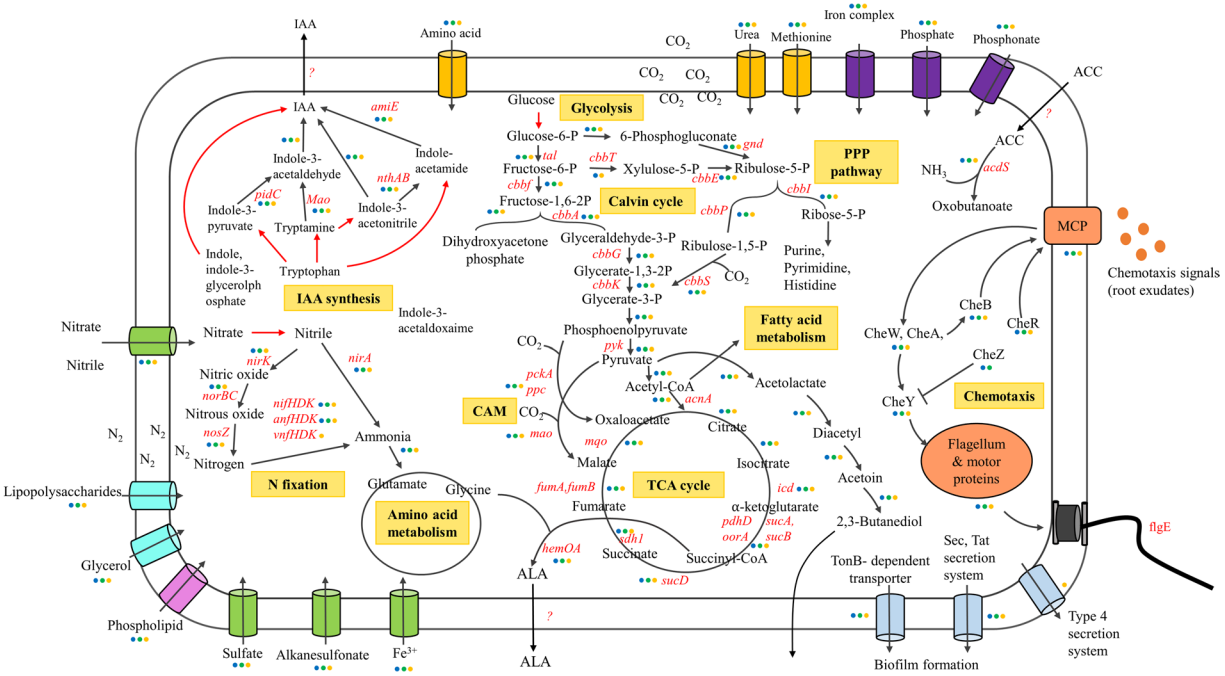

Figure 5. Schematic depiction of genes involved in metabolism (PPP, TCA cycle, glycolysis, nitrogen assimilation), rhizosphere adaptation and plant growth promotion in *R. palustris*. Genes annotated in each strain are marked with colored circles representing PS3 (blue), YSC3 (green), and CGA009 (orange). Red arrows represent nonspecific genes that were annotated among the three strains. "?" represents unknown function.

genes in the PS3 and YSC3 strains encode dioxygenases involved in the degradation of aromatic compounds, such as 3,4-dihydroxyphenylacetate 2,3-dioxygenase (locus tags: RPPS3_16850, RPPS3_37890, RPYSC3_16530, and RPYSC3_38130), homogentisate 1,2-dioxygenase (RPPS3_46330 and RPYSC3_46820), and hydroxyquinol 1,2-dioxygenase (RPPS3_21770 and RPYSC3_21800) (Supplementary Tables S5 and S6). Genes involved in ring cleavage pathways of homogentisate and phenylacetate were also identified in PS3 and YSC3, such as the *bed* genes (RPPS3_06600 and 06630–06740; RPYSC3_06760 and 06790–06900) (Supplementary Tables S5 and S6), which are associated with anaerobic benzoate degradation[28]. Additionally, CGA009 has been found to be able to use fatty acids and dicarboxylic acids via a conserved gene cluster associated with the fatty acid beta-oxidation pathway[6,29]. Similarly, we observed that the PS3 and YSC3 strains had a complete gene cluster for the fatty acid beta-oxidation pathway. The *R. palustris* pathways involved in degrading aromatic compounds provide not only extraordinary metabolic versatility but also high utility for bioremediation (e.g., methoxylated aromatics and aromatic amides)[7,29,30] and bioenergy production (e.g., hydrogen gas)[12]. We noticed no monosaccharide (such as glucose, mannose, xylose, arabinose, or fructose) transporter-related gene in any of the three *R. palustris* genomes. A previous study reported that CGA009 has limited ability to grow on sugars due to the absence of genes encoding glucose transporters, fructose transporters or hexokinases in its genome[6]. However, some studies have reported *R. palustris* strains that could consume glucose or fructose for cell growth[13,31,32]. In our previous study[13], we found that PS3 and YSC3 could use some monosaccharides, such as fructose and glucose. In addition, there are genes encoding multiple sugar ABC transport systems (RPPS3_01220, RPPS3_01230, RPPS3_033890, RPPS3_35020, RPPS3_35050, RPPS3_35450, RPPS3_43670, RPPS3_45360, RPYSC3_01220, RPYSC3_01230, RPYSC3_35200, RPYSC3_35230, RPYSC3_35650, RPYSC3_44090 and RPYSC3_45830) and TonB-dependent transporters in the *R. palustris* genomes (Supplementary Tables S5 and S6). TonB-dependent transporters have been considered to be involved in dietary polysaccharide processing in bacteria[33]. Therefore, we deduced that the multiple sugar ABC transport systems or TonB-dependent transporters are associated with the uptake of single sugar molecules for *R. palustris*. However, this hypothesis remains to be verified.

Nitrogen fixation and nitrogen utilization. Biological nitrogen fixation is the process via which nitrogen is converted to ammonia by the nitrogenase complex of microorganisms[34]. All known diazotrophs contain at least one of the three closely related subtypes of nitrogenase-related genes: *nif* (encoding molybdenum nitrogenase), *vnf* (encoding vanadium nitrogenase), and *anf* (encoding iron nitrogenase)[35]. According to previous studies, CGA009 was characterized as a nitrogen-fixing bacterium and harbors the above three gene subtypes[6,22]. On the other hand, only *anf* and *nif* nitrogenase-related genes and no *vnf*-related gene were found in the genomes of PS3 and YSC3. Nevertheless, both strains could fix nitrogen under light-microaerobic conditions[13]. According to genomic analysis, these two strains have a gene cluster encoding the nitrate/nitrite transport pathways (RPPS3_21380-21400 and RPYSC3_21410-21430) (Supplementary Tables S5 and S6); however, no explicit nitrate reductase genes were identified in the two genomes. The PS3 and YSC3 strains have genes encoding proteins associated with denitrification (RPPS3_33410, 41010, 14290–14300 and 20700; RPYSC3_41430, 1438–1439

and 20720) (Supplementary Tables S5 and S6), resembling the denitrification-associated genes in the CGA009 strain. In addition to nitrogen fixation, ferredoxin-nitrite reductase, encoded by *nirA* (RPPS3_37380 and RPYSC3_37610), can directly convert nitrite to ammonium, while ammonium can be taken up from the environment via two ammonium transporters (RPPS3_02860 and 02880; RPYSC3_02920 and 02940) (Supplementary Tables S5 and S6). As shown in Fig. 5, ammonium can be assimilated by glutamine synthetase (RPPS3_10270, 30150 and 41690; RPYSC3_10150, 30130 and 42060) and further converted to glutamate by glutamate synthetase (RPPS3_04850 and 08970; RPYSC3_04930 and 09180) (Supplementary Tables S5 and S6) for amino acid metabolism.

Root colonization. Root colonization by bacteria is regarded as an essential step for PGPRs to promote plant growth[3]. We compared genes associated with root colonization, such as genes involved in chemotaxis, cell motility, and biofilm formation[36]. All three strains possess three sets of the *che* genes (i.e., *cheA*, *cheB*, *cheR*, *cheW*, and *cheY*) (Supplementary Fig. S2). Cluster I comprises eight chemotaxis genes, which is the most complete cluster. Moreover, both PS3 and YSC3 contain the *cheZ* gene (RPPS3_11990 and RPYSC3_11730), which is annotated as a hypothetical protein in CGA009[6]. Genes encoding methyl-accepting chemotaxis proteins (RPPS3_00100, RPPS3_04430, RPPS3_11420, RPPS3_17980, RPPS3_36270, RPPS3_42600, RPPS3_44180, RPYSC3_00110, RPYSC3_18180, RPYSC3_36490, RPYSC3_42970, RPYSC3_44590, TX73_RS00710, TX73_RS02235, TX73_RS18110, TX73_RS21940, TX73_RS21960, TX73_RS21965, TX73_RS22735, TX73_RS23690 and TX73_RS23695) exist in all three strains. For cell motility, there were 50, 46, and 39 flagella-related genes in PS3, YSC3, and CGA009, respectively (Supplementary Tables S5 and S6 and NC_005296.1). Moreover, we noted that the cell migration rates of the three strains varied substantially. Microscopy showed that PS3 had the fastest migration speed, followed by YSC3. By contrast, CGA009 was almost immobile Supplementary Videos S1–S3). Several genes involved in biosynthesis or transportation of polysaccharides were identified in all three strains, for example, *exo* genes, which are responsible for exopolysaccharide (EPS) biosynthesis[22]. The *lptG* and *lptF* genes are responsible for lipopolysaccharide transportation[37]. Genes known to be associated with biofilm formation (as reported in the KEGG database), such as *pel*, *psl*, and *glg*, were not identified in these *R. palustris* strains; however, all three strains showed the ability to form biofilms during cultivation in PNSB broth (Supplementary Fig. S3a), and CGA009 shown higher biofilm formation than did PS3 and YSC3. In addition, biofilm formation was not significantly different between the PS3 and YSC3 strains (Supplementary Fig. S3).

Deduced plant growth promotion-related genes. The mechanisms for PGP by rhizobacteria include nitrogen fixation, improvement of nutrient availability, and phytohormone production[3,38]. As described above, all three *R. palustris* strains contain the conserved gene cluster that encodes nitrogenase (Supplementary Fig. S4a), which is consistent with the positive phenotyping result obtained for nitrogen fixation. We also found that the *R. palustris* strains harbor genes encoding nitrite reductase and nitric oxide reductase, which convert nitrite to nitric oxide and nitrous oxide. These strains also contain ferredoxin-nitrite reductase, which can directly reduce nitrite to ammonium (Fig. 5). These findings suggest that via enzymatic conversion, *R. palustris* is able to provide plants with available sources of nitrogen.

Phosphate solubilization is also an important mode of action for plant growth[4]. We identified several genes encoding phosphatases, C-P lyases, inositol-phosphate phosphatases, and organic acids in the genomes of all three strains (Supplementary Fig. S4b). Unexpectedly, in our plate assay, these three strains did not present clear zones around the colonies, which indicates that these strains are unable to solubilize phosphate (Supplementary Fig. S5). Some PGPRs can produce phytohormones to stimulate plant growth[39–41]. In our previous study, we conducted a colorimetric assay to demonstrate that both PS3 and YSC3 were able to produce the plant hormone IAA in the presence of tryptophan[13]. As shown in Fig. 5, these two strains possess most of the genes involved in the biosynthetic pathway of IAA in bacteria[42]. However, some genes encoding essential proteins, such as tryptophan-pyruvate aminotransferase (TAA1), tryptophan aminotransferase (TAM1), aromatic amino acid decarboxylase (DDC), tryptophan 2-monooxygenase (MAO), tryptophan side chain oxidase (TSO) and tryptophan monooxygenase (IaaM), were absent in the genomes of these strains. To corroborate their IAA production ability, we employed a more sensitive and accurate method (HPLC) for evaluation (Supplementary methods). As shown in Supplementary Fig. S6, all of these tree strains can produce IAA in the presence of tryptophan. It remains unclear whether the absence of these genes in the *R. palustris* genomes is an artifact of annotation or whether these bacteria have alternative genes for these functions.

ACC deaminase genes were identified in the genomes of PS3 and YSC3 (RPPS3_24510 and RPYSC3_24830, respectively) (Supplementary Tables S5 and S6) but were absent in the genome of CGA009. *R. palustris* can produce 5-aminolevulinic acid (ALA), which is regarded as an effective compound for PGP under abiotic stress[14,43–45]. The genes *hemO* and *hemA*, which are associated with the biosynthesis of ALA, were identified in all three strains. Detailed information about the genes associated with PGP is shown in Supplementary Fig. S4.

Effect of root exudates of Chinese cabbage on biofilm formation and relative gene expression levels. Root exudates and their organic acid components are considered important factors for biofilm formation and colonization by PGPRs of the rhizosphere[1]. To elucidate the role of root exudates in microbial activity, we used a hydroponic solution containing root exudates for cultivation of the bacterial strains. As shown in Fig. 6a, the growth rates of both PS3 and YSC3 increased slightly upon treatment with the root exudates (-R) in comparison with those of the control (-NS) groups; however, there was no statistically significant difference at most of the time points. With respect to bacterial biofilm formation, we quantified the crystal violet-stained biofilms at an optical density of 570 nm (OD_{570}). As shown in Fig. 6b, there was no significant difference in the accumulation of biofilm between PS3 and YSC3 while they were cultivated in the hydroponic solution. On the other hand, more biofilm

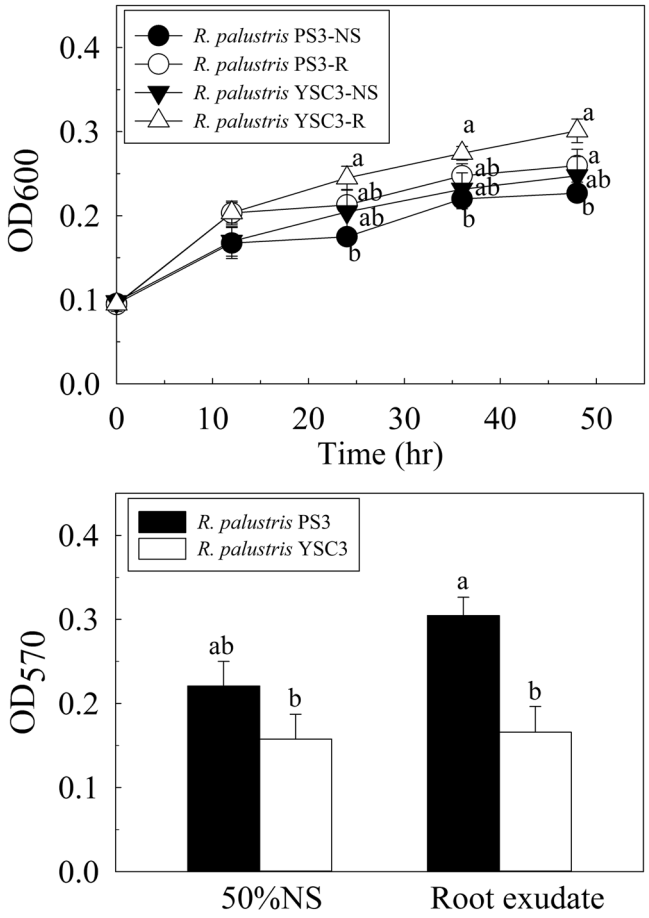

Figure 6. Effects of Chinese cabbage root exudates on growth and biofilm formation of the *R. palustris* PS3 and YSC3 strains. (**a**) Growth curve of *R. palustris* strains in Hoagland NS and root exudate solution. (**b**) Biofilm formation was evaluated by 0.1% crystal violet staining for 15 min at 24 h postincubation. Both *R. palustris* strains were incubated in either half-strength Hoagland NS or root exudate solution (10% (v/v)). The letters indicate statistically significant differences based on Student's t-test ($P < 0.05$).

was formed by PS3 than by YSC3, while root exudates were supplemented in the hydroponic solution. We also noted that biofilm formation by YSC3 was not altered in the presence of root exudates.

The expression patterns of genes associated with bacterial colonization and biofilm formation in response to root exudates were analyzed in a time-course study. As shown in Fig. 7, the relative expression levels of flagella-related genes (Fig. 7a,b) of YSC3 were higher than those of PS3 at most time points during growth. We found that the expression of *fliM* and *flgB* in YSC3 increased with time and that the expression of *fliE* peaked at 12 h and gradually declined. Moreover, according to the cluster integrity, we selected several *che* genes located in cluster I to quantify the expression levels. The results showed that the expression of the chemotaxis-related genes *cheR*, *cheW* and *cheA* of PS3 was upregulated and peaked at 12 h, and these expression levels were significantly higher than those of YSC3 at this time point (Fig. 7d–f). There was no significant difference in the expression of the biofilm formation-related genes *fliE* or *exoR* or the *eps* genes between PS3 and YSC3 (Fig. 7c,g,h).

Discussion

R. palustris strains PS3 and YSC3 were isolated from paddy fields located in neighboring cities in northern Taiwan. These strains have a closer evolutionary relationship than the other characterized *R. palustris* strains (Fig. 2). The chromosomal organization of these two strains is highly conserved, and the strains share 98.59% of their protein-coding genes (Fig. 2c,d and Supplementary Fig. S1 and S7). However, although these strains are closely phylogenetically related, only strain PS3 is able to promote plant growth[13,16].

While treating individual bacterial cultures with root exudates, substantial differences in biofilm formation and relative gene expression levels were observed between PS3 and YSC3 (Figs 6 and 7). Root exudates contain various carbohydrate-derived compounds (e.g., glucose, maltose, xylose, citric acid, malic acid, and succinic acid)[36,46,47] and are the most important nutrient sources for rhizospheric microorganisms. In our previous study, we proved that both PS3 and YSC3 can utilize various carbon sources, including the carbon sources mentioned above[13]. Furthermore, many metabolic pathways of the core carbohydrates were identified in the genomes of PS3 and YSC3 (Fig. 5). Therefore, we inferred that these two bacteria are able to utilize carbohydrates derived from root exudates. We noted that the bacterial growth of the PS3 and YSC3 strains was not enhanced in half-strength

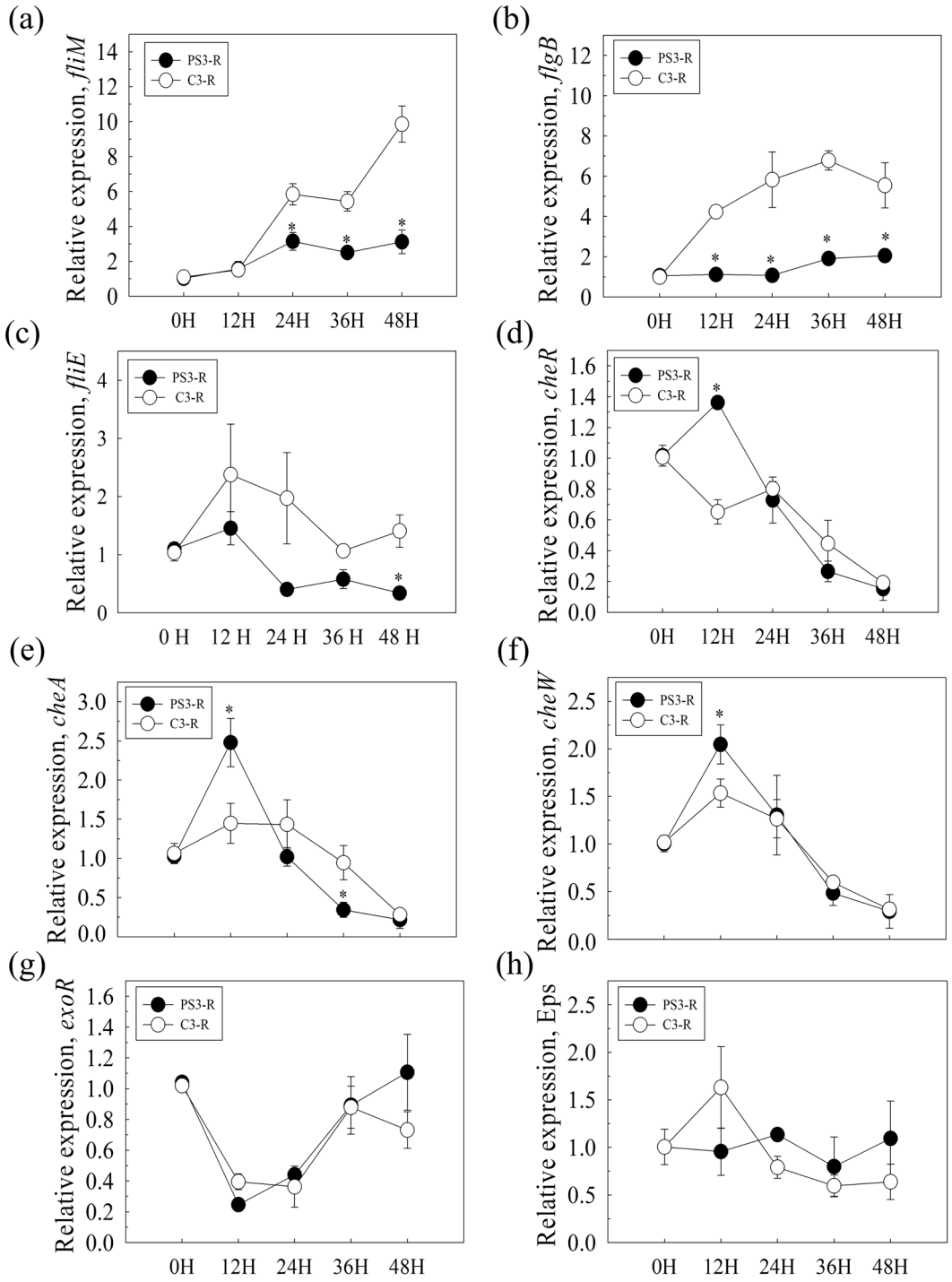

Figure 7. Gene expression patterns of *R. palustris* strains in response to Chinese cabbage root exudate solution. *R. palustris* strains were incubated with Chinese cabbage root exudates, and then, the expression of flagella (*fliM*, *flgB*, *fliE*), chemotaxis (*cheR*, *cheW*, *cheA*) and biofilm formation (Eps and *exo*) genes was determined by qPCR relative to an internal control gene, *clpX*. Relative expression values (SE) were obtained from three biological repeats and measured for three technical repeats. Asterisks indicate significant differences based on Student's t-test ($P < 0.05$).

Hoagland solution containing root exudates (Fig. 6a). We hypothesized that the nutrient levels in this culture medium were too low to sustain normal bacterial growth of *R. palustris*.

In addition to carbohydrates, aromatic hydrocarbons are another type of abundant plant-derived compounds in the rhizosphere. Aromatic hydrocarbons are mainly derived from secondary metabolites (such as flavonoids and phenols) and lignin structures[48]. *R. palustris* can degrade a variety of aromatic compounds[6,7,49]. In the present study, several genes associated with degradation of aromatic compounds were identified in the PS3 and

YSC3 genomes. These putative enzymes are involved in either oxygenase-dependent ring cleavage pathways or the anaerobic benzoate degradation pathway (Supplementary Tables S5 and S6). Accordingly, this finding suggests that the *R. palustris* strains can utilize a variety of carbon sources at different levels of oxygen, even under low-oxygen conditions (hypoxia). This result may explain why PS3 can have beneficial effects on plant growth in either soil (aerobic) or hydroponic solution (aerobic-anaerobic interfaces)[13,16]. It would be advantageous for *R. palustris* to act as a PGPR to utilize additional nutrients in agricultural systems under conditions where oxygen demand exceeds supply, such as during flooding of the rice rhizosphere.

Efficient colonization by PGPRs of roots has been considered a key trait conferring beneficial effects to plants, and this ability is closely associated with chemotaxis and biofilm formation[50]. We found that the genetic arrangements of the chemotaxis-related gene cluster (*cheA*, *cheB*, *cheW*, *cheR* and *cheY*) and the flagellar biosynthesis-related gene cluster (*flhA*, *flhB*, *fliP*, *fliQ*, and *fliR*) are very similar among the genomes of PS3, YSC3 and CGA009 (Fig. 5 and Supplementary Tables S5 and S6). Moreover, genes associated with biosynthesis of exopolysaccharides, such as the *exo*, *kps*, and *upp* genes, were identified in the three strains (GenBank: NC_005296, Supplementary Tables S5 and S6). The *upp* gene has already been found to be an important gene in the mediation of biofilm formation by *R. palustris* under photoheterotrophic growth conditions[51]. Although these gene clusters showed very similar genetic arrangements in the three bacteria, the abilities of these strains to form biofilms differed. As shown in Supplementary Fig. S3, CGA009 produced more biofilm than did the other two strains.

Rhizobia are able to supply nitrogen sources to host plants via symbiotic nitrogen fixation in root nodules. In contrast, free-living nitrogen-fixing bacteria release the ammonia synthesized by cells into the environment, and some of this ammonia is converted to nitrite/nitrate[52]. As mentioned, both PS3 and YSC3 have the nitrogenase genes and are able to fix nitrogen under light-microaerobic condition. Upon inoculating these bacteria into the hydroponic nutrient solution (NS) for cultivating plants, we noted that the concentration of ammonia did not change substantially in the NS (data not shown), indicating that free-living N_2-fixation did not occur under such aerobic culture conditions. Accordingly, we deduced that biological nitrogen fixation is not the primary mode of action for PGP by PS3.

Phosphorus is one of the most important macronutrients, but the availability of phosphorus in soil is limited. Phosphate-solubilizing bacteria can convert insoluble phosphorus (both organic and inorganic) to available forms for plant utilization, and this property is regarded as an essential mode of action for PGP[3,4]. PS3, YSC3 and CGA009 contain many genes involved in phosphate solubilization, such as *phn*, *gcd* and *pqq* (Supplementary Fig. S4b). The *phn* gene family encodes phosphonatases and C-P lyases, which are the enzymes that perform C-P cleavage in organophosphonates[53]. Furthermore, this gene family is also associated with the release of phosphate ions from organic matter, such as fertilizers. On the other hand, genes involved in phosphate solubilization via the production of organic acids were also identified in these *R. palustris* strains. For example, the *gcd* gene, encoding glucose dehydrogenase, and the *pqq* gene, encoding pyrroloquinoline quinone (PQQ), are associated with the production of gluconic acid (GA) in a well-known organic acid-based mechanism of inorganic phosphate solubilization[53]. However, we noted that all three strains lacked orthologs of the *pqqA* gene in the PQQ synthetic pathway (Supplementary Fig. S4b). This finding might suggest that these three strains are unable to synthesize GA. However, it has been reported that *pqqA* is not essential for biosynthesis of PQQ in *Methylobacterium extorquens* AM1[54]. Therefore, the GA production of these three bacteria requires further elucidation. In addition, these bacteria did not harbor related genes encoding phosphatases or phytases, which are the most relevant proteins associated with phosphate solubilization in the environment[53]. Moreover, our data showed that these three strains were not capable of solubilizing inorganic phosphorus from insoluble compounds (Supplementary Fig. S5), even though these strains possess most of the phosphate solubilization-related genes. This result is also consistent with previous reports that *R. palustris* lacks the ability to solubilize phosphate[55,56]. The commonly observed absence of phosphate-solubilization activity among *R. palustris* strains indicates that this function is probably no longer required for sustaining the growth of these bacteria in the environment. Bacteria generally lose some essential biosynthetic functions when the corresponding metabolite is present in sufficient amounts in the bacterial growth environment or is provided by a consortium of organisms[57]. Whether the reduction of metabolic burden for basic cellular processes in *R. palustris* results in adaptive benefits over other genotypes[58], as well as the causal mechanisms that explain this observation, remains unclear.

We observed that PS3 could modulate root system architecture and promote plant growth[13,16], indicating the production of phytohormones and other signals during the interactions between *R. palustris* and host plants. It has been demonstrated that enhanced root proliferation, such as increased root size and lateral root number, is closely associated with bacterial IAA levels[39]. IAA biosynthesis in bacteria can be divided into tryptophan-dependent and tryptophan-independent pathways[42]. However, we noted that genes involved in the conversion of tryptophan to other intermediates were absent in the annotation (Fig. 5 and Supplementary Fig. S4c). We identified some genes involved in the synthesis of indole-3-glycerolphosphate and indole in PS3, YSC3 and CGA009; these genes included *trpBA* (RPPS3_00730, RPPS3_00740, RPYSC3_00730, RPYSC3_00740, TX73_RS00360 and TX73_RS00365) and *tnaA* (RPPS3_35930, RPYSC3_36170 and TX73_RS18205). These intermediates are predictive precursors of IAA synthesis in tryptophan-independent pathways[59], suggesting that these *R. palustris* strains are able to synthesize IAA via a yet-unidentified pathway(s).

Some genes associated with environmental stress tolerance were identified in the genomes of the *R. palustris* strains. Examples of these genes include *acdS* (ACC deaminase; locus tags: RPPS3_24510 and RPYSC3_24830), *hemO*/*hemA* (RPPS3_08610, RPYSC3_08830 and TX73_RS04400 for PS3, YSC3 and CGA009, respectively) and the *hemA* genes (RPPS3_15310, RPYSC3_15390 and TX73_RS04400 for PS3, YSC3 and CGA009, respectively), which encode ALA synthase (Supplementary Fig. S4d). In many PGPRs, such as *Pseudomonas fluorescens*, *Achromobacter piechaudii* and *P. putida*, ACC deaminase can alleviate the detrimental effects of environmental stress and can enhance the stress tolerance of plants by degrading the ethylene precursor ACC[60,61]. ALA is a precursor of porphyrin-containing compounds, such as vitamin B12, chlorophyll, heme and phytochrome[62–65].

Several studies have indicated that exogenous application of ALA can effectively promote plant growth and aid in the stress tolerance of plants[66–69]. For example, Nunkaew *et al*. found that applying the broths of *R. palustris* TK103 and PP803 could promote the growth of rice under high-salt conditions due to the high ALA content[14].

As described above, PS3 and YSC3 exhibited a very close phylogenetic relationship and shared several conserved regions and genetic arrangements in their chromosomes. The conservation of genetic arrangement is usually used to predict functions of protein-coding genes[70]. Although we identified many putative genes that were associated with known PGP traits in both *R. palustris* strains, only PS3 can successfully promote the growth of plants[13]. Previous studies have indicated that root exudates can regulate transcription in PGPRs[71–73]. As shown in Figs 6 and 7, root exudates of Chinese cabbage had an effect on microbial activities such as biofilm formation as well as on gene expression patterns specific to flagella-related genes (*fliM*, *fliB, fliE*) and chemotaxis-related genes (*cheR, cheW*, and *cheA*) of PS3 and YSC3. The flagella of bacteria are primarily involved in cellular motility but also have sensory functions to sense changes in the environment[74]. Chemotaxis is the movement of bacteria in response to stimuli; bacteria move toward favorable chemicals or away from unfavorable chemicals[75]. Therefore, we deduced that the differences in the effectiveness of PGP by the two bacterial strains were due to the different physiological responses of these strains to specific compounds in the root exudates that act as signal molecules.

Recent studies have indicated that quorum sensing (QS) by PGPRs is involved in biofilm formation, plant colonization and PGP and in triggering induced systemic resistance[76–78]. These beneficial effects are mediated via QS signaling molecules, such as N-acylhomoserine lactone (AHL), which regulate gene expression in response to bacterial population density and interactions with plants[79,80]. Surprisingly, *R. palustris* uses *p*-coumaroyl-homoserine lactone (pC-HSL), an aryl-HSL, as a signaling molecule[81]. pC-HSL synthase was also identified in the genomes of the PS3 and YSC3 strains (RPPS3_03320 and RPYSC3_03390). The synthesis of pC-HSL requires an exogenous source of *p*-coumarate, which is usually present in root exudates[82,83]. Accordingly, we inferred that this aromatic compound triggers the synthesis of the QS molecule of *R. palustris* and mediates interactions with the plant host. pC-HSL is conserved in PGPR strains other than *R. palustris*, such as *Bradyrhizobium* BTAi1[81]. Therefore, it is possible that *R. palustris* can use pC-HSL to have beneficial effects on plant growth.

Summary

This is the first study to carry out a comparative analysis of *R. palustris* strains that are effective and ineffective in PGP. The PS3 and YSC3 strains are closely related to each other and have similar genomic structures and compositions. Although these strains have many plant growth-promoting genes in common, only the former exhibited PGP. This result suggests that the presence of PGP-associated genes in a bacterium is not sufficient for the bacterium to have beneficial effects on plant growth. Rather, physiological responses to the presence of plant hosts and successful establishment of interactions with the host appear to be critical. To elucidate the underlying molecular mechanisms associated with PGP by *R. palustris* PS3, further experiments are needed. For example, gene deletion and parallel analyses can be used to determine the phenotypic and functional properties associated with plant-bacteria interactions.

Methods

Preparation of phototrophic bacterial inoculant. The *R. palustris* strains PS3 and YSC3 are PNSBs and were both isolated from Taiwanese paddy soils[19]. PS3 is an effective PGPR, whereas YSC3 is not. For bacterial inoculant preparation, a single colony was selected and inoculated into 3 mL of PNSB broth as described previously[13]. The culture was then incubated for 24 h at 37 °C (200 rpm). Subsequently, 2.5 mL of these cultures was transferred into 250-mL Erlenmeyer flasks containing 50 mL of fresh PNSB broth. The cultures were incubated under the conditions described above, and the log-phase bacterial cells were harvested for genomic DNA extraction.

Genomic DNA preparation. A 1-mL suspension of the log-phase bacterial culture was collected in a 2.0-mL Eppendorf tube and centrifuged at 3,000 × g at 4 °C. Subsequently, the supernatant was removed, and the Eppendorf containing the cell pellet was snap-frozen in liquid nitrogen. The cell pellet was homogenized by adding sterile steel beads and rapidly shaking the microcentrifuge tubes back and forth at 9,000 rpm for 1 min in a SH-100 homogenizer (Kurabo, Japan). The homogenization process was repeated three times. The Gentra® Puregene® Kit (QIAGEN) was used for genomic DNA purification according to the manufacturer's protocol. The quantity and quality of the total DNA were assessed using UV spectrophotometry (Nanodrop ND-1000, J & H Technology Co., Ltd.), and the OD260/280 value of the DNA was higher than 1.80. Agarose gel electrophoresis (0.75%) was used to ensure that the gDNA was intact. Samples containing greater than 25 μg of gDNA were used to perform whole-genome sequencing.

Whole-genome sequencing. We utilized the MiSeq (Illumina) and the PacBio RSII (Pacific Biosciences) platforms to perform whole-genome shotgun sequencing. The sequencing service was provided by Genomics BioSci & Tech Co., Ltd. (New Taipei City, Taiwan). For Illumina MiSeq sequencing, the DNA library was constructed using the Illumina TruSeq Nano DNA HT Sample Prep Kit according to the TruSeq DNA Sample Preparation protocol (Illumina). This library was diluted and sequenced with 600 paired-end cycles on the Illumina MiSeq instrument by following the standard protocol. For the PS3 strain, the insert size was 500 bp, and 10,471,982 read-pairs and ~3.6 Gb of raw data were obtained; for the YSC3 strain, the insert size was 500 bp, and 11,242,474 read-pairs and ~3.8 Gb of raw data were obtained. For PacBio SMRT sequencing, the DNA library was constructed according to the PacBio SampleNet – Shared Protocol (Pacific Biosciences). After dilution, the library was loaded onto the instrument with the DNA Sequencing Kit 4.0 v2 (part number PB100-612-400) and a SMRT Cell 8 Pac for sequencing. Primary filtering analysis was performed with the RS instrument, and secondary analysis was performed using the SMRT analysis pipeline, version 2.1.0. For the PS3 strain, the average length of

the reads was 7,112 bp, and 164,831 reads and ~1.1 Gb of raw data were obtained; for the YSC3 strain, the average length of the reads was 6,342 bp, and 192,795 reads and ~1.2 Gb of raw data were obtained.

***De novo* genome assembly.** The *de novo* genome assembly was based on the paired-end Illumina reads and the PacBio reads. The raw Illumina reads were trimmed at the first position from both the 5′- and 3′-ends that had quality scores lower than 20 by the software Trimmomatic[84]. After discarding these reads, all Illumina reads were shorter than 210 bp, and high-quality sets of 10,470,949 (PS3 strain, ~2.6 Gb of raw data) and 11,241,446 read-pairs (YSC3 strain, ~2.8 Gb of raw data) were obtained. These trimmed reads were individually matched with the corresponding PacBio reads and used as the input for SPAdes Genome Assembler, version 3.5[85], with default parameters. Finally, the whole-genome sequences were obtained, and the genomic sizes of PS3 and YSC3 were 5,269,926 bp and 5,371,816 bp, respectively.

Genome annotation. Annotations of the PS3 and YSC3 genomes were based on the procedures described by Cho, *et al.*[86]. The programs RNAmmer[87], tRNAscan-SE[88], and PRODIGAL[89] were used for gene prediction. The genomic sequence of *R. palustris* CGA009[6] was used as the reference, and the initial annotation of each protein-coding gene was conducted by OrthoMC[90] with a BLAST[91] e-value cutoff of 1e-15 and an inflation value of 1.5. Then, BLASTP[91] searches against the NCBI non-redundant (nr) protein database, BlastKOALA[92], and the PATRIC platform[93] were used for manual curation to improve the annotation. For functional categorization, all protein-coding genes were used to run BLASTP[91] searches against the COG functional category database as described by Galperin, *et al.*[94] with an e-value cutoff of 1e-10. The program CIRCOS[95] was used to plot the gene locations, GC-skew and GC content.

Phylogenetic analysis. To infer the relatedness among the *R. palustris* strains, phylogenetic trees were constructed based on MLSA and *puf* genes. For MLST analysis, three housekeeping genes, *recA*, *rpoB* and *dnaK*, were selected. The sequences of these three genes were retrieved from GenBank. Then, individual gene sequences were validated by alignment using ClustalW multiple alignment program[96] with the default settings. Subsequently, these genes were combined to form a *recA-rpoB-dnaK* concatenated sequence by BioEdit[97]. MEGA7.0.14[98] was used to construct the topological tree using the maximum likelihood program[99]. The general time-reversible model and gamma distributed with invariant model (GTR + G + I)[100] were evaluated from the alignment in the maximum likelihood framework. To estimate the level of support for each branch, the 1,000 bootstrap[101] samples of the alignment were generated by using the maximum likelihood program[99] in MEGA7.0.14[98]. The *puf* genes consisted of *pufL* and *pufM*, which encode the core proteins of the photosynthetic reaction center. The sequences of the *puf* genes from other *R. palustris* strains were downloaded from GenBank. The individual gene sequences were aligned using BioEdit[97] with the ClustalW multiple alignment program[96] with the default settings. After gene concatenation, the resulting multiple sequence alignment was used to construct the phylogenetic trees by using the maximum likelihood program[99] with the general time-reversible model and gamma distributed with invariant model (GTR + G + I)[100]. The 1,000 bootstrap[101] replicates were used to estimate the level of support for each internal branch.

Comparative genomic analyses. We performed comparative genomic analyses of the genomes of the PS3 and YSC3 strains and the sequenced *R. palustris* type strain CGA009[6]. Pairwise alignments of all three strains were carried out by MUMmer version 3.23[102] with default parameters. The conserved genes and homologous gene clusters were identified using OrthoMCL[90] with the same settings as described above. Genes involved in metabolic pathways were analyzed by KEGG Mapper. Genomic island prediction was performed by Zisland Explorer[24] with default parameters.

Collection of Chinese cabbage root exudate solution. To collect the root exudates, Chinese cabbage seeds (*Brassica rapa* L. ssp. *chinensis*, "Maruba Santoh") were selected and purchased from Formosa Farming Materials Co., Ltd. (Taipei, Taiwan). The seeds were immersed in 70% alcohol for 2 min and then in 3% hydrogen peroxide solution for 7 min for surface sterilization. Then, the seeds were washed thoroughly with sterile distilled water and germinated for 1 day at 25 °C in the dark. Subsequently, well-germinated seeds were transferred to soaked cotton and cultivated under continuous (24-h photoperiod) light-emitting diode lighting (~210 μmol $m^{-2}s^{-1}$). After one week, the seedlings were transferred to hydroponic tanks (35 L) in a plant factory facility (College of BioResources and Agriculture, National Taiwan University). Twenty-four seedlings were cultivated in each of the tanks, which were equipped with air pumps to homogenize the solution and maintain the dissolved oxygen. Half-strength Hoagland solution was used as an NS (0.255 g L^{-1} KNO_3, 0.245 g L^{-1} $MgSO_4 \bullet 7H_2O$, 0.04 g L^{-1} NH_4NO_3, 0.034 g L^{-1} KH_2PO_4, 11.25 mg L^{-1} Fe-EDTA, 1.43 mg L^{-1} H_3BO_3, 0.0255 mg L^{-1} $CuSO_4$, 0.11 mg L^{-1} $ZnSO_4 \bullet 7H_2O$, 0.95 g L^{-1} $MnCl_2 \bullet 4H_2O$, 0.06 mg L^{-1} $Na_2MoO_4 \bullet 2H_2O$ and 0.59 g L^{-1} $Ca(NO_3)_2 \bullet 4H_2O$)[103]. The initial pH value was adjusted to 6.0 by H_3PO_4. After 7 days of cultivation, the NSs containing root exudates were collected and filtered through 0.22-μm filter membranes. The sterility of these root exudate solutions was checked by plating onto nutrient agar plates.

Effect of root exudates on the growth of R. palustris strains. A single bacterial colony was selected, inoculated into 3 mL of PNSB broth as described previously[13], and incubated for 24 h at 37 °C (200 rpm). Then, the absorbance at 600 nm was adjusted to 1.0 using fresh PNSB broth, and 0.5 ml of the above broths were inoculated into 250-mL Erlenmeyer flasks containing 50 mL of fresh 50% Hoagland solutions as well as the root exudate solutions described above. The growth concentration was determined by measuring the optical density at 600 nm (OD_{600}) using a spectrophotometer (Ultrospec 2100 pro, Amersham Biosciences).

Effect of root exudates on the biofilm production of R. palustris. Biofilm formation assay was performed according to a protocol proposed by Tram, *et al.*[104] with some modifications. A single bacterial colony was selected, inoculated into a 10-mL sterile plastic tube containing 3 mL of PNSB broth[13], and then incubated at 37 °C and 200 rpm for 24 h. Hoagland solution was used in this experiment as the hydroponic solution. The above culture broth (20 μL) was taken and inoculated into a 96-well plate in which each well contained 180 μL of Hoagland solution with or without root exudates. Bacteria grown in the wells were incubated at 37 °C under stirring (500 rpm) in darkness. For biofilm quantification, the broth in the well was slowly emptied and then rinsed with sterile distilled, deionized water (DDW) to remove the incomplete biofilm. The plate was air dried for 5 min, and the biofilm was then stained with 200 μL of 0.1% crystal violet for 15 min. The crystal violet solution was removed, and the well was washed with DDW three times prior to observation. Subsequently, 200 μL of 95% ethanol was added into the well and shaken vigorously by vortex. Following, the absorbance at 570 nm was determined by using a multilabel reader (VICTOR3 1420-050, PerkinElmer).

Gene expression analysis of R. palustris in response to root exudates. *R. palustris* broth was inoculated (10% (v/v)) into 200 mL of half-strength Hoagland solution and 200 mL of the abovementioned root exudate solution. The cells were then incubated at 25 °C and 150 rpm in the dark. Bacterial cells were sampled at different time intervals for RNA extraction. Bacterial cell pellets were collected by centrifugation (5000 × g for 5 min at 4 °C). Subsequently, the cell pellets were snap-frozen in liquid nitrogen and homogenized by adding sterile steel beads and rapidly shaking the microcentrifuge tubes back and forth at 9,000 rpm for 1 min in an SH-100 homogenizer (Kurabo, Japan). The homogenization process was repeated three times. RNA purification was performed by the Direct-zol™ RNA MiniPrep Kit (Zymo Research, USA) according to the manufacturer's instructions. For reverse transcription, 2 μg of total RNA was reacted with random hexamers and the SuperScript III reagent to synthesize first-strand cDNA according to the protocol for SuperScript® III Reverse Transcriptase (Invitrogen, USA). Quantitative PCR analysis of gene expression was performed by using the SYBR Green Real-Time PCR Master Mix Kit (Kapa Biosystems, USA), and the fluorescence intensity was measured by the LightCycler 480 system (Roche, Germany). The real-time PCR conditions were as follows: denaturation at 95 °C for 3 min, followed by 45 cycles of 95 °C for 10 s, 60 °C for 20 s and 72 °C for 1 s. A program of 95 °C for 5 s and 60 °C for 1 min was used to obtain a melting curve. All qPCR analyses were performed in three biological replicates. The housekeeping gene *clpX* was used as the reference gene for transcript normalization. All primer pairs used for quantitative RT-PCR are listed in Supplementary Table S8. The fold change in the expression of target genes in each treatment was calculated using the $2^{-\Delta\Delta Ct}$ method[105].

Statistical analysis. Analyses of variance were performed with *R* version 3.4.3. Fisher's least significant difference (LSD) test was used for multiple range analyses to determine significant differences between groups of data. The results were considered significant at $P < 0.05$.

Data availability. The data associated with genomic information for *R. palustris* PS3, YSC3 and CGA009 strains in this paper are available in the NCBI genome database under accession numbers CP019966.1, CP019967.1 and NC_005296.1, respectively.

References

1. Kloepper, J. W. & Schroth, M. N. In *Proceedings of the 4th international conference on plant pathogenic bacteria*. (ed. Station de Pathologie Végétale et Phyto-Bactériologie) 879–882 (1978).
2. Ahemad, M. & Kibret, M. Mechanisms and applications of plant growth promoting rhizobacteria: Current perspective. *J. King Saud Univ. Sci.* **26**, 1–20 (2014).
3. Lugtenberg, B. & Kamilova, F. Plant-growth-promoting rhizobacteria. *Annu Rev Microbiol* **63**, 541–556 (2009).
4. Goswami, D., Thakker, J. N. & Dhandhukia, P. C. Portraying mechanics of plant growth promoting rhizobacteria (PGPR): a review. *Cogent Food Agric* **2**, 1127500–1127518 (2016).
5. Beneduzi, A., Ambrosini, A. & Passaglia, L. M. P. Plant growth-promoting rhizobacteria (PGPR): Their potential as antagonists and biocontrol agents. *Genet Mol Biol* **35**, 1044–1051 (2012).
6. Larimer, F. W. *et al*. Complete genome sequence of the metabolically versatile photosynthetic bacterium *Rhodopseudomonas palustris*. *Nat Biotechnol* **22**, 55–61 (2004).
7. Austin, S. *et al*. Metabolism of multiple aromatic compounds in corn stover hydrolysate by *Rhodopseudomonas palustris*. *Environ Sci Technol* **49**, 8914–8922 (2015).
8. Idi, A., Nor, M. H. M., Wahab, M. F. A. & Ibrahim, Z. Photosynthetic bacteria: an eco-friendly and cheap tool for bioremediation. *Rev Environ Sci Bio* **14**, 271–285 (2015).
9. Oda, Y., Star, B., Huisman, L. A., Gottschal, J. C. & Forney, L. J. Biogeography of the purple nonsulfur bacterium *Rhodopseudomonas palustris*. *Appl Environ Microb* **69**, 5186–5191 (2003).
10. Zhang, D. *et al*. Bioprocess modelling of biohydrogen production by *Rhodopseudomonas palustris*: Model development and effects of operating conditions on hydrogen yield and glycerol conversion efficiency. *Chem Eng Sci* **130**, 68–78 (2015).
11. Liu, Y., Ghosh, D. & Hallenbeck, P. C. Biological reformation of ethanol to hydrogen by *Rhodopseudomonas palustris* CGA009. *Bioresource Technol* **176**, 189–195 (2015).
12. Shi, X. Y., Li, W. W. & Yu, H. Q. Optimization of H-2 photo-fermentation from benzoate by *Rhodopseudomonas palustris* using a desirability function approach. *Int J Hydrogen Energ* **39**, 4244–4251 (2014).
13. Wong, W. T. *et al*. Promoting effects of a single *Rhodopseudomonas palustris* inoculant on plant growth by Brassica rapa chinensis under low fertilizer input. *Microbes Environ* **29**, 303–313 (2014).
14. Nunkaew, T., Kantachote, D., Kanzaki, H., Nitoda, T. & Ritchie, R. J. Effects of 5-aminolevulinic acid (ALA)-containing supernatants from selected *Rhodopseudomonas palustris* strains on rice growth under NaCl stress, with mediating effects on chlorophyll, photosynthetic electron transport and antioxidative enzymes. *Electron J Biotechn* **17**, 19–26 (2014).
15. Kornochalert, N., Kantachote, D., Chaiprapat, S. & Techkarnjanaruk, S. Use of *Rhodopseudomonas palustris* P1 stimulated growth by fermented pineapple extract to treat latex rubber sheet wastewater to obtain single cell protein. *Ann Microbiol* **64**, 1021–1032 (2014).

16. Hsu, S. H., Lo, K. J., Fang, W., Lur, H. S. & Liu, C. T. Application of phototrophic bacterial inoculant to reduce nitrate content in hydroponic leafy vegetables. *Crop Environ Bioinf* **12**, 30–41 (2015).
17. Liu, W. *et al*. Whole genome analysis of halotolerant and alkalotolerant plant growth-promoting rhizobacterium *Klebsiella* sp. D5A. *Sci Rep* **6**, 26710–26719 (2016).
18. Magno-Perez-Bryan, M. C. *et al*. Comparative genomics within the *Bacillus* genus reveal the singularities of two robust *Bacillus amyloliquefaciens* biocontrol strains. *Mol Plant Microbe Interact* **28**, 1102–1116 (2015).
19. Shen, X., Hu, H., Peng, H., Wang, W. & Zhang, X. Comparative genomic analysis of four representative plant growth-promoting rhizobacteria in *Pseudomonas*. *BMC Genomics* **14**, 271–290 (2013).
20. Gupta, A. *et al*. Whole genome sequencing and analysis of plant growth promoting bacteria isolated from the rhizosphere of plantation crops coconut, cocoa and arecanut. *PLoS One* **9**, e104259 (2014).
21. Taghavi, S. *et al*. Genome sequence of the plant growth promoting endophytic bacterium Enterobacter sp. 638. *PLoS Genet* **6**, e1000943 (2010).
22. Oda, Y. *et al*. Multiple genome sequences reveal adaptations of a phototrophic bacterium to sediment microenvironments. *Proc Natl Acad Sci USA* **105**, 18543–18548 (2008).
23. Oda, Y. *et al*. Functional genomic analysis of three nitrogenase isozymes in the photosynthetic bacterium *Rhodopseudomonas palustris*. *J Bacteriol* **187**, 7784–7794 (2005).
24. Wei, W. *et al*. Zisland Explorer: detect genomic islands by combining homogeneity and heterogeneity properties. *Brief Bioinform* **18**, 357–366 (2016).
25. Okamura, K., Takata, K. & Hiraishi, A. Intrageneric relationships of members of the genus *Rhodopseudomonas*. *J Gen Appl Microbiol* **55**, 469–478 (2009).
26. Leipe, D. D. & Landsman, D. Histone deacetylases, acetoin utilization proteins and acetylpolyamine amidohydrolases are members of an ancient protein superfamily. *Nucleic Acids Res* **25**, 3693–3697 (1997).
27. Harwood, C. S. & Gibson, J. Anaerobic and aerobic metabolism of diverse aromatic compounds by the photosynthetic bacterium *Rhodopseudomonas palustris*. *Appl Environ Microb* **54**, 712–717 (1988).
28. Hirakawa, H., Hirakawa, Y., Greenberg, E. P. & Harwood, C. S. BadR and BadM proteins transcriptionally regulate two operons needed for anaerobic benzoate degradation by *Rhodopseudomonas palustris*. *Appl Environ Microb* **81**, 4253–4262 (2015).
29. Harrison, F. H. & Harwood, C. S. The pimFABCDE operon from *Rhodopseudomonas palustris* mediates dicarboxylic acid degradation and participates in anaerobic benzoate degradation. *Microbiology* **151**, 727–736 (2005).
30. Karpinets, T. V. *et al*. Phenotype fingerprinting suggests the involvement of single-genotype consortia in degradation of aromatic compounds by *Rhodopseudomonas palustris*. *PLoS One* **4**, e4615 (2009).
31. Wang, Y. Z., Liao, Q., Zhu, X., Tian, X. & Zhang, C. Characteristics of hydrogen production and substrate consumption of *Rhodopseudomonas palustris* CQK 01 in an immobilized-cell photobioreactor. *Bioresour Technol* **101**, 4034–4041 (2010).
32. Oh, Y. K., Seol, E. H., Lee, E. Y. & Park, S. Fermentative hydrogen production by a new chemoheterotrophic bacterium *Rhodopseudomonas palustris* P4. *Int J Hydrogen Energ* **27**, 1373–1379 (2002).
33. Schauer, K., Rodionov, D. A. & de Reuse, H. New substrates for TonB-dependent transport: do we only see the 'tip of the iceberg'? *Trends Biochem Sci* **33** (2008).
34. Kim, J. & Rees, D. C. Nitrogenase and biological nitrogen fixation. *Biochemistry* **33**, 389–397 (1994).
35. Bishop, P. E. & Joerger, R. D. Genetics and molecular biology of alternative nitrogen fixation systems. *Annu Rev Plant Phys* **41**, 109–125 (1990).
36. Ahmad, F., Husain, F. M. & Ahmad, I. In *Microbes and microbial technology: Agricultural and environmental applications* (eds Iqbal Ahmad, Farah Ahmad, & John Pichtel) 363-391 (Springer New York, 2011).
37. Ruiz, N., Gronenberg, L. S., Kahne, D. & Silhavy, T. J. Identification of two inner-membrane proteins required for the transport of lipopolysaccharide to the outer membrane of *Escherichia coli*. *Proc Natl Acad Sci USA* **105**, 5537–5542 (2008).
38. Vessey, J. K. Plant growth promoting rhizobacteria as biofertilizers. *Plant Soil* **255**, 571–586 (2003).
39. Shao, J., Xu, Z., Zhang, N., Shen, Q. & Zhang, R. Contribution of indole-3-acetic acid in the plant growth promotion by the rhizospheric strain *Bacillus amyloliquefaciens* SQR9. *Biol Fert Soils* **51**, 321–330 (2014).
40. Talboys, P. J., Owen, D. W., Healey, J. R., Withers, P. J. A. & Jones, D. L. Auxin secretion by *Bacillus amyloliquefaciens* FZB42 both stimulates root exudation and limits phosphorus uptake in Triticum aestivium. *BMC Plant Biol* **14**, 51–59 (2014).
41. Spaepen, S. & Vanderleyden, J. Auxin and plant-microbe interactions. *Cold Spring Harb Perspect Biol* **3**, https://doi.org/10.1101/cshperspect.a001438 (2011).
42. Spaepen, S., Vanderleyden, J. & Remans, R. Indole-3-acetic acid in microbial and microorganism-plant signaling. *FEMS Microbiol Rev* **31**, 425–448 (2007).
43. Nishikawa, S. & Murooka, Y. 5-Aminolevulinic acid: Production by fermentation, and agricultural and biomedical applications. *Biotechnol Genet Eng Rev* **18**, 149–170 (2001).
44. Morales-Payan, J. P. & Stall, W. M. Papaya transplant growth as affected by 5- aminolevulinic acid and nitrogen fertilization. *Proc Fla State Hort Soc* **118**, 263–265 (2005).
45. Zhao, Y. Y. *et al*. Effects of exogenous 5-aminolevulinic acid on photosynthesis, stomatal conductance, transpiration rate, and PIP gene expression of tomato seedlings subject to salinity stress. *Genet Mol Res* **14**, 6401–6412 (2015).
46. Rovira, A. D. Plant root exudates. *Bot Rev* **35** (1969).
47. Vacheron, J. *et al*. Plant growth-promoting rhizobacteria and root system functioning. *Front Plant Sci* **4** (2013).
48. Adler, E. Lignin chemistry - past, present and future. *Wood Sci Technol* **11**, 169–218 (1977).
49. Harwood, C. S., Burchhardt, G., Herrmann, H. & Fuchs, G. Anaerobic metabolism of aromatic compounds via the benzoyl-CoA pathway. *FEMS Microbiol Rev* **22**, 439–458 (1998).
50. Ramey, B. E., Koutsoudis, M., von Bodman, S. B. & Fuqua, C. Biofilm formation in plant-microbe associations. *Curr Opin Microbiol* **7**, 602–609 (2004).
51. Fritts, R. K., LaSarre, B., Stoner, A. M., Posto, A. L. & McKinlay, J. B. A Rhizobiales-specific unipolar polysaccharide adhesin contributes to *Rhodopseudomonas palustris* biofilm formation across diverse photoheterotrophic conditions. *Appl Environ Microbiol* **83**, e03035–03016 (2017).
52. Bhattacharyya, P. N. & Jha, D. K. Plant growth-promoting rhizobacteria (PGPR): Emergence in agriculture. *World J Microbiol Biotechnol* **28**, 1327–1350 (2012).
53. Rodriguez, H., Fraga, R., Gonzalez, T. & Bashan, Y. Genetics of phosphate solubilization and its potential applications for improving plant growth-promoting bacteria. *Plant Soil* **287**, 15–21 (2006).
54. Toyama, H. & Lidstrom, M. E. *pqqA* is not required for biosynthesis of pyrroloquinoline quinone in *Methylobacterium extorquens* AM1. *Microbiology* **144**, 183–191 (1998).
55. Batool, K., Tuz Zahra, F. & Rehman, Y. Arsenic-redox transformation and plant growth promotion by purple nonsulfur bacteria *Rhodopseudomonas palustris* CS2 and *Rhodopseudomonas faecalis* SS5. *Biomed Res Int* **2017**, 6250327 (2017).
56. Koh, R. H. & Song, H. G. Effects of application of *Rhodopseudomonas* sp. on seed germination and growth of tomato under axenic conditions. *J Microbiol Biotechnol* **17**, 1805–1810 (2007).
57. D'Souza, G. & Kost, C. Experimental evolution of metabolic dependency in bacteria. *PLoS Genet* **12**, e1006364 (2016).
58. D'Souza, G. *et al*. Less is more: Selective advantages can explain the prevalent loss of biosynthetic genes in bacteria. *Evolution* **68**, 2559–2570 (2014).

59. Prinsen, E., Costacurta, A., Michiels, K., Vanderleyden, J. & Vanonckelen, H. *Azospirillum brasilense* indole-3-acetic acid biosynthesis: evidence for a non-tryptophan dependent pathway. *Mol Plant Microbe Interact* **6**, 609–615 (1993).
60. Saravanakumar, D. & Samiyappan, R. ACC deaminase from *Pseudomonas fluorescens* mediated saline resistance in groundnut (Arachis hypogea) plants. *J Appl Microbiol* **102**, 1283–1292 (2007).
61. Mayak, S., Tirosh, T. & Glick, B. R. Plant growth-promoting bacteria that confer resistance to water stress in tomatoes and peppers. *Plant Sci* **166**, 525–530 (2004).
62. Bykhovsky, V. Y., Demain, A. L. & Zaitseva, N. I. The crucial contribution of starved resting cells to the elucidation of the pathway of vitamin B12 biosynthesis. *Crit Rev Biotechnol* **17**, 21–37 (2008).
63. Wang, L. J. *et al*. Promotion by 5-aminolevulinic acid of germination of pakchoi (*Brassica campestris* ssp *chinensis* var. communis Tsen et Lee) seeds under salt stress. *J Integr Plant Biol* **47**, 1084–1091 (2005).
64. Tabuchi, K., Mizuta, H. & Yasui, H. Promotion of callus propagation by 5-aminolevulinic acid in a *Laminaria japonica* sporophyte. *Aquac Res* **41**, 1–10 (2009).
65. Sasaki, K., Watanabe, M., Tanaka, T. & Tanaka, T. Biosynthesis, biotechnological production and applications of 5-aminolevulinic acid. *Appl Microbiol Biotechnol* **58**, 23–29 (2002).
66. Korkmaz, A., Korkmaz, Y. & Demirkiran, A. R. Enhancing chilling stress tolerance of pepper seedlings by exogenous application of 5-aminolevulinic acid. *Environ Exp Bot* **67**, 495–501 (2010).
67. Liu, D. *et al*. 5-Aminolevulinic acid enhances photosynthetic gas exchange, chlorophyll fluorescence and antioxidant system in oilseed rape under drought stress. *Acta Physiol Plant* **35**, 2747–2759 (2013).
68. Youssef, T. & Awad, M. A. Mechanisms of enhancing photosynthetic gas exchange in date palm seedlings (*Phoenix dactylif*era L.) under salinity stress by a 5-aminolevulinic acid-based fertilizer. *J Plant Growth Regul* **27**, 1–9 (2008).
69. Naeem, M. S. *et al*. 5-Aminolevulinic acid alleviates the salinity-induced changes in *Brassica napus* as revealed by the ultrastructural study of chloroplast. *Plant Physiol Biochem* **57**, 84–92 (2012).
70. Tamames, J. Evolution of gene order conservation in prokaryotes. *Genome Biol* **2**, RESEARCH0020 (2001).
71. Zhang, N. *et al*. Whole transcriptomic analysis of the plant-beneficial rhizobacterium *Bacillus amyloliquefaciens* SQR9 during enhanced biofilm formation regulated by maize root exudates. *BMC Genomics* **16**, 685 (2015).
72. Yuan, J. *et al*. Organic acids from root exudates of banana help root colonization of PGPR strain Bacillus amyloliquefaciens NJN-6. *Sci Rep* **5**, 13438 (2015).
73. Wu, L. *et al*. Plant-microbe rhizosphere interactions mediated by *Rehmannia glutinosa* root exudates under consecutive monoculture. *Sci Rep* **5**, 15871 (2015).
74. Chilcott, G. S. & Hughes, K. T. Coupling of flagellar gene expression to flagellar assembly in *salmonella enterica serovar typhimurium* and Escherichia coli. *Microbiol Mol Biol R* **64**, 694–708 (2000).
75. Wadhams, G. H. & Armitage, J. P. Making sense of it all: Bacterial chemotaxis. *Nat Rev Mol Cell Bio* **5**, 1024–1037 (2004).
76. Jung, B. K. *et al*. Quorum sensing activity of the plant growth-promoting rhizobacterium *Serratia glossinae* GS2 isolated from the sesame (*Sesamum indicum* L.) rhizosphere. *Ann Microbiol* **67**, 623–632 (2017).
77. Zuniga, A., Donoso, R. A., Ruiz, D., Ruz, G. A. & Gonzalez, B. Quorum-sensing systems in the plant growth-promoting bacterium *Paraburkholderia phytofirmans* PsJN exhibit cross-regulation and are involved in biofilm formation. *Mol Plant Microbe Interact* **30**, 557–565 (2017).
78. Zuniga, A. *et al*. Quorum Sensing and Indole-3-Acetic Acid Degradation Play a Role in Colonization and Plant Growth Promotion of *Arabidopsis thaliana* by *Burkholderia phytofirmans* PsJN. *Mol Plant Microbe Interact* **26**, 546–553 (2013).
79. Degrassi, G. *et al*. Plant growth-promoting *Pseudomonas putida* WCS358 produces and secretes four cyclic dipeptides: Cross-talk with quorum sensing bacterial sensors. *Curr Microbiol* **45**, 250–254 (2002).
80. Imran, A. *et al*. *Ochrobactrum* sp Pv2Z2 exhibits multiple traits of plant growth promotion, biodegradation and N-acyl-homoserine-lactone quorum sensing. *Ann Microbiol* **64**, 1797–1806 (2014).
81. Schaefer, A. L. *et al*. A new class of homoserine lactone quorum-sensing signals. *Nature* **454**, 595–600 (2008).
82. Eisenhauer, N. *et al*. Root biomass and exudates link plant diversity with soil bacterial and fungal biomass. *Sci Rep* **7**, 44641 (2017).
83. Badri, D. V. & Vivanco, J. M. Regulation and function of root exudates. *Plant Cell Environ* **32**, 666–681 (2009).
84. Bolger, A. M., Lohse, M. & Usadel, B. Trimmomatic: a flexible trimmer for Illumina sequence data. *Bioinformatics* **30**, 2114–2120 (2014).
85. Bankevich, A. *et al*. SPAdes: a new genome assembly algorithm and its applications to single-cell sequencing. *J Comput Biol* **19**, 455–477 (2012).
86. Cho, S. T. *et al*. Genome analysis of *Pseudomonas fluorescens* PCL1751: A *Rhizobacterium* that controls root diseases and alleviates salt stress for its plant host. *PLoS One* **10**, e0140231 (2015).
87. Lagesen, K. *et al*. RNAmmer: Consistent and rapid annotation of ribosomal RNA genes. *Nucleic Acids Res* **35**, 3100–3108 (2007).
88. Lowe, T. M. & Eddy, S. R. tRNAscan-SE: A program for improved detection of transfer RNA genes in genomic sequence. *Nucleic Acids Res* **25**, 955–964 (1997).
89. Hyatt, D. *et al*. Prodigal: Prokaryotic gene recognition and translation initiation site identification. *BMC Bioinformatics* **11**, 119–129 (2010).
90. Li, L., Stoeckert, C. J. Jr. & Roos, D. S. OrthoMCL: Identification of ortholog groups for eukaryotic genomes. *Genome Res* **13**, 2178–2189 (2003).
91. Camacho, C. *et al*. BLAST+: Architecture and applications. *BMC Bioinformatics* **10**, 421–429 (2009).
92. Kanehisa, M., Sato, Y. & Morishima, K. BlastKOALA and GhostKOALA: KEGG Tools for Functional Characterization of Genome and Metagenome Sequences. *J Mol Biol* **428**, 726–731 (2016).
93. Wattam, A. R. *et al*. Improvements to PATRIC, the all-bacterial bioinformatics database and analysis resource center. *Nucleic Acids Res* **45**, 535–542 (2017).
94. Galperin, M. Y., Makarova, K. S., Wolf, Y. I. & Koonin, E. V. Expanded microbial genome coverage and improved protein family annotation in the COG database. *Nucleic Acids Res* **43**, 261–269 (2015).
95. Krzywinski, M. *et al*. Circos: An information aesthetic for comparative genomics. *Genome Res* **19**, 1639–1645 (2009).
96. Thompson, J. D., Higgins, D. G. & Gibson, T. J. CLUSTAL W: improving the sensitivity of progressive multiple sequence alignment through sequence weighting, position-specific gap penalties and weight matrix choice. *Nucleic Acids Res* **22**, 4673–4680 (1994).
97. Hall, T. A. BioEdit: a user-friendly biological sequence alignment editor and analysis program for Windows 95/98/NT. *Nucleic Acids Symp Ser* **41**, 95–98 (1999).
98. Kumar, S., Stecher, G. & Tamura, K. MEGA7: Molecular Evolutionary Genetics Analysis Version 7.0 for Bigger Datasets. *Mol Biol Evol* **33**, 1870–1874 (2016).
99. Martens, M. *et al*. Advantages of multilocus sequence analysis for taxonomic studies: a case study using 10 housekeeping genes in the genus Ensifer (including former *Sinorhizobium*). *Int J Syst Evol Microbiol* **58**, 200–214 (2008).
100. Tavaré, S. In *American mathematical society: Lectures on mathematics in the life sciences* Vol. 17, 57–86 (Amer Mathematical Society, 1986).
101. Felsenstein, J. Confidence limits on phylogenies - an approach using the bootstrap. *Evolution* **39**, 783–791 (1985).
102. Kurtz, S. *et al*. Versatile and open software for comparing large genomes. *Genome Biol.* **5**, R12 (2004).

103. Hoagland, D. R. & Arnon, D. I. The water-culture method for growing plants without soil. *Circular. California Agricultural Experiment Station* **347**, 1–32 (1950).
104. Tram, G., Korolik, V. & Day, C. J. MBDS solvent: An improved method for assessment of biofilms. *Adv Microbiol* **3**, 200–204 (2013).
105. Livak, K. J. & Schmittgen, T. D. Analysis of relative gene expression data using real-time quantitative PCR and the 2(T)(-Delta Delta C) method. *Methods* **25**, 402–408 (2001).

Acknowledgements

We thank Genomics BioSci & Tech Co., Ltd. (New Taipei City, Taiwan) for providing Illumina and PacBio sequencing services. This study was supported by grants from the Ministry of Science and Technology (MOST 103-2622-B-002-008-CC2, 102-2313-B-002-011-MY3, 105-2313-B-002-045, 106-3114-B-005-001 and 106-2622-B-002-005-C).

Author Contributions

K.J.L. carried out the experiment, experimental data analysis, bioinformatic data analysis and manuscript writing. C.W.L. performed the bioinformatics analysis for the genome assembly. S.S.L. provided the bioinformatic platform for data analysis. C.H.K. performed the bioinformatics for gene prediction and annotation as well as manuscript writing. C.T.L. is the corresponding authors in charge of the project design and manuscript writing.

Additional Information

Supplementary information accompanies this paper at https://doi.org/10.1038/s41598-018-31128-8.

Competing Interests: The authors declare no competing interests.

Publisher's note: Springer Nature remains neutral with regard to jurisdictional claims in published maps and institutional affiliations.

PLOS ONE

RESEARCH ARTICLE

Development of a low-cost culture medium for the rapid production of plant growth-promoting *Rhodopseudomonas palustris* strain PS3

Kai-Jiun Lo[1], Sook-Kuan Lee[1], Chi-Te Liu[1,2]*

1 Institute of Biotechnology, National Taiwan University, Taipei, Taiwan, **2** Agricultural Biotechnology Research Center, Academia Sinica, Nankang, Taipei, Taiwan

* chiteliu@ntu.edu.tw

OPEN ACCESS

Citation: Lo K-J, Lee S-K, Liu C-T (2020) Development of a low-cost culture medium for the rapid production of plant growth-promoting *Rhodopseudomonas palustris* strain PS3. PLoS ONE 15(7): e0236739. https://doi.org/10.1371/journal.pone.0236739

Editor: Leonidas Matsakas, Luleå University of Technology, SWEDEN

Received: April 24, 2020

Accepted: July 13, 2020

Published: July 30, 2020

Data Availability Statement: All relevant data are within the paper and its Supporting Information files

Funding: This article was subsidized by Ministry of Science and Technology and National Taiwan University (NTU), Taiwan. This study was supported by grants from the Ministry of Science and Technology, Taiwan (MOST 108-2313-B-002-058-MY3 and 108-2321-B-005 -018 -).

Competing interests: The authors have declared that no competing interests exist.

Abstract

Rhodopseudomonas palustris PS3 is one of the purple phototrophic non-sulfur bacteria (PNSB), which have plant growth-promoting effects on various plants. To expand the scale of PS3 fermentation in a time- and cost-effective fashion, the purpose of this work was to evaluate the use of low-cost materials as culture media and to optimize the culture conditions via response surface methodology. Corn steep liquor (CSL) and molasses were identified as potential materials to replace the nitrogen and carbon sources, respectively, in the conventional growth medium. The optimum culture conditions identified through central composite design were CSL, 39.41 mL/L; molasses, 32.35 g/L; temperature, 37.9˚C; pH, 7.0; and DO 30%. Under the optimized conditions, the biomass yield reached 2.18 ± 0.01 g/L at 24 hours, which was 7.8-fold higher than that under the original medium (0.28 ± 0.01 g/L). The correlation between the predicted and experimental values of the model was over 98%, which verified the validity of the response models. Furthermore, we verified the effectiveness of the *R. palustris* PS3 inoculant grown under the newly developed culture conditions for plant growth promotion. This study provides a potential strategy for improving the fermentation of *R. palustris* PS3 in low-cost media for large-scale industrial production.

Introduction

Rhodopseudomonas palustris is one of the purple phototrophic non-sulfur bacteria (PSNB). Since it can process nutrients through various metabolic pathways, such as photosynthetic, photoheterotrophic, chemoheterotrophic and chemoautotrophic pathways, *R. palustris* can inhabit a variety of environments [1]. It is already known that *R. palustris* contains many useful characteristics and is broadly used in industry for bioremediation, sewage treatment, removal of phytotoxic compounds, etc. [2, 3]. This strain is able to convert complex organic compounds into biomass and bioenergy, regardless of whether the substrates are plant-derived, pollutant or aromatic compounds [1, 4–7]. *R. palustris* has also been reported to act as a promising biofertilizer for promoting crop yield and improving soil fertility [8–10]. Previously, we

isolated an *R. palustris* strain, called as the PS3, from Taiwanese paddy soil that *not only had beneficial* effects on plant growth but also enhanced the efficiency of the uptake of the applied fertilizer nutrients [8, 11]. Accordingly, this strain has been considered an elite microbial inoculant for agricultural applications.

For the purpose of the commercialization or the large-scale field application of the selected microbes, fermentation production is an essential prerequisite. The yield per unit biomass of the mass production is influenced by several factors, such as the medium composition (carbohydrate and nitrogen sources, minerals, etc.), the culture conditions (pH, temperature, agitation and aeration, etc.) and the mode of fermentation (batch, fed-batch and continuous fermentations) [12]. The scaling-up of microbial processes is commonly undertaken in lab-scale process development with expensive medium components such as yeast extract, beef extract, and peptone [13]. These high-cost media result in a limitation on commercialization. To reduce the cost of fermentation, complex raw materials derived from plant and animal residues, as well as from agricultural and food industrial wastes, are mainly used [14]. For example, cheese whey, corn steep liquor (CSL), corn syrup, distillery yeast, molasses, soybean and starch are widely applied [15–19]. These relatively inexpensive raw materials have already been used as suitable nutrients for ensuring the growth of bacteria and for the production of different primary and secondary metabolites [17, 20–22].

Response surface methodology (RSM), also called the Box–Wilson methodology, is a useful tool to optimize the factors of fermentation processes by applying mathematics and statistics [23]. This technique is an experimental design based on the fit of a polynomial regression model for testing the multiple factors that influence the responses by varying the factors simultaneously, and fewer experiments are needed to study the effects of all factors [24, 25]. Through RSM, the interaction effects of individual factors can also be determined. The common experimental designs for RSM are central composite design (CCD) and Box-Behnken design (BBD). Although BBD has been suggested to reduce the number of trials required for a large number of variables, this advantage will disappear when in four or more factors [23]. Moreover, because CCD consists of a factorial or fractional factorial design with center points augmented with a group of axial points, it is often applied in sequential experiments and can be used in the estimation of model curvature [23]. Overall, the RSM procedure includes the selection of independent variables, the delimitation of the experimental factor region, the evaluation of the model's fitness, and finally, the attainment of optimum values and verification [23, 24].

The van Niel medium and modified van Niel medium have been designed for *R. palustris* fermentation [26, 27]. Du et al [28] cultivated *R. palustris* strain DH with the original van Niel medium for 7 days, and the derived biomass was ~0.3 g/L. Carlozzi and Sacchi [29] incubated *R. palustris* strain 42OL in a modified van Niel medium to which sodium acetate was added, and the derived biomass was 1.42 g/L/d. Chang et al [30] modified the original medium with sodium acetate and peptone, and the derived biomass of *R. palustris* strain YSC3 was 0.36 g/L after 2 days of incubation. However, the use of these media may be uneconomical for industrial application due to their high cost and long incubation time. The cost is primarily due to expensive nitrogen sources, such as yeast extract and peptone. On the other hand, some media have low-cost sources; for example, Xu et al [31] used *Stevia* residue extractions supplied with NH_4Cl as a medium to culture *R. palustris*, and the highest obtained biomass was 1.5 (OD_{660}) (approximately equivalent to 0.77 g/L) after 96 hours of cultivation. Kornochalert et al [9] obtained the 0.9 g/L *R. palustris* in latex rubber sheet wastewater supplied with pineapple extract after 96 hours of fermentation. In our previous study, we used a modified van Niel medium with malate and yeast extract as the carbon and nitrogen sources for the fermentation of *R. palustris* PS3, and the biomass was 0.07 g/L after 24 hours of cultivation. Although this

broth showed promising plant growth-promoting effects on several crops [8, 11, 32], the cost was too high for industrial application. Therefore, the purpose of this study was to develop an optimal fermentation protocol for *R. palustris* PS3 that is cost-effective, results in high biomass yield, and has a short fermentation time. We evaluated some agro-industrial by-products, including corn steep liquor (CSL), beetroot extract (BRE), soybean flour (SF), soybean protein isolate (SPI), molasses and corn starch, for use as substrates for *R. palustris* PS3 cultivation in terms of cost reduction and tested them with RSM to obtain the optimal fermentation conditions. Furthermore, we inoculated the newly developed fermentation broth into plants to verify its plant growth-promoting effect.

Materials and methods

Microorganism and bacterial preparation

R. palustris PS3 was isolated from Taiwanese paddy soil and showed promising beneficial effects on plant growth in our previous studies [8, 11]. This bacterium was grown in 3 mL of modified van Niel medium [8] (designated PNSB medium hereafter) at 37˚C and 200 rpm. The PNSB medium consisted of KH_2PO_4 1.0 g/L, NH_4Cl 1.0 g/L, $MgSO_4•7H_2O$ 0.2 g/L, $FeSO_4•7H_2O$ 0.01 g/L, $CaCl_2$ 0.02 g/L, $MnCl_2•4H_2O$ 0.002 g/L, $Na_2MoO_4•2H_2O$ 0.001 g/L, yeast extract 0.5 g/L, and malate 5.0 g/L, pH = 7.0. After 24 hours incubation, 2 mL of the above bacterial broth was incubated in a 250 mL Erlenmeyer flask containing 50 mL PNSB medium and then cultured at 37˚C with shaking at 200 rpm. After 24 hours incubation, the bacterial broth was diluted with fresh PNSB medium and adjusted to an optical density approximately equal to OD_{600} = 1.0. This diluted bacterial broth was used as a seed culture for further experiments.

Screening of nitrogen and carbon sources for medium optimization

Different nitrogen (yeast extract, NH_4Cl, corn steep liquor (CSL) (TAIROUN PRODUCTS Co., Ltd., Taiwan), beetroot extract (BRE) (Hauert HBG Dünger AG, Switzerland), soybean flour (SF), soybean protein isolate (SPI) and NH_4NO_3) and carbon (malate, sodium acetate, glucose, fructose, molasses (TAIWAN SUGAR Co. Ltd., Taiwan) and corn starch (TAIROUN PRODUCTS Co., Ltd., Taiwan)) sources were used to optimize the composition of the PNSB medium. The initial concentrations of the individual carbon and nitrogen sources followed those in the PNSB medium described above and were sterilized separately by autoclave. For preliminary screening of alternative nitrogen sources, a final concentration of 1.5 g/L of each nitrogen-containing candidate material was introduced to substitute NH_4Cl (1.0 g/L) as well as yeast extract (0.5 g/L) in the presence of 5.0 g/L malate (carbon source). For preliminary screening of alternative carbon sources, a final concentration of 5.0 g/L of each carbon-containing candidate material was introduced to substitute malate (5.0 g/L) in the presence of CSL (1.5 g/L) as the selected nitrogen source.

For the experiments, the seed culture mentioned above was centrifuged at 3,000 rpm for 5 min at 4˚C and then suspended in phosphate buffer solution (PBS). The final OD_{600} was adjusted to 1.0, inoculated (10% v/v) into 50 mL of the respective modified media in a 250 mL Erlenmeyer flask, and then cultured at 37˚C with shaking at 200 rpm.

Measurement of cell growth

The population of PS3 cells was estimated by a standard plate count method. Enrichment culture broth was serially diluted by fresh PNSB medium, and spread onto PNSB agar plate. Incubated the plate at 37˚C in the dark and then calculated the number of colony forming unit (CFU) per milliliter. On the other hand, the cell concentration was also measured by optical

density with a spectrophotometer at 600 nm. The bacterial culture broth was diluted in distilled water to obtain an optical density less than 0.6, and the OD_{600} was multiplied by the dilution times. Biomass (grams per liter) was assayed from the OD_{600} value by using a calibration standard curve. Viable counts were determined by the plate counting method.

Construction of the response surface model by central composite design (CCD)

Based on the results of factor screening, the following independent variables, including the medium components (molasses and CSL) as well as the fermentation conditions (temperature and pH), were selected for optimization by central composite design (CCD). The CCD consists of three parts: a factorial design, a central points, and axial points [23]. In order to reduce the experimental trials, fractional factorial design was substituted for factorial design. For CCD construction, we performed a 2^{4-1} (four factors) fractional factorial design (FFD) using R software with the package "rsm". Then, the design was augmented by eight axial points and four replications of the center points. This design resulted in a total of 20 experiments [33]. The distance of the axial points (1.682) from the central point was developed by the software with the default settings (rotatable if possible) [33]. Before performing a regression analysis, the factors will be normalized. Codification of the levels of variables needs transforming the real studied value to the range without dimension (-1 to +1). The various factors were coded according to the following equation:

$$x_i = \frac{E_i - E_0}{\Delta E_i} \qquad \text{Eq (1)}$$

where x_i is the coded variable of the factor, E_i is study value of variable, E_0 is the real value of the variable at the center point, and ΔE_i is the step-altered value, which represents the difference from the real value in the higher or lower value from the real value at the central point. In present study, the ΔE_i for CSL, molasses, temperature and pH value are 5 mL/L, 4 g/L, 1.5˚C and 0.3, respectively. The various factors and levels for the CCD are shown in Table 1. The matrix corresponding to the CCD and the total experimental data from 20 runs are shown in S1 Table in S1 File. The trail no. 1 to 8 represented fractional factorial design (FFD); trail no. 9 to 12 were attributed to center point; and trail no. 13 to 20 were referred as axial points. The experimental data of the CCD were fitted with a quadratic second-order polynomial equation by a multiple regression technique. The regression equation is shown as Eq (2):

$$Y = \beta_0 + \sum_{i=1}^{k} \beta_i x_i + \sum_{i=1}^{k} \beta_{ii} x_i^2 + \sum_{i=1}^{k-1} \sum_{j=1+i}^{k} \beta_{ij} x_i x_j \qquad \text{Eq (2)}$$

where Y is the predicted response, β_0 is the intercept, and β_i, β_{ii} and β_{ij} are the linear, quadratic and cross-interaction regression constant coefficients, respectively. x_i and x_j are the coded

Table 1. Level and code of variables in the CCD experiments.

Independent variable	Coded levels				
	-1.682	**-1**	**0**	**1**	**1.682**
Corn steep liquor (mL/L)	31.59	35	40	45	48.41
Molasses (g/L)	28.27	31	35	39	41.73
Temperature (˚C)	35.9	37	38.5	40	41
pH	6.06	6.4	6.9	7.4	7.74

The various factors were coded according to Eq (1).

https://doi.org/10.1371/journal.pone.0236739.t001

independent variables for factors. The quality of the fitting of the second-order equation model to the data was described by the coefficient of determination R-squared, and the statistical significance was evaluated by the F-test. The significance of the regression coefficients was analyzed by a t-test. The computer software used was R, version 3.6.2 [34].

Batch-culture experiments in a benchtop bioreactor

To perform the response surface methodology assay, a 5-L stirred tank bioreactor (BTF-A5L, BIOTOP Inc, Taiwan) was used to carry out all of the batch-culture experimental trials. We inoculated 300 mL of bacterial culture into 3 L of fresh medium. The conditions for molasses, CSL, temperature and pH value were set according to the experimental design matrix corresponding to the CCD described. The pH value of the cultures was controlled by pH-stat and automatically adjusted with 2 N NaOH and 2 N HCl.

In planta experiments to verify the plant-growth promotion effect of the newly developed fermentation broth

Chinese cabbage seeds (*Brassica rapa* L. spp. *pekinensis* cv. "Michelle") were purchased from Formosa Farming Materials Co., Ltd. (Taipei, Taiwan). The seeds were immersed in 70% alcohol for 3 min and then in 3% hydrogen peroxide solution for 7 min for surface sterilization, followed by a thorough washing with sterile distilled water. These seeds were germinated for 1 day at 25˚C in the dark. For hydroponic cultivation, well-germinated seeds were transferred to completely wet cotton and cultivated under continuous (24-h photoperiod) light-emitting diode (LED) light (~210 μmol $m^{-2}s^{-1}$). After one week, the seedlings were transferred to hydroponic tanks (35 L) in a plant factory facility (College of BioResources and Agriculture, National Taiwan University). Twenty-four seedlings were cultivated in each tank, and each tank was equipped with an air pump to homogenize the solution and maintain the dissolved oxygen. Hoagland's solution (0.51 g L^{-1} KNO_3, 0.49 g L^{-1} $MgSO_4•7H_2O$, 0.08 g L^{-1} NH_4NO_3, 0.068 g L^{-1} KH_2PO_4, 22.5 mg L^{-1} Fe-EDTA, 2.86 mg $L^{-1}H_3BO$, 0.051 mg L^{-1} $CuSO_4$, 0.22 mg L^{-1} $ZnSO_4•7H_2O$, 1.81 g L^{-1} $MnCl_2•4H_2O$, 0.12 mg L^{-1} $Na_2MoO_4•2H_2O$ and 1.18 g L^{-1} Ca $(NO_3)_2•4H_2O$) was used as a nutrient sources [35]. The concentrations of the hydroponic nutrient solution were measured by an electrical conductivity meter (EC meter) (Spectrum® Technologies, Inc.) and adjusted with concentrated hydroponic nutrient solution to maintain an EC value of 1.2–1.3 dS m^{-1}. The initial pH value of the hydroponic nutrient solution was adjusted by H_3PO_4 and 2N KOH to 7.0. The cultivation environment was set at 25˚C, 70% humidity, and 210 μmol.m^{-2}.s^{-1} light intensity for 16 hours. We poured 250 mL of the liquid culture (OD_{600} = 0.1, equivalent to ~ 10^8 colony-forming units [CFU]/mL) into the tank, resulting in a final bacterial concentration of 10^6 CFU/mL. After seven days post inoculation (7 dpi), another 250 mL of the liquid culture was applied to each tank. Seventeen days after planting (DAP), the Chinese cabbages were harvested, and the fresh and dry weights were measured. For soil cultivation, well-germinated seeds were transferred to cultivatable soil under controlled illumination with a 16-hour photoperiod (~210 μmol $m^{-2}s^{-1}$). After one week, the seedlings were transferred to pots containing approximately 300 g cultivatable soil. The cultivation environment was set to be consistent with that under hydroponic cultivation. Two milliliters of the respective culture broth (OD_{600} = 0.1, equivalent to ~ 10^8 colony-forming units [CFU]/mL) and 0.05g chemical fertilizer were added into each pot once a week as described previously [8]. The chemical fertilizer was purchased from SINON Co., Ltd. (New Taipei City, Taiwan) which consists of 14% ammonium nitrogen, 15% citric acid-soluble Phosphorus (13.5% water-soluble phosphorus), and 10% water- soluble potassium. At 28 DAP, the Chinese cabbages were harvested, and their fresh and dry weights were measured.

Statistical analysis

Analyses of variance (ANOVA) were performed with R version 3.6.2 [34]. Fisher's least significant difference (LSD) test was used for multiple range analyses to determine the significant differences between the groups of data. The results were considered significant at P = 0.05.

Results

Selection of appropriate components for optimization of *R. palustris* strain PS3 medium

Carbon and nitrogen sources provide important nutrients for bacterial growth. To screen suitable carbon and nitrogen sources for viable PS3 cell production, a "one-factor-at-a-time" method (OFAT, or single-variable *optimization* strategy) was used. We selected corn steep liquor (CSL), beetroot extract, soybean flour (SF), soybean protein isolate (SPI), and NH_4NO_3 as the individual nitrogen sources and malate, sodium acetate, glucose, fructose, molasses, and corn starch as the individual carbon sources. These materials are common, low-cost agro-industrial byproducts and are the most common nutrient sources in industrial fermentations [14, 36]. Fig 1 shows the effect of the different selected nitrogen and carbon sources on the growth of the *R. palustris* PS3 strain. In the presence of 5 g/L malate as single carbon source, the highest turbidity (OD_{600}) was observed when using SF or SPI as the sole nitrogen source, followed by that of the strain incubated with CSL, BRE and PNSB and that from fermentation in NH_4NO_3 (Fig 1A). To estimate the cell concentration of the PS3 culture, we also verified the correlation between turbidity (OD_{600}) and colony-forming unit (CFUs) counts. As shown in S1 Fig in S1 File, the OD_{600} and CFUs values were positively correlated during the fermentation progress (24 hr). As shown in Fig 1B, when using CSL as the sole nitrogen source, the cell viability of *R. palustris* PS3 was $1.14 \pm 0.72 \times 10^9$ CFU/mL, which was comparable to that with the original nitrogen source (NH_4Cl and yeast extract in PNSB medium) and higher than with the other nitrogen sources. Although the soybean flour (SF) and soybean protein isolate (SPI) also showed high OD_{600} values, their CFUs were dramatically lower than the others. This implied that the turbidities (OD_{600}) of these two microbial samples did not reflect the number of viable cells produced (CFU). This inconsistency may be attributed to their poor solubility in the individual media, which interfered with the turbidity readout. Accordingly, CSL is considered a potential nitrogen source for the production of *R. palustris* PS3. After 1.5 mL/L CSL was determined as the nitrogen source for the modified medium, we further screened appropriate carbon sources. We found that molasses and sodium acetate significantly increased the biomass of *R. palustris* PS3 compared with those under the other carbon sources (Fig 1C), with OD_{600} values of 0.641 ± 0.033 and 0.628 ± 0.032, respectively. On the other hand, higher viable cell counts were present in the molasses and malate treatments than in the other treatments, and the biomass was approximately 10^9 CFU/mL (Fig 1D). We noticed that when sugars were used as carbons (i.e., glucose and fructose), the corresponding cell viability (CFU/mL) was significantly lower than that resulting from the use of organic acid (i.e., malate and sodium acetate) or molasses. Accordingly, molasses could be a suitable substrate to replace malate as a carbon source for *R. palustris* PS3 cultivation. Taken together, we selected CLS and molasses as nitrogen and carbon sources for future experiments.

Screening suitable fermentation conditions

For the purpose of screening suitable fermentation conditions, the range and levels of test variables were evaluated. We made a preliminary investigation for the concertation effects of CSL and molasses on the growth of *R. palustris* PS3 by OFAT (S2A and S2B Fig in S1 File).

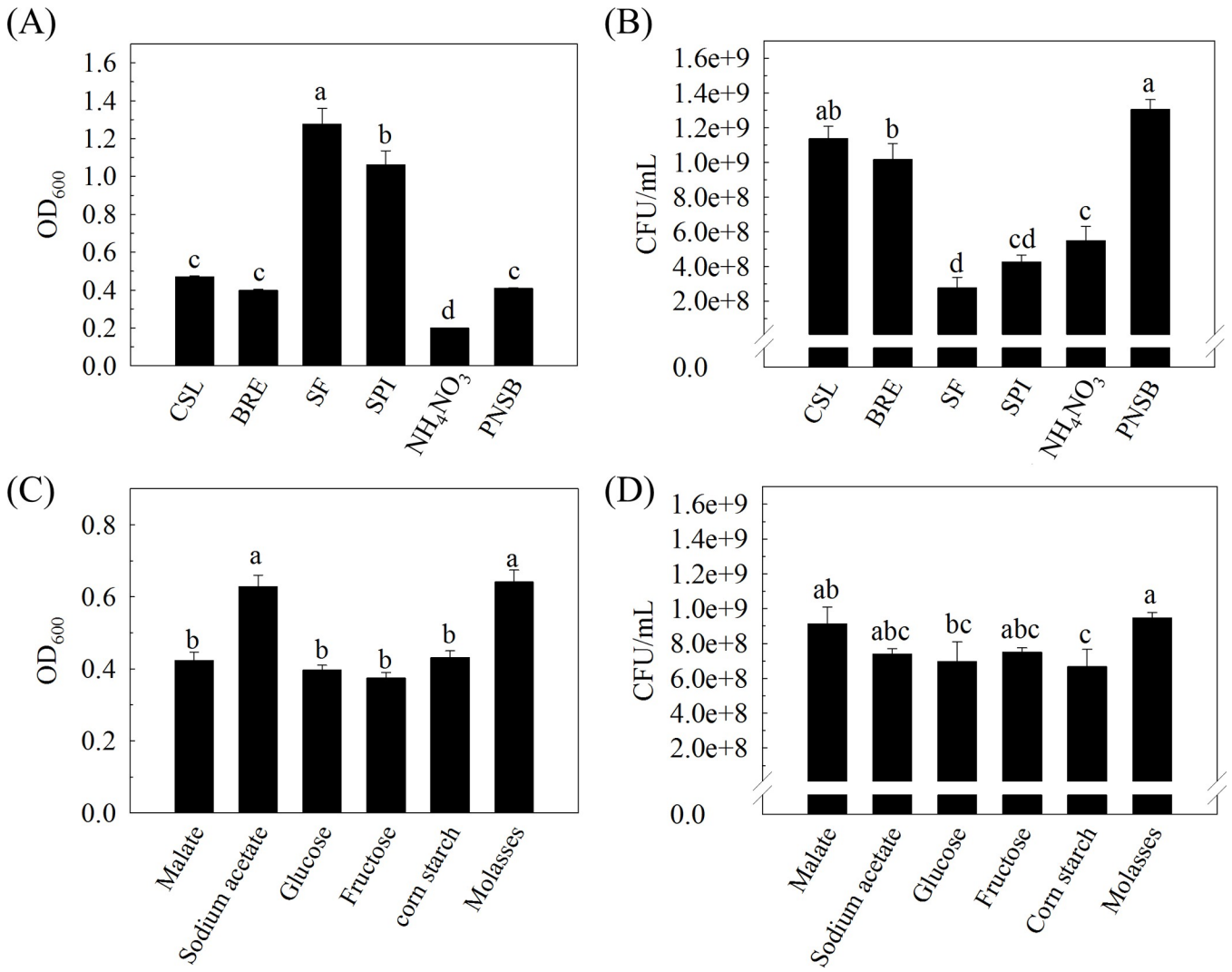

Fig 1. Selection of appropriate components for an optimized *R. palustris* medium. The effect of different nitrogen (A, B) and carbon sources (C, D) on the growth of *R. palustris* PS3 culture under 200 rpm and 37˚C for 24 hours. In the nitrogen source screening experiments (A and B), each nitrogen source (1.5 g/L) was used to replace 1.0 g/L NH_4Cl and 0.5 g/L yeast extract in the PNSB treatment. In the carbon source screening experiments (C and D), 1.5 g/L CSL was used as the nitrogen source in the medium, and the concentration of each carbon source was set at 5 g/L. CSL: corn steep liquor; BRE: beetroot extract; SF: soybean flour; SPI: soybean protein isolate; PNSB: modified van Niel medium [8]. Vertical bars represent the standard error of each mean, and bars with different letters indicate statistically significant differences at P = 0.05 according to LSD test.

https://doi.org/10.1371/journal.pone.0236739.g001

Subsequently, the effects of pH values, temperatures and dissolved oxygen (%) were respectively evaluated for PS3 growth (S2C-S2E Fig in S1 File). These derived data were used for fractional factorial design (FFD).

All of the experiments in FFD were performed in the 5 L desktop bioreactor. The factor screening process and the experimental design for the range and levels of test variables, as well as results for the FFD are shown in S2 Table in S1 File. The experimental data were analyzed by ANOVA with a first-order regression model (S1 Eq in S1 File). The results of the regression analyses are shown in S3 Table in S1 File and were analyzed by Fisher's F-test and Student's t-test. Student's t-test was used to evaluate the significance of the factor regression coefficients. The proposed linear model for the biomass (g/L) of *R. palustris* PS3 is shown in S2 Eq in S1 File. As shown in S3 Table in S1 File, the model *p* value is significantly lower than 0.05, and the

coefficient and adjusted coefficient of determination R^2 were calculated to be 0.9999 and 0.9996, respectively. The coefficients of the factors are 0.76188 (CSL), 0.58188 (molasses), 0.00438 (dissolved oxygen), 0.34688 (temperature) and -0.08312 (pH), respectively (S3 Table in S1 File). In addition, for the regression *p* value, all of the target factors showed a significant effect except that of dissolved oxygen (DO). Therefore, we set the dissolved oxygen as constant at 30% for the subsequent experiments. To further identify the appropriate range of variables for RSM, we conducted the steepest ascent path method to clarify the levels of factors. The steepest ascent path was designed according to S2 Eq in S1 File., and the results are shown in S4 Table in S1 File. The search direction and length of each factor were CSL 5 mL/L, molasses 3.82 g/L, temperature 0.7˚C and pH -0.3, respectively. Based on the data, we found that the biomass significantly increased with each step, reaching 2.44 g/L in step 4. After step 5, the biomass of *R. palustris* PS3 dramatically decreased and was even lower than the original biomass.

Optimization of culture conditions by RSM

According to the results of the factorial design experiment (S3 Table in S1 File), we took CSL, molasses, temperature and pH as the major variables affecting the performance of *R. palustris* PS3 growth. We conducted a four-coded-level central composite design (CCD) to optimize the levels of these variables. The corresponding experimental results of the CCD design are shown in Table 2 and were fitted with a second–order polynomial equation (Eq 2). The

Table 2. The coded levels and real values for the experimental design and results of CCD.

Trial no.	Coded levels of factors				Biomass (g/L)	
	x_1	x_2	x_3	x_4	Experimental	Predicted
1	-1	+1	+1	-1	0.88	0.74
2	-1	-1	-1	-1	1.45	1.34
3	+1	+1	+1	+1	0.91	0.86
4	+1	-1	+1	-1	0.25	0.21
5	-1	-1	+1	+1	1.09	1.02
6	-1	+1	-1	+1	1.59	1.47
7	+1	+1	-1	-1	1.09	1.00
8	+1	-1	-1	+1	1.75	1.72
9	0	0	0	0	2.29	2.18
10	0	0	0	0	2.21	2.18
11	0	0	0	0	2.31	2.18
12	0	0	0	0	2.23	2.18
13	+1.682	0	0	0	1.43	1.44
14	-1.682	0	0	0	1.63	1.78
15	0	+1.682	0	0	1.94	2.06
16	0	-1.682	0	0	2.13	2.16
17	0	0	+1.682	0	0.47	0.54
18	0	0	-1.682	0	1.59	1.68
19	0	0	0	+1.682	1.01	1.05
20	0	0	0	-1.682	0.18	0.30

Letters: x_1 = CSL (mL/L), x_2 = molasses (g/L), x_3 = temperature (˚C) and x_4 = pH value. Trial no. 1 to 8 represented fractional factorial design (FFD), trial no. 9 to 12 were referred as central point, and trial no. 13 to 20 were represented as axial points. The coefficient of determination, R2, between the predicted and experimental values was calculated to be 0.98.

https://doi.org/10.1371/journal.pone.0236739.t002

proposed polynomial model for biomass production in *R. palustris* PS3 is shown in Eq (3):

$$\text{Biomass (g/L)} = 4.2267 - 0.1918x_1 - 0.0562x_2 - 0.6582x_3 + 0.4321x_4 - 0.3882x_1^2 - 0.0442x_2^2 - 0.7315x_3^2 - 1.0302x_4^2 + 0.0165x_1x_2 - 0.1448x_1x_3 + 0.2340x_1x_4 \quad \text{Eq (3)}$$

The variables x_1, x_2, x_3 and x_4 represent the CSL, molasses, temperature and pH value, respectively. The results of the regression analyses were evaluated by Fisher's *F*-test and Student's *t*-test. As shown in Table 3, the regression coefficients and corresponding *p* values of the linear terms of CSL, temperature, pH value and interaction terms between CSL and temperature or pH value had a significant effect on *R. palustris* PS3 biomass production (p value < 0.05). However, the molasses term and other interaction terms were not significant at the 5% level. Moreover, other interaction terms between molasses, temperature and pH value were omitted from the predicted model. The coefficient and adjusted coefficient of determination, R^2, for the regression model fit were calculated to be 0.9962 and 0.9896, respectively. This means that more than 98% of the variability of the regression model could be explained by the regression equation. The response-surface full quadratic model of biomass for *R. palustris* PS3 was also tested by ANOVA. The *F* value of the model was 151.99, and the *p* value was less than 0.0001 (2.84×10^{-7}), indicating that the model was highly significant (Table 3). The lack-of-fit *F* value and *p* value were 3.16 and 0.186, respectively, which implied that the lack of fit was insignificant. These results supported that the second-order model adequately approximated the response surface of *R. palustris* PS3 biomass production. After canonical transformation of Eq (3), the optimum fermentation combination was obtained as follows: CSL, 39.41 mL/L; molasses, 32.35 g/L,

Table 3. The variance analysis of the second-order regression model for biomass production.

Source	DF	SS	MS	*F*-value	Coef.	*p*-value
Model	12	31.9509	2.6626	151.99		2.84E-07
Blocks	1	0.4613	0.4613	26.33		0.0003
Linear	4	9.0117	2.2529	128.6		1.2E-06
x_1	1	0.5024	0.5024	28.68	-0.1918	0.00104
x_2	1	0.0432	0.0432	2.46	-0.0562	0.15911
x_3	1	5.9164	5.9164	337.72	-0.6582	2.8E-07
x_4	1	2.5498	2.5498	145.55	0.4321	6E-06
Square	4	21.5663	5.3916	307.76		5.9E-08
x_1^2	1	2.143	2.143	122.33	-0.3882	1E-05
x_2^2	1	0.0278	0.0278	1.59	-0.0442	0.23298
x_3^2	1	7.6097	7.6097	434.38	-0.7315	1.4E-07
x_4^2	1	15.0951	15.0951	861.66	-1.0302	1.3E-08
2-Way Interaction	3	0.608	0.2027	11.57		0.00412
x_1x_2	1	0.0022	0.0022	0.12	0.0165	0.73435
x_1x_3	1	0.1677	0.1677	9.57	-0.1448	0.0172
x_1x_4	1	0.4382	0.4382	25.01	0.234	0.00153
Error	7	0.1226	0.0175			
Lack-of-Fit	4	0.0991	0.0248	3.16		0.186
Pure Error	3	0.0235	0.0078			
Total	19	32.0735				

Letters: x_1 = CSL (mL/L), x_2 = molasses (g/L), x_3 = temperature (˚C) and x_4 = pH value.

https://doi.org/10.1371/journal.pone.0236739.t003

temperature, 37.9˚C, pH 7.0 and the DO was constant at 30%. The model predicted that the maximum response of *R. palustris* PS3 biomass production would be 2.31 g/L.

Effects of various factors on *R. palustris* PS3 biomass production

The 3D response surface contour plots were constructed in R software to analyze the interaction effects of four variables (CSL, molasses, temperature and pH value). The plots showed the effect of two variables on the response while the other factors were set at the "zero" level; the levels tested were 40 mL/L CSL, 35 g/L molasses, 38.5˚C temperature and 6.9 pH (Fig 2). These contour plots represent the projection maps the 3D response surfaces onto two-dimensions planes with contours delineating changes in 3D space, which provide relative clear pictures of the responses derived from each factor. As shown in Fig 2A and 2B and 2E, the elliptical and inclined form of contour plots inferred that the interactions between CSL and molasses, CSL and temperature, CSL and pH value are evident. These results can also be confirmed by the variance analysis of regression model for biomass production (Table 3). On the other hand, the biomass production of *R. palustris* PS3 significantly increased with increasing CSL, temperature and pH. However, too high a concentration or condition level of these factors resulted in the opposite effect. On the other hand, it was noted that molasses did not acutely affect the biomass production of *R. palustris* PS3 under our experimental design, although increasing the concentration resulted in a slight increase-then-decrease pattern. These results were consistent with the polynomial regression analyses (Table 3), i.e., biomass production was significantly influenced by CSL, temperature and pH value. On the other hand, the 3D surface projection was confined to the smallest curve of the contour diagram suggesting that it contained an optimum condition in the levels of variables. Moreover, the 3D response surface presented a "roof form". Taken together, these data suggest that the model has a maximum stationary point, which contains the maximum biomass production of *R. palustris* PS3 strain.

Verification of optimization

To verify the predicted biomass production of *R. palustris* PS3, confirmation fermentation with the predicted optimal culture conditions (CSL, 39.41 mL/L; molasses, 32.35 g/L, temperature, 37.9˚C, pH 7.0 and DO 30%) was performed. As shown in Table 4, after 24 hours of fermentation, the biomass production of *R. palustris* PS3 was 2.18 ± 0.01 g/L, which was approximately 7.8 times higher than that obtained in the original PNSB medium (0.28 ± 0.01g/L). The validated biomass production showed a high correlation (95%) with the predicted biomass from the response model. This result suggests that the proposed model Eq (3) is effective for *R. palustris* PS3 biomass production. The estimated cost of this newly developed medium was about 0.16 US$/L, which was approximately 30% of the original PNSB medium (0.53 US $/L). The detailed material cost of each component in respective medium was shown in S5 Table in S1 File.

Validation of the plant growth-promoting effect of the newly developed fermentation broth

To confirm the plant growth-promoting effect of PS3 with the newly developed fermentation broth, we cultivated Chinese cabbage in either hydroponic or soil system with different treatments. As shown in S6 Table in S1 File, the fermented culture broth of PS3 contained 0.05 ±0.17 g/Kg of total organic carbon and 16.98 ±0.17 g/Kg of total nitrogen (S6 Table in S1 File), indicating the C/N ratio of this broth was approximated 1.77. The morphologies of 17 DAP and 28 DAP Chinese cabbage cultivated under different treatments are shown in Fig 3A–3F. In the hydroponic system, the Chinese cabbage treated with the PS3 inoculant was obviously

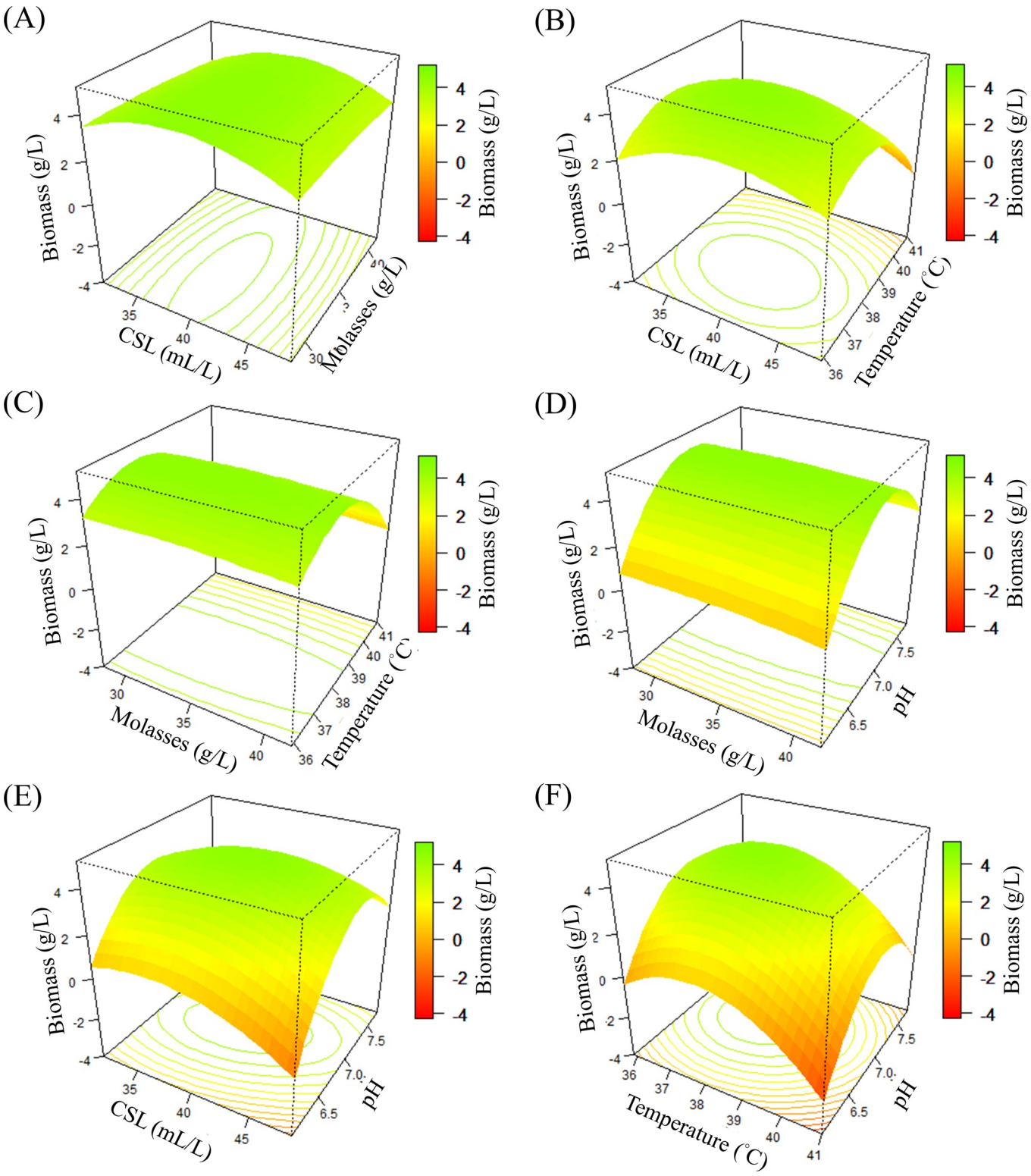

Fig 2. Three-dimensional response surfaces and contour plots of the effects of three factors on *R. palustris* PS3 biomass production. When two factors were plotted, the other two factors were set at the coded level, zero. Each condition was as follows: CSL, 40 mL/L; molasses, 35 g/L; temperature, 38.5˚C and pH value, 6.9. (A): CSL and molasses were plotted at 38.5˚C and pH 6.9; (B) CSL and temperature were plotted at 35 g/L molasses and pH 6.9; (C) molasses and temperature were plotted at 40 mL/L CSL and pH 6.9; (D) molasses and pH were plotted at 40 mL/L CSL and 38.5˚C; (E): CSL and pH were plotted at 35 g/L molasses and 38.5˚C; (F): temperature and pH were plotted at 40 mL/L and 35 g/L molasses. CSL: corn steep liquor.

https://doi.org/10.1371/journal.pone.0236739.g002

Table 4. Comparison of PNSB medium and optimal medium parameters for *R. palustris* PS3 biomass production for 24 hours.

Factor	PNSB medium	Optimal medium
Molasses (g/L)	-	32.35
Malate (g/L)	5	-
CSL (mL/L)	-	39.41
Yeast extract (g/L)	1	-
NH_4Cl (g/L)	0.5	-
Agitation (rpm)	200	-
Aeration (vvm)	1.22	-
pH	7	7
Temperature (˚C)	37	37.9
Biomass (g/L)	0.28 ± 0.01	2.18 ± 0.01
Material cost (US$/L)	0.53	0.16

The fermentation experiments were carried out in a 5-L bioreactor.

Material cost was calculated according to S5 Table in S1 File, which shown detailed cost information for each component in respective medium.

https://doi.org/10.1371/journal.pone.0236739.t004

larger than that treated with CF or conventional growth medium. There was no significant difference in the size of Chinese cabbage treated with the medium and with CF. The fresh and dry shoot weights of Chinese cabbage cultivated in the hydroponic system with different treatments are shown in Fig 3G–3H (fresh/dry weight of CF: 45.87 ± 1.39 g/2.51 ± 0.076 g, PS3: 57.20 ± 1.54 g/2.81 ± 0.078 g, medium: 48.86 ± 1.14 g/2.35 ± 0.067 g). Compared to those of the CF group, the fresh and dry shoot weights of the PS3 treatment increased by 25% and 12%, respectively. Likewise, the fresh and dry shoot weights of PS3 Chinese cabbage cultivated in the soil system were also superior to those of the other treatments (fresh/dry weight of CF: 11.11 ± 0.84 g/1.75 ± 0.36 g, PS3: 14.27 ± 0.71 g/2.50 ± 0.23 g, medium: 13.31 ± 0.71 g/2.12 ± 0.24 g, respectively) (Fig 3I and 3J). Compared to those of the CF group, the fresh and dry shoot weights were 28% and 48% increased, respectively, with the PS3 treatment. We confirmed that the fermentation broth of *R. palustris* PS3 produced under the newly developed culture conditions had beneficial effects on plant growth.

Discussion

R. palustris PS3 has been shown to have beneficial effects on several crops [8, 11, 32]. To scale up the biomass production of PS3 for commercial purposes, we developed optimal fermentation conditions that are cost-effective and have a high product yield and a short fermentation time. Based on the derived RSM model (Eq (3)), the predicted optimal culture conditions were 39.41 mL/L CSL, 32.35 g/L molasses, 37.9˚C and 7.0 pH. As shown in Table 4, the optimized medium resulted in *R. palustris* PS3 biomass production (2.18 ± 0.01 g/L at 24 hours fermentation) that was 7.8-fold higher than that with the original PNSB medium (0.28 ± 0.01g/L at 24 hours fermentation). Accordingly, this optimal fermentation condition for *R. palustris* PS3 is not only highly productive but also cost- and time-effective. It has been indicated that the sources of nitrogen and carbon play a critical role in the production of microbial secondary metabolites [37, 38]. Variation in fermentation condition results in changes in the yields and compositions of these secondary metabolites, which potentially affect activity, biomass and original effectiveness of microorganisms [39–41]. Therefore, we deduced that the secondary

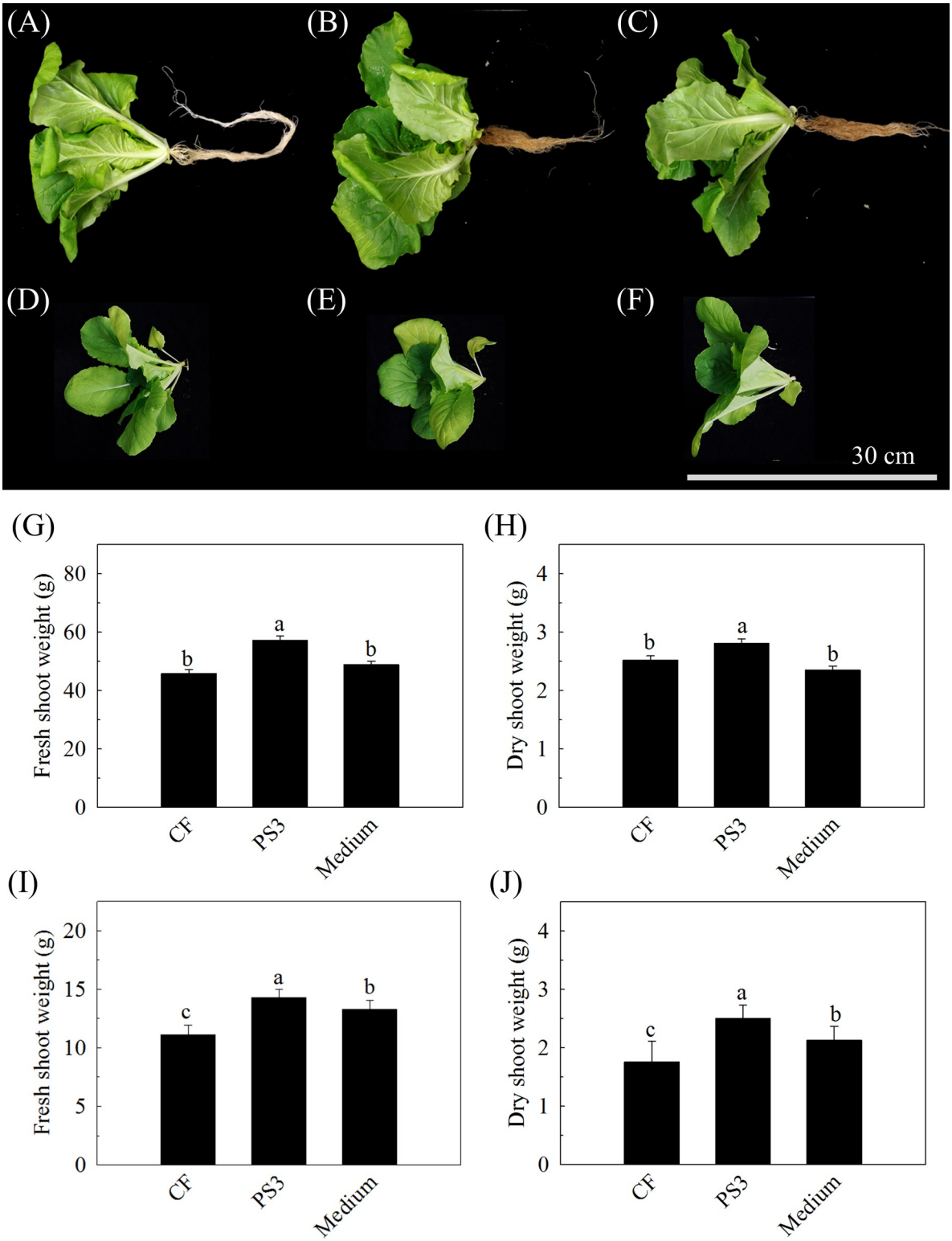

Fig 3. Plant growth-promoting effects of *R. palustris* PS3 incubated with the newly developed culture conditions on leafy vegetable. *Brassica rapa chinensis* (Chinese cabbage) was cultivated with pure chemical fertilizer under either hydroponic or soil system. "CF" indicates the control group (chemical fertilizer treatment), "PS3" indicates the treatment (CF) supplemented with the fermentation broth of *R. palustris* PS3, "medium" indicates the treatment (CF) supplemented with fresh medium, respectively. (A)-(F) show the morphology of Chinese cabbage cultivated in hydroponic (A:CF, B: PS3 and C: medium) and soil systems (D: CF, E: PS3 and F: medium) with the different

treatments at 17 DAP and 28 DAP, respectively. (G-J) are the fresh and dry shoot weights of Chinese cabbage cultivated in hydroponic (G and H) and soil systems (I and J), respectively. Vertical bars represent the standard error and bars with different letters indicate statistically significant differences at P = 0.05 according LSD test.

https://doi.org/10.1371/journal.pone.0236739.g003

metabolites of PS3 using CLS and molasses as nitrogen and carbon sources can effectively stimulate the growth of this bacterium, although the profiles of the substances remains to be elucidated.

For industrial fermentation, the composition of the medium is critical, since it significantly affects the product concentration, yield and volumetric productivity. Furthermore, the cost of raw materials can range from 40% to 80% of the total costs of fermentation and affect the ease and cost of downstream product separation [42]. *R. palustris* is already known as the most metabolically versatile bacteria, which was able to catabolize various carbon and nitrogen sources, such as glucose, fructose, malic acid, acetic acid, ammonium nitrate, glutamine, yeast extract and so on [8, 26, 43, 44]. In this study, we evaluated several low-cost materials derived from common nutrients or agro-industrial byproducts for the fermentation of *R. palustris* PS3 and found that a variety of nitrogen and carbon sources could be utilized (Fig 1). These results may be attributed to the extraordinary metabolic versatility of *R. palustris* PS3 [45]. Noteworthily, the growth rates of *R. palustris* PS3 varied in response to different carbon or nitrogen sources (Fig 1). For nitrogen sources, the viable count of PS3 cultured with complex substrates, such as CSL, BRE or yeast extract supplied with NH_4Cl (i.e., the PNSB treatment), was significantly higher than that of PS3 cultured with a sole nitrogen source (i.e., NH_4NO_3) (Fig 1B). These complex substrates all contain nitrogen-rich substances [46–49], and were well solubilized in our cultivation medium. On the other hand, although SF and SPI are also complex nitrogen sources, the cell counts of these two treatments were relatively low (Fig 1B). We deduced that it was due to their low solubility in the medium as described above or because their primary components (β-conglycinin, glycinin, and lipophilic proteins) are not easily metabolized by *R. palustris* PS3. However, further experimentation is still needed.

For carbon sources, as shown in Fig 1D, the viable count of PS3 cultured with molasses was higher than those of PS3 cultured with sugars (i.e., glucose or fructose). Molasses is a by-product of the sugar manufacturing process and may be obtained from beet or sugarcane; it contains abundant saccharides (such as sucrose, glucose, and fructose) and small amounts of organic acids (such as acetic acid and lactic acid) [50, 51]. It has been reported that *R. palustris* biomass production is stimulated by the co-utilization of multiple carbon sources [52]. Similar phenomenon was also observed in other microorganisms. For example, the growth rate of cultivated *E. coli* was higher with a combination of two substrates (i.e., mannose, xylose, glycerol, maltose or glucose supplemented with succinate, pyruvate, oxaloacetate, glycerol or glucose, respectively) than with a single substrate (mannose, xylose, glycerol, maltose or glucose, respectively) [53]. *Lactobacillus brevis* subsp. *lindneri* CB1 cultivated with maltose and citrate mixtures resulted in a faster cell growth rate than that of the strain cultivated with maltose alone, and the growth rate and viable counts (OD_{620}) derived from the former media were 1.8-fold and 1.2-fold higher, respectively [54]. Comparison with either glucose alone or malate alone as a carbon source, the growth rate of *B. subtilis* 168 increased 1.25-fold when cultured in medium containing glucose and malate mixtures [55]. It is already known that *R. palustris* can readily utilize organic acids as carbon sources [56]. Since organic acids such as acetic acid and lactic acid are contained in molasses [51], it is possible that *R. palustris* co-metabolized several of the carbon sources in molasses, although further experimentation is needed.

The relationship between the target factors and *R. palustris* PS3 biomass production was explained by mathematical models and ANOVA. The linear regression model and ANOVA in

FFD suggested that increasing the concentration of molasses could increase biomass production (S2 Eq and S3 Table in S1 File). This result is quite reasonable because bacterial cells require carbon sources to survive. However, the results of the second-order regression model and ANOVA (Table 3) indicated that molasses did not significantly influence the growth of *R. palustris* PS3 (Eq (3) and Table 3). We deduced that this discrepancy between the first- and second-order regression models might be attributed to CSL, which contains organic acids [48]. Increasing the concentration of CSL might supply a carbon source to partially substitute for molasses. In a previous study, it was mentioned that CSL could serve as a supplement to replace carbon sources for some microorganisms [57]. It also indicated that the carbon source was already sufficient in our CCD experiments. The effects of molasses concentration can also be observed in Fig 2A, 2C and 2D. Increasing or reducing the concentration of molasses did not significantly alter the biomass of *R. palustris* PS3.

In contrast, the factors CSL, temperature and pH value significantly influenced the growth of *R. palustris* PS3 (Table 3). It was observed that for greater and lower levels of CSL, temperature and pH value, there was a reduction in the response (Fig 2). Not surprisingly, a higher or lower pH value reduced the growth of *R. palustris* PS3, while the optimal pH value proposed by the RSM model for the fermentation of *R. palustris* was 7.0 (Table 4). This result was consistent with our previous study, which found that the pH range for *R. palustris* PS3 growth was 5.0 to 9.0, and the optimum pH was 7.0 [8]. Interestingly, the mathematical model suggested that the optimal temperature for *R. palustris* PS3 fermentation was 37.9˚C, which was different from our previous finding (30˚C) [8]. We inferred that this dissimilarity could be attributed to the culture medium composition. Our proposed model showed that the interaction between CSL and temperature dramatically influenced *R. palustris* PS3 biomass production (Table 3). However, no study has indicated the effects of temperature and nutrients on *R. palustris* metabolism. Likewise, a higher temperature suppressed the growth of *R. palustris* PS3, though S2 Eq in S1 File indicated that increasing the temperature could increase *R. palustris* PS3 biomass production (Fig 2B, 2C and 2F). In the CCD experiments, the biomass production in trials No. 1, 3, 4, 5 and 17 was significantly lower than that in the other trials (Table 2). Regarding the effect of CSL on the growth of *R. palustris* PS3, we considered that an extra nitrogen source was absolutely important to *R. palustris* growth. It is known that *R. palustris* can obtain nitrogen from air by biological nitrogen fixation (BNF) [1]. However, BNF is very sensitive to the O_2 concentration and is only carried out under microaerobic conditions. Thus, under the aerobic culture conditions of this study, BNF did not occur. Accordingly, supplementation with exogenous nitrogen in the culture medium was necessary.

Molasses and CSL can be applied individually as fertilizers in agriculture. For example, it has been found that the soil quality was remarkably improved by the application of molasses [58, 59]. There were also reports showing that molasses could increase the yield and quality of crops [60, 61]. CSL was shown to have beneficial effects on plants [62, 63], and supplementation of with exogenous CSL in soil promoted the growth of the root system of soybean [62]. It has been suggested that the organic nitrogen in CSL is converted to nitrate via microbial ammonification and nitrification and directly utilized by plants [64]. However, it has also been reported that CSL and molasses might have negative effects on plant growth. Zhu et al [62] reported that high concentration of CSL (more than 2%) will inhibit plant growth. In addition, fertilization of molasses singly or in combination with some PGPRs (*Bacillus* spp. *Azospirillum* spp. or *Azotobacter* spp.) showed a negative influence on seed germination *in vitro* [65]. In this study, the newly developed medium containing molasses (32.35 g/L) and CSL (39.41 mL/L) was verified for its effect on plant growth. Since the PS3 fermentation broth showed positive effects on plant growth in both soil and hydroponic systems (Fig 3). It suggests that this medium is suitable not only for phototrophic bacteria production but for application in

agricultural production. Such an approach to farming is regarded as environmentally friendly and can be used to reduce excessive chemical fertilizer application and ensure sustainable crop production.

Furthermore, it is notable that PS3 fermentation broth obtained from newly developed medium that is consistent with PS3 cultured in modified PNSB, it shown the plant growth promotion effect (Fig 3). In our previous work [8], to examine whether the plant beneficial effects of *R. palustris* PS3 were elicited by viable cells or conferred by organic compounds from the PNSB medium or dead/ decaying cells, the 65˚C heat-killed bacterial suspension was applied to replace the vegetative *R. palustris* cells. The results showed that neither medium nor dead *R. palustris* cells was able to promote plant growth [8]. These results indicated that the effectiveness observed were mainly exerted by the viable cells of *R. palustris* PS3. Notably, it was also demonstrated that not only the population (i.e viability) but also the metabolic activity (i.e vitality) of PS3 cells is crucial for the plant beneficial traits [32]). On the other hand, in our another study [45], we carried out a comparative analysis of effective (strain PS3) as well as ineffective (strain YSC3) *R. palustris* strains in plant-growth promotion. PS3 and YSC3 exhibited a very close phylogenetic relationship and shared several conserved regions and genetic arrangements in their chromosomes. Although these strains have many plant growth-promoting (PGP) genes in common, only PS3 exhibited beneficial traits. We noticed that the transcripts of genes associated with bacterial colonization and biofilm formation in response to root exudates were higher in PS3 than those in YSC3 strain [45]. These data suggested that PS3 responds better to the presence of plant hosts. It indicates that the physiological responses of this bacterium to its plant hosts as well as successful establishment of interactions with plant hosts appear to be critical factors for PS3 to promote plant growth. Taken together, we deduced that the beneficial effects of PS3 were mainly offered by the viable cells of this bacterium through interactions with the host.

Conclusion

This paper presented an experimental design for the optimization of *R. palustris* PS3 biomass production with an alternative, low-cost medium containing agricultural byproducts. CSL and molasses were identified as potential nitrogen and carbon sources for *R. palustris* fermentation. The utilization of CSL and molasses as raw materials for *R. palustris* fermentation can aid in reducing agro-industrial waste. The response surface methodology revealed the factors that greatly influence *R. palustris* PS3 growth, namely, CLS, temperature and pH value. *R. palustris* PS3 biomass production increased significantly, by 7.8-fold, from 0.28 ± 0.01 g/L to 2.18 ± 0.01 g/L, compared to that under the basal medium/conditions when the strain was cultivated in the optimal culture conditions (CSL, 39.41 mL/L; molasses, 32.35 g/L; temperature, 37.9˚C; pH, 7.0 and DO 30%) developed by statistical experimental methods. The in planta experiments verified that the newly developed fermentation broth retained the plant growth-promoting functions of *R. palustris* PS3. Compared with those in previous studies, our newly developed fermentation process could successfully produce high levels of *R. palustris* in a shorter time. This study described the prospective uses of agro-industrial techniques for *R. palustris* biofertilizer production.

Supporting information

S1 File.
(DOCX)

Acknowledgments

We thank Prof. Yan-Zhang Sun (Department of Plant Pathology and Microbiology, National Taiwan University) for kindly providing the 5-L stirred tank bioreactor. This article was subsidized by National Taiwan University under the Excellence Improvement Program for Doctoral Students (sponsored by Ministry of Science and Technology).

Author Contributions

Conceptualization: Sook-Kuan Lee.

Data curation: Kai-Jiun Lo.

Formal analysis: Kai-Jiun Lo.

Funding acquisition: Chi-Te Liu.

Investigation: Kai-Jiun Lo, Sook-Kuan Lee.

Methodology: Kai-Jiun Lo.

Project administration: Chi-Te Liu.

Resources: Chi-Te Liu.

Software: Kai-Jiun Lo.

Supervision: Chi-Te Liu.

Validation: Chi-Te Liu.

Visualization: Kai-Jiun Lo.

Writing – original draft: Kai-Jiun Lo.

Writing – review & editing: Kai-Jiun Lo, Sook-Kuan Lee, Chi-Te Liu.

References

1. Larimer FW, Chain P, Hauser L, Lamerdin J, Malfatti S, Do L, et al. Complete genome sequence of the metabolically versatile photosynthetic bacterium *Rhodopseudomonas palustris*. Nat Biotechnol. 2004; 22(1):55–61. https://doi.org/10.1038/nbt923 PubMed PMID: WOS:000187745400027. PMID: 14704707
2. Idi A, Nor MHM, Wahab MFA, Ibrahim Z. Photosynthetic bacteria: an eco-friendly and cheap tool for bioremediation. Rev Environ Sci Bio. 2015; 14(2):271–85. https://doi.org/10.1007/s11157-014-9355-1 PubMed PMID: WOS:000354408400006.
3. Austin S, Kontur WS, Ulbrich A, Oshlag JZ, Zhang W, Higbee A, et al. Metabolism of multiple aromatic compounds in corn stover hydrolysate by *Rhodopseudomonas palustris*. Environ Sci Technol. 2015; 49 (14):8914–22. https://doi.org/10.1021/acs.est.5b02062 PMID: 26121369; PubMed Central PMCID: PMC5031247.
4. Oda Y, Star B, Huisman LA, Gottschal JC, Forney LJ. Biogeography of the purple nonsulfur bacterium *Rhodopseudomonas palustris*. Appl Environ Microbiol. 2003; 69(9):5186–91. https://doi.org/10.1128/aem.69.9.5186-5191.2003 PubMed PMID: WOS:000185437000017. PMID: 12957900
5. Zhang D, Xiao N, Mahbubani KT, del Rio-Chanona EA, Slater NKH, Vassiliadis VS. Bioprocess modelling of biohydrogen production by *Rhodopseudomonas palustris*: Model development and effects of operating conditions on hydrogen yield and glycerol conversion efficiency. Chem Eng Sci. 2015; 130:68–78. https://doi.org/10.1016/j.ces.2015.02.045 PubMed PMID: WOS:000353485800007.
6. Liu Y, Ghosh D, Hallenbeck PC. Biological reformation of ethanol to hydrogen by *Rhodopseudomonas palustris* CGA009. Bioresour Technol. 2015; 176:189–95. https://doi.org/10.1016/j.biortech.2014.11.047 PMID: 25461002.
7. Shi XY, Li WW, Yu HQ. Optimization of H-2 photo-fermentation from benzoate by Rhodopseudomonas palustris using a desirability function approach. Int J Hydrogen Energ. 2014; 39(9):4244–51. https://doi.org/10.1016/j.ijhydene.2014.01.016 PubMed PMID: WOS:000333881500011.

8. Wong WT, Tseng CH, Hsu SH, Lur HS, Mo CW, Huang CN, et al. Promoting effects of a single *Rhodopseudomonas palustris* inoculant on plant growth by *Brassica rapa chinensis* under low fertilizer input. Microbes Environ. 2014; 29(3):303–13. Epub 2014/08/19. https://doi.org/10.1264/jsme2.me14056 PMID: 25130882; PubMed Central PMCID: PMC4159042.
9. Kornochalert N, Kantachote D, Chaiprapat S, Techkarnjanaruk S. Use of *Rhodopseudomonas palustris* P1 stimulated growth by fermented pineapple extract to treat latex rubber sheet wastewater to obtain single cell protein. Ann Microbiol. 2014; 64(3):1021–32. https://doi.org/10.1007/s13213-013-0739-1 PubMed PMID: WOS:000340087200015.
10. Nunkaew T, Kantachote D, Kanzaki H, Nitoda T, Ritchie RJ. Effects of 5-aminolevulinic acid (ALA)-containing supernatants from selected Rhodopseudomonas palustris strains on rice growth under NaCl stress, with mediating effects on chlorophyll, photosynthetic electron transport and antioxidative enzymes. Electron J Biotechn. 2014; 17(1):19–26. https://doi.org/10.1016/j.ejbt.2013.12.004 PubMed PMID: WOS:000334440900008.
11. Hsu SH, Lo KJ, Fang W, Lur HS, Liu CT. Application of phototrophic bacterial inoculant to reduce nitrate content in hydroponic leafy vegetables. Crop Environ Bioinf. 2015; 12:30–41.
12. Yang X. Scale-up of microbial fermentation process. In: Baltz R DA, Davies J, Bull A, Junker B, Katz L, Lynd L, Masurekar P, Reeves C, Zhao H, editor. Manual of industrial microbiology and biotechnology. 3rd ed. Washington, DC: American Society of Microbiology; 2010. p. 669–75.
13. Crater JS, Lievense JC. Scale-up of industrial microbial processes. FEMS Microbiol Lett. 2018; 365 (13). doi: ARTN fny13810.1093/femsle/fny138. PubMed PMID: WOS:000441114700001.
14. Thomsen MH. Complex media from processing of agricultural crops for microbial fermentation. Appl Microbiol Biotechnol. 2005; 68(5):598–606. Epub 2005/08/06. https://doi.org/10.1007/s00253-005-0056-0 PMID: 16082554.
15. Moraes IO, Capalbo DMF, Moraes RO. Multiplicação de agentes de controle biológico. Controle biológico de doenças de plantas. Brasília: EMBRAPA; 1991. p. 253–72.
16. Xiao ZJ, Liu PH, Qin JY, Xu P. Statistical optimization of medium components for enhanced acetoin production from molasses and soybean meal hydrolysate. Appl Microbiol Biotechnol. 2007; 74(1):61–8. Epub 2006/10/18. https://doi.org/10.1007/s00253-006-0646-5 PMID: 17043817.
17. Yang TW, Rao ZM, Zhang X, Xu MJ, Xu ZH, Yang ST. Effects of corn steep liquor on production of 2,3-butanediol and acetoin by *Bacillus subtilis*. Process Biochem. 2013; 48(11):1610–7. https://doi.org/10.1016/j.procbio.2013.07.027 PubMed PMID: WOS:000327920600002.
18. Shamala TR, Vijayendra SV, Joshi GJ. Agro-industrial residues and starch for growth and co-production of polyhydroxyalkanoate copolymer and alpha-amylase by *Bacillus* sp. CFR-67. Braz J Microbiol. 2012; 43(3):1094–102. Epub 2012/07/01. https://doi.org/10.1590/S1517-838220120003000036 PMID: 24031933; PubMed Central PMCID: PMC3768888.
19. Cha SH, Lim JS, Yoon CS, Koh JH, Chang HI, Kim SW. Production of mycelia and exo-biopolymer from molasses by *Cordyceps sinensis* 16 in submerged culture. Bioresour Technol. 2007; 98(1):165–8. Epub 2006/01/03. https://doi.org/10.1016/j.biortech.2005.11.007 PMID: 16387491.
20. Dhaliwal SS, Oberoi HS, Sandhu SK, Nanda D, Kumar D, Uppal SK. Enhanced ethanol production from sugarcane juice by galactose adaptation of a newly isolated thermotolerant strain of *Pichia kudriavzevii*. Bioresour Technol. 2011; 102(10):5968–75. https://doi.org/10.1016/j.biortech.2011.02.015 PubMed PMID: WOS:000291125800058. PMID: 21398115
21. Liu BB, Yang MH, Qi BK, Chen XR, Su ZG, Wan YH. Optimizing L-(+)-lactic acid production by thermophile *Lactobacillus plantarum* As 1 3 using alternative nitrogen sources with response surface method. Biochem Eng J. 2010; 52(2–3):212–9. https://doi.org/10.1016/j.bej.2010.08.013 PubMed PMID: WOS:000284571200015.
22. Shen NK, Liao SM, Wang QY, Qin Y, Zhu QX, Zhu J, et al. Economical succinic acid production from sugarcane juice by Actinobacillus succinogenes supplemented with corn steep liquor and peanut meal as nitrogen sources. Sugar Tech. 2016; 18(3):292–8. https://doi.org/10.1007/s12355-015-0401-2 PubMed PMID: WOS:000375790600009.
23. Bezerra MA, Santelli RE, Oliveira EP, Villar LS, Escaleira LA. Response surface methodology (RSM) as a tool for optimization in analytical chemistry. Talanta. 2008; 76(5):965–77. https://doi.org/10.1016/j.talanta.2008.05.019 PubMed PMID: WOS:000259750800001. PMID: 18761143
24. Yolmeh M, Jafari SM. Applications of response surface methodology in the food industry processes. Food Bioprocess Tech. 2017; 10(3):413–33. https://doi.org/10.1007/s11947-016-1855-2 PubMed PMID: WOS:000394285200001.
25. Zhang B, Guowei S, Bao C, Cao J, Tan Y. Optimization of culture medium for *Lactobacillus bulgaricus* using box-behnken design. Acta Univ Cibiniensis, Ser E: Food Technol. 2017;21. https://doi.org/10.1515/aucft-2017-0001

26. Dönmez GÇ, Öztürk A, çakmakçı L. Properties of the Rhodopseudomonas palustris strains isolated from an alkaline lake in turkey. Turk J Biol. 1999; 23(4):457–63.

27. van Niel CB. The culture, general physiology, morphology, and classification of the non-sulfur purple and brown bacteria. Bacteriol Rev. 1944; 8(1):1–118. PMID: 16350090.

28. Du C, Zhou J, Wang J, Yan B, Lu H, Hou H. Construction of a genetically engineered microorganism for CO_2 fixation using a *Rhodopseudomonas*/*Escherichia coli* shuttle vector. FEMS Microbiol Lett. 2003; 225(1):69–73. Epub 2003/08/06. https://doi.org/10.1016/S0378-1097(03)00482-8 PMID: 12900023.

29. Carlozzi P, Sacchi A. Biomass production and studies on *Rhodopseudomonas palustris* grown in an outdoor, temperature controlled, underwater tubular photobioreactor. J Biotechnol. 2001; 88(3):239–49. https://doi.org/10.1016/s0168-1656(01)00280-2 PubMed PMID: WOS:000169906200004. PMID: 11434969

30. Chang TH, Wang R, Peng YH, Chou TH, Li YJ, Shih YH. Biodegradation of hexabromocyclododecane by Rhodopseudomonas palustris YSC3 strain: A free-living nitrogen-fixing bacterium isolated in Taiwan. Chemosphere. 2020; 246:125621. Epub 2020/01/03. https://doi.org/10.1016/j.chemosphere.2019.125621 PMID: 31896015.

31. Xu J, Feng Y, Wang Y, Lin X. Characteristics of purple nonsulfur bacteria grown under stevia residue extractions. Lett Appl Microbiol. 2013; 57(5):420–6. Epub 2013/07/11. https://doi.org/10.1111/lam.12129 PMID: 23837648.

32. Lee SK, Lur HS, Lo KJ, Cheng KC, Chuang CC, Tang SJ, et al. Evaluation of the effects of different liquid inoculant formulations on the survival and plant-growth-promoting efficiency of *Rhodopseudomonas palustris* strain PS3. Appl Microbiol Biotechnol. 2016; 100(18):7977–87. https://doi.org/10.1007/s00253-016-7582-9 PubMed PMID: WOS:000382008000016. PMID: 27150383

33. Lenth RV. Response-surface methods in R, using rsm. J Stat Softw. 2009; 32(7):1–17. Epub 2009-10-14. https://doi.org/10.18637/jss.v032.i07

34. R Core Team. R: a language and environment for statistical computing. Vienna, Austria: R Foundation for Statistical Computing; 2019.

35. Hoagland DR, Arnon DI. The Water-culture method for growing plants without soil: University of California, College of Agriculture, Agricultural Experiment Station; 1950. 31 p.

36. Liu S. Chapter 2—An overview of biological basics. In: Liu S, editor. Bioprocess Engineering. 2nd ed: Elsevier; 2017. p. 21–80.

37. Ruiz B, Chavez A, Forero A, Garcia-Huante Y, Romero A, Sanchez M, et al. Production of microbial secondary metabolites: regulation by the carbon source. Crit Rev Microbiol. 2010; 36(2):146–67. Epub 2010/03/10. https://doi.org/10.3109/10408410903489576 PMID: 20210692.

38. Singh V, Haque S, Niwas R, Srivastava A, Pasupuleti M, Tripathi CK. Strategies for fermentation medium optimization: An in-depth review. Front Microbiol. 2016; 7:2087. Epub 2017/01/24. https://doi.org/10.3389/fmicb.2016.02087 PMID: 28111566; PubMed Central PMCID: PMC5216682.

39. Navarrete-Bolaños JL. Improving traditional fermented beverages: How to evolve from spontaneous to directed fermentation. Eng Life Sci. 2012; 12(4):410–8. https://doi.org/10.1002/elsc.201100128

40. Waites MJ, Morgan NL, Rockey JS, Higton G. Industrial microbiology: An introduction: Wiley; 2001.

41. Comelli RN, Seluy LG, Isla MA. Optimization of a low-cost defined medium for alcoholic fermentation—a case study for potential application in bioethanol production from industrial wastewaters. New Biotechnol. 2016; 33(1):107–15. https://doi.org/10.1016/j.nbt.2015.09.001 PubMed PMID: WOS:000364861700013. PMID: 26391675

42. Li KX, Liu S, Liu XH. An overview of algae bioethanol production. Int J Energ Res. 2014; 38(8):965–77. https://doi.org/10.1002/er.3164 PubMed PMID: WOS:000337729900001.

43. Imhoff JF, Trüper HG. The genus Rhodospirillum and related genera. In: Balows A, Trüper HG, Dworkin M, Harder W, Schleifer K-H, editors. In the prokaryotes. 2nd ed. New York: Springer; 1992. p. 2141–55.

44. Merugu R, Rudra M, Ayinampudi S, Ramesh D, Nageshwari B, Rajyalaxmi K, et al. Influence of different cultural conditions on photoproduction of hydrogen by Rhodopseudomonas palustris KU003. ISRN Renew Energy. 2011;2011. https://doi.org/10.5402/2011/328984

45. Lo KJ, Lin SS, Lu CW, Kuo CH, Liu CT. Whole-genome sequencing and comparative analysis of two plant-associated strains of Rhodopseudomonas palustris (PS3 and YSC3). Sci Rep. 2018; 8(1):12769. Epub 2018/08/26. https://doi.org/10.1038/s41598-018-31128-8 PMID: 30143697; PubMed Central PMCID: PMC6109142.

46. Silveira MM, Wisbeck E, Hoch I, Jonas R. Production of glucose-fructose oxidoreductase and ethanol by *Zymomonas mobilis* ATCC 29191 in medium containing corn steep liquor as a source of vitamins. Appl Microbiol Biotechnol. 2001; 55(4):442–5. https://doi.org/10.1007/s002530000569 PubMed PMID: WOS:000168842900009. PMID: 11398924

47. Hull SR, Yang BY, Venzke D, Kulhavy K, Montgomery R. Composition of corn steep water during steeping. J Agr Food Chem. 1996; 44(7):1857–63. https://doi.org/10.1021/jf950353v

48. Xiao X, Hou Y, Du J, Liu Y, Liu Y, Dong L, et al. Determination of main categories of components in corn steep liquor by near-infrared spectroscopy and partial least-squares regression. J Agr Food Chem. 2012; 60(32):7830–5. https://doi.org/10.1021/jf3012823 PMID: 22838730

49. Mirmiran P, Houshialsadat Z, Gaeini Z, Bahadoran Z, Azizi F. Functional properties of beetroot (Beta vulgaris) in management of cardio-metabolic diseases. Nutr Metab. 2020; 17(1). doi: ARTN 310.1186/s12986-019-0421-0. PubMed PMID: WOS:000513724400001.

50. Najafpour GD, Shan CP. Enzymatic hydrolysis of molasses. Bioresour Technol. 2003; 86(1):91–4. Epub 2002/11/08. https://doi.org/10.1016/s0960-8524(02)00103-7 PMID: 12421015.

51. Nelson EK. Some organic acids of sugar cane molasses. J Am Chem Soc. 1929; 51(9):2808–10. https://doi.org/10.1021/ja01384a030

52. Govindaraju A, McKinlay JB, LaSarre B. Phototrophic lactate utilization by *Rhodopseudomonas palustris* is stimulated by coutilization with additional substrates. Appl Environ Microbiol. 2019;85(11). doi: UNSP e00048-1910.1128/AEM.00048-19. PubMed PMID: WOS:000468578100002.

53. Hermsen R, Okano H, You C, Werner N, Hwa T. A growth-rate composition formula for the growth of *E. coli* on co-utilized carbon substrates. Mol Syst Biol. 2015; 11(4):801. Epub 2015/04/12. https://doi.org/10.15252/msb.20145537 PMID: 25862745; PubMed Central PMCID: PMC4422558.

54. Gobbetti M, Corsetti A. Co-metabolism of citrate and maltose by *Lactobacillus brevis* subsp. *lindneri* CB1 citrate-negative strain: Effect on growth, end-products and sourdough fermentation. Eur Food Res Technol. 1996; 203(1):82–7. https://doi.org/10.1007/BF01267775

55. Kleijn RJ, Buescher JM, Le Chat L, Jules M, Aymerich S, Sauer U. Metabolic fluxes during strong carbon catabolite repression by malate in *Bacillus subtilis*. J Biol Chem. 2010; 285(3):1587–96. Epub 2009/11/18. https://doi.org/10.1074/jbc.M109.061747 PMID: 19917605; PubMed Central PMCID: PMC2804316.

56. McKinlay JB, Harwood CS. Calvin cycle flux, pathway constraints, and substrate oxidation state together determine the H-2 biofuel yield in photoheterotrophic bacteria. Mbio. 2011; 2(2). doi: ARTN e00323-1010.1128/mBio.00323-10. PubMed PMID: WOS:000296843700009.

57. Liggett RW, Koffler H. Corn steep liquor in microbiology. Bacteriol Rev. 1948; 12(4):297–311. https://doi.org/10.1128/Mmbr.12.4.297–311.1948 PubMed PMID: WOS:A1948UY02600002. PMID: 16350125

58. Pyakurel A, Dahal B, Rijal S. Effect of molasses and organic fertilizer in soil fertility and yield of spinach in Khotang, Nepal. IJASBT. 2019; 7:49–53. https://doi.org/10.3126/ijasbt.v7i1.23301

59. Bagheri B, Karimi-Jashni A, Zerafat MM. Application of molasses as draw solution in forward osmosis desalination for fertigation purposes. Environ Technol. 2019:1–11. https://doi.org/10.1080/09593330.2019.1645215 PMID: 31311445

60. Samavat S, Samavat S. The effects of fulvic acid and sugar cane molasses on yield and qualities of tomato. Int Res J Appl Basic Sci. 2014; 8(3):266–8.

61. Şanlı A, Karadoğan T, Tosun B. The effects of sugar beet molasses applications on root yield and sugar content of sugar beet (Beta vulgaris L.). Tarla Bitkileri Merkez Araştırma Enstitüsü Dergisi. 2015; 24 (2):103–8.

62. Zhu MM, Liu EQ, Bao Y, Duan SL, She J, Liu H, et al. Low concentration of corn steep liquor promotes seed germination, plant growth, biomass production and flowering in soybean. Plant Growth Regul. 2019; 87(1):29–37. https://doi.org/10.1007/s10725-018-0449-6 PubMed PMID: WOS:000457940100004.

63. Chinta YD, Kano K, Widiastuti A, Fukahori M, Kawasaki S, Eguchi Y, et al. Effect of corn steep liquor on lettuce root rot (Fusarium oxysporum f.sp. lactucae) in hydroponic cultures. J Sci Food Agr. 2014; 94 (11):2317–23. Epub 2014/01/10. https://doi.org/10.1002/jsfa.6561 PMID: 24403175.

64. Shinohara M, Aoyama C, Fujiwara K, Watanabe A, Ohmori H, Uehara Y, et al. Microbial mineralization of organic nitrogen into nitrate to allow the use of organic fertilizer in hydroponics. Soil Sci Plant Nutr. 2011; 57(2):190–203. https://doi.org/10.1080/00380768.2011.554223

65. A S, Widawati S. Effect of Plant Growth Promoting Rhizobacteria and Molasses on Seed Germination and Seedling Growth of Sorghum bicolor L.Moench. The 1st Science and Technology Research Partnership for Sustainable Development Program (SATREPS); 2017; Bogor, Indonesia2017. p. 94–9.